THIRD INTERNATIONAL CONFERENCE ON STABILITY OF SHIPS AND OCEAN VEHICLES

VOLUME II

ADDENDUM 1

STAB'86

22-26

September 1986

GDAŃSK-POLAND

STAB '86

MARIN
Maritiem Research Instituut Nederland
Haagsteeg 2 Postbus 28 6700 AA Wageningen

Third
International
Conference
on

Stability of Ships and Ocean Vehicles

22-26
September 1986
Gdańsk-Poland

Volume II
Addendum 1

C O N T E N T S

Third International Conference on Stability of Ships and Ocean Vehicles, Gdańsk, Sept 1986

STAB'86

ASYMMETRIC NONLINEAR ROLLING: INFLUENCE ON STABILITY

A. Cardo, A. Francescutto

R. Nabergoj, G. Trincas

ABSTRACT

In this paper we consider the nonlinear rolling motion of a heeled ship in a regular beam sea. By means of a perturbation method, we derive approximate expressions relating the maximum amplitude of the oscillation to the excitation intensity. The experimentally observed difference in amplitude connected with the direction of the waves relative to the initial bias, is explained in terms of the coupling roll-heave effect. The results obtained clarify the understanding of the nonlinear rolling phenomenon.

1. INTRODUCTION

As pointed out in the conclusions of STAB'82 [1,2], the ship stability and safety problem is still far from a univocal solution valid in all physical conditions. It was recommended to strenghten the efforts with all means at our disposal, in the light of the fact that a conclusive response cannot come out from pure experimental, analytical or numerical approaches. This is particularly true for the rolling motion which represents the major risk for capsizing.

The rolling motion, due to its higly nonlinear nature, is still insufficiently known, also in the deterministic domain [3]. Following the introduction to English SAFESHIP project [4] one may state: "Model experiments had been carried out for some time in this country and elsewhere to seek an explanation for capsize losses. Apart from the fact that such experiments are expensive and time-consuming they yield incomplete information e.g. because of the number of parameters involved and the impracticability of isolating their separate effects. It was believed therefore that a theoretically oriented project would provide a more comprehensive basis for future stability regulations, observing the almost infinite combinations of hull and environmental parameters at various load conditions, speeds and wave directions. this tends, in our view, to rule out a purely experimental solutions."

The rolling motion is usually studied for a ship in the upright equilibrium position. In the last few years, considerable efforts have been devoted to this sector, both from the theoretical and experimental points of view. The understanding of the problem, although not fully satisfactory, can be considered very encouraging. However, in the very important case in which the ship is initially in a heeled equilibrium position, the present state of research appears to be insufficient. Only a few papers concerning both the experimental [5,6] and the theoretical [7-11] aspects of the phenomenon have been published on this particular subject. The analytical results fit the experimental data quite well, but

where y is the adimensional roll angle measured from the heeled equilibrium position.

It can be proved that equations (4) and (5) are equivalent. Indicating with x_0 the static heel angle and assuming $x=x_0+y$, the first equation is reduced to the second by a change of variable and viceversa. Therefore, in the following discussion, only equation (5) will be considered. Note that x_0 is positive for a ship biased towards waves and negative for a ship biased away from waves.

The hydrodynamic coefficients of a heeled ship are changed with respect to those of a ship in the upright position [8]. For example, it would be necessary to consider that in the heeled condition the damping model cannot be described by an odd polynomial and even terms have to be introduced in the power expansion. We will maintain, both for simplicity and for lack of necessary experimental knowledge, that all the hydrodynamic coefficients are constant.

In the main resonance region the approximate analytical solution of equation (5) is

$$y(\tau) = C\cos(\omega\tau+\psi) + a_0 + a_2\cos 2(\omega\tau+\psi) \quad . \qquad (6)$$

The amplitude and the phase of the steady state solution are given by the following equations

$$g_0C^6+g_4C^4+g_5C^2-e_\omega^2 = 0 \quad ,$$
$$tg\psi = -(a_4+a_3C^2)/(D_1+\frac{3}{4}\hat{a}_3C^2) \quad . \qquad (7)$$

The quantities e_i and g_i are given in Appendix, and

$$a_0 = -\frac{1}{2}a_2\omega_0^{-2}C^2 \quad ,$$
$$a_2 = \frac{1}{2}a_2(4\omega^2-\omega_0^2)^{-1}C^2 \quad , \qquad (8)$$
$$\hat{a}_3 = a_3-\frac{4}{3}a_2^2\omega_0^{-2}[1-\frac{1}{2}\omega_0^2(4\omega^2-\omega_0^2)^{-1}] \quad .$$

The parameter $\hat{a}_3$, here introduced, plays the role of an "equivalent nonlinearity" for the righting moment in heeled conditions.

The frequency response curve of a heeled ship exhibits the typical features of the nonlinear resonance. In particular, both the theoretical analysis and the numerical simulations indicate that the ship posesses, apart from synchronism, other nonlinear resonances such as ultraharmonic and subharmonic resonances. The difference between the nonlinear rolling in heeled and in upright conditions consists of the fact that the tuning ratios 1/2 and 2 play the predominant role instead of the tuning ratios 1/3 and 3 [3,12].

The response curve in synchronism shows the well known backbone aspect. The bending of the resonance peak has the effect of shifting the maximum oscillation amplitude at a frequency $\omega>\omega_0$ if $\hat{a}_3>0$ or $\omega<\omega_0$ if $\hat{a}_3<0$. This circumstance brings about a different weight in the effective damping of the motion, that is the damping for $\hat{a}_3>0$ becomes lower than that for $\hat{a}_3<0$ and consequently lowers the maxima. In particular, when $\hat{a}_3=0$, the righting arm nonlinearity has no influence on the response, because the effects of the quadratic and cubic nonlinearities cancel each other. The quadratic nonlinearity is responsible for an additional heeling, i.e. the rolling oscillation is not centered exactly at x_0. Expression (8) indicates that a_0 is opposite in sign to a_2. Since a_2 is usually opposite to x_0, the ship suffers an additional bias with the same sign of the static heel. As a consequence, the dynamic bias angle is larger in magnitude than the corresponding static heel of the ship.

We observe that both the maximum amplitude and the width of the resonance curve are strongly dependent, for a given excitation, on the value of the damping coefficients. The agreement between the analytical solutions and the numerical computation is found to be very satisfying [12]. In particular, the perturbation method adopted shows its validity in the forecast of the maximum rolling amplitude as a function of the excitation [14,15].

are generally in a very complex and involved mathematical form, so that they cannot be simply used in practice. In other words, one cannot handle simple formulas to compute the evolution of the ship's response, the maximum rolling amplitudes, the onset of nonlinear resonances different from synchronism, etc. The knowledge of these roll characteristics is particularly important when the ship is not in its own best conditions to react to the sea excitation.

The unfavourable situation of a heeled ship can arise from different, internal and external causes, e.g. shift of cargo, water on deck, unsymmetrical damage and the action of constant heeling moments due to wind or caused by manoeuvring. The purpose of the present paper is to develop an analytical method for predicting the wave-excited motions of ships which have a heeled equilibrium position and are running in regular beam seas. This method is based on the linear wave excitation theory, and the ship response is formulated in the frequency domain. The ship equation takes into account explicitly the restoring and damping nonlinearities.

2. EQUATION OF MOTION

The independent rolling can be described by the following differential equation

$$I\ddot{\phi} + D(\phi,\dot{\phi}) + M_r(\phi,t) = E(t) \quad , \qquad (1)$$

where ϕ is the rolling angle with respect to the calm sea surface, I is the mass moment of inertia including the added mass, $D(\phi,\dot{\phi})$ is the dissipative term, $M_r(\phi,t)$ is the righting arm, and $E(t)$ is the heeling moment due to external forces.

Equation (1) can be written in adimensional terms by using suitable angle and time scales for the problem. With these substitutions [12], one obtains

$$\ddot{x} + d(x,\dot{x}) + m_r(x,t) = e(t) \quad . \qquad (2)$$

The meaning of the various terms in equation (2) remains unchanged.

Later on, the righting arm will be considered as a function of the angle only, except for Section 4 where a coupling between roll-heave oscillations is introduced through an explicit dependence on time. Moreover, it is usual to assume a power series expansion in roll angle and roll speed for the dissipative term. A realistic damping model takes into account both the speed and the angle nonlinearities [13]. Here the usual cubic model will be assumed.

The righting moment will be expressed by a power series expansion including only odd terms in the angle. In particular, a cubic polynomial may be used for a sufficiently realistic analysis. The coefficient of the cubic term is chosen so as to give a "good" fit to the true curve.

With these assumptions [12], the equation of motion for a ship in upright equilibrium position and subjected to a regular beam sea becomes

$$\ddot{x} + 2\mu\dot{x} + \delta_2\dot{x}^3 + \omega_0^2 x + \alpha_3 x^3 = e_\omega \cos\omega\tau \quad . \qquad (3)$$

On the other hand, the motion of a ship in the heeled equilibrium position can be described by different theoretical models according to the particular nature of the heeling, i.e. due to initial instability, to internal or external causes. If the ship is heeled by an internal cause (cargo shifting, asymmetric damage, etc.) or by an external cause (wind, towing, etc.) one still takes equation (2) into consideration to represent the rolling motion. In this case, however, the excitation includes a further term which may be considered as constant, i.e.

$$\ddot{x} + 2\mu\dot{x} + \delta_2\dot{x}^3 + \omega_0^2 x + \alpha_3 x^3 = e_0 + e_\omega \cos\omega\tau \quad , \qquad (4)$$

where x is measured from the upright position. In the case of initial instability, it is commonly assumed that the righting moment is no longer an odd function of the heeling angle. Limiting the approximation still to a cubic polynomial, one can write

$$\ddot{y} + 2\mu\dot{y} + \delta_2\dot{y}^3 + \omega_0^2 y + \alpha_2 y^2 + \alpha_3 y^3 = e_\omega \cos\omega\tau \quad , \qquad (5)$$

3. MAXIMUM AMPLITUDES

One has the possibility of working with equation (7) in order to obtain simple formulas with the same prediction capabilities. This was done in Refs.[14,15] for a ship in the upright position. The results fit surprisingly well both the numerical calculations and the experimental data. For a heeled ship a similar approach can be adopted. The detailed calculations are close to those shown in Ref.[14].

The equation relating the maximum amplitude of the resonant component of the oscillation to the intensity of the excitation, is expressed by

$$8\omega_0(\mu I_m+\frac{3}{8}\delta_3\omega_0^2 I_m^3)-e_\omega^2=0 \quad . \tag{9}$$

Formula (9) gives the maximum amplitude of the rolling oscillations about the dynamic heel angle, in a first order of approximation. It is of immediate practical interest, giving an improvement of the classical formulas because it takes into account both the linear and the nonlinear damping effects. The quadratic and cubic righting arm nonlinearities do not appear explicitly in this expression. This fact does not invalidate the theoretical predictions, not even in the case where the nonlinearity is rather strong. The nonlinearity of the righting arm is responsible for a bending in the frequency response curve causing the system to be more "sensitive" to the excitation in a frequency range which is wider than that of the linear case. Consequently, it causes a frequency shift in the location of the maximum but does not strongly affect the corresponding maximum amplitude. However, the righting arm nonlinearities can be indirecty introduced in equation (9) through the dependence of the natural frequency on the amplitude, i.e. by means of the formula

$$\omega_m=\omega_0(1-\frac{3}{8}\hat{a}_3 I_m^2) \quad , \tag{10}$$

so rendering slightly more cumbersome the estimation of the maxima.

The theoretical predictions have been compared with the experimental observations carried out on ship models at Southampton University [16]. The model was suitably tethered to restrain it in drift and in yaw, while allowing it to roll, heave and sway. The results indicate that, for the same excitation intensity, the maximum amplitude of the rolling oscillations may assume considerably different values, depending on the direction of the propagation of the waves relative to the initial heel. Unfortunatelly, this effect cannot be explained by means of equation (9), the predictions of which are totally independent on the initial heel. To account for this experimental evidence the rolling equation must be improved, i.e. the coupling between roll and heave motions must be explicitly considered.

4. INFLUENCE OF THE ROLL-HEAVE COUPLING

To include the effect of the roll-heave coupling in the equation of ship motion an explitly time dependent righting moment has been considered by several authors [7,9,11]. This mathematical model is still very simplified, but incorporates sufficient details at this stage of the knowledge and allows a simple approximate analysis. In this case, equation (5) can be written in the following form

$$\ddot{y}+2\mu\dot{y}+\delta_2\dot{y}^3+[1-p\cos(\omega\tau+\delta)](\omega_0^2 x+a_2 x^2+a_3 x^3)$$
$$=e_\omega\cos\omega\tau \quad . \tag{11}$$

Equation (11) represents a forced nonlinear Mathieu equation, characteristic of problems with parametric excitation. Simplified forms of this equation have been extensively studied in longitudinal sea waves. In the case of a beam sea, this mathematical model leads also to a parametric instability related to the onset of a rolling oscillation which is subharmonic 1/2 of the excitation. However, in this paper, we are not concerned with the stability of the solutions of equation (11), but interested in obtaining an upper bound for the amplitude of the rolling oscillations belonging to the stable region

3. MAXIMUM AMPLITUDES

One has the possibility of working with equation (7) in order to obtain simple formulas with the same prediction capabilities. This was done in Refs.[14,15] for a ship in the upright position. The results fit surprisingly well both the numerical calculations and the experimental data. For a heeled ship a similar approach can be adopted. The detailed calculations are close to those shown in Ref.[14].

The equation relating the maximum amplitude of the resonant component of the oscillation to the intensity of the excitation, is expressed by

$$2\omega_0(\mu y_m + \frac{3}{8}\delta_2\omega_0^2 y_m^3) - e_\omega^2 = 0 \quad . \qquad (9)$$

Formula (9) gives the maximum amplitude of the rolling oscillations about the dynamic heel angle, in a first order of approximation. It is of immediate practical interest, giving an improvement of the classical formulas because it takes into account both the linear and the nonlinear damping effects. The quadratic and cubic righting arm nonlinearities do not appear explicitly in this expression. This fact does not invalidate the theoretical predictions, not even in the case where the nonlinearity is rather strong. The nonlinearity of the righting arm is responsible for a bending in the frequency response curve causing the system to be more "sensitive" to the excitation in a frequency range which is wider than that of the linear case. Consequently, it causes a frequency shift in the location of the maximum but does not strongly affect the corresponding maximum amplitude. However, the righting arm nonlinearities can be indirecty introduced in equation (9) through the dependence of the natural frequency on the amplitude, i.e. by means of the formula

$$\omega_m = \omega_0(1 - \frac{3}{8}\alpha_3 y_m^2) \quad , \qquad (10)$$

so rendering slightly more cumbersome the estimation of the maxima.

The theoretical predictions have been compared with the experimental observations carried out on ship models at Southampton University [16]. The model was suitably tethered to restrain it in drift and in yaw, while allowing it to roll, heave and sway. The results indicate that, for the same excitation intensity, the maximum amplitude of the rolling oscillations may assume considerably different values, depending on the direction of the propagation of the waves relative to the initial heel. Unfortunatelly, this effect cannot be explained by means of equation (9), the predictions of which are totally independent on the initial heel. To account for this experimental evidence the rolling equation must be improved, i.e. the coupling between roll and heave motions must be explicitly considered.

4. INFLUENCE OF THE ROLL-HEAVE COUPLING

To include the effect of the roll-heave coupling in the equation of ship motion an explitly time dependent righting moment has been considered by several authors [7,9,11]. This mathematical model is still very simplified, but incorporates sufficient details at this stage of the knowledge and allows a simple approximate analysis. In this case, equation (5) can be written in the following form

$$\ddot{y} + 2\mu\dot{y} + \delta_2\dot{y}^3 + [1 - p\cos(\omega\tau + \delta)](\omega_0^2 x + \alpha_2 x^2 + \alpha_3 x^3) = e_\omega \cos\omega\tau \quad . \qquad (11)$$

Equation (11) represents a forced nonlinear Mathieu equation, characteristic of problems with parametric excitation. Simplified forms of this equation have been extensively studied in longitudinal sea waves. In the case of a beam sea, this mathematical model leads also to a parametric instability related to the onset of a rolling oscillation which is subharmonic 1/2 of the excitation. However, in this paper, we are not concerned with the stability of the solutions of equation (11), but interested in obtaining an upper bound for the amplitude of the rolling oscillations belonging to the stable region

of the ship parameters.

To this end, a perturbative solution has been searched for in the main resonance region. The resulting analytical expression is represented by

$$y(\tau) = C\cos(\omega\tau+\phi) + a_0' + a_2'\cos 2(\omega\tau+\phi) + b_2'\sin 2(\omega\tau+\phi) \quad (12)$$

where

$$a_0' = -\frac{1}{2}a_2\omega_0^{-2}C^2 + \frac{1}{2}pC\cos(\phi-\delta)$$

$$a_2' = \frac{1}{2}a_2(4\omega^2-\omega_0^2)^{-1} - \frac{1}{2}\omega_0^2(4\omega^2-\omega_0^2)^{-1}pC\cos(\phi-\delta)$$

$$b_2' = -\frac{1}{2}\omega_0^2(4\omega^2-\omega_0^2)^{-1}pC\sin(\phi-\delta) \quad (13)$$

The amplitude and the phase of the resonant component show a rather complicate dependence on the model parameters and will not be reported here.

Also in this case a perturbative approximate solution was found for the maximum amplitude, starting from the maximum amplitude of the uncoupled rolling equation. If Y_m is the solution of equation (9) and Y_m' is the maximum rolling amplitude in presence of roll-heave coupling, one can write $Y_m' = Y_m + \delta Y$. With proper mathematical calculations up to the first order of approximation, it results

$$\delta Y = \frac{1}{3}a_2 pe^{-1}\omega^3 Y_m^3(c_3+c_4Y_m^2)(D_1+\frac{3}{4}\hat{a}_3Y_m^2) \times (g_5+2g_4Y_m^2+3g_0Y_m^4)^{-1} \quad (14)$$

Equation (14) explicitly depends on a_2 and thus accounts for a difference in the maximum rolling amplitude of a heeled ship, according to the direction of wave progation relative to the initial bias. The experimental results show that the bias towards waves makes the model much more likely to capsize as compared to a model with zero bias or with a bias away from the wave direction. This accurs even if the maximum rolling amplitudes reached by the model biased towards waves are in all cases lower then those shown by the model biased away from waves. The latter phenomenon is justified in terms of equation (14): since a_2 is usually opposite to x_0, one obtains that $\delta Y<0$ for a ship heeled towards waves and $\delta Y>0$ for a ship heeled away from waves.

5. CONCLUSIONS

The rolling of a heeled ship in a beam sea has been studied by several authors both from an experimental and a theoretical point of view. In these papers, different analytical methods have been applied to modelize the phenomenon which, in several cases, includes also the coupling between roll and heave motions. This explaines quite satisfactorily the experiments. However, the analytical results are always presented in a rather involved form useful for numerical computations only, and are not easily definable in terms of the weights of the many factors influencing the phenomenon.

This paper shows similar results, but they are given in terms of maximum rolling amplitudes and additional bias angle. The simple formulas obtained are useful for handmade computations: they represent therefore an important tool in the preliminary design stage and allow the formulation of stability criteria enlighting the relative importance of the ship parameters.

A comparison of the theoretical predictions with experimental data has been carried out for a ship in upright equilibrium position [15], showing a very satisfactory agreement. At present, similar conclusions cannot be reached for a heeled ship, mainly due to the partly unknown parameters of the tested models and to the scattering of the available data.

APPENDIX

$$D_1 = \omega_0^2 - \omega^2,$$

$$c_3 = \frac{3}{4}\delta_2\omega^3,$$

$$c_4 = 2\mu\omega,$$

$$g_0 = \frac{9}{16}\hat{a}_3^2 + c_3^2,$$

$$g_4 = 2c_3c_4 + \frac{3}{2}\hat{a}_3D_1,$$

$$g_5 = D_1^2 + c_4^2.$$

REFERENCES

1. Kuo, C., "Summary of Stability '82", The Second International Conference on

Stability of Ships and Ocean Vehicles, Tokyo, The Society of Naval Architects of Japan, 1983, pp. 779-787.

2. Jens, J.L.E. and Kobilinsky, L., "IMO Activities in Respect of International Requirements", The Second International Conference on Stability of Ships and Ocean Vehicles, Tokyo, The Society of Naval Architects of Japan, 1983, pp. 751-764.

3. Cardo, A., Francescutto, A. and Nabergoj, R., "Deterministic Nonlinear Rolling: A Critical Review", Bull. A.T.M.A., Vol. 85, 1985, pp. 1-23.

4. Bird, H. and Morrall, A., "Research Towards Realistic Stability Criteria", The Safeship Project: Ship Stability and Safety, The Royal Institution of Naval Architects, London, 1986, pp. 1.1-1.12.

5. Tamiya, S., "On the Characteristics of Unsymmetrical Rolling of Ships", Selected Papers from the Journal of the Society of Naval Architects of Japan, Vol. 4, 1970, pp. 76-95.

6. Wright, J.G.H. and Marshfield, W.B., "Ship Roll Response and Capsize Behaviour in Beam Seas", Transactions of the Royal Institution of Naval Architects, Vol. 122, 1980, pp. 129-148.

7. Feat, G. and Jones, D., "Parametric Excitation and the Stability of a Ship Subjected to a Steady Heeling Moment", International Shipbuilding Progress, Vol. 28, 1981, pp. 263-267.

8. Lee, C.M. and Kim, K.H., "Prediction of Motion of Ships in Damaged Conditions in Water", The Second International Conference on Stability of Ships and Ocean Vehicles, Tokyo, The Society of Naval Architects of Japan, 1983, pp. 287-301.

9. Bass, D.W., "On the Response of Biased Ships in Large Amplitude Waves", International Shipbuilding Progress, Vol. 30, 1983, pp. 2-9.

10. Nayfeh, A.H. and Khdeir, A.A., "Nonlinear Rolling of Ships in Regular Beam Seas", International Shipbuilding Progress, Vol. 33, 1986, pp. 40-49.

11. Nayfeh, A.H. and Khdeir, A.A., "Nonlinear Rolling of Biased Ships in Regular Beam Waves", International Shipbuilding Progress, Vol. 33, 1986, pp. 84-93.

12. Cardo, A., Francescutto, A. and Nabergoj, R., "Ultraharmonics and Subharmonics in the Rolling Motion of a Ship: Steady-state Solution", International Shipbuilding Progress, Vol. 28, 1981, pp. 234-251.

13. Cardo, A., Francescutto, A. and Nabergoj, R., "On Damping Models in Free and Forced Rolling Motion", Ocean Engineering, Vol. 9, 1982, pp. 171-179.

14. Cardo, A., Francescutto, A. and Nabergoj, R., "On the Maximum Amplitudes in Nonlinear Rolling", The Second International Conference on Stability of Ships and Ocean Vehicles, Tokyo, The Society of Naval Architects of Japan, 1983, pp. 93-102.

15. Cardo, A., Francescutto, A. and Nabergoj, R., "Nonlinear Rolling Response in a Regular Sea", International Shipbuilding Progress, Vol. 31, 1984, pp. 204-208.

16. Marshfield, W.B., private communication.

Third International Conference on Stability of Ships and Ocean Vehicles, Gdańsk, Sept. 1986

STAB'86

CAPSIZE PREDICTION USING A TEST-TRACK CONCEPT

E. Deakins, N.R. Cheesley

G.R. Crocker, C.T. Stockel

ABSTRACT

This interim report describes the ongoing work since 1982, at Plymouth Polytechnic, into the probabilistic assessment of vessel safety against capsize in a representative range of likely to be encountered environmental and operating conditions.

The proposed risk framework utilises probabilistic procedures which have recently been applied to operability studies. The method is capable of accounting for variations in seastate, vessel design features and load condition as well as vessel speed and heading subject to master's intervention.

The concept of a test-track is introduced as a means of standardising, particularly for regulatory purposes, the operating scenarios which should be included in any analysis which seeks to predict, in a realistic manner, vessel capsize safety.

The preliminary analysis described utilises a linear superposition technique to predict vessel response and the concept of a "potentially dangerous" roll motion is introduced to avoid the necessity to predict large non-linear capsize roll angles.

This work is affiliated to the United Kingdom Safeship project.

1. INTRODUCTION

Ship stability is a property which is not amenable to simple definition. To naval architects stability means "safety against capsizing" in a very general sense and the development of the underlying theory has had a long period of evolution which is still far from complete. Current international stability criteria can be traced directly to the work, in 1939, of Rahola [34] who proposed that a ship's measure of safety be related to certain properties of still-water righting lever (GZ) curves. However, in recent years it has been argued that these criteria, which neglect the action of the seaway, cannot be a sufficient indicator of vessel capsize resistance in the seaway [9]. Furthermore, it is generally agreed that any new and improved criteria should seek to take account of the variability of the environmental conditions encountered, the vessel's design features as well as the variation in load conditions and master's action [22].

It is in the area of structural design, especially, that there has been a movement away from the deterministic approaches, where satisfactory rules are gradually evolved by a process of trial and error, to one where the variability in the demands made on and the capability of a structural element to resist the load actions imposed is taken into account [12, 38]. In such a probabilistic approach it is recognised that a structural element will have to withstand loads of different magnitude and frequency during its lifetime and similarly that its capability to resist these loads will not have a single deterministic value, Fig 1.

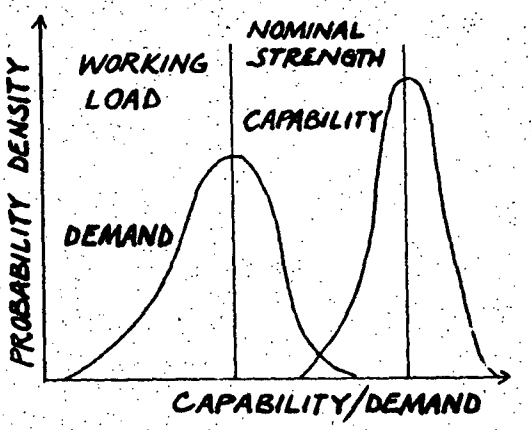

Fig 1
Variation of Demand and Capability of a Structural Element

The problem to overcome in such an approach is to ascertain the nature of the tails of the demand and capability distributions since it is in the overlap region that the comparatively rare high demand and low capability may occur simultaneously to cause failure.

An overall strategy for probabilistic stability assessment, based on modern structural design methods [12] is shown in Fig 1a and this can be compared with the traditional (current) stability assessment.

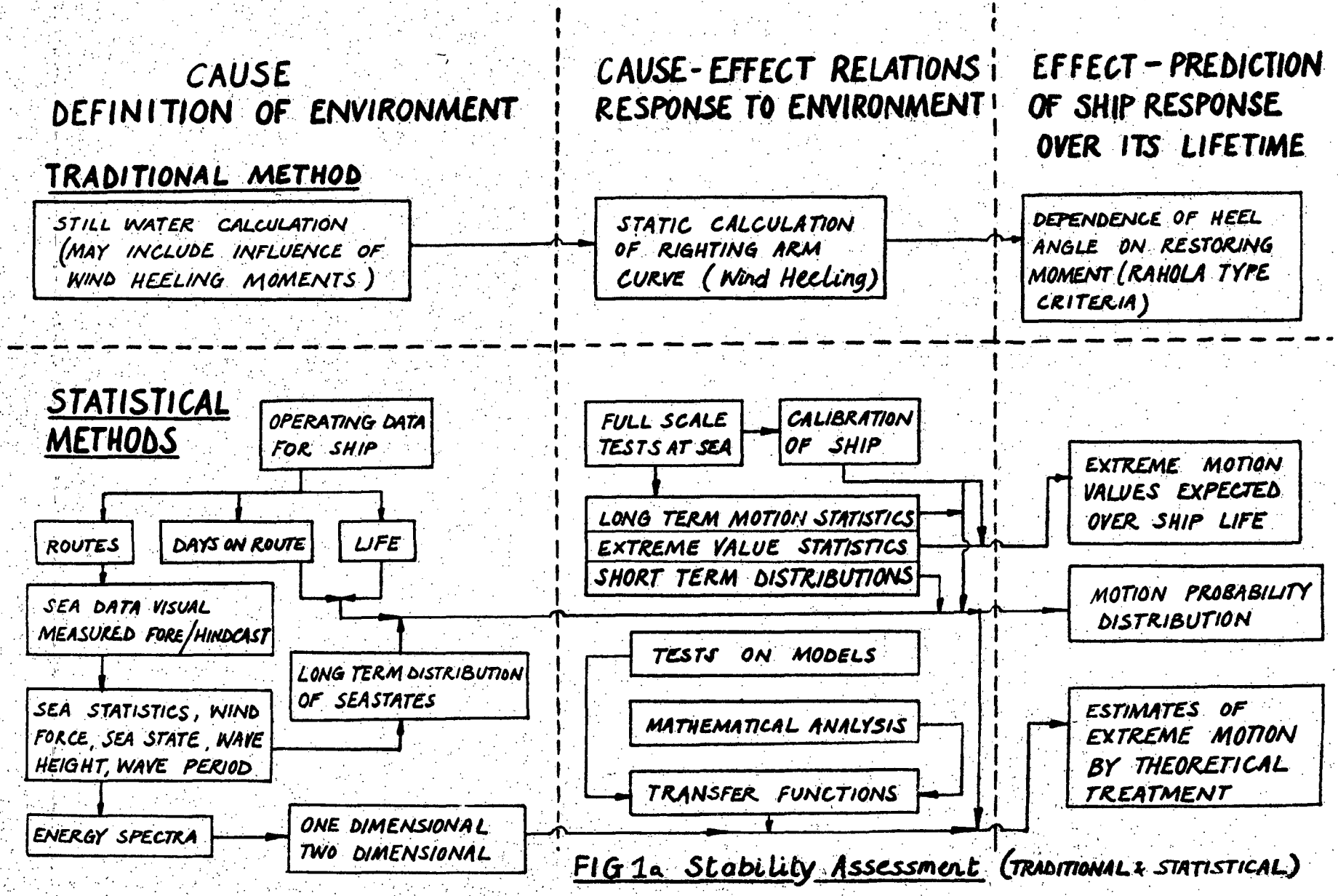

FIG 1a Stability Assessment (TRADITIONAL & STATISTICAL)

As well as being much more extensive, the modern approach features experimental and analytical models backed up by full scale trials where appropriate.

The main purpose of the work at Plymouth is to explore the feasibility of developing and applying such a probability analysis framework as a basis for ship safety from capsize which may lead to improved stability, design and regulation criteria. It is also hoped that the framework will help mesh together the different and often highly individual analytical techniques for modelling the various capsize phenomena, in a concise and efficient manner.

1.1 Assessment of Risk in the Marine Environment

The concept of risk is not new. In many instances where a large body of information exists, based on accident history, an appropriate interrogation of the database can assign the risk of death, injury or other loss involved in partaking of a particular activity, eg, Table 1.

Risk Source	FAFR	
Average for British Industry	4	
Chemical Industry	3.5	FAFR=Fatal
Steel Industry	8	Accident
Fishing	35	Frequency
Coal Mining	40	Rate
Construction Workers	67	= No of
Air crew	250	deaths
Staying at home	3	per 10^8
Driving a car	60	hours of
Rock climbing	4000	risk
		exposure
		[21]

Table 1
Risk levels by Activity

Unfortunately no database currently exists which is capable of providing sufficient detail to assign the probability of an individual vessel's risk of capsize. This is hardly surprising given the nature of a capsizal which is frequently rapid with little resulting casualty wreckage to provide evidence of the likely causes. Whilst some useful information can be obtained from the casualty records, such as the general nature of the capsize and the surrounding circumstances, no suitably detailed information can be obtained regarding the sequence or the probability of causal events which would be particularly useful for a more traditional risk analysis such as "fault-tree" [3].

Even if this information was available it would not be appropriate to extrapolate it to cover many of the unique projects which are undertaken in the marine environment today.

The alternative is to develop an appropriate prediction technique which aims to incorporate that information which is available from casualty records (where it exists) as well as catering for those casualties which nearly occurred ie, the "near misses". Fortunately probability methods have recently been developed [20] which have direct application to the problem of assessing the risk of a vessel capsizing in a seaway. These will now be discussed within the context of application to capsize assessment.

2. THE TEST-TRACK CONCEPT

2.1 Problem Outline

Risk prediction can be generally stated as determining the probability that a pre-assigned event will occur in a number of trials (or over a period of time). This definition is particularly suited to games of chance, to assess the likelihood of obtaining a particular face value of a die, for example, in so many trial throws.

When applying probability concepts to the problem of vessel capsizing, it is more appropriate to consider the probability of a critical roll response being exceeded since this will determine the area of the overlapping tails in Fig 1 ie, the probability that the operational and environmental demands exceed the vessel capability to resist the demands.

In operability-type studies such as fatigue analysis it is necessary to consider every cycle of vessel response during its lifetime since all cycles

contribute to fatigue failure. In (survivability) risk-type studies this is not the case since quite often only the severest seastates will cause the severest motions, and, provided that the relatively rare catastrophic responses in mild seas can be accounted for, this suggests that the amount of computation can be reduced in some way. Obviously, it is not sufficient to seek the 'worst cases' on an ad hoc basis and some ordered approach is desirable.

2.2 Test Tracks and Proving Ground

In an attempt to 'trap' the worst-case scenarios, the proposed method consists essentially of a subject vessel being required to successfully (ie, without capsizing) negotiate a series of "test-tracks" which have been designed to represent the range of critical (potentially capsize causing) scenarios that it will encounter over its lifetime.

In the automobile industry, in particular, this type of procedure is common. A road vehicle is made to perform a series of manoeuvres over varying terrain in a variety of conditions (environmental, load, speed etc) where each test-track represents one such set of conditions. For example there will exist a handling and stability test-track, a steep gradient test-track and so on. The total test-track set is termed the "proving-ground" and its overall nature reflects the vehicle's intended use and type. Thus a sports car will have a different set of test-tracks to negotiate than an articulated lorry, though some will be identical. See Fig 2.

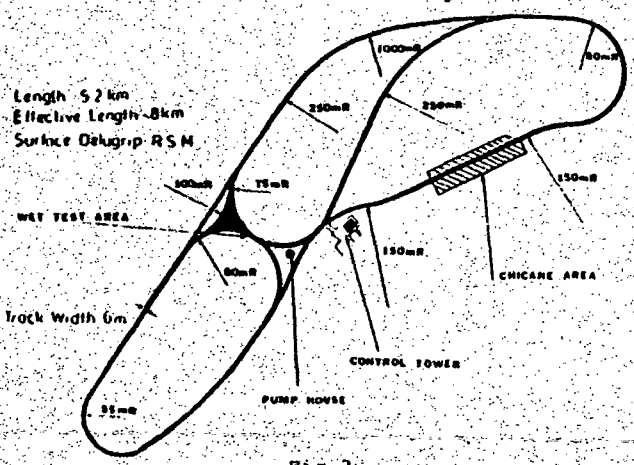

Fig 2
Handling and Stability Circuit at MIRA [40]

The main advantages to the vehicle designer of using this approach are:-

a) The full range of operating conditions, including the very important severe conditions, can be produced in a manner difficult to achieve on the open road, for example, (also making repeatability of results possible).

b) Vehicles are tested under tightly controlled conditions where individual characteristics such as handling can be assessed, in isolation if necessary, and compared against previous and other vehicles' results.

c) Attention is focused on individual elements eg, vehicle suspension settings so that if a poor performance characteristic manifests itself on one particular test-track the design can be precisely retested after suitable modification.

The authors believe that these are valuable procedures which can be used to assess the capability of a seagoing vessel to perform its duty in safety. However, leaving aside the immense difficulty of physical modelling of severe sea conditions, sheer expense would preclude the use of a purely physical marine proving ground for every single vessel. Thus it is envisaged that at first the test-tracks will be largely analytical in nature with some experimental back-up for certain difficult aspects until, as the theory improves, eventually no physical experimentation would be required (?)

For this preliminary investigation and for illustration of the overall 'package' a wholly analytical frequency domain analysis will be used. Obviously this means that certain physical capsize phenomena which may be best suited to time domain analysis (such as the broaching-to phenomenon) will not be modelled and thus the test-tracks will not be fully activated initially. Section 4 addresses the basis for using a linear frequency domain analysis for what are essentially non-linear large angle capsize phenomena.

2.3 Choice of Test-Track

As with the road vehicle case, the vessel type and intended zone or zones of operation dictate the nature of the proving ground, and thus the individual test-tracks, that the seagoing vessel will be required to negotiate successfully. Thus, for example, a vessel which is intended for operation in a sea-area which is well sheltered or has shelter to hand will not have to negotiate the more stringent test-tracks required of a vessel intended for extended operation in high icing latitudes. Indeed, some form of licensing might be desirable for individual operational zones since this would assist in avoiding the potential overdesign or underdesign of vessels which the current 'blanket' regulations may encourage.

A vessel which is intended for international operation would be subjected to the worst possible weather conditions (Appendix 2.2).

By considering individual test-track performance the effect on the performance of design and operational features can be considered in detail whilst overall proving ground performance will allow comparison of total performance and safety levels across a fleet of vessels for example though this "average" value should be treated with caution.

A typical subject vessel can be expected to operate, over its lifetime, in a wide range of environmental and displacement conditions and to be subject to different masters' action. The correct choice of test-tracks to isolate the potential capsize scenarios from amongst all possible operating scenarios encountered by the vessel during its lifetime is vital if certain critical operations are not to be overlooked along the way. Whereas it is computationally desirable that the proving ground should only encompass all of the possible scenarios which could cause capsize, it is obviously not possible to pre-define them, and it is thus necessary to initially consider that all scenarios are potentially capsize causing. However, if an initial assumption is made that only the severest seastates cause the severest responses the amount of computation for any scenario is reduced if the order of severity of seastates to which the vessel is subjected (everything else remaining unchanged) is progressively reduced from the most severe possible in the operating zone under consideration. Once the predicted response level falls below the limiting safe value the computer program moves on to consider the next scenario and so on. (Section 5) The results of Multi-variate (pattern recognition) analysis of casualty date (for the broad vessel type and size) is also used to ensure that no proven (frequently recurring) capsize scenarios have been missed, particularly in mild seas. These positively identified "capsize nuclei" (each one representing a distillation of many similar casualties) form critical scenarios for consideration and are embedded in the test-tracks with respect to time and location. Fig 3.

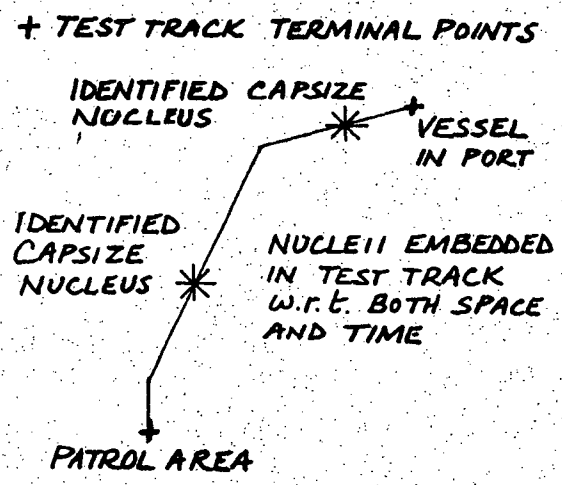

Fig 3
Vessel Steaming to Patrol Area
Test-Track containing 2 identified capsize nuclei

3. APPLICATION OF THE METHOD

3.1 Managing the Lifetime of Risk

The method of handling all the scenarios comprising a lifetime of risk is best illustrated with the aid of an example. The subject vessel being used for the present study is a fisheries protection vessel which has an operational area encompassing the Northern North Sea and North Eastern Atlantic in the region of the 100 fathom line around North West Scotland. There are also occasional sorties of up to

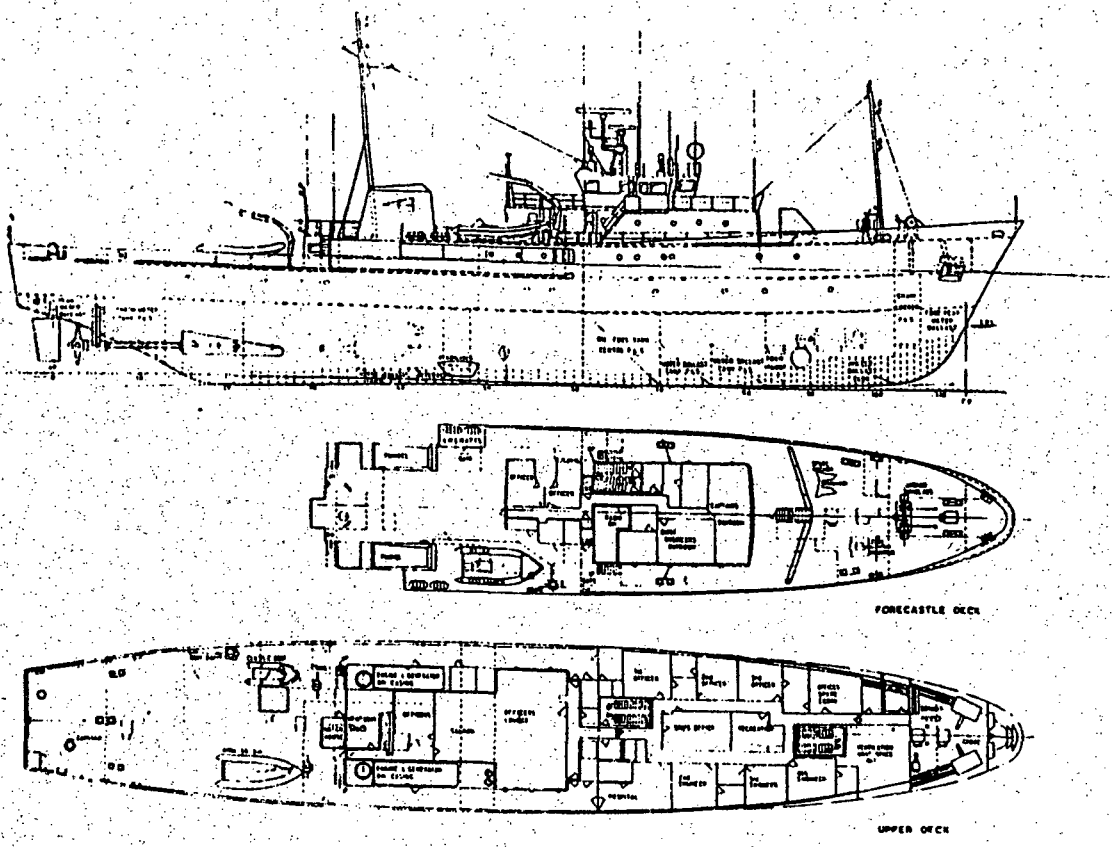

Fig. 4. General Arrangement: Fishery Protection Vessel.

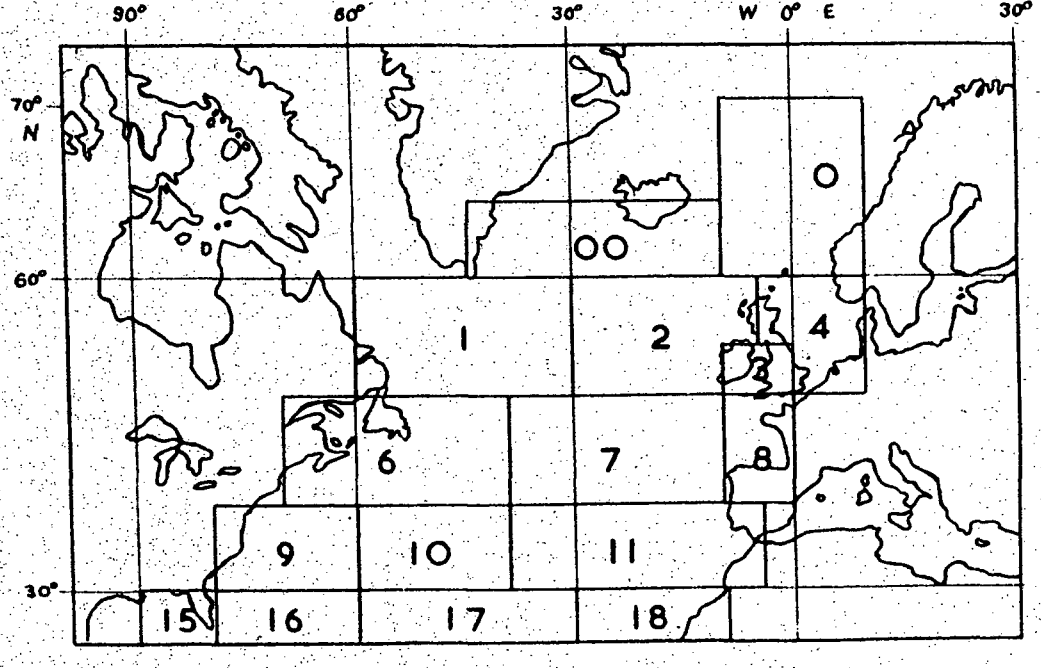

Fig. 5. North Atlantic Basin Climatology Regions [8].

200 miles into the open North Atlantic.

Principal vessel particulars are given in Table 2 and Figure 4 shows the general arrangement.

Length Overall	71.33 m
Length b.p.	64.00 m
Beam mld.	11.60 m
Design Displacement	1532 tonnes

Table 2 - Principal Particulars

The prediction method aims to calculate $P(\phi_c < \phi)$, the cumulative probability of a 'critical roll motion' (ϕ_c) being exceeded, at least once, during the vessels lifetime of operation. This value is of course represented by the proving ground result. Additionally the probabilities of exceedance during certain individual vessel operations, represented by individual test-track results, is being sought.

The 'critical roll motion, ϕ_c' is defined, in the first instance, as the value of roll angle beyond which there is increasing concern that the vessel will be in danger of capsizing. This is referred to as the potentially dangerous roll angle, though it may subsequently be defined to include velocity or acceleration terms. (These aspects are discussed in Section 4).

The cumulative probability $P(\phi_c < \phi)$ can be obtained from a knowledge of the underlying lifetime response probability density function $P(\phi)$. This in turn can be found by taking (ie, computer-predicting) independent trial samples of roll response over the vessels lifetime together with the independent single trial probabilities of occurrence. These independent trial results are then combined using Bernoulli trial procedures, (Appendix 1).

A preliminary analysis is necessary to determine the vessel's intended missions (operating practices and operating areas). For ease of illustration it is assumed that our subject vessel will only ever operate in the sea areas labelled 2 and 4 in Fig 5.

This indicates the boundaries of the sea-areas in the North Atlantic Basin into which the climatology data is divided in Ref [8]. It is assumed that each sea-area has its own distinct climatology and that this is homogenous (uniform) within the area boundaries shown.

Thus the sea-areas 2 and 4 together comprise the proving ground for the subject vessel.

Typical missions identify routes within the proving ground which form the individual test-tracks. One of these is shown in Fig 6.

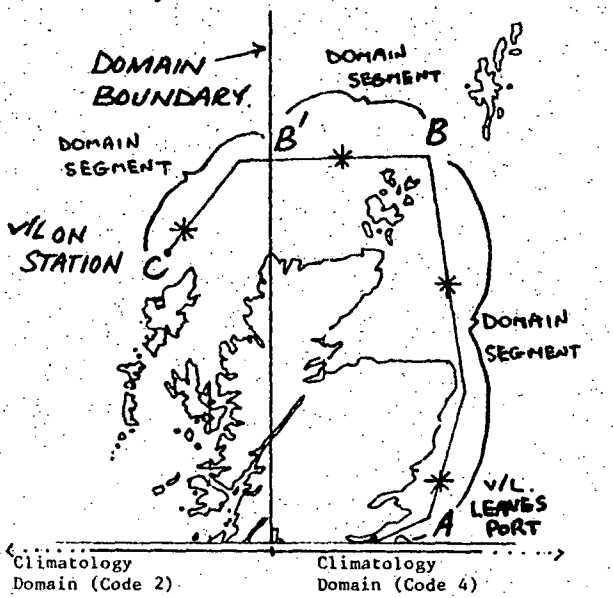

Key: Test-Track = ABB'C

Assumption: Displacement is constant between legs AB and BC. Leg BC crosses the domain boundary at B'. * indicates independent trial sampling points.

Fig 6

Application of the Method

A typical mission is involved in proceeding from the home port (Position A in the Figure) to the patrol area at position C where time is spent on station before returning to A by the same route. It can be seen that the intended track is ABB'C which crosses the domain boundary at B'. Thus the test-track is subdivided into 2 separate spatial domains where the climatology is assumed homogeneous. Each spatial domain is further subdivided into domain segments which are segments along the intended track where the vessel's displacement condition ($\Delta, k_{xx}, k_{yy}, k_{zz}$) can be assumed constant. Thus in Figure 6, between AB and BC the displacement conditions are assumed constant and different. (For convenience, and to facilitate comparison of performance with

the existing stability criteria, the actual load conditions which are used are taken from the vessel's stability booklet to represent the complete range of vessel capability).

3.2 Independent Trial Samples

In order to be able to use the simple procedures, for manipulating probabilities which are given in Appendix 1, for risk and operability studies, it is necessary to ensure that all the predicted responses (trial samples of the underlying lifetime response probability density function) are independent. This necessitates that the response obtained from one scenario shall not have been influenced by any previous responses obtained along a domain segment ie, the response obtained should have no 'memory'.

Thus it is required to know how many independent trial samples of the underlying response distribution can be taken in each domain segment since this has an important bearing on the probabilities obtained (Appendix 1). For this purpose an independence interval was introduced by Hutchison [20]. This 'interval' represents the minimum distance in time and/or space that a vessel must travel before the seastates (and by inference the resulting responses) can be considered independent trial samples of the underlying seastate probability density function. This is an important concept since conditional information concerning the seastate (and thus the responses obtained) at one instant strongly alters the probability distribution for seastates (responses) at nearby times or locations but the influence of the conditional data diminishes as one moves further away in time or space until eventually the underlying seastate (response) probability distribution is again dominant.

Hutchison proposed a simple form of metric for the number of independent ship exposure cycles, N_* where

$$N_* = \sqrt{\left(\frac{T}{T_*}\right)^2 + \left(\frac{VT}{L_*}\right)^2} \qquad [20]$$

where T_* = independence period, hours

L_* = independence distance, nautical miles

T = exposure time, hours

V = average vessel speed

The independence period/distance is the time/distance required between two observations to be independent. See Fig 6. Further work is required in this area but values for the independence period of between 13 and 26 hours have been quoted based on some available seastate process sampling rates on a scale significant to ship routeing [20].

In fact a simpler measure

$$N = \frac{\text{Exposure distance } R}{VT_*}$$

is more appropriate if vessel speed relative to the advancing weather conditions is used.

3.3 Applied Probability Concepts

A particular design which is operating in a domain segment (ie, of a particular load condition) will have a motion response dependent upon the combination of broad factors route, climatology and seamanship. These factors are considered in detail in Appendix 2.

It is apparent that the single trial probability of obtaining a roll response level (ϕ) is equal to the single trial probability of encountering the particular load condition, route, climatology and seamanship giving rise to the response.

Thus the single trial probability of obtaining the predicted roll response ϕ, given the load condition Δ, location L and season S.

$P^1(\phi/\Delta,L,S)$, where P^1 indicates the single trial probability, is equal to the single trial probability of encountered seastate (H_s',T_m,F), relative heading to waves (μ) and speed (V) given load condition (Δ), location (L) and season (S). Thus

$$P^1(\phi/\Delta,L,S) = P^1(H_s',T_m,F,\mu,V/\Delta,L,S)$$

The value of $P^1(H_s', T_m, F, \mu, V/\Delta, L, S)$ is obtained by manipulation of the component probabilities given in Table 3 from Appendix 2. There are several ways of combining these probabilities but in the present study the adopted procedure is as follows:

(a) For a given domain segment ($\Delta, k_{xx}, k_{yy}, k_{zz}$ constant), the relative heading to waves, before any modifying seamanship, is given by $[\mu_o = C - \phi']$ where C is the course and ϕ the predominant wave direction.

Now, the joint probability of seastate, heading, wave spectrum and speed (prior to seamanship) given the location and season is

$$P(H_s, T_m, F, \mu_o, V_o/L, S)$$
$$= P(C, V_o/L, S).P(H_s, T_m, F, \phi/L, S)$$
$$= P(C, V_o/L, S).P(H_s T_m, F, [C - \mu_o]/L, S)$$

(b) Incorporating the avoidance type seamanship $P(H_s'/H_s)$ gives after avoidance:

$$P(H_s', T_m, F, \mu_o, V_o/L, S) =$$
$$P(H_s'/H_s).P(H_s, T_m, F, \mu_o, V_o/L, S)$$

(c) Incorporating the pacifying type seamanship, $P(V, \mu/H_s', T_m, F, V_o, \mu_o)$ yields the required joint probability of seastate, heading and speed (after seamanship action) given the location and season ie,

$$P(H_s', T_m, F, \mu, V/L, S) =$$
$$P(V, \mu/H_s', T_m, F, V_o, \mu_o).$$
$$P(H_s', T_m, F, V_o, \mu_o/L, S) \text{ or}$$
$$P(H_s', T_m, F, \mu, V/L, S) =$$
$$P(V, \mu/H_s', T_m, F, V_o, \mu_o).\ P(H_s'/H_s).$$
$$P(C, V_o/L, S).P(H_s, T_m, F, [C - \mu_o]/L, S)$$

This is the single independent trial probability of obtaining the predicted roll response ϕ resulting from this scenario in a given domain segment for 1 set of conditions. There are many such sets or combinations of conditions which must be considered.

Probability	Description
$P(L,S)$	Joint Probability of V/L location and season
$P(C,V_o/L,S)$	Joint Probability of intended course and speed given the location and season
$P(H_s', T_m, F, \phi/L, S)$	Joint Probability of encountered significant waveheight and mean wave period, wave family spectrum and predominant wave direction given location and season
$P(H_s'/H_s)$	Probability of encountering a seastate of severity H_s' after taking avoidance action given that H_s would have been encountered if no bad weather avoidance had been attempted
$P(V, \mu/H_s', T_m, F, V_o, \mu_o)$	Joint Probability of new speed and new heading to waves after master's alteration in response to excessive motions caused by seastate severity and original speed and heading

Table 3
Component Probabilities used in the Analysis (Appendix 2)

At this stage of combining all the possible combinations, the opportunity is taken to obtain directly the single trial probability of roll angle ϕ exceeding the critical value ϕ_c, $P^1(\phi_c < \phi)$. To every scenario a response level ϕ is predicted, such as the expected maximum roll angle which has a value dependent on the duration of exposure to each seastate, (ultimately the independence period - Appendix A2.4).

If a counting functional is constructed from:-

$$\gamma_\phi = \begin{bmatrix} 1 \text{ for } \phi_c < \phi \\ 0 \text{ otherwise} \end{bmatrix}$$

the cumulative single trial probability of exceeding the critical roll ϕ_c in the domain segment (for a given load condition, location and season) is given by

$$P^1(\phi_c<\phi/L,S) =$$

$$\int_0^{2\pi}\int_0^{\infty}\int_0^{2\pi}\int_{F=1}^{F=f} P(V,\mu/H_s',T_m,F,V_o,\mu_o).P(H_s'/H_s).$$

$$P(C,V_o/L,S).P(H_s,T_m,F,[C-\mu_o]/L,S).\gamma\phi$$

$$d\mu_o,dH_s,dC,dF$$

If required, further counting functionals can be added to this equation, eg:

$$\gamma''_\phi = \begin{vmatrix} 1 \text{ for } \ddot{\phi}_c < \ddot{\phi} \\ 0 \text{ otherwise} \end{vmatrix}$$

would give the cumulative single trial probability of roll angle ϕ exceeding ϕ_c with ϕ roll acceleration $\ddot{\phi}$ exceeding $\ddot{\phi}_c$.

$$P^1(\phi_c<\phi,\ddot{\phi}_c<\ddot{\phi}).$$

The number of independent trials in the domain segment is found from

$$N = \frac{R}{VT_*}$$

where R is the distance along the course track between entrance and exit boundaries of a domain segment eg, distances AB,BB',B'C in Figure 6

V = vessel speed relative to weather speed of advance

T_* = independence period.

Then the probability of $(\phi_c < \phi)$ in N independent trials in the domain segment is given by (Appendix 1):

$$P^N(\phi_c<\phi/L,S) = 1 - [1-P^1(\phi_c<\phi/L,S)]^N$$

Since the $P^N(\phi_c < \phi)$ processes are independent processes in each domain segment L, domain D and season S the probability that ϕ exceeds ϕ_c at least once on a single independent test-track is given by

$$P^1(\phi_c<\phi) = 1 - \left\{\prod_{LDS}[1-P^N(\phi_c<\phi/L,S)]\right\}$$

this is the <u>required single test-track result</u>.

For Q repeated identical test-tracks in a lifetime of operation

$$P^Q(\phi_c<\phi) = 1 - [1-P^1(\phi_c<\phi)]^Q$$

Since the proving ground involves several <u>distinct types</u> of test-track

$$P^{\Sigma Q_i}(\phi_c<\phi) = 1 - \prod[1-P^1(\phi_c<\phi)]^{Q_i}$$

where Q_i = number of test-tracks of type i gives the <u>proving ground</u> result ie, the overall risk that ϕ exceeds ϕ_c for a lifetime of operation.

Thus $P^{\Sigma Q_i}(\phi_c<\phi) =$

$$1 - \prod\left[1 - \left(1 - \left\{\prod_{LDS}[1 - P^N(\phi_c<\phi/L,S)]\right\}\right)\right]^{Q_i}$$

$$= 1 - \prod\left[1-\left(1-\left\{\prod_{LDS}[1-(1-(1-P^1(\phi_c<\phi/L,S))^N)]\right\}\right)\right]^{Q_i}$$

where $P^1(\phi_c<\phi/L,S) =$

$$\int_0^{2\pi}\int_0^{\infty}\int_0^{2\pi}\int_{F=1}^{F=f} P(V,\mu/H_s',T_m,F,V_o,\mu_o).P(H_s'/H_s).$$

$$P(C,V_o/L,S).P(H_s,T_m,F,[C-\mu_o]/L,S).\gamma\phi\ d\mu_o,dH_s,dC,dF$$

4. <u>SCOPE OF THE PRESENT WORK</u>

The previous section has outlined the method of manipulating probabilities of independent response samples so that the probability of exceeding, at least once, a critical roll motion can be found for each of the test-tracks and the proving ground.

Of equal importance is the prediction of the motions themselves in what is essentially a large angle non-linear phenomenon.

Poor stability (operational or icing effects)
Wave amidships causing stability loss
Mathien effect (periodic resonance with waves)
Broaching-to (directional instability in following waves)
Heavy seas from one side
Breaking Waves
Cargo Shift
Water on Deck

<u>Table 4 [39] Capsize Phenomena</u>

Investigations of casualty data and experiments with scale models has led to the categories of capsize shown in Table 4. Especially for smaller vessels physical wave effects can be critical, especially in some local conditions which may be encountered off the Norwegian coast for example [39].

It follows that every test-track segment should be analysed to take account of all possible capsize phenomena, especially when smaller vessels are under investigation. Consideration should also be given to the possibility of one phenomenon giving rise to another eg, heavy seas from one side causing cargo shift. This would lead to the ideal demand/capability assessment of Figure 7 which is necessarily a mix of analytical techniques (time domain and frequency domain) and experimental techniques at this time. The largest roll motion obtained from all these procedures would be carried forward in the calculation. However in these early stages, for illustration, only certain of the capsize phenomena are being investigated, through the use of the linear superposition theory. The basis for this choice is now explained.

4.1 The Potentially Dangerous Roll Angle

When a vessel capsizes, from whatever cause, it assumes a large angle of inclination from which it cannot recover. It follows that the measure of the vessel's overall capsize safety should be its capability to resist this ultimate roll motion during its lifetime. This requires a reliable method for predicting the large roll angles which can properly handle the non-linear nature of the roll damping and restoring moments as well as the important coupling of roll, sway, yaw motions giving rise to considerable roll motion damping. In addition, for risk analysis purposes, the method should ideally be capable of taking account of the key parameters such as the environment, speed and heading to waves as well as changes in hull form and load condition. A method which could also simultaneously predict pitch and heave motions would be particularly useful in a computer simulation because the magnitude of the vertical motion and acceleration together with associated physical phenomena such as slamming may cause the master to change speed/heading to seek acceptable motion limits.

Unfortunately such a general theory for non-linear system response to stochastic processes which is suitable for a risk analysis does not currently exist. Methods which are available tend to either give accurate prediction of uncoupled large roll angles for an intact vessel stopped in beam seas, for example [35] or else to have the scope for a risk analysis study but not the capability to predict the large roll angles. The linear superposition principle of St Denis and Pierson [16] falls under the latter category. Whilst it can give reasonably good results for coupled pitch and heave motions the prediction of large amplitude coupled lateral motions is less satisfactory because of the inherent motion non-linearities.

Thus a further important feature of the present analysis is that the prediction of the actual large angle capsize is not attempted per se. Instead a lesser roll angle termed the "potentially dangerous roll angle" is chosen beyond which it is assumed that a capsize is likely. Thus the potential for disaster is being predicted rather than the disaster itself. This novel approach can be justified for the following reasons:-

a) Long before the vessel reaches its capsize angle there is often great likelihood of cargo shifting.

b) Simultaneously there is great likelihood of water downflooding as well as water trapped on deck.

This would necessitate the accurate prediction of large angle damage stability and roll taking account of possible cargo shifting effects and water on deck and further complicated by large changes in hydrodynamic coefficients as the deck edge is immersed. Until such methodologies become available, it is proposed that the linear theory be stretched to the limit of its capabilities in order to estimate the occurrence of a roll motion judged "potentially dangerous".

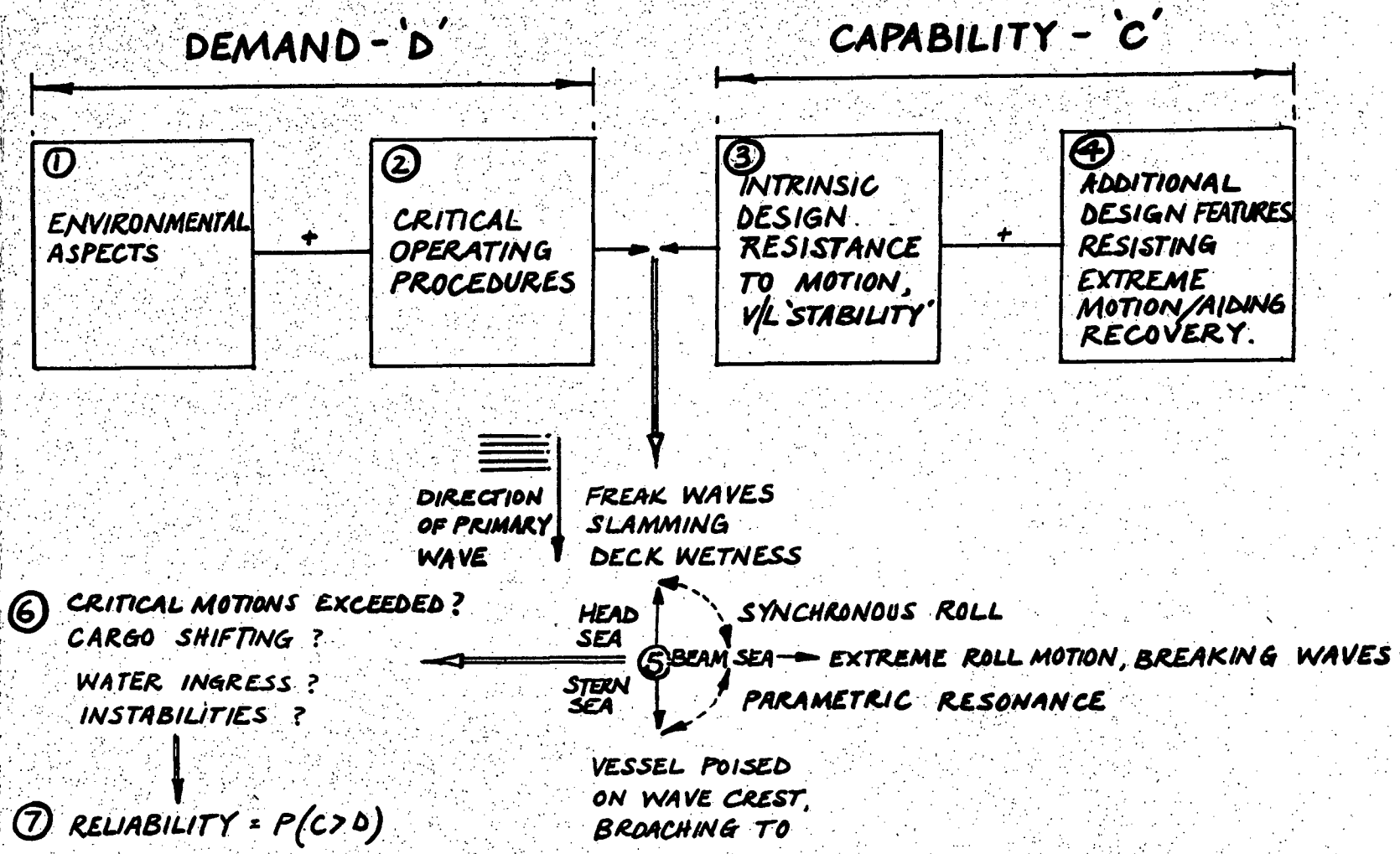

FIG 7 : VESSEL DEMAND & CAPABILITY

Based on discussions and correspondence with fleet operators and serving commanding officers [33] an angle from the upright of 30 degrees has been selected for the subject vessel (length of 60 m) as the potentially dangerous roll angle. This does not imply that when a vessel rolls to 30 degrees it will capsize. It does, however, reflect the view that beyond this angle there is increasing cause for concern by the vessel operators and that a vessel "regularly" rolling to 30 degrees and beyond should be considered suspect. This would be reflected in a high probability of 30 degrees being exceeded in a particular operational scenario. Through the SAFESHIP project Brook [11] has demonstrated that, provided the righting lever curve is approximately linear to the angle in question it is more important, for roll prediction, to include coupled motions through linear theory rather than to use an uncoupled non-linear prediction method. He also demonstrated that in some cases the coupled-linear roll angles were greater than the coupled non-linear roll angles and sometimes less. (See Table 5)

Wave Direction	30 degrees		
Ship	1	2	3
	ϕ max 2 hrs		
Coupled, Non-linear	18.1	11.7	9.9
Coupled linear	14.6	9.1	7.2
Uncoupled Non-linear	-	-	-

Wave Direction	90 degrees		
Ship	1	2	3
	ϕ max 2 hrs		
Coupled, Non-linear	34.3	19.0	21.7
Coupled linear	40.5	16.2	26.0
Uncoupled Non-linear	25.2	54.2	5.2

Ship 1 = Offshore Supply V/L (53 m)
Ship 2 = Stern Trawler (60 m)
Ship 3 = Coastal Tanker (67 m)

Table 5 from Ref [11]

The linear nature of the subject vessel's GZ curve is illustrated in Fig 8 for angles up to well in excess of 30 degrees.

It is envisaged that in due course better motion prediction methods, having the required scope for risk studies, will become available and the linear spectral analysis used in this work will be superseded. This argument will not be pursued here any further since the primary aim of this work is to synthesise the components of demands made on the vessel and the capability of the vessel itself, where the demand and capability is constantly changing over the vessel's lifetime.

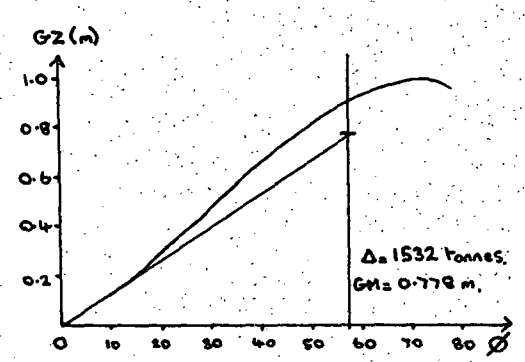

Fig 8

GZ curve - Fisheries Protection Vessel

5. THE COMPUTER SIMULATION

The foregoing sections have outlined how the probability of exceeding a "potentially dangerous" roll motion can be estimated, making use of independent (Bernoulli) trial concepts. It has also been proposed that every vessel be subjected to a set of (mostly) analytical test-tracks which together comprise the proving ground appropriate in nature to the vessel being considered. This aspect is particularly suited to regulatory purposes where vessels are subject to standard procedures and assumptions.

Work is continuing on the computer program which is required for implementation of the method; however Figure 9 indicates the overall extensive nature of the program as far as it can be envisaged at this time. The figure

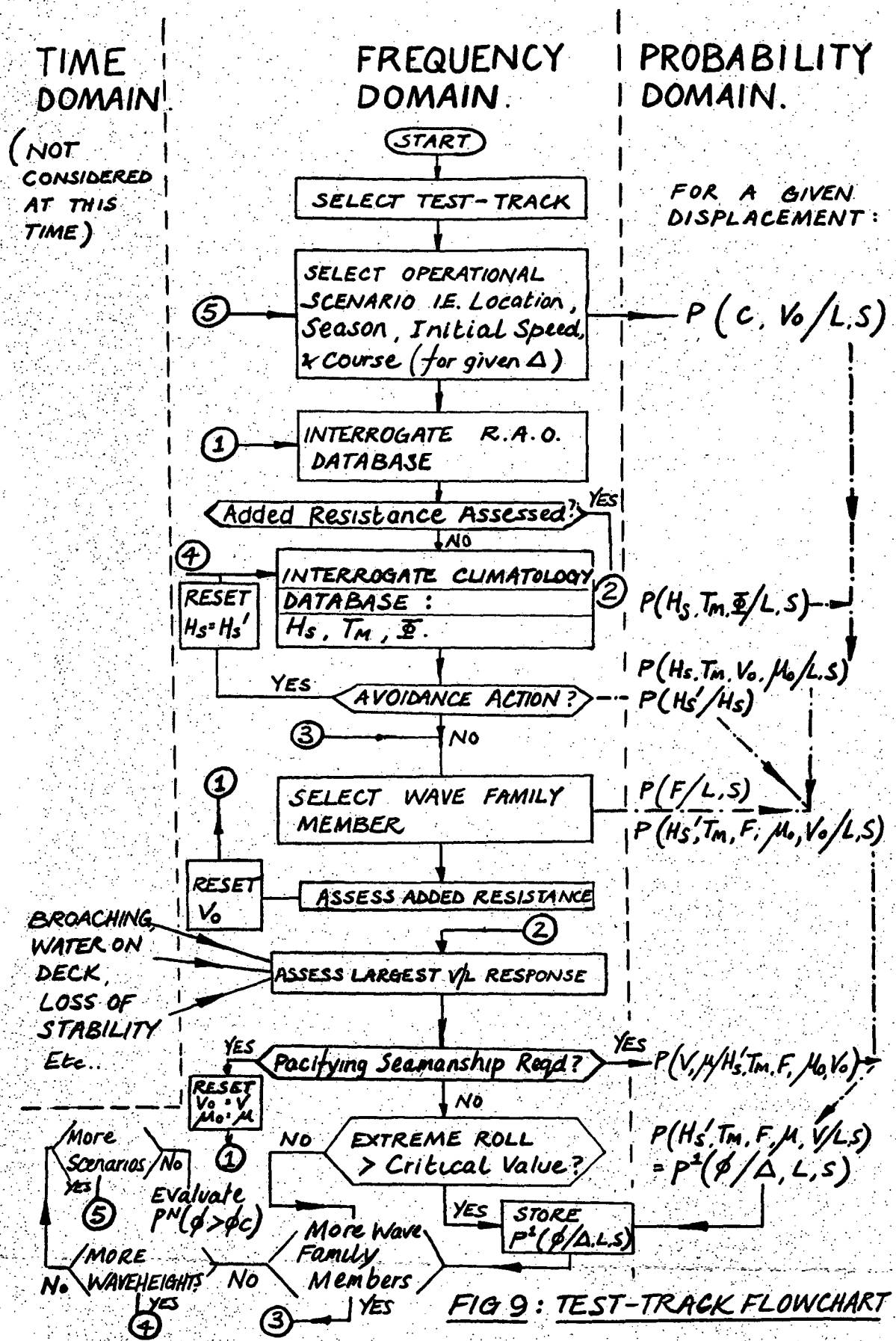

FIG 9: TEST-TRACK FLOWCHART

illustrates how a complete study would seek to encompass the time, frequency and probability domains though only the frequency and probability aspects are being considered in the present study.

The figure also indicates to which stages in the frequency domain calculation the component probabilities relate. Essentially the computer simulation reduces to the manipulation of 3 databases containing climatology, component probability and complex functioned response amplitude operator information respectively. An important feature of the RAO database is that it reflects the sensitivity of motion response to internal ship parameters such as hull form and load condition as well as to external parameters such as encountered wave conditions [36] for example.

Once a particular scenario has been established ie, the load condition and intended speed and heading for a particular location and season, the appropriate climatology and RAO information is combined to assess the degree of added resistance in waves once any avoidance seamanship (Appendix A2.3) has been carried out. With new vessel speed as argument the vessel's vertical responses are predicted and scrutinised for resulting severe motions and sealoads which are likely to cause the master to alter speed or heading (Appendix A2.3).

If these motions perceived by the master are acceptable the extreme roll response is then evaluated (Appendix 2.4). However, in the event that critical motions are exceeded the heading and/or speed is varied (conducive with best progress in the desired direction) until the perceived motions are again within acceptable limits. The vessel may have to assume a hove-to attitude at this time but in any event the roll response is still evaluated, taking account of the exposure time to each scenario through the use of the independence period (Appendix 2.2).

Provided that the roll motion is larger than the potentially dangerous value the scenario probability is carried forward for inclusion in the calculation to find the cumulative probability of critical motion exceedance, as outlined in Section 3.3. Thus the prediction method proceeds through all possible combinations of:-

a)	Wave spectrum family members	(max. 11)
b)	Courses	Heading to waves (7)
c)	Wave primary heading	
d)	Significant waveheight	(10)
e)	Modal period	(10)
f)	Speeds	(10)
		£77,000

for a given single load condition, location and season.

It is apparent that the amount of computation for the several required load conditions, locations and seasons is potentially enormous, and while this can be reduced (from 77,000 to about 8,000) by excluding certain physically impossible seastates and by assuming that responses vary linearly with significant waveheight for the same modal period, on the other hand these aspects also introduce their own data handling difficulties.

At the present time the main calculation has not been carried out, thus it is difficult to make estimates of the eventual computing requirements. However, a recent roughly equivalent operability study [5] used about 2 hours of mainframe computer time for around 1,300 calculations the cost of which can be expected to fall as the processing capabilities of computers continue to increase. It should be emphasised that this is a once-only survivability calculation which it is being proposed should be carried out in the design stages before a vessel is even launched. No further assessment would be required unless the vessel is subsequently required to operate in different geographical zones or it undergoes alterations which materially affect its response to waves.

6. SUMMARY AND REQUIRED FURTHER WORK

In any engineering enterprise, particularly where human life is exposed to dangerous conditions, it is the responsibility of the designer as well as the statutory authorities concerned to ensure that the vehicle, structure etc, is

safe, judged by the scientific knowledge of the day.

In this interim report a procedure has been outlined, which is intended as a once-only calculation, to evaluate by using independent (Bernoulli) trial concepts the probability that a "potentially dangerous" roll motion will be exceeded at least once in a series of typical missions (test-tracks) which have been identified as being representative of a vessel's operating lifetime.

In the present pilot study the interpretation of the term 'test-track' is that it represents an identified typical mission of the subject vessel. This is necessary because it is not known à priori which scenarios could cause capsizing and thus the marine equivalent of the automobile test-tracks, where individual characteristics are exclusively tested, are not derivable (until, possibly, experience has been gained with the method). However, while this causes difficulty at present for novel vessel types, the proposed present analysis is able to incorporate specific scenarios which historic casualty data have indicated as frequently recurring and potentially capsize causing. (using pattern recognition analysis)

It is felt that, while the results obtained are not likely to be mathematically rigorous, the proposed overall framework is of vital importance since:-

a) The problem of vessel capsizing is a pressing one which cannot wait until every aspect of every analytical technique has been perfected.

b) There exists a patchwork of analytical and experimental techniques for predicting the various capsize phenomena and these ultimately need to be fitted into an overall risk framework.

c) Lack of mathematical rigour does not prevent the results generated being used in a comparative manner in these early stages.

d) It will highlight areas for further research.

Thus the proposed method is primarily a framework for evaluating, in a realistic manner, the effects of the variation in demand and capability which will enable the comparative risk of a critical roll motion being exceeded while accounting for likely operational scenarios. There are 6 basic elements to consider:-

(i) Identify the critical scenarios which give rise to large roll motion and possible capsize.

(ii) Assign the probability of encountering each of the critical scenarios which have been identified in (i).

(iii) Predict the 6 degrees of freedom motion response for each operational scenario.

(iv) Manipulate scenario responses and associated probabilities using independent (Bernoulli) trial procedures to find the probability that a critical roll response will be exceeded at least once during an individual typical mission as well as during a lifetime of operation.

(v) Compare the probabilities obtained against an accepted risk level.

(vi) Adjust the operational procedures and/or the design to improve the risk levels (if necessary).

Unfortunately the procedure raises more questions than it answers. Given that a full treatment, as proposed, would reflect the risk of a large roll motion being exceeded by all of the mechanisms which have been identified eg, broaching-to, Mathien effect etc, etc, there still remain some fundamental unanswered questions which would form research projects in their own right, eg:

(i) Is roll angle alone a sufficient description of the capsize potential?

(ii) What assurance against capsize risk is acceptable to the industry since perfect safety is not possible?

(iii) How may the risks be reduced to the acceptable standard?

(iv) Can the method yield a set of stability criteria as simple to enforce as those currently in use?

A large angle prediction method to incorporate all of the non-linearities and to take account of the associated dynamic effects will probably be a long time coming. Thus, it is particularly important that a method which seeks to predict the onset of capsize has a proper measure of potentially dangerous motion which may contain velocity and/or acceleration terms. The illustration of such a joint probability process is shown in Fig 10. (By assuming narrow bandedness of the response the roll angle, velocity and acceleration can be shown to be independent processes and the probability of a critical angle/velocity combination being exceeded can thus be deduced. This is represented by the shaded portion in Fig 10).

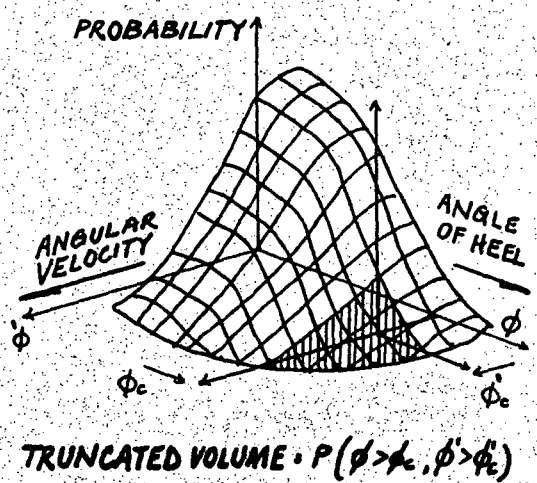

Fig 10

Unfortunately little is known about what the critical values of velocity/acceleration should be. Whilst it is reasonably possible to set limiting acceleration values, for example on the cargo lashings, it is no simple matter to do the same for bulk cargoes let alone to consider sliding 'liquefaction' instability of damp fine grained minerals for example [17].

Assuming that the capsize phenomenon can be quantified the issue of acceptable risk levels is a vexing one. Essentially the analysis of costs versus benefits, such a measure of acceptable risk seeks to incorporate the 'value' of a human life [21] and to assess how an individual accepts risk whether consciously or unconsciously. It seems reasonable that a starting point is to demonstrate that an individual's risk of fatality has been reduced by appropriate measures which arise from the type of analysis proposed, without involving oneself in absolute values of risk (provided that they are comparable with the majority of current 'equivalent' industrial risks). In any event absolute safety cannot ever be guaranteed and an appropriate acceptable risk level is needed as the measure of survivability.

Ultimately, through refinement of the method it may be possible to formulate a set of stability criteria which take realistic account of the environmental and operational variations and yet are as simple to apply as the current regulations. However, simplicity of application is no longer a strict necessity given the potential speed and capacity of the new generation of parallel-processor computers, and thus a standard agreed procedure would seem most appropriate for future stability requirements (with an appropriate risk of capsize as the desirable aim). Indeed it is more important that one builds into the procedure the experience of serving ship's officers and crews.

The proposed method is very much a first attempt and contains many areas for further research. In addition to the obvious uncertainties inherent within the motions prediction there is also uncertainty regarding the value of the independence period T_* which determines the number of independent trials, N_* in a domain segment and thus the probabilities obtained.

Finally, although the method is initially being applied to a 64 m fisheries

protection vessel it is actually suitable for any fixed or moving ocean vehicle or structure. Perhaps one day these might even individually be licensed to operate in specific areas with known risk levels from both an operability and survivability point of view.

AUTHORS

E. DEAKINS, B.Sc. (Hons.)
Lecturer, Department of Marine Technology.

N.R. CHEESLEY, B.Sc., M.Sc., C.Eng., M.R.I.N.A.
Principal Lecturer, Department of Marine Technology.

C.T. STOCKEL, B.Sc., Ph.D., M.B.C.S., M.R.I.N.
Principal Lecturer, Department of Computing.

G.R. CROCKER, B.Sc., Ph.D., F.S.S.
Lecturer, Department of Mathematics and Statistics.

All authors from PLYMOUTH POLYTECHNIC.

NOMENCLATURE

C	Vessel (true) course
D	Domain
F	Wave spectrum family member
H_s, H_s'	Significant Waveheight before/after avoidance seamanship
k_{xx}, k_{yy}, k_{zz}	Radius of gyration with respect to axes
L	Geographical location
L_*	Independence distance
N, N_*	Number of independent trial samples
Q	Identical test-track number
R	Domain segment length
S	Season
T, T_*	Independence period
T_m	Mean wave period
V_o, V	Ship speed before/after pacifying seamanship
$\gamma_\phi, \gamma''_\phi$	Counting functional with respect to roll angle/acceleration
Δ	Displacement
μ_o, μ	Relative heading to waves before/after pacifying seamanship
σ	Random variable
σ_c	'Critical' random variable
ϕ, ϕ', ϕ''	Roll angle/velocity/acceleration
$\phi_c, \phi_c', \phi_c''$	Critical (potentially dangerous) roll angle/velocity/acceleration
Φ	Predominant wave direction
$P(\sigma)$	Probability density
$P^1(\sigma)$	Single independent trial probability
$P^N(\sigma)$	Multiple independent trial probability
$P^1(\sigma_c<\sigma)$	Cumulative single trial probability of $(\sigma_c<\sigma)$
$P^N(\sigma_c<\sigma)$	Cumulative multiple trial probability of $(\sigma_c<\sigma)$

REFERENCES

(1) Aerttsen, G et al;
"Service Performance and Seakeeping Trials on Two Conventional Trawlers". Trans NEC 1965.

(2) Aerttsen, G;
"Service Performance and Seakeeping Trials of MV Jordaens". Tran RINA Vol 108, 1966.

(3) Aldwinckle, D S et al;
"Reliability and Safety Assessment Methods for Ships and Other Installations", Lloyds Register of Shipping Report No 82, 1983.

(4) Andrew, R N et al;
"Full Scale Comparative Measurements of the Behaviour of Two Frigates in Severe Head Seas", Trans RINA, Vol 123, 1981.

(5) Andrew, R N et al;
"The Assessment of Ship Seakeeping Performance in Likely to be Encountered Wind and Wave Conditions", Intl Symp on Wave and Wind Climate Worldwide, RINA 1984.

(6) Andrews, K S et al;
"Wave Climate Synthesis", NMI Report R149, January 1983.

(7) Baitis, A E et al;
"Human Factors Considerations Applied to Operations of the FFG8 and Lamps Mk III, ASNE Day 1984.

(8) Bales, S et al;
"Standardized Wave and Wind Environments for NATO operational areas", DTNSRDC Report SPD 0919-01 July 1981.

(9) Bird, H et al;
"State of Art; Past, Present and Future", Intl Conf on Stability of Ships and Ocean Vehicles, Glasgow 1975.

(10) Bledsoe, M D et al;
"Seakeeping Trials on Three Dutch Destroyers", Trans SNAME, Vol 68, 1960.

(11) Brook, A K;
"A practical assessment of the rolling behaviour of ships at the design stage and in service", BSRA Contract Report W1067 (Confidential).

(12) Caldwell, J B;
"The Theory and Synthesis of Thin-Shell Ship Structures".

(13) Chatfield, C;
"Statistics for technology", Chapman and Hall (publ) 1981.

(14) Chazal, E A;
"Status Report on the Application of Stress and Motion Monitoring in Merchant Vessels", SNAME STAR Symp 1980.

(15) Conolly, J E;
Standards of Good Seakeeping for Destroyers and Frigates in Head Seas", Intl Symp Dynamics of Marine Vehicles in Waves, Inst Mech Eng, 1975.

(16) St Denis, M et al;
"On the Motions of Ships in Confused Seas" Trans SNAME 1953.

(17) Green, P V et al;
"Behaviour of Damp Fine-grained Bulk Mineral Cargoes", Trans (TM) Inst Marine Engineers, 1981.

(18) Hogben, N et al;
"Ocean Wave Statistics", HMSO, London 1967.

(19) Hosodo, R et al;
"A Method for Evaluation of Seakeeping Performance in Ship Design Based on Mission Effectiveness Concept".

(20) Hutchison, B L;
"Risk and Operability Analysis in the Marine Environment", SNAME (Trans) Vol 89, 1981.

(21) Jenssen, T K;
"Risk Criteria for marine and related activities", Det Norske Veritas Technical Report 76-240, 1976.

(22) Kastner, S;
"Simulation and Assessment of Roll Motion Stability", 2nd Intl Stability Conference, Tokyo, 1982.

(23) Kehoe, J W;
"Destroyer Seakeeping - Ours and Theirs", Proc US Naval Inst 1973.

(24) Lloyd, A R J M et al;
"Criteria for ship speed in Rough Weather", 18th Am Towing Tk Conf Vol 2, 1977.

(25) Lloyd, A R J M;
"Ship Motions, Wind and the Helicopter", Symp on Helicopters and the Marine Environment, Royal Aeronautical Society. June 1982.

(26) Maruo, H;
"The Excess Resistance of a ship in a rough sea" Intl Shipbuilding Progress, Vol 4, No 35, 1957.

(27) Ochi, M K;
"On Prediction of Extreme Value", Jnl of Ship Research, Vol 17, 1973.

(28) Ochi, M K;
"Prediction of Slamming Characteristics and Hull Responses for Ship Design", Trans SNAME, Vol 81, 1973.

(29) Ochi, M K;
"Wave Statistics for the Design of Ships and Ocean Structures", Trans SNAME, Vol 86, 1978.

(30) Ochi, M K et al;
"Effect of Various Spectral Formulations in Predicting Responses of Marine Vehicles and Ocean Structures", 9th OTC, Houston, 1977.

(31) Ochi, M K;
"A Series of Jonswap Wave Spectra for Offshore Structure Design", 2nd Intl Conf on Behaviour of Offshore Structures, London, 1979.

(32) Ochi, M K;
"On 6-parameter wave spectra", Proc 15th Conf on Coastal Engineering, 1976.

(33) Personal Correspondence;

(34) Rahola, J;
"The Judging of the Stability of Ships" and the Determination of the Minimum Amount of Stability PhD Thesis, Helsinki, 1939.

(35) Roberts, J B et al;
"A Probabilistic Model of Ship Roll Motions for Stability Assessment", Intl Conf on the Safeship Project, RINA June 1986.

(36) Schmitke, R T;
"The Influence of Displacement, Hull Form, Appendages, Metacentric Height and Stabilization on Frigate Rolling in Irregular Seas" SNAME STAR Symp, June 1980.

(37) Schoenberger, R W;
"Subjective Response to Very Low Frequency Vibration", Aviation, Space and Environmental Medicine. June 1975.

(38) Stiansen, S G et al;
"Reliability Methods in Ship Structures", RINA 1979 Spring Papers.

(39) Varheim, R et al;
"Small Cargo Vessels which have capsized in Heavy Weather", Seminar on Norwegian "Ships in Rough Seas" (SIS) Project, RINA (publ) 1982.

(40) Williams, A R et al;
"The Design and Use of the Dunlop/MIRA handling and stability circuit" Conference on Road Vehicle Handling, Nuneaton 1983.

APPENDIX 1: INDEPENDENT (BERNOULLI) TRIAL CONCEPTS

a) Independence of samples or random processes is an important concept. Independence can be defined as existing if either of the following two conditions are satisfied [13]:-

i) $P(A/B) = P(A)$ [and $P(B/A) = P(B)$]

is the probability of A given that B has already occurred is the same as the probability of A regardless of whether B has occurred.

ii) $P(A,B) = P(A).P(B)$

ie, the joint probability of A and B occurring is the product of the probabilities of A and B occurring separately.

Another way of looking at (i) is that for an independent trials process the sampling process does not alter the underlying probability for the next individual trial, thus knowing that an event has occurred has no bearing on the next event to occur.

b) In general, the probability of at least one event (σ) in N independent trials is

$$P^N(\sigma) = 1 - [P^1(\phi)]^N$$

where $P^N(\sigma)$ = probability of at least one event σ in N independent trials. $P^N(\sigma)$ varies not quite linearly with the value of N [20].

$P^1(\phi)$ = probability of <u>not</u> obtaining the event σ on a single independent trial.

Specifically, when considering the probability of roll motion (ϕ) <u>exceeding</u> a critical value (ϕ_c) in N independent trials.

$$P^N(\sigma_c<\sigma) = 1 - [P^1(\sigma_c>\sigma)]^N$$

$$= 1 - [1-P^1(\sigma_c<\sigma)]^N.$$

APPENDIX 2: FACTORS FOR CONSIDERATION

Fundamentally each test-track reduces into the four considerations of Route, Climatology, Seamanship and Response. A full treatment of these aspects is beyond the scope of the present work. However, an underlying aim is to render them useful for regulatory purposes, through simplification without undue loss in realism.

A2.1 Route

The route embodies consideration of geographical location (L), season (S), initial or intended course (C) and initial speed (V_o). The problem of determining the route is to determine the joint probability distribution of the location, season, initial course and initial speed ie, $P(L,S,C,V_o)$.

Consideration of the test-track segment being used will govern the joint probability of location and season, $P(L,S)$ where L is actually representing a distance along the vessels intended track for which the displacement condition ($\Delta, k_{xx}, k_{yy}, k_{zz}$) can be assumed constant. The test-track segment also governs the conditional probability distribution of initial course and speed given the location and season, $P(C,V_o/L,S)$.

Then the required probability

$$P(L,S,C,V_o) = P(C,V_o/L,S).P(L,S).$$

A2.2 Climatology

This aspect is of vital importance in the analysis and, despite increased effort, is still far from resolved. It is required to determine the conditional probability of significant waveheight (H_s), mean wave period (T_m), wave spectrum family member (F) and predominant wave direction (ϕ) given a location (L) and season (S) ie,

$$P(H_s,T_m,F,\phi/L,S) = P(F/L,S).P(H_s,T_m,\phi/L,S).$$

The necessary climatological data, $P(H_s,T_m,\phi/L,S)$ are to be found in many formats and in many sources [6, 8, 18]. Reference [8] is an extensive database which is convenient and has been chosen for use in the present study. It contains climatological data for different geographical areas and seasons of the year. An important recent development has been a method for correcting the masses of raw visual observations held in many meteorological archives [6].

A further consideration is how realistic are the predicted responses if we use the commonly available simple spectral formulations such as Pierson-Moskowitz, Bretschneider's two-parameter, Darbyshire's fetch-limited etc, which have been developed for some idealised conditions? In reality the shape of wave spectra observed in the ocean varies considerably (for the same waveheight) depending upon the geographical location, duration and fetch of wind, stage of growth and decay of a storm, and existence of swell.

Unfortunately data is very scarce regarding the occurrence and severity of severe seas and this data is particularly important in an extreme risk analysis. Ochi [29] presents a method to estimate the frequency of occurrence of seas of various severity from available data based on the underlying probability function. He also presents a method to predict the severest sea condition likely to be encountered.

In order to cover a variety of spectral shapes which a vessel may encounter in her lifetime two families of wave spectra are used in the present work. One of the familes consists of 11 members for an arbitrarily specified sea severity and is called the Ochi-6 parameter wave spectral family.

$$\Phi\zeta(\omega) = \frac{1}{4}\sum_j \frac{\left[\frac{4\lambda_j+1}{4}\cdot\omega_{mj}^4\right]^{\lambda_j}}{\Gamma(\lambda_j)}\cdot\frac{H_{s\,j}^2}{\omega^{4\lambda_j+1}}\cdot e^{-\frac{(4\lambda_j+1)}{4}(\omega_{mj}/\omega)^4}$$

where j = 1,2 stands for the lower and higher frequency components respectively.

An example is given in Fig 11 for a significant waveheight of 3 m using the values, which were derived from 800 available spectra observed in the North Atlantic [32]. Consideration of the

underlying spectrum parameter probability functions yields the required probability of encountering in a given location and season the particular wave spectrum family member, P(F/L,S).

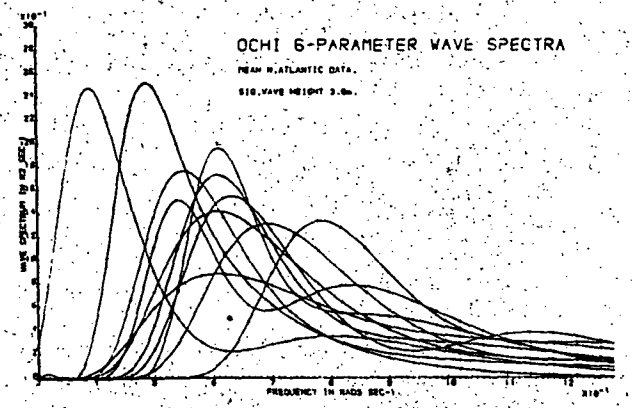

Fig 11

6-Parameter Spectrum

It should be noted that the 6-parameter wave spectrum family covers a wider variety of shapes than other commonly used spectra and that some have double peaks indicating the co-existence of swell and sea waves.

In using the Ochi-6 parameter family of wave spectra for the short-term prediction for each sea severity, one of the family members yields the largest response with confidence coefficient of 0.95 while another yields the smallest response with confidence coefficient 0.95. Hence by connecting the points obtained in each sea severity, the upper and lower response bounds can be established eg, Fig 12.

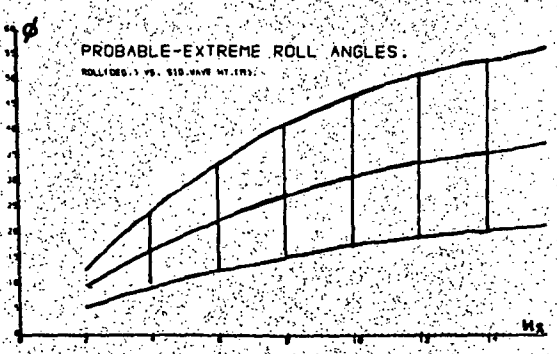

Fig 12

Probable Extreme Roll Angle

Ochi and Bales [30] have demonstrated that, for a range of vessels and offshore structures, the bounds obtained by using the 6-parameter family with N Atlantic data reasonably covers the variation of responses computed using measured spectra in various locations of the world. Fig 13.

A similar analysis has been performed for a family of Jonswap wave spectra suitable for fetch limited seas, to cover the variation in expected spectral shape [31].

The current investigation uses both 6-parameter and Jonswap spectral families for open-sea and fetch limited seas respectively.

In order to account for short-crestedness of the seaway and following the recommendation in [8] from which the wave climatology is extracted, cosine squared spreading of wave energy is assumed. This aspect requires further attention by oceanographers.

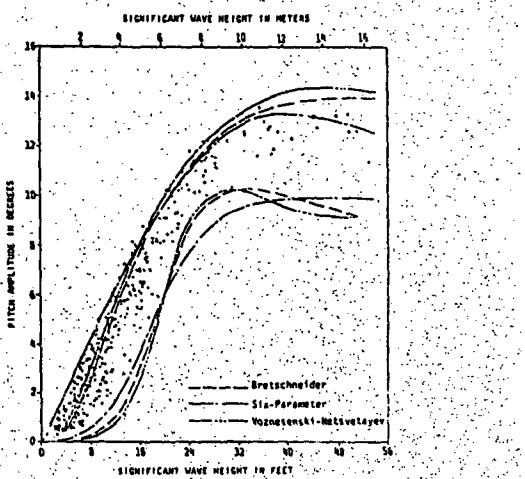

Fig 13

Mariner Probable Extreme Pitch Values (head seas)

A2.3 Seamanship

This factor can have a large influence on both the motion probabilities obtained and the motions themselves once the severe seastates have been encountered. Firstly, by manoeuvring to avoid a storm area (or in the case of certain particularly small vessels by not sailing at all until the storm has passed) the vessel is using avoidance seamanship. This is a function of the accuracy of weather forecasts and

the skill of the ship's officers. Secondly a vessel experiencing excessive motions and sea loads may be manoeuvred to reduce these to perceived acceptable levels. The vessel is using what might be termed pacifying seamanship which is a function of the motion/sea loads information available to the ship's officers and their skill in reducing these motions and sea loads.

Avoidance type seamanship can be represented by a Markov mapping [20] ie, P(i/j) from the probability of encountering each seastate in the absence of avoidance seamanship to the probability of encounter with avoidance seamanship. An example transition matrix $P(H_s'/H_s)$ is given in Table 6 where H_s' is the seastate encountered after avoidance action and H_s the seastate which would have been obtained in the absence of avoidance action.

Pacifying seamanship consists primarily in changes of speed and/or heading once a severe seastate has been encountered. These can be represented as conditional properties of speed, V and relative heading to waves, given the seastate actually encountered after appropriate avoidance (H_s', T_m, F) and unaltered speed V_o and relative heading μ_o ie, $P(V, \mu/H_s', T_m, F, V_o, \mu_o)$ where μ, μ_o are functions of ship course C and wave direction ϕ.

Seastate which would have been encountered		H_s				
		1	2	3	4	5
Encountered seastate after avoidance seamanship H_s'	1	1.0	0	0	0	0
	2	0	1.0	0.2	0	0
	3	0	0	0.8	0.5	0.1
	4	0	0	0	0.5	0.6
	5	0	0	0	0	0.3
		1.0	1.0	1.0	1.0	1.0

Table 6

Ship speed in a seaway comprises the involuntary speed reduction due to the added resistance and reduced propulsive efficiency in waves together with the voluntary speed reduction due to the master's action to reduce excessive motions and sea loads.

Although the present study is primarily concerned with the higher seastates where master's voluntary action overrides any consideration of natural speed reduction, nevertheless the approximate increase in added resistance is accounted for by using a conveniently available method due to Maruo [26], to estimate the initial attained speed of the vessel on any heading. This is an area requiring further work but recourse can be made to experimental results if necessary.

The problem of voluntary slowdown/change of heading criteria to reduce motions and loads is no less difficult. It is inevitable that any proposed criteria will be subjective ie, based upon the master's previous experience, will depend upon how well the master perceives the motions and loads from his conning position, and will also be vessel dependent.

Once criteria have been agreed a more objective response from the master should be possible, if suitable instrumentation is provided, to indicate the motions and loads being imposed together with suggested critical motion/load limits and even possible optimum courses of action to reduce these to acceptable levels. [14]

In the meantime, and for the purposes of the present study, it has been necessary to assign a set of criteria which it will be assumed the master will adhere to in order that his vessel will be rendered more seakindly. The master is likely to take action to avoid damage to his vessel's structure, engines, or cargo and to avoid undue discomfort to his passengers and crew. There have been several studies with both merchant and warships eg, [1,2,10,15,23] into limiting motion criteria for different types of vessel, but several of the proposed criteria suffered from the drawback that they could not be readily assessed from the master's conning position and were also not relevant to the environment being experienced by the crew. For example Conolly proposed a criterion based upon slamming at 0.2 L bp abaft the fore perpendicular [15] and Aerttsen used the amplitude of acceleration at the fore perpendicular [2]. To address these deficiencies Lloyd and Andrew [24] proposed

the following measures of ship behaviour in connection with predictions of voluntary speed loss in rough weather:-

i) Slam-induced whipping vibration acceleration at bridge not to exceed 0.05 g in a 15 minute sampling period.

ii) Subjective motion magnitude (SM) weighted according to personnel location and averaged along ship length SM = 15.

iii) Average deck wetness interval at F.P. not less than 100 secs.

iv) Average propeller emergence interval to be greater than 30 secs.

The actual estimates for the limiting conditions were based on seakeeping trials with destroyers [10] and the cargo ship JORDAENS [2].

The Slamming Criterion (1) has been subsequently amended because it is possible, by using the original criterion, to apparently improve the seakeeping performance by moving the bridge to the region of a node where there is no whipping response and thus no speed limitation. The amended slamming criterion refers to the "average whipping acceleration experienced over the entire ship" which should not exceed 0.18 g and is based on full scale trials with 2 frigates [4]. Aertssen, meanwhile in the discussion to [4] proposed a value of 0.20 g for the bridge whipping acceleration based on trials with the trawler Belgian Lady [1].

The Subjective Motion Magnitude (SM) concept [24] attempts to quantify the motion environment within the ship experienced by the crew and to relate this to human response to ship motions. The original concept was proposed by Schoenberger [37].

Whilst subsequent full scale trials and results of questionnaires have borne out the original proposed SM value of 12-15 over a 12 hour period in head seas, and it is therefore expected that higher values might be tolerable in the short term, it is generally agreed that a subjective magnitude criterion should not be based solely upon vertical accelerations in head seas but that rolling and lateral plane motions should also be accounted for in one single SM value if possible. Hosodo et al [19] proposed a method based on reliability engineering techniques by treating the human being as a series system and obtained an overall "human effectiveness" by multiplying individual effectiveness appropriate to each motion level being experienced. Baitis et al [7] also reported studies to determine criteria for limiting motions based on vertical with lateral forces.

The average deck wetness interval has been changed to 40 seconds following full scale trials [4], although this figure takes no account of sensitive equipment or men on deck. The above represents a great deal of ongoing work which, for the reasons outlined, are inconclusive except for some particular full scale trials results, mostly on 2 frigates. For this reason the following limiting motion criteria will be assumed in the present study.

Criterion	Fisheries Protection (64m)	Stern Trawler (58M)
No of slams +	60 per hour	60 per hour
SM ‡	12	15
No of deck wetness ‡	90 per hour	90 per hour
No of propeller emergences	120 per hour	120 per hour

Table 7

[All of these values reflect the calculation assumptions and do not therefore necessarily reflect the physical situation observed].

NB + For this length of vessel slamming whipping is not considered a problem. A slam is deemed to occur when the impact velocity > $0.093\ (g/L)^{1/2}$ [28].

‡ Especially relevant in a survivability study when the master will aim to keep the seas on the bow.

‡ Method of calculation takes no account of distortion by hull of incident waves nor static/dynamic swell-up.

If the subject vessel exceeds one or more of these motion criteria it will be caused to alter heading/speed conducive to the continued "success" of the mission, which will reduce the motions to acceptable levels, otherwise the vessel will achieve a hove-to position if motions and loads cannot be reduced to acceptable levels.

A2.4 Responses

In Section 4.1 the concept of a "potentially dangerous" roll angle was introduced. This was stated to be a pre-assigned roll angle (30 degrees in the present case) beyond which it can be assumed that the vessel will be considered potentially unsafe from a capsize point of view. Before the required probability of exceedance of the potentially dangerous roll motion ϕ_c can be ascertained, $P(\phi > \phi_c)$ an appropriate response statistic ϕ is required. For operability studies this ϕ-response is likely to be an average-type process such as the significant roll response, whereas when considering survivability some measure of the expected maximum is required.

A useful development by Ochi [27] is the extreme response value which will be exceeded with a pre-assigned small probability, the 'design-extreme value'. This is necessary because the most probable extreme value $\bar{\sigma}_n$, which can be used for comparison with the observed extreme value, has a high probability (0.632) of being exceeded for a large number of observations n, if the process is narrow band, where the most probable extreme value:-

$$\bar{\sigma}_n = \sqrt{2 \ln \left\{ \frac{2\sqrt{1-\varepsilon^2}}{1+\sqrt{1-\varepsilon^2}} n \right\}} \sqrt{m_o} \quad \text{for } \varepsilon \leq 0.9$$

and ε is the spectral bandwith parameter of the σ process.

$$\varepsilon = \sqrt{\frac{m_o m_4 - m_2^2}{m_o m_4}}$$

where m_o, m_2, m_4 are the zeroth, second and fourth moments of the response process.

In terms of exposure time the most probable extreme value $\bar{\sigma}_T$ is given by [27].

$$\bar{\sigma}_T = \sqrt{2 \ln \left\{ \frac{60^2 T}{2\pi} \sqrt{\frac{m_2}{m_o}} \right\}} \sqrt{m_o}$$

where T = exposure time in hours. (It is argued in Ref [20] that T should be the independence period T_*). The design extreme value $\hat{\sigma}$ is similarly given in terms of number of observations and exposure time:-

$$\hat{\sigma}_n = \sqrt{2 \ln \left\{ \frac{2\sqrt{1-\varepsilon^2}}{1+\sqrt{1-\varepsilon^2}} \cdot \frac{n}{\alpha} \right\}} \sqrt{m_o}$$

$$\hat{\sigma}_T = \sqrt{2 \ln \left\{ \frac{60^2 T}{2\pi\alpha} \sqrt{\frac{m_2}{m_o}} \right\}} \sqrt{m_o}$$

for small α and for $\varepsilon \leq 0.9$.

Choosing α as 0.01 for example, implies that only one vessel in 100 sister vessels operating under statistically identical environments may suffer from a response greater than the predicted value in a given period of time.

Third International Conference on Stability of Ships and Ocean Vehicles, Gdańsk, Sept. 1986 STAB'86

THE INFLUENCE OF LOAD CONDITION IN THE CAPSIZING OF SHIPS

R.E.D. Bishop
W.G. Price
P. Temarel

ABSTRACT

The equations governing linear antisymmetric motions of a rigid ship are formulated and the nature of a complete solution of them is explored. The possibility that motion in waves can be both resonant and dynamically unstable is reiterated and suggested as an explanation of ship losses. It was found that the hypothesis produced what appear to be illuminating results, even on the basis of a much simplified theory, for the coastal tanker EDITH TERKOL which was actually lost at sea.

1. INTRODUCTION

The losses of fishing vessels in recent years have been discussed by Reilly [1]. The statistics are not difficult to come by but, as that writer points out, their interpretation is not at all straightforward. It is not proposed to discuss the details here but the general picture that emerges is far from reassuring:

i) Total losses have risen in recent years;
ii) The increase is mainly attributable to foundering of old ships; that is to say the main cause of increased losses is entry of water into hulls.

It is worth noting that, while water inside the hull may cause capsize, Reilly found no particular increase in the incidence of intact capsize.

This suggests that two factors are fundamental

a) Greater attention needs to be paid to seakeeping and to shipping of green water;
b) Water clearance and weather-tightness are critically important.

It would appear that, of these, (b) is really a matter of detailed design and of hull maintenance. It is with (a) that this paper is concerned.

2. SEAKEEPING

To a first approximation we are concerned with the antisymmetric motions of roll, yaw and sway. It is impossible for one to occur without the other two, so all are coupled together. (If it is assumed that motion occure in one degree of freedom only - i.e. in roll - it is likely that predictions will be grossly inaccurate.) There are two possible causes of large antisymmetric motions, so far as linear theory is concerned, namely resonance and dynamic instability. These two phenomena raise very different considerations.

Resonance. The phenomenon of resonance is important because its effect is to increase the range of encounter frequency over which responses are significant. In principle, there is no special difficulty in determining conditions of resonance.

Dynamic Instability. By contrast conditions of linear dynamic instability appear never to have been adequately defined in the literature, let alone determined for a particular vessel. The motion is comparable to flutter or divergence of aircraft but the presence of waves raises special difficulties. (The naval architects' traditional separation of directional stability from hydrostatic stability is probably quite unjustified; the latter is likely to be a special case of the former, it would seem.) What is lacking is the ability to determine a boundary of instability.

The purpose of this paper is twofold. It is first to draw attention to a hypothesis that has, in fact, been advanced by the writers before [2,3]. It is that a helmsman can counter the effects of resonance or dynamic instability but cannot cope with both together. That is to say, it is suggested that a vessel which is capable of being simultaneously resonant and dynamically unstable in a seaway is inherently capable of being uncontrollable while executing large motions. This hypothesis introduces the second aim of this paper, namely to define linear dynamic instability in a seaway.

3. EQUATIONS OF MOTION

If conventional body axes are fixed with their origin at the centre of mass of a rigid hull, the equations of motion may be written down in terms of motions defined by reference to them. The equations are

$$m(\dot{v} + rU) = \Delta Y$$
$$I_{xx}\dot{p} - I_{xz}\dot{r} = \Delta K$$
$$I_{zz}\dot{r} - I_{xz}\dot{p} = \Delta N$$

where m is the mass, I_{xx} and I_{zz} are moments of inertia, I_{xz} is a product of inertia, U is constant forward velocity, v is sway velocity and p, r are angular velocities of roll and yaw respectively. The components ΔY, ΔK, ΔN are components of sway force, roll moment and yaw moment due to fluid loading.

The most general expressions available for the fluid loading components are those introduced by Cummings [4] and generalised later by Bishop et.al. [5,6]. They employ the concept of convolution and, unlike 'derivatives', make allowance for memory effects which are undoubtedly present. When the expressions are introduced into the equations of motion, the latter become:

$$m(\dot{v}+rU) = \int_{-\infty}^{\infty} y_v(\tau)[v_w(t-\tau) - v(t-\tau)]d\tau + \int_{-\infty}^{\infty} y_p(\tau)[p_w(t-\tau) - p(t-\tau)]d\tau + \int_{-\infty}^{\infty} y_r(\tau)[r_w(t-\tau) - r(t-\tau)]d\tau ,$$

$$I_{xx}\dot{p}-I_{xz}\dot{r} = -\rho g\nabla GM\phi + \int_{-\infty}^{\infty} k_v(\tau)[v_w(t-\tau) - v(t-\tau)]d\tau + \int_{-\infty}^{\infty} k_p(\tau)[p_w(t-\tau) - p(t-\tau)]d\tau + \int_{-\infty}^{\infty} k_r(\tau)[r_w(t-\tau) - r(t-\tau)]d\tau ,$$

$$I_{zz}\dot{r}-I_{xz}\dot{p} = \int_{-\infty}^{\infty} n_v(\tau)[v_w(t-\tau) - v(t-\tau)]d\tau + \int_{-\infty}^{\infty} n_p(\tau)[p_w(t-\tau) - p(t-\tau)]d\tau + \int_{-\infty}^{\infty} n_r(\tau)[r_w(t-\tau) - r(t-\tau)]d\tau,$$

where the subscript w signifies "of the water". That is to say the fluid actions depend on the relative motions of the water and the hull. The quantity $\phi(t)$ is roll angle so that $\phi(t) \equiv p(t)$. The quantities $y_v(\tau)$, ... are impulse reponse functions.

If there are sinusoidal waves on the water and the frequency of encounter is ω_e, then we may define a column vector

$$\{v_w(t),\ p_w(t),\ r_w(t)\} = \{\bar{v}_w,\ \bar{p}_w,\ \bar{r}_w\}e^{i\omega_e t}$$

where $\bar{v}_w$, $\bar{p}_w$, $\bar{r}_w$ are constants. Consider now a ship motion given by the vector

$$\{v(t),\ p(t),\ r(t)\} = \{v_o,\ p_o,\ r_o\}e^{\lambda t} .$$

so that, if $\phi(t) = \phi_o e^{\lambda t}$,

$$\{v(t),\ p(t),\ r(t)\} = \{v_o,\ \lambda\phi_o,\ r_o\}e^{\lambda t} .$$

With these admitted motions, let us take a typical convolution integral:

$$\int_{-\infty}^{\infty} y_p(\tau)[p_w(t-\tau) - p(t-\tau)]d\tau = \bar{p}_w e^{i\omega_e t}\int_{-\infty}^{\infty} y_p(\tau)e^{-i\omega_e\tau}d\tau - p_o e^{\lambda t}\int_{-\infty}^{\infty} y_p(\tau)e^{-\lambda\tau}d\tau = Y_p(i\omega_e)\,\bar{p}_w e^{i\omega_e t} - Y_p(\lambda)\,p_o e^{\lambda t}$$

where $Y_p(i\omega_e)$ and $Y_p(\lambda)$ are, respectively, the Fourier transform and the Laplace transform of the impulse response function $y_p(\tau)$.

The equations of motion may now be put in a convenient matrix form. They become

$$\begin{bmatrix} m\lambda+Y_v(\lambda) & \lambda Y_p(\lambda) & mU+Y_r(\lambda) \\ K_v(\lambda) & \lambda^2 I_{xx}+\lambda K_p(\lambda)+\rho g\nabla GM & -\lambda I_{xz}+K_r(\lambda) \\ N_v(\lambda) & -\lambda^2 I_{xz}+\lambda N_p(\lambda) & \lambda I_{zz}+N_r(\lambda) \end{bmatrix} \begin{Vmatrix} v_o \\ \phi_o \\ r_o \end{Vmatrix} e^{\lambda t} =$$

$$\begin{bmatrix} Y_v(i\omega_e) & Y_p(i\omega_e) & Y_r(i\omega_e) \\ K_v(i\omega_e) & K_p(i\omega_e) & K_r(i\omega_e) \\ N_v(i\omega_e) & N_p(i\omega_e) & N_r(i\omega_e) \end{bmatrix} \begin{Vmatrix} \bar{v}_w \\ \bar{p}_w \\ \bar{r}_w \end{Vmatrix} e^{i\omega_e t}.$$

In matrix notation, this may be written as

$$\underset{\sim}{D}(\lambda)\,\underset{\sim}{q}_o e^{\lambda t} = \underset{\sim}{E}(i\omega_e)e^{i\omega_e t} ,$$

where $\underset{\sim}{q}_o \equiv \{v_o, \phi_o, r_o\}$ and $\underset{\sim}{E}(i\omega_e)$ are column vectors.

4. FORCED MOTION

A steady state forced motion, such that $\underset{\sim}{q}(t) = \underset{\sim}{q}_o e^{i\omega_e t}$, is found as the solution of

$$\underset{\sim}{D}(i\omega_e)\underset{\sim}{q}_o e^{i\omega_e t} = \underset{\sim}{E}(i\omega_e)e^{i\omega_e t} .$$

That is to say

$$\underset{\sim}{q}(t) = \underset{\sim}{D}^{-1}(i\omega_e)\ \underset{\sim}{E}(i\omega_e)e^{i\omega_e t} .$$

The resonance condition is found as the minimum of $|\underset{\sim}{D}(i\omega_e)|$ though the sharpness of its magnification depends on the fluid damping.

5. FREE MOTION

A more complete solution of the equation of motion may be found from the condition $\underline{q}_w(t) = \underline{0}$. This requires that there is a free motion, in addition to the forced one, such that $\underline{q}(t) = \underline{q}_o e^{\lambda t}$ where

$$\underline{D}(\lambda)\underline{q}_o e^{\lambda t} = \underline{0} .$$

This requires that the characteristic equation

$$|\underline{D}(\lambda)| = 0$$

has roots λ_1, λ_2, λ_3, ... such that

$$|\underline{D}(\lambda_1)| = 0 \quad , \quad |\underline{D}(\lambda_2)| = 0, \ \ldots$$

The ship suffers dynamic instability if any of these roots has a positive real part.

It will be noticed that the condition of dynamic instability cannot be found directly. This is because a characteristic equation, $|\underline{D}(\lambda_1)| = 0$ say, cannot be formulated until its solution $\lambda = \lambda_1$ is known. In general, some form of iterative procedure would appear to be required. There are, however, certain degenerate (though not unfamiliar) approaches that are at least of interest:

a) Using slow motion derivatives in the equations $|\underline{D}(\lambda)| = 0$ in place of the Laplace transforms [7],

b) Using oscillatory coefficients in the equations in place of Laplace transforms [2].

It is also worth noting that approaches to the Laplace transforms can be made, at least in theory, by measuring the Fourier transforms with a Planar Motion Mechanism and extrapolating the results so found in the complex plane by means of Taylor expansions [8].

6. THE COASTAL TANKER 'EDITH TERKOL'

The EDITH TERKOL was such that

$$L_{pp} = 58.6\text{m} \ ; \ B = 9.65\text{m} \ ; \ D = 4.15\text{m} \ .$$

Details of her loading conditions with level keel are:

Loading condition (tonnes)	Draught amidships (m)
595 (ballast)	1.586
830	2.1
1020	2.6
1280	3.2
1589 (full load)	3.8

For each of the five draughts, values of GM = 0.2, 0.4, 0.6, 0.8 and 1.0m were taken so as to produce a range of resonance frequencies.

Considerable effort was made to assemble a consistent set of hydrodynamic data on this ship. Results were computed for both slow motion derivatives and oscillatory coefficients and comparisons were made with results published by van Leeuwen [9], Inoue et.al.[10] and Gerritsma [11]. (The slow motion derivatives provided means of correcting the oscillatory coefficients for low encounter frequencies.) This assembly of data was a major undertaking in its own right and, when it was thought that adequately reliable results had been found, the oscillatory coefficients were used to determine regions of dynamic instability as suggested by approach (b) mentioned above.

Possible coincidence of dynamic instability and resonance was investigated in the manner explained in ref.2. That is to say, 'shaded' regions of instability were found on suitable polar charts and resonance loci were plotted; coincidence could occur when a locus fell inside a shaded area of instability. For a Froude Number of 0.2, such plots were made for each of the 5 selected draughts and the various GM values gave 5 resonance loci on each. Two examples of the polar charts are shown in Fig.1.

The results can be summarised as follows:

1. The deeper the draught the smaller the region of instability. The region was the largest for the ballast condition.
2. In general, the smaller the GM value the more likely was coincidence of resonance and instability to occur.
3. In the full load condition only the GM=0.2m locus fell in the area of instability, whereas in the ballast condition only contours for GM > 0.8m fell outside it.

The actual loci were published in a report to the U.K. Department of Transport [12]. The results found can be represented as shown in fig.2 by curve A. The area above curve A is "safe" and that below "unsafe".

It is of interest now to compare these findings with those found by employing other criteria. The results of model tests for this vessel were published by Kure and Bang [13] and the conditions under which they did and did not achieve capsize in a model basin are marked on fig.2 by o and x respectively.

Curves B and C are derived from IMO criteria. That of curve B shows GM as stated by IMO Res.167 while curve C follows from IMO Weather Criteria. (The IMO data were kindly supplied by Mr H. Bird of the Dept. of Transport, London.)

7. CONCLUSIONS

This paper investigates the conditions which linear theory suggests would present a helmsman with difficult problems of control. In particular, it is explained how logical equations of motion can be written, i.e. equations the form of whose solutions do not have to be known before the equations can be formulated. It is demonstrated that even linear theory presents a serious mathematical obstacle to progress.

It is suggested that there are ad hoc approaches for getting round the mathematical difficulty. One of these is employed with data relating to a particular ship, the coastal tanker EDITH TERKOL, which was lost in a seaway. It was found that, although she appears to have complied with existing stability requirements, those criteria may be optimistic. Moreover, the computed results are more closely in agreement with the results of model tests than the IMO curves or recent published studies [14]. While the writers would accept that these results are far from conclusive, they do suggest that they can scarcely be ignored.

REFERENCES

1. Reilly, M.S.J. The safety of UK fishing vessels 1961-80. J.of Navigation, 37, 1984, 60-82.
2. Bishop, R.E.D., Price, W.G. and Temarel, P. On the role of encounter frequency in the capsizing of ships. Second Internat.Conf.on Ship Stability, Tokyo, 1982, Paper SIII-2a, 43-51.
3. Bishop, R.E.D., Price, W.G. and Temarel, P. Some recent research on the dynamics of capsizing. Proc.SAFESHIP Seminar, RINA, 1982, 49-67.
4. Cummings, W.E. The impulse response function of ship motions. Schiffstechnik, 7, 1962, 101-109.
5. Bishop, R.E.D., Burcher, R.K. and Price, W.G. The uses of functional analysis in ship dynamics. Proc.Roy.Soc., A332, 1973, 23-35.
6. Bishop, R.E.D., Price, W.G. and Temarel, P. A functional representation of fluid actions on ships. Internat.Shipb.Progress, 31,1984, 239-250.
7. Bishop, R.E.D., Burcher, R.K. and Price, W.G. Application of functional analysis to oscillatory ship model testing. Proc.Roy.Soc., A332, 1973, 37-49.
8. Bishop, R.E.D., Price, W.G. and Temarel, P. General linear antisymmetric motions of a rigid ship. Proc.Internat.Conf.on The SAFESHIP Project : Ship Stability and Safety, 1986.
9. van Leeuwen, G. The lateral damping and added mass of an oscillating ship model. Shipbuilding Lab.Report 23, Delft, 1964.
10. Inoue, S., Hirano, M. and Kijima, K. Hydrodynamic derivatives of ship manoeuvring. Internat.Shipb.Progress, 28, 1981, 112-125.
11. Gerritsma, J. Hydrodynamic derivatives as a function of draught and ship speed. Shipbuilding Lab.Report 477, Delft, 1979.
12. Bishop, R.E.D., Price, W.G. and Temarel, P. The influence of load conditions in the capsizing of ships. Report S8 on the SAFESHIP Project, Dept. of Transport, London.
13. Kure, K. and Bang, C.J. The ultimate half roll. First Internat.Conf.on Stability of Ships and Ocean Vehicles, Glasgow, 1975.
14. Vassalos, D. A critical look into the development of ship stability criteria based on work/energy balance. Trans.RINA, Paper W4, 1985.

R.E.D. Bishop, F.Eng, FRS.
W.G. Price, D.Sc(Eng), F.Eng.
P. Temarel, C.Eng, Ph.D.

Brunel University
Uxbridge, Middx., UB8 3PH
U.K.

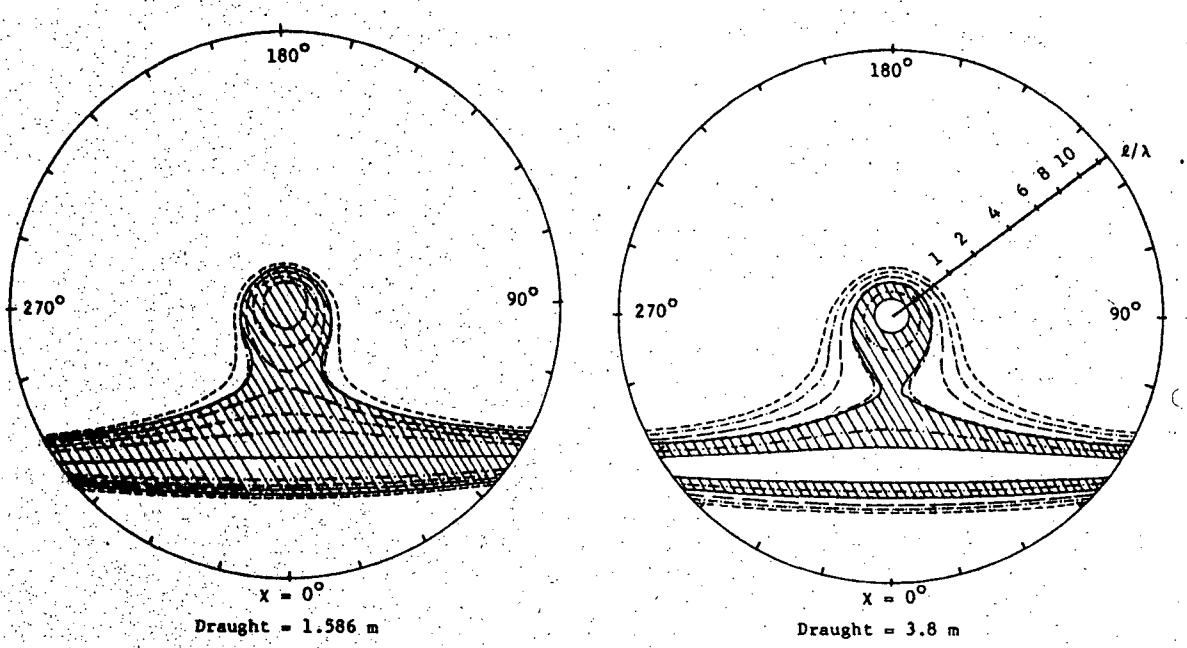

FIG.1 Polar Charts for the EDITH TERKOL travelling at Froude number Fn=0.2 in sinusoidal waves. The hatched area shows the region of instability and the other lines give the resonance conditions for

GM = 1.0m (---); 0.8m (-.-.-); 0.6m (——); 0.4m (--.--); 0.2m(-..-..-) .

($\chi = 180°$ corresponds to head waves; $\ell \equiv L_{pp}$ and λ = wave length).

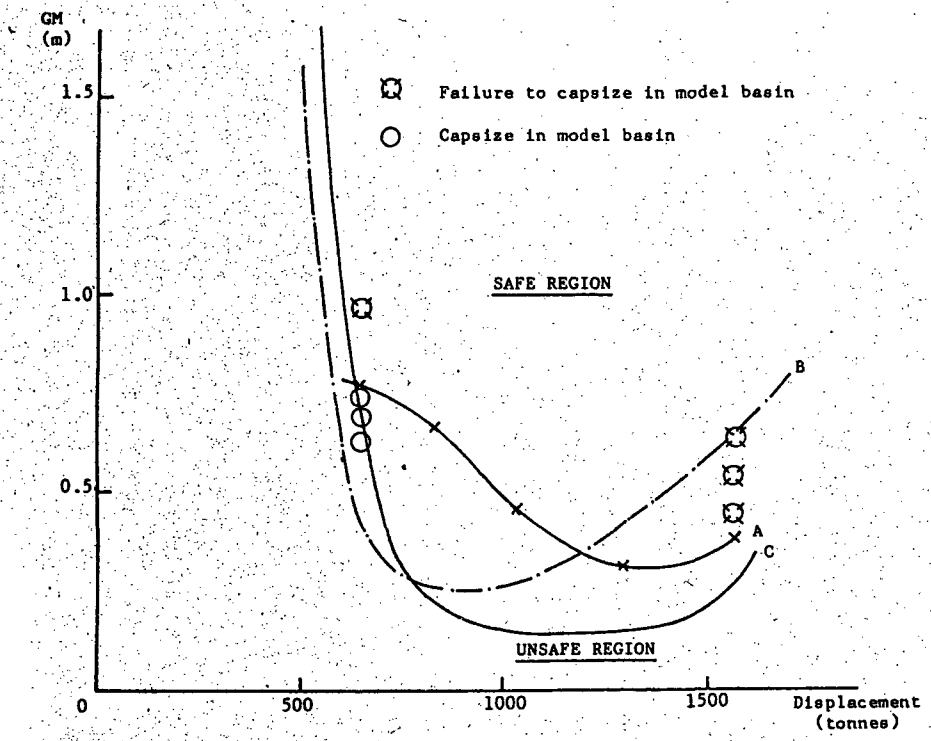

FIG.2 Limits of safe operation of EDITH TERKOL predicted by :

A the present calculations

B IMO/Ref.13

C IMO Weather Criteria

Third International Conference on Stability of Ships and Ocean Vehicles, Gdańsk, Sept. 1986

STAB'86

A COMPARISON OF VESSEL SAFETY ASSESSMENTS BASED ON STATICAL STABILITY CRITERIA AND ON SIMULATED ROLL RESPONSE CHARACTERISTICS IN EXTREME SEA STATES

A.K. Brook, MSc, CEng
British Maritime Technology Limited

ABSTRACT

The safe operating condition of a vessel is currently determined from stability criteria which are based on properties of a vessel's statical restoring curve. No allowance is made explicitly for environment conditions, vessel motions and the roll damping properties of the vessel. This paper describes how vessel safety can be assessed from the statistics of the roll response of a vessel obtained from a time simulation of the coupled non-linear equations of motions. The safety of a number of vessels in extreme sea-states has been assessed using this technique at operating conditions which correspond to the minimum GM specified by the IMO stability criteria A167. The ability of existing stability criteria to specify safe operating conditions for these vessels has been evaluated.

1 INTRODUCTION

The rolling motion of a vessel in an irregular sea-way can be determined from a time simulation of the coupled sway, roll and yaw equations of motion. Appendix I describes equations of motion which are based on those used for a linear seakeeping analysis but incorporate the non-linear roll restoring and roll damping effects. Details of how the irregular wave and wind effects can be represented are also given in Appendix I.

From a simulation the safety of a vessel can be assessed from the statistics of the roll response of the vessel. The probability of extreme roll motions occurring can be determined by fitting a suitable probability distribution to the histogram of the roll response. However a distinction needs to be made between assessing safety in terms of capsize and in terms of exceedence of large roll angles. In order for a simulation to be used to validly predict the occurrence of a capsize the equations of motion need to account for phenonemon such as water on deck, down flooding and shifting cargo and in extreme sea-states the effect of breaking waves also needs to be given consideration. These effects have not been represented in the present analysis. It is obviously desirable that the probability of large roll angles occurring should be small and this is considered in this paper rather than the question of capsize. The safety of a vessel can be assessed by determining the probability of exceedence of a given angle, which in this study is taken to be 30 degrees.

Currently ship operators and designers determine the safe operational condition of a vessel for a range of vessel displacements by calculating the minimum GM which satisfies statical stability criteria based on the non-linear restoring characteristics of the vessel. The IMO A167 criteria for merchant vessels, which many governments require operators to comply with, are described in Appendix II. The IMO A167 criteria have been supplemented with similar criteria for certain classes of vessels such as fishing and offshore supply vessels. Recently IMO has recommended that vessels should comply with a weather criterion which is also described in Appendix II. This criterion takes into account the response of the vessel to a beam wind and the roll of the vessel due to wave action. Details of other existing and proposed stability criteria are given in Ref.[1].

This paper describes the results of an assessment of the roll response of a number of vessels from a simulation of the coupled non-linear equations of the sway, roll and yaw motions of the vessels. The simulations have been undertaken for extreme sea-states at the minimum GM for which the vessels satisfy the IMO A167 and weather criteria. An evalution of the criteria has been made by assessing the safety of the vessels from the statistics of the roll response.

2 DETERMINATION OF VESSEL ROLL RESPONSE AND SAFETY ASSESSMENT FROM SIMULATION TECHNIQUES

The continuous sway, roll and yaw response of a vessel can be obtained from a time simulation of the coupled non-linear equations described in Appendix I. Ref.[2] describes a comparison between the RMS roll response from a simulation with the measured RMS roll from model tests and full-scale trials on the fishery protection vessel 'Sulisker'. It was found that reasonable agreement was obtained between simulations and model tests or full-scale trials, providing the non-linear roll damping is determined accurately. Reference [2] also presents results from simulations which have been undertaken for six selected vessels at two load conditions. The significance of the non-linear roll damping, coupling, frequency variation of the added mass and damping coefficients and the effect of wind gusting has been investigated for each of the vessels and it was found that:

Coupling with sway in beam seas was significant for some vessels.

The frequency variation of the added mass and damping coefficients can be neglected and simulations can be undertaken using constant coefficients at the natural roll frequency.

The RMS roll response is sensitive to the magnitude of the non-linear roll damping which needs to be accurately determined from reliable theoretical methods or model experiments.

A steady extreme wind can cause some vessels to heel significantly.

The effect of wind gusting is significant for some vessels even if the heel angle, due to the mean wind, is small.

The roll response of the vessel can be analysed to give a histogram of the roll amplitudes measured from the even keel position. A Rayleigh distribution can be fitted to this histogram where the distribution depends on the root mean square (RMS) of the continuous roll record. From this distribution the following statistical information can be obtained:

- **Probability of the Roll Amplitude Exceeding a Given Roll Amplitude ϕ_{MAX}**

The probability of the roll amplitude exceeding a specified roll amplitude ϕ_{MAX} is given by:

$$Q(\phi > \phi_{MAX}) = e^{-\frac{1}{2}\left(\frac{\phi_{MAX}}{RMS}\right)^2} \qquad (1)$$

- **Expected Maximum Roll Amplitude**

The expected or average maximum roll amplitude is given to a good approximation by:

$$E(\phi_{MAX}) = RMS\sqrt{2}\left((\log_e N)^{\frac{1}{2}} + \frac{0.2886}{(\log_e N)^{\frac{1}{2}}}\right) \qquad (2)$$

where the RMS roll is obtained from N roll amplitudes.

- **Roll Amplitude with a Percentage Chance of Being Exceeded**

The roll amplitude with a percentage chance P of being exceeded in N amplitudes is given (for small P) by:

$$\phi_{MAX,P} = RMS\sqrt{2}\,(\log_e \frac{100N}{P})^{\frac{1}{2}} \qquad (3)$$

A second histogram can be formed from the distribution of N_p peak roll angles occurring in N_p groups of M roll amplitudes, where M is typically 15-20 amplitudes ($N = MN_p$).

A double exponential distribution can be fitted to this histogram from which the following statistical information can be obtained.

- **Probability of the Peak Amplitude Exceeding a Given Roll Amplitude ϕ_{MAX}**

The probability of the peak roll amplitude exceeding a specified roll amplitude ϕ_{MAX} is given by:

$$Q(\phi_p > \phi_{MAX}) = 1 - e^{-e^{-\alpha(\phi_{MAX}-u)}} \qquad (1)$$

where α and u are the parameters of the fitted distribution.

- **Expected Maximum Roll Amplitude**

The expected or average maximum roll amplitude occurring in N_p groups is given to a good approximation by:

$$E(\phi_{MAX}) = u + \frac{\log_e N_p}{\alpha} \qquad (2)$$

- **Peak Roll Amplitude with a Percentage Chance of Being Exceeded**

The peak roll angle which has a percentage chance P of being exceeded in N_p groups is given (for small P) by:

$$\phi_{MAX,P} = u + \frac{\log_e \frac{100\,N_p}{P}}{\alpha} \qquad (3)$$

$E(\phi_{MAX})$ and $\phi_{MAX,P}$ can thus be calculated from both the Rayleigh distribution of roll amplitudes and from the double exponential distribution of group maxima. For many vessels these are in good agreement but in some cases the double exponential distribution was found to give more reliable results. This is consistent with the statistics being derived from the extreme motions of the vessel, in contrast to the statistics from the Rayleigh distribution which are based on the RMS of the continuous roll record.

An assessment of a vessel's safety in a given sea-state and for a given loading condition can be obtained from the roll amplitude $\phi_{MAX,P}$ which has a percentage change P of being exceeded. For this study a vessel is judged safe if $\phi_{MAX,1\%}$ is no more than 30 degrees.

The expected maximum roll amplitude gives an inadequate assessment of vessel safety since, being an average value, it can frequently be exceeded.

In the following sections the statutory minimum GM of five sample vessels have been obtained from the IMO criteria which are described in Appendix II. An assessment has been made of the safety of the vessels when subject to extreme beam wind and wave conditions at the minimum GM values.

3 SAFE OPERATING CONDITION FROM IMO CRITERIA

The safe operating condition of a vessel at a given load condition can be specified in terms of the minimum GM value which satisfies the existing IMO stability criteria. The A167 criteria (Appendix II) do not take into account the environmental effects or roll damping properties of the vessel.

Table 1 Minimum GM Requirements to Satisfy IMO A167 and Weather Criteria

	SUPPLY VESSEL		STERN TRAWLER		FISHERY PROTECTION	VEHICLE CARRIER		CONTAINER	
Lpp (m)	52.6		56.9		64.0	80.0		135.0	
Beam (m)	12.2		12.2		11.6	16.0		23.0	
Speed (knots)	12		12		14	14		19	
Displ.(tonnes)	2122	1299	1881	1582	1532	2706	1943	17620	10439
Draught (m)	4.9	3.4	4.8	4.3	4.6	3.9	3.1	8.2	5.2
Trim (m)	0.0	0.58	0.2	1.9	0.0	0.5	2.3	0.0	1.5
Bilge Breadth (m)	0.3		0.3		0.37	0.5		0.5	
Length (m)	13.0		12.6		16.0	24.0		40.5	
KM (m)	6.07	5.86	6.15	6.33	5.43	7.48	8.10	9.84	10.48
GM (m) Operating	1.72	1.16	0.72	0.46	0.78	0.38	0.60	1.70	2.35
GM (m) A167	1.52*	0.28*	0.35+	0.45+	0.31Δ	0.30Δ	0.50Δ	0.82Δ	0.52Δ
GM_W(m)# Weather Criteria	1.34	0.21	0.27	0.37	0.44	1.18	1.88	0.59	0.19
Mean Wind Speed (knots) [Ref.3]	90	76	74	71	73	60	60	68	65
GM_W(m)& (Mean Wind Speed 80 knots)	1.30	0.24	0.32	0.48	0.52	2.14	3.38	0.69	0.35
Recommended Minimum GM	1.52*	0.28*	0.35+	0.45+	0.44#	1.18#	1.88#	0.82Δ	0.52Δ
	1.52*	0.28*	0.35+	0.48&	0.52&	2.14&	3.38&	0.82Δ	0.52Δ

* Offshore Supply Rules

\+ Fishing Boat Rules

Δ A167

\# GM to limit heel due to steady wind to 10 degrees from Weather Criteria (with variable wind speed)

& GM to limit heel due to steady wind to 10 degrees from Weather Criteria (modified for fixed mean wind speed of 80 knots)

The weather criteria however takes into account wind effects and relates it to the roll angle of the vessel due to wave action and an allowance is made for the roll damping properties of the vessel.

Table 1 shows the minimum GM which is required for five selected vessels to satisfy both the IMO A167 and weather criteria. The vessels range in size from 50 to 135 metres and include a supply vessel, stern trawler, fishery protection vessel, vehicle carrier and container vessel. Two load conditions have been considered for each of the vessels except for the fishery protection vessel.

Table 1 shows that for some of the vessels the statutory minimum GM from A167 is considerably less than the operating GM whereas for some of the vessels the operating GM is close to the IMO minimum. The minimum GM which is shown in Table 1 for the weather criterion is such that the heel angle due to the steady wind will not exceed 10 degrees.

The minimum GM calculated from the existing weather criterion is based on a constant wind pressure per unit area for all vessels as described in Appendix II and no allowance is made explicitly for a design wind speed. The mean wind speed which corresponds to that implied by the weather criterion has been calculated from available wind heeling coefficients which are reported in Ref.[3]. These wind speeds are shown in Table 1 and they vary considerably according to the vessel type.

The weather criterion recommends an increased GM for two of the vessels, namely the fishery protection vessel and vehicle carrier, but the corresponding wind speeds are only 73 and 60 knots respectively. However, based on observed wind data, a design wind speed of 80 knots is desirable and the minimum GM from the weather criterion on the basis of this wind speed is also shown in Table 1 for each vessel. A considerable increase in the minimum GM is required for the vehicle carrier in this case. An increase in GM is also obtained for the fishery protection vessel but for the other vessels the GM is still less than the A167 criteria except for the stern trawler at one condition.

The recommended minimum operating GM shown in Table 1 is the value from A167 unless the weather criterion recommends a higher value. Only in the case of the vehicle carrier does the minimum GM

exceed the existing operating value for the vessel.

4 VESSEL SAFETY AT MINIMUM GM FROM SIMULATION

The safety of the vessels shown in Table 1 has been assessed at the minimum GM which satisfies the IMO A167 or equivalent vessel class criteria. Simulations have been undertaken for a duration of one hour real time and the irregular wave and wind forces and moments have been generated such that they have a repeat time equal to the duration of the simulation.

The added mass and damping coefficients and the regular wave forces, from which the irregular wave forces are generated, have been calculated from a seakeeping program which is based on Ref.[4]. The non-linear roll damping effects have been calculated theoretically from methods developed by BMT based on Ref.[5]. Recently a comparison has been made between this theoretical approach and experimental roll damping coefficients for the fishery protection vessel 'Sulisker'. The theoretical method was found to give good agreement with experimental results for this vessel and also for hull forms derived from the parent hull form [Ref.2].

The IMO A167 criteria does not take into account environmental condition but in order to investigate the safety of a vessel from a simulation the extreme wind and wave conditions need to be specified. Significant wave heights of 8 and 12 metres have been considered which represent gale and storm conditions. A mean wind speed of 80 knots has been used which allows for gusts in excess of 100 knots. An example of the histograms of roll amplitudes and the Rayleigh and double exponential distributions are shown in Fig.1 for one of the vessels. The effect of wind gusting for the same vessel is also shown in Fig.2.

The RMS roll response and the peak roll angle $\phi_{MAX,1}$ which has a 1% chance of being exceeded is shown in Table 2 for each of the vessels at the minimum GM specified by IMO A167 as given in Table 1. The response of the vessel to waves and to wind and waves is shown. The safety of the supply vessel, stern trawler and fishery protection vessel is not satisfactory since $\phi_{MAX,1}$ is in excess of 30 degrees which has been chosen as a representative safe angle of roll. $\phi_{MAX,1}$ exceeds the vanishing angle ϕ_0 of the restoring curve for the supply vessel and stern trawler at some of the sea-states and load conditions and hence the vessel is at risk of capsizing in these conditions.

The action of the wind results in an increase of up to 20% in $\phi_{MAX,1}$ depending on the vessel type and GM. However the vehicle carrier, which did not roll significantly due to wave action, heels excessively up to 67 degrees in the ballast condition and $\phi_{MAX,1}$ is in excess of 80 degrees.

The IMO weather criterion has been introduced to improve the safety of such vessels. However in its present form it does not recommend that the heel angle of the vessel should be limited. Table 1 shows the minimum GM obtained from the weather criterion for each of the vessels such that the heel angle will not exceed 10 degrees. As mentioned previously this results in an increase in the minimum GM only for the fishery protection vessel and the vehicle carrier. Table 3 shows a comparison between the response of these vessels for the GM values from IMO A167 and from the weather criteria, for a 12 metre significant wave height and 80 knot mean wind. The increase in GM results in an improvement in $\phi_{MAX,1}$ but the values are still considerably in excess of 30 degrees. The vehicle carrier heels to nearly 20 degrees rather than the expected 10 degrees because, as shown in Table 1,

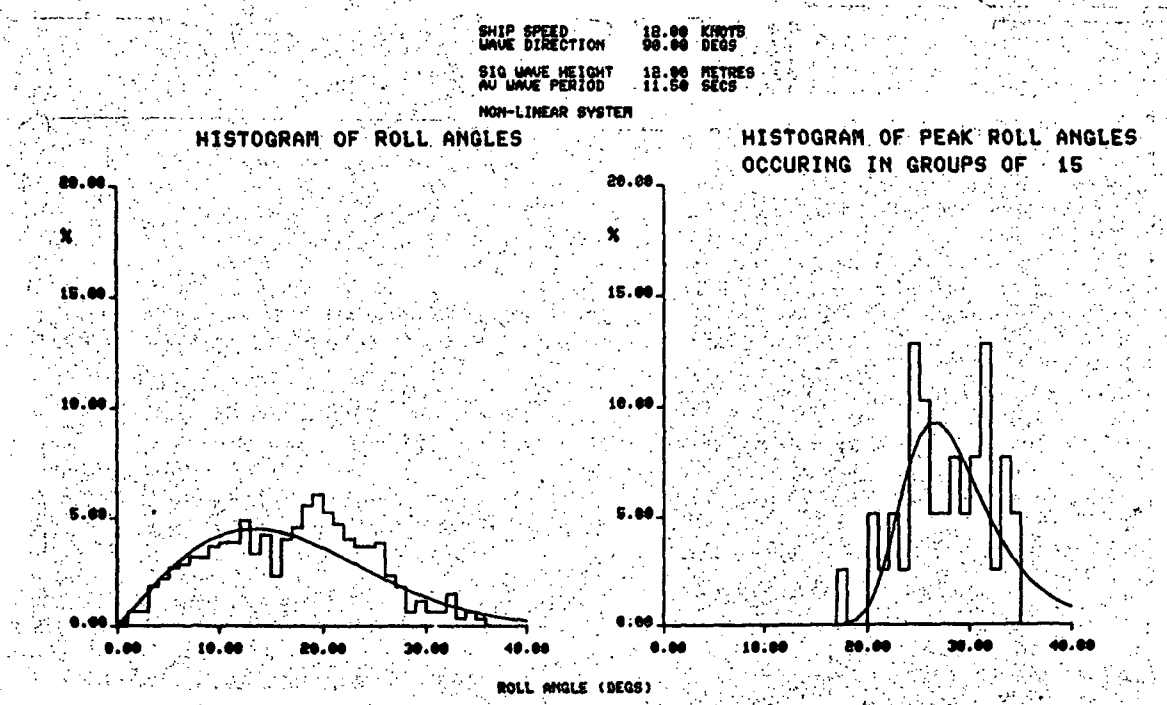

Fig.1 Histogram of Vessel Roll Response

Table 2 Assessment of Vessel Safety from Simulation at Minimum GM Specified by IMO A167 or Equivalent in Beam Wind and Waves (Roll Response Statistics)

Sig. Wave Height (m)	Av. Wave Period (secs)	Mean Wind Speed (knots)		SUPPLY VESSEL		STERN TRAWLER		FISHERY PROTECTION	VEHICLE CARRIER		CONTAINER	
			Draught (m)	4.9	3.4	4.8	4.3	4.6	3.9	3.1	8.2	5.2
			GM (m)	1.52	0.28	0.35	0.45	0.31	0.30	0.50	0.82	0.52
			T_N (sec)	7.1	17.6	16.3	13.3	16.0	22.3	16.8	18.6	23.7
			ϕ_0 (deg)	62	59	73	72	>90	>90	>90	48	47
8	9.5	0	RMS (deg)	12.4	9.8	9.7	7.4	12.4	1.1	1.7	3.8	3.5
			$\phi_{MAX,1}$ (deg)	64#	44*	53*	36*	66*	14	9	21	20
12	11.5	0	RMS (deg)	15.8	13.4	14.8	10.3	18.4	1.8	2.8	6.2	5.9
			$\phi_{MAX,1}$ (deg)	91#	59#	72#	50*	78*	10	14	35*	30
8	9.5	80	RMS (deg)	12.7	12.3	14.1	15.3	18.7	43.6	67.2	6.3	8.4
			HEEL (deg)	1.7	7.0	9.4	12.7	12.5	42.8	67.0	4.8	7.3
			$\phi_{MAX,1}$ (deg)	68#	51*	63*	55*	74*	80*	107*	29	27
12	11.5	80	RMS (deg)	16.1	15.4	18.2	16.8	22.2	43.6	67.2	8.1	9.7
			HEEL (deg)	2.3	7.5	9.9	12.7	11.7	42.2	67.0	5.2	7.4
			$\phi_{MAX,1}$ (deg)	94#	78#	87#	66*	96*	82*	106*	40*	36*

* Vessel unsafe - $\phi_{MAX,1} > 30°$ # Vessel capsize - $\phi_{MAX,1} > \phi_0$

T_N - Natural roll period ϕ_0 - Vanishing angle of restoring curve

Table 3 Assessment of Vessel Safety from Simulation at Minimum GM - Comparison between IMO A167 and Weather Criteria (Beam Wind and Waves - Sig. Wave Ht. 12m; Mean Wind Speed 80 knots)

	FISHERY PROTECTION VESSEL	VEHICLE CARRIER	
Draught (m)	4.6	3.9	3.1
ϕ_0 (degs)	>90	>90	>90
GM(m) - A167	0.31	0.30	0.50
RMS (degs)	22.2	43.6	67.2
HEEL (degs)	11.7	42.6	67.0
$\phi_{MAX,1}$ (degs)	96*	82*	106*
GM(m) - Existing Weather Criteria	0.44	1.18	1.88
RMS (degs)	19.8	19.2	20.7
HEEL (degs)	9.4	17.8	19.0
$\phi_{MAX,1}$ (degs)	84*	66*	82*
GM(m) - Weather Criteria (Wind Speed 80 knots)	0.52	2.14	3.38
RMS (degs)	18.3	12.0	11.2
HEEL (degs)	8.4	10.2	9.8
$\phi_{MAX,1}$ (degs)	84*	50*	48*

* Vessel unsafe - $\phi_{MAX,1} > 30°$

Vessel capsize - $\phi_{MAX,1} > \phi_0$

ϕ_0 - Vanishing angle of restoring curve.

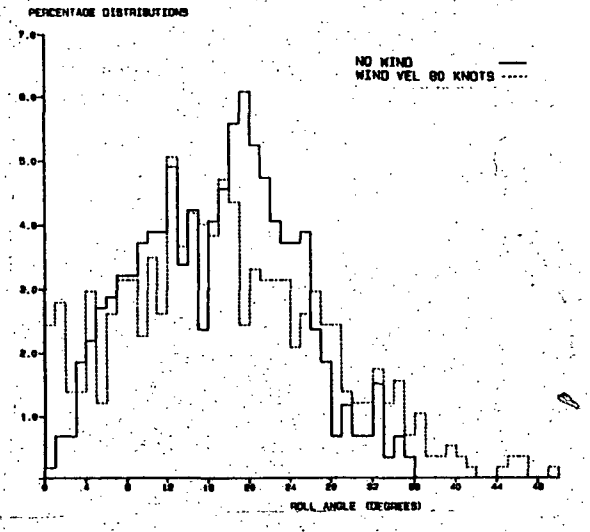

Fig.2 Histogram of Roll Angle - Effect of Wind Gusting

the assumed wind pressure in the weather criterion only represents a mean 60 knot wind. Table 1 also shows the minimum GM from the weather criterion which has been modified to utilise an 80 knot mean wind for these vessels and to limit the angle of heel to 10 degrees. Table 3 also shows the response of these vessels at these GM values, the response of the vehicle carrier being improved considerably such that $\phi_{MAX,1}$ is 50 degrees, which for a high sided vessel may be acceptable.

The safety of the fishery protection vessel has not been improved significantly through application of the weather criterion because the vessel is unsafe under the action of waves. The results in Table 2 demonstrate that there is a need for stability criteria which take account of the response of a vessel to wave action as well as the vessel's operating condition, weather condition and roll damping characteristics.

Table 4 Assessment of Vessel Safety from Simulation at Operating GM in Beam Waves (Roll Response Statistics)

			SUPPLY VESSEL		STERN TRAWLER		FISHERY PROTECTION
Sig. Wave Height (m)	Av. Wave Period (secs)	Draught (m)	4.9	3.4	4.8	4.3	4.6
		GM (m)	1.72	1.16	0.72	0.46	0.78
		T_N (sec)	6.6	8.9	11.1	14.4	9.7
		ϕ_0 (deg)	72	90	90	72	>90
8	9.5	RMS (deg)	11.7	8.0	10.0	7.4	10.6
		$\phi_{MAX,1}$ (deg)	58*	34*	48*	36*	47*
12	11.5	RMS (deg)	14.2	9.1	12.7	10.3	12.3
		$\phi_{MAX,1}$ (deg)	75#	40*	63*	50*	58*

* Vessel unsafe - $\phi_{MAX,1} > 30°$. # Vessel capsize - $\phi_{MAX,1} > 90$.

T_N - Natural roll period. ϕ_0 - Vanishing angle of restoring curve.

Table 1 shows that the operating GM of most of the vessels exceed the minimum values specified by A167. The safety of the three vessels which were judged to be unsafe due to wave action has been assessed at their operating GM and the results are shown in Table 4. The increase in the GM has resulted in an improvement in the safety of the vessels but $\phi_{MAX,1}$ is still in excess of 30 degrees.

5 CONCLUSIONS AND RECOMMENDATIONS FOR IMPROVING VESSEL SAFETY

The safety of five vessels has been assessed in extreme beam wind and wave conditions. The safety of the vessels at the minimum GM values which satisfy the IMO A167 stability criteria has been evaluated from the roll response statistics of the vessels which have been obtained from time-domain simulations based on the coupled non-linear equations of motion. Three vessels, namely a supply vessel, stern trawler and fishery protection vessel were judged to be unsafe since the maximum peak roll angles considerably exceeded the chosen safe limiting angle of 30 degrees.

The effect of extreme wind resulted in the vehicle carrier heeling up to 67 degrees and rendered the vessel unsafe. Wind effects on the other vessels resulted in higher roll response. The IMO weather criterion recommends a higher GM for the fishery protection vessel and vehicle carrier. It has been shown that the existing weather criterion could be improved by limiting the allowable heel angle due to the mean wind to some chosen value, such as 10 degrees. The specification of wind speed rather than wind pressure is desirable since it was found that the wind pressure can represent mean wind speeds as low as 60 knots for some vessels.

Whilst the application of the weather criterion can improve the safety of a vessel susceptible to wind action there is clearly a need for a criterion which takes account of the wave action on a vessel. Modifying the existing IMO A167 statical criteria to impose a significantly higher GM for the smaller vessels in order to improve their safety in extreme sea-states is clearly undesirable due to the implications to a vessel's owner and operator. There is also a need for vessel safety to be undertaken in a more rational way and for allowance to be made for the extreme environmental conditions and roll damping characteristics of the vessel. It is undesirable that vessels should be specified as safe to operate only in limited weather conditions. However a practical way of improving vessel safety would be to provide criteria which take into account a vessel's roll damping characteristics. This would allow designers to evaluate vessel safety subject to specified extreme wind and wave conditions and, in conjunction with the existing IMO requirements, determine the required damping characteristics of a vessel. The designer could apply the criteria in such a manner that a trade-off between metacentric height and the roll damping characteristics of the vessel could be undertaken.

The procedure by which a vessel's safety is evaluated subject to extreme environmental conditions, roll damping characteristics and vessel motions could be undertaken with the simulation techniques described in this paper. An alternative approach, which is less demanding in terms of the design process is to determine roll bounds from mathematical techniques which also take into account the environmental effects, vessel load condition and damping characteristics. References [6] and [7] describe the theory and application of such an approach based on Lyapunov techniques. The advantage of these techniques is that the improvement of the vessel's safety can be undertaken at the design stage and the vessel's master and operator need only ensure that the load condition of his vessel is satisfactory, as at present.

ACKNOWLEDGEMENTS

The author would like to thank the Directors of British Maritime Technology (BMT) and the UK Department of Transport who sponsored the

development of the simulation techniques, for permission to publish this paper.

REFERENCES

1 BIRD, H. and MORRALL, A.M. 'The SAFESHIP Project - A Basis for Better Design Criteria and Stability Regulations' Third International Conference on Stability of Ships and Ocean Vehicles STAB '86, Gdansk, Poland, Sept.1986.

2 BROOK, A.K. 'The Role of Simulation in Determining the Roll Response of a Vessel in an Irregular Seaway' RINA International Conference on The Safeship Project: Ship and Stability Safety, London, Jun 1986.

3 AAGE, C. 'Wind Coefficients for Nine Ship Models' Hydro-Og Aerodynamisk Laboratorium Aerodynamics Section, Rep. No.A.3, 1971.

4 VUGTS, J.H. 'The Hydrodynamic Forces and Ship Motions in Oblique Waves' Netherlands Ship Research Centre, Rep. No.1505, 1971.

5 BEARMAN, P.W., DOWNIE, M.J. and GRAHAM, J.M.R. 'Calculation Method for Separated Flows with Applications to Oscillatory Flow Past Cylinders and Roll Damping of Barges' 14th Symposium Naval Hydrodynamics, 1983.

6 CALDEIRA-SARAIVA, F. 'The Boundedness of Rolling Motions of a Ship by Lyapunov's Method' Third International Conference on Stability of Ships and Ocean Vehicles STAB '86, Gdansk, Poland, Sept.1986.

7 PHILLIPS, S.R. 'Applying Lyapunov Methods to Investigate Roll Stability' Third International Conference on STability of Ships and Ocean Vehicles STAB '86, Gdansk, Poland, Sept.1986.

8 IKEDA, Y. 'A Prediction Method for Ship Roll Damping' Dept. of Naval Architecture, University of Osaka, Japan, Rep. No.00405, 1978.

APPENDIX I
EQUATIONS OF MOTION OF VESSEL IN IRREGULAR SEA-WAY

The linear equations of the coupled sway, roll and yaw motions of a ship in regular waves are given in Ref.[4]. The equations can be expressed, with the origin at the centre of gravity, as follows where the roll equation has been extended to include the non-linear roll and restoring terms:

$$\begin{aligned}
&(\Delta+a_{22})\ddot{y}+b_{22}\dot{y}+a_{24}\ddot{\phi}+b_{24}\dot{\phi}+a_{26}\ddot{\phi}+b_{26}\dot{\phi} = X_2(t)\\
&a_{42}\ddot{y}+b_{42}\dot{y}+(a_{44}+I_{44})\ddot{\phi}+b_{44}\dot{\phi}+f(\dot{\phi},\phi) + \Delta g GZ(\phi)\\
&\quad +a_{46}\ddot{\phi}+b_{46}\dot{\phi} = X_4(t) \qquad (A1)\\
&a_{62}\ddot{y}+b_{62}\dot{y}+a_{64}\ddot{\phi}+b_{64}\dot{\phi}+(a_{66}+I_{66})\ddot{\phi}+b_{66}\dot{\phi} = X_6(t)
\end{aligned}$$

where Δ is the ship's displacement; a_{ij}, b_{ij} are the added mass and damping coefficients of response i coupled with response j (calculated from a seakeeping program), I_{44}, I_{66} are roll and yaw moments of inertia; GZ is the restoring curve; X_2, X_4, X_6 are the sway, roll and yaw forces and moments and $F(\dot{\phi},\phi)$ is the non-potential roll damping.

- **Non-potential Damping**

The non-potential roll damping includes contributions from friction b_f, vortex shedding from the naked hull b_e, and appendages such as bilge keels b_{bk}, and a lift contribution in the case of a ship with forward speed b_L. The friction and lift contributions can be estimated from theoretical methods described in Ref.[8] whilst the vortex shedding from the naked hull and appendages can be determined from the BMT method which has been based on Ref.[5]. The friction and lift components are linear terms where the friction term depends on frequency and the lift term is independent of frequency. The vortex shedding terms are non-linear and are taken as proportional to the square of the roll velocity and are independent of wave frequency. Hence:

$$F(\dot{\phi}) = [b_L(v)+b_f(\omega,v)]\dot{\phi} + [b_e(v)+b_{bk}(v)]\dot{\phi}|\dot{\phi}| \qquad (A2)$$

- **Excitation Forces and Moments**

The irregular wave forces and moments can be obtained by summing, over a range of wave frequencies, the regular wave forces which are calculated from a seakeeping program. The wave amplitude at a particular frequency is related to the spectral ordinate by:

$$a(\omega_i) = \sqrt{2S(\omega_i)\delta\omega_i} \qquad (A3)$$

where $S(\omega)$ is the wave spectrum.

Hence the wave force or moment at a given time t is given by:

$$X(t) = \sum_{i=1}^{N} R(\omega_i)\sqrt{2S(\omega_i)\delta\omega_i}\cos(\omega_i t + \phi_F(\omega_i) + \varepsilon(\omega_i)) \qquad (A4)$$

where $R(\omega_i)$ is the force or moment per unit wave amplitude, $\phi_F(\omega_i)$ is the phase angles of the force or moment with respect to the wave, and $\varepsilon(\omega_i)$ is a random phase angle. The wave amplitudes $a(\omega_i)$ can also be randomised.

- **Wind Gusting**

The steady wind moment acting on a vessel can be obtained from non-dimensional coefficients C_K given in Ref.[3] where:

$$M_{WIND} = \frac{1}{2}\rho_A C_K A_L H V^2 \qquad (A5)$$

where ρ_A is the density of air, A_L is the transverse windage area, H is the distance above the waterline of the centre of area and V is the wind speed in metres/sec. Wind gusting is generated in the same

way as for irregular waves where in equation (A4) $R(\omega_1)$ and $\phi_F(\omega_1)$ are not included and a wind spectrum is used.

The effect of changes in windage area due to the motion of the vessel has not been included.

APPENDIX II
IMO CRITERIA

• A167

The operating condition of a vessel needs to satisfy, with reference to Fig.A1, the following criteria:

A - area under curve up to 30 degrees to be not less than 0.055 metre-radian.

B - area under curve up to x degrees to be not less than 0.09 metre-radian.

C - area between 30 degrees and x degrees to be not less than 0.03 metre-radian.

x - 40 degrees or any lesser angle at which the lower edges of any openings in the hull, superstructure or deckhouses which lead below deck and cannot be closed weathertight, would be immersed.

E - maximum GZ to occur at angle not less than 30 degrees and to be at least 0.20 metres.

F - initial GM to be not less than 0.15 metre.

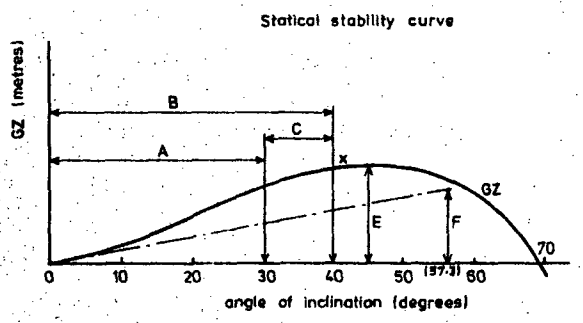

Fig.A1

• Weather Criterion

It is recommended that the ability of a ship to withstand the combined effects of beam wind and rolling should be demonstrated for each normal condition of loading, with reference to Fig.A2, as follows:

1 The ship is subjected to a steady wind pressure acting perpendicular to the ship's centreline which results in a steady wind heeling lever (ℓw_1).

2 From the resultant angle of equilibrium (θ_0), the ship is assumed to roll due to wave action to an angle of roll (θ_1) to windward.

3 The ship is then subjected to a gust wind pressure which results in a gust wind heeling lever (ℓw_2).

4 Under these circumstances, area b should be equal to or greater than area a.

The angles in the figure below are defined as follows:

θ_0 = angle of heel under action of steady wind

θ_1 = angle of roll to windward due to wave action

θ_2 = angle of downflooding (θ_f) or 50° or θ_0 whichever is less, where:

θ_f = angle of heel at which openings in the hull, superstructures or deckhouses which cannot be closed weathertight immerse.

θ_0 = angle of second intercept.

Expressions for the wind lever ℓw_1 and the angle of roll θ_1 to windward due to wave action are given in the criteria. The wind lever ℓw_2 assumes a constant wind pressure for all vessels of 0.0514 tonnes/m^2. The angle of roll θ_1 takes into account vessel particulars, load condition and whether bilge keels are included.

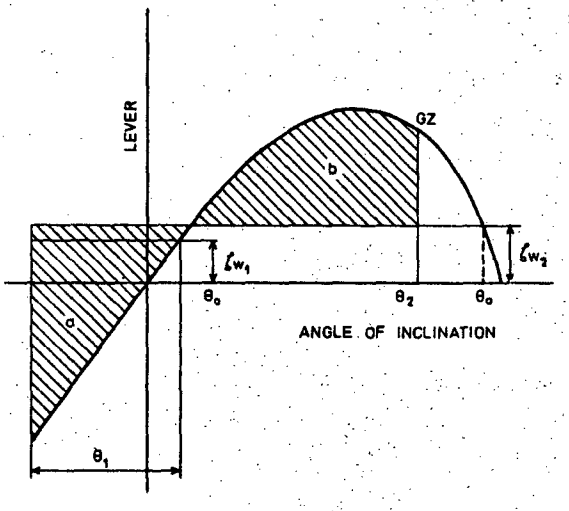

Fig.A2

Third International Conference on Stability of Ships and Ocean Vehicles, Gdańsk, Sept. 1986

STAB'86

COMPUTING CAPSIZING FREQUENCIES OF SHIPS IN A SEAWAY

H. Söding, E. Tongue

ABSTRACT

As part of a research project aimed at computing the probability of capsizing in a seaway, the question is dealt with how to derive this probability from simulations or model experiments. To establish the limit between safe and unsafe ships, quite low capsizing rates are of interest which cannot be directly determined by counting the number of capsizes during the simulation, because this would require too much simulation time. Therefore it is proposed to perform simulations or measurements in a steeper seaway and to extrapolate the capsizing probability to more moderate seaways. For this extrapolation, two methods are proposed which are based on a semi-empirical relationship and on numerically integrating the Fokker-Planck equation, respectively.

INTRODUCTION

A major research project of our institute aims at a computational method to assess the danger of capsizing of ships in a natural seaway by means of excessive wave-induced motions. Causes of capsizing like cargo shift, loss of deck cargo on one side, severe unsymmetrical flooding etc. are disregarded, as are motions due to breaking transverse waves. However, included into our investigation is a rolling motion analysis of ships with symmetrically or asymmetrically flooded compartments.

The main tool for this investigation is a detailed roll motion simulation. We are convinced that, at least in many cases, motions in the other five degrees of freedom are coupled to the rolling motion to an extent that necessitates the inclusion of all six rigid-body motions into roll motion simulations. In case of damaged ships or ships with substantial partly filled tanks, further degrees of freedom are necessary to describe the fluid motions within these spaces. We expect also that it is not appropriate for such simulations to disregard all hydrodynamic influences, assuming a hydrostatic pressure distribution along the hull. The reason for this is that a larger ship of, say, 100 or 200 m length with deck load up to the capsizing safety margin has maximum still-water righting levers in the size range of 1 % only of the ship's breadth (Fig. 1). Thus, because hydrostatic and weight forces nearly cancel each other, relatively small hydrodynamic influences become important. Even if the hydrostatic pressure distribution were appropriate for the rolling motion alone, for heaving and pitching motions hydrodynamic influences are definitely necessary to be taken into account; and because of the above-mentioned coupling between all these motions, the inclusion of at least some hydrodynamic terms is held to be necessary for adequate roll motion simulations.

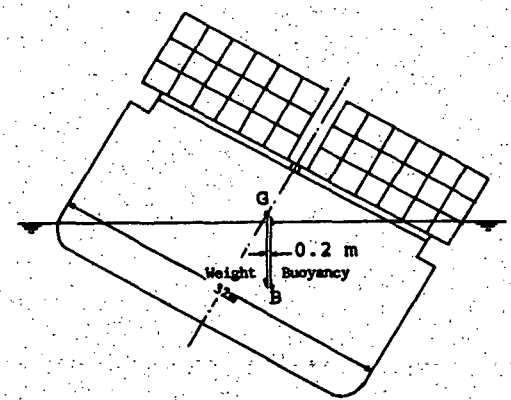

Fig. 1: Relative size demonstration of GZ and ship's breadth

On the other hand, calculating nonlinear ship motions by means of solving a three-dimensional boundary value problem to determine fluid motions and pressures around the ship in each time instant is clearly impossible today. Therefore we use an intermediate between these extremes, applying analogues of the strip method or the strip method itself for certain parts of the problem. Details of these simulation methods are shown in the papers by H. Böttcher, P. Kröger and F. Petey presented to this conference.

Böttcher describes an accurate, quite involved motion simulation method which, however, will require extensive manual preparation work and computer time for its application; it is still in the development stage. A much simpler method is described by Kröger; it will, hopefully, nonetheless be accurate enough at least for computing relative figures for capsizing safety of different ships, loading cases and wave conditions. Finally, the paper of Petey presents several methods and results of computing fluid motions in tanks with a free surface or in damaged compartments, including the inflow and outflow of fluid through openings and the generation of free-surface jumps causing substantial roll damping. The procedures may be combined with the afore-mentioned and with other methods of ship motion simulations to determine the mutual influence of ship and internal fluid motions.

The aim of these simulations is to determine, as a measure of capsizing safety, the mean capsizing frequency f_c or its inverse, the mean time between successive capsizing events,

$$T_c = \frac{1}{f_c} \qquad (1)$$

for a ship with a certain speed and heading in a given loading case and sea state defined by a wave spectrum. These quantities are related to two other frequently-used safety measures: the probability that the ship capsizes at least once during a single roll period of duration T_R,

$$P_R = 1 - \exp(-f_c T_R) \qquad (2)$$

or during another, arbitrary time interval T

$$P_T = 1 - \exp(-f_c T) \qquad (3)$$

As for realistic cases P_R is small compared to 1, we can approximate (2) by

$$P_R = f_c T_R \qquad (4)$$

Inserting this into (3) gives a relation between P_T and P_R applicable for $P_R \ll 1$:

$$P_T = 1 - \exp\left(-\frac{P_R T}{T_R}\right) \qquad (5)$$

PROBLEM

The problem treated in the rest of this paper is how to determine P_R from simulations; the other three safety measures f_c, T_c and P_T follow then directly from the above formulae. In principle, P_R may be determined simply by simulating the roll motions during N successive roll periods. In case that the ship capsizes during this simulation, both the roll angle Φ and the roll angular velocity $\dot{\Phi}$ are changed to 0, and the simulation is continued. If, during N roll cycles, the ship capsizes K times, the best estimate of P_R is

$$P_R = \frac{K}{N} \qquad (6)$$

The formula requires that P_R is $\ll 1$ because otherwize the unrealistic starting conditions $\Phi = \dot{\Phi} = 0$ have too much influence on K. Fortunately, this condition is satisfied automatically in cases of practical interest. To avoid excessive random deviations of the estimate (6) from the true value of P_R, K should at least be 2 or 3. That means, if we want to determine P_R values corresponding to a mean time between capsizes of T_c = 1 year, the simulation has to cover about 2 to 3 years of real time. If the investigation has to be repeated for several sea states, loading conditions etc., we clearly arrive at unrealistic computing times.

SOLUTION 1

EXTRAPOLATION OVER SIGNIFICANT WAVE HEIGHT

THEORETICAL CONSIDERATIONS

To attain realistic simulation times even for estimating quite small capsizing probabilities, we investigate as well theoreti-

cally as numerically the dependence of P_R upon significant wave height H, leaving constant all other parameters of the seaway even if this leads to an unrealistic wave steepness. The idea is to simulate the ship motions with a relatively large value H_1 of significant wave height to obtain several capsizing events within tolerable computing time; to estimate $P_R(H_1) = K/N$ in this seaway; and then to estimate the capsizing probabilty $P_R(H)$ in a seaway of smaller, realistic significant height H by means of a general extrapolation rule for $P_R(H)$.

To find such an extrapolation rule, we assume provisionally that a ship capsizes if it hits waves which exceed a certain critical height h. The mean frequency of occurrence of waves exceeding height h, f(h,H), depends on the significant wave height H of the seaway. According to the above assumption, the ratio of capsizing probabilities in seaways differing only in significant height corresponds to the frequency ratio of exceeding h in both seaways:

$$\frac{P_R(H)}{P_R(H_1)} = \frac{f(h,H)}{f(h,H_1)} \qquad (7)$$

From the above assumption follows also that the mean frequency of exceeding h is equal to the mean capsizing frequency:

$$f(h,H) = f_c(H) = \frac{P_R(H)}{T_R} \qquad (8)$$

where the last expression follows from (4). A corresponding relation holds for H_1:

$$f(h,H_1) = f_c(H_1) = \frac{P_R(H_1)}{T_R} \qquad (9)$$

The ratio $P_R(H)/P_R(H_1)$ follows from these relations if we use the well-known Rayleigh distribution to determine f(h,H):

$$f(h,H) = f_o \cdot \exp\left(-\frac{(h/2)^2}{2m_o(H)}\right) \qquad (10)$$

Here f_o designates the mean zero-upcrossing period of the seaway, and m_o is the variance of the sea surface height, which is related to the significant wave height by

$$m_o(H) = \left(\frac{H}{4}\right)^2 \qquad (11)$$

From (8), (10) and (11) follow

$$f(h,H) = f_o \cdot \exp\left(-\frac{2h^2}{H^2}\right) = \frac{P_R(H)}{T_R} \qquad (12)$$

and a corresponding formula for H_1:

$$f(h,H_1) = f_o \cdot \exp\left(-\frac{2h^2}{H_1^2}\right) = \frac{P_R(H_1)}{T_R} \qquad (13)$$

Solving (13) for h^2 results in

$$h^2 = \frac{1}{2} \cdot H_1^2 \cdot \ln\left(\frac{T_R f_o}{P_R(H_1)}\right) \qquad (14)$$

From (12) and (13) we get the desired ratio

$$\frac{P_R(H)}{P_R(H_1)} = \exp\left(-\frac{2h^2}{H^2} + \frac{2h^2}{H_1^2}\right) \qquad (15)$$

from which h^2 can be eliminated with the aid of (14):

$$\frac{P_R(H)}{P_R(H_1)} = \left(\frac{P_R(H_1)}{T_R f_o}\right)^{\frac{H_1^2}{H^2} - 1} \qquad (16)$$

This is the provisional extrapolation rule which allows us to determine $P_R(H)$ from $P_R(H_1)$. It may be written also in the symmetrical form

$$H^2 \cdot \ln\left(\frac{P_R(H)}{T_R f_o}\right) = H_1^2 \cdot \ln\left(\frac{P_R(H_1)}{T_R f_o}\right) = C \text{ (constant over H)} \qquad (17)$$

Stated in words: The logarithm of $P_R(H)$, plotted over H^{-2}, is a linear function with slope C according to (17). Due to the approximations used, this relation is expected to hold only for sufficiently small values of $P_R(H)$ (Fig. 2).

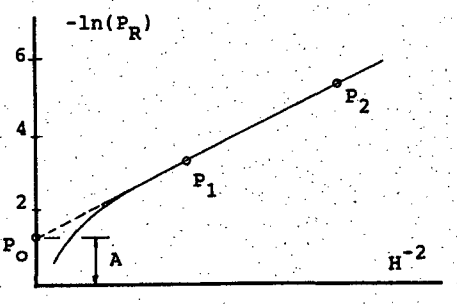

Fig. 2: Dependence of P_R on H (schematicly)

Now we generalize our provisional assumptions about the capsizing conditions as follows: The ship is assumed to capsize with probability p if n successive waves encountering the ship all have heights exceeding h. Under this assumption, the previous equations change as follows:

$$\frac{P_R(H)}{P_R(H_1)} = \frac{f(h,n,H)}{f(h,n,H_1)} \qquad (7a)$$

$$p \cdot f(h,n,H) = f_c(H) = \frac{P_R(H)}{T_R} \qquad (8a)$$

$$f(h,n,H) = f_o \cdot \exp\left(-\frac{n(\frac{h}{2})^2}{2m_o(H)}\right) \qquad (10a)$$

$$f(h,n,H) = f_o \cdot \exp\left(-\frac{2nh^2}{H^2}\right) = \frac{P_R(H)}{p\,T_R} \qquad (12a)$$

$$h^2 = \frac{1}{2n} \cdot H_1^2 \cdot \ln\left(\frac{p\,T_R f_o}{P_R(H_1)}\right) \qquad (14a)$$

$$\frac{P_R(H)}{P_R(H_1)} = \left(\frac{P_R(H_1)}{p\,T_R f_o}\right)^{\frac{H_1^2}{H^2} - 1} \qquad (16a)$$

$$H^2 \cdot \ln\left(\frac{P_R(H)}{pT_R f_o}\right) = H_1^2 \cdot \ln\left(\frac{P_R(H_1)}{pT_R f_o}\right) = C \qquad (17a)$$

(17a) shows that the number n of waves necessary to capsize a ship has no effect on the extrapolation. The logarithm of $P_R(H)$, plotted over H^{-2}, is a straight line as before; however, its slope C now depends upon the unknown and poorly defined quantity p. Therefore, the slope or, correspondingly, the quantity pT_Rf_o has to be determined by numerical computations. pT_Rf_o is related to the quantity A in Fig. 2:

$$A = -\ln(p\,T_R\,f_o) \qquad (18)$$

This fact follows from (17a) for H approaching infinity.

NUMERICAL EXPERIMENTS

To test these ideas, we used the following severely simplified rolling motion equation which allowed to simulate large numbers of roll periods, but which nonetheless is expected to show the same general tendencies as the real rolling motion of a ship:

$$I\ddot{\Phi} + D\dot{\Phi}|\dot{\Phi}| + (C_1 + C_2\alpha)\Phi + C_3\Phi|\Phi| + C_4\alpha = C_5 \qquad (19)$$

Here Φ designates the roll angel, α the wave slope. The latter was determined as a superposition of at least 30 sinusoidal oscillations with irrational frequency ratio, random phase and amplitudes corresponding to a given wave spectrum. I and D model the moment of inertia and a quadratical roll damping, resp. C_1 corresponds to the mean initial stability, whereas C_2 defines a change of initial stability due to the seaway, leading to parametric excitation. Negative C_3 values are used to obtain a parabolic righting lever curve (Fig. 3) which allows capsizing. C_4 defines the direct wave excitation. C_5 is a constant heeling moment.

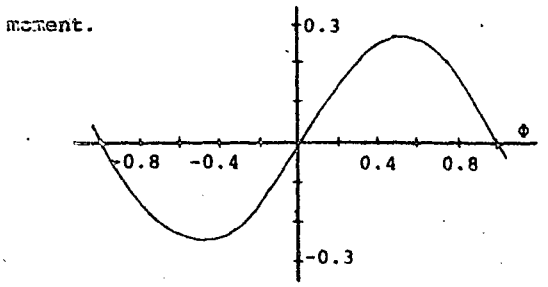

Fig. 3: Righting lever curve used for the simulations; $GZ = \Phi - \Phi|\Phi|$

A large number of simulations was performed with different sets of constants in (19) and different spectra of α by means of a 4th order Runge-Kutta integration of (19) over time with constant step size typically of 1/12 natural roll period. (Each step includes four evaluations of (19).) Figs. 4 and 5 show the results $\Phi(t)$, including several capsizes, for two cases without and with parametric excitation, resp. The number of roll periods simulated per run exceeded 200.000 in some cases. By counting the number N of roll cycles and the number K of capsizes for simulations with different significant wave heights, the probabilities $P_R(H)$ were determined. Fig. 6 shows four examples of $\ln(P_R(H))$ plotted over S_α^{-1} = constant·H^{-2}. Disregarding random fluctuations due to the finite number of capsizes observed, the curves correspond nicely to the expected linear trend for $P_R < \exp(-3)$ or (in one case) $\exp(-4)$. The quantity A of Fig. 2 is relatively constant, ranging from 1.0 to 1.5.

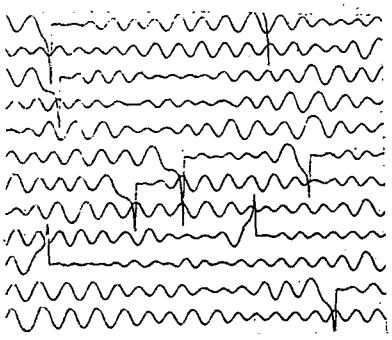

Fig. 4: Simulation of rolling motion, (Eq. 19)

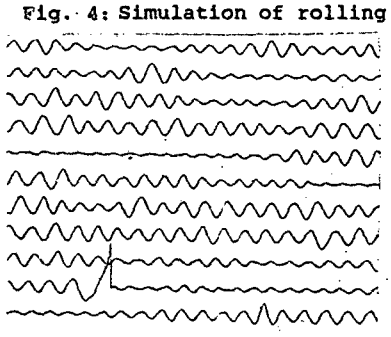

Fig. 5: Simulation of rolling motion, (Eq. 19)

Fig. 6: Dependence of capsizing probability P_R upon the excitation spectrum S_α assumed to be constant between ω_1 and ω_2 and zero outside of this interval, according to motion simulations using equation 19 with the following constants:

Curve	I	D	C_1	C_2	C_3	C_4	C_5	ω_1	ω_2
I	1	0.1	1	0	-1	0.1265	0	0.5	1.25
II	1	0.1	1	1	-1	0.2	0	1.5	2.25
III	1	0.1	1	1	-1	1	0	1.5	2.25
IV	1	0.1	1	0	-1	0.1	0.1	0.5	1.25

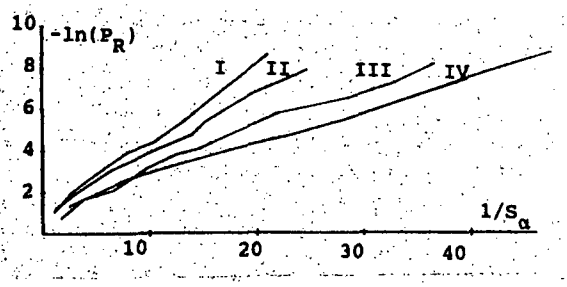

APPLICATION

Thus, two procedures can be proposed to estimate small capsizing probabilities from relatively short motion simulations:

1. Choose a significant wave height H_1 which leads to a capsizing at about every 30th roll cycle.
   Simulate about 400 roll cycles.
   Estimate the capsizing probability $P_R(H_1)$ in that seaway as Number of Capsizes over Number of Roll Cycles and enter it as P_1 into a plot like Fig. 2.
   Choose A =1.25 and construct the straight line through the points P_0 and P_1 of Fig. 2.

This plot, then, gives $P_R(H)$ for arbitrary significant wave heights H. With more computing effort, a better approximation could be attained:

2. Choose two significant wave heights H_1 and H_2 leading to capsizing probabilities of about 1/30 and 1/250, resp. (H_2 may be estimated by procedure 1.)
   Determine $P_R(H_1)$ and $P_R(H_2)$ by simulation as described above, using about 400 and 2000 roll cycles to determine H_1 and H_2, resp.
   Enter $P_R(H_1)$ and $P_R(H_2)$ as P_1 and P_2 into a plot like Fig. 2 and connect P_1 and P_2 by a straight line.

SOLUTION 2

APPLICATION OF THE FOKKER-PLANCK EQUATION

THEORETICAL BACKGROUND

If we describe the ship's position and orientation by means of the 6-component vector $\underline{x}$ and its translational and rotational velocities by $\dot{\underline{x}}$, the motion equation can be approximated by

$$\ddot{\underline{x}} + \underline{b}(\underline{x},\dot{\underline{x}}) = \underline{e}(\underline{x},\dot{\underline{x}},t) \qquad (20)$$

The 6-component vector function $\underline{b}$ describes damping and restoring forces (and moments, as is understood also in the following) whereas $\underline{e}$ contains the random excitation due to the seaway. $\underline{e}$ is presupposed to have the mean value 0 for all $\underline{x}$, $\dot{\underline{x}}$; thus, a difference between, e.g., still water righting levers and mean righting levers in a seaway is included in $\underline{b}$, not in $\underline{e}$.

In (20) it is assumed that acceleration-dependent forces are proportional to the accelerations, and that all forces and moments upon the ship depend only on position $\underline{x}$, velocity $\dot{\underline{x}}$, acceleration $\ddot{\underline{x}}$ and (in case of excitation) time t. The previous motion history is assumed to have no influence. This is in contrast, e. g., to strip theory which regards the motion history by frequency-dependent masses and damping constants. On the other hand, (20) is more general than strip theory in allowing nonlinear damping and restoring as well as coupling, e. g., between damping, restoring and exciting forces and moments. Such a coupling between position $\underline{x}$ and excitation $\underline{e}$ is responsible for the parametric excitation which is of particular importance for roll motions.

We further assume that for $\underline{x}$ and $\dot{\underline{x}}$ fixed, $\underline{e}$ is a stationary, Gaussian, white random process. By this we mean that the i-th component (i=1,...,6) of $\underline{e}$ can be written as

$$e_i = \lim_{\substack{\Delta\omega\to 0 \\ \omega_1\to 0 \\ \omega_n\to\infty}} \sum_{n=1}^{N} \sqrt{2S\Delta\omega_n}\; Y_i \cos(\omega_n t+\varepsilon_i+\varepsilon_n) \qquad (21)$$

Here, the spectrum $S(\underline{x},\dot{\underline{x}})$ of the primary

excitation (the seaway) and the transfer function amplitude $Y_i(\underline{x},\dot{\underline{x}})$ and phase $\varepsilon_i(\underline{x},\dot{\underline{x}})$ are presupposed to be independent of ω at least in the frequency range which is of main importance for the roll motion excitation. However, they may and, normally, will depend upon the ship's state of motion $\underline{x}$ and $\dot{\underline{x}}$. ε_n is a random phase angle equally distributed between 0 and 2π ; it depends on n, but is equal for the 6 components i.

As is shown in the Appendix, under these conditions the joint probability distribution $p(\underline{x},\dot{\underline{x}})$ of $\underline{x}$ and $\dot{\underline{x}}$ satisfies the stationary Fokker-Planck equation

$$\frac{\pi}{2}\sum_{i=1}^{6}\sum_{j=1}^{6}\left(s\,Y_iY_j\cos(\varepsilon_i-\varepsilon_j)p\right)_{\dot{x}_i\dot{x}_j} - \sum_{i=1}^{6}\dot{x}_i\,p_{x_i} + \sum_{j=1}^{6}(b_i\,p)_{\dot{x}_i} = 0 \qquad (22)$$

Here, the indices x_i, $\dot{x}_i$ and $\dot{x}_j$ designate partial derivatives. Thus, (22) is a homogeneous linear partial differential equation for the one unknown function p depending upon the 12 unknowns x_i and $\dot{x}_i$. It will be extremely difficult to find accurate numerical solutions of (22) in case of 6 degrees of freedom. However, at least two degrees of freedom seem to be amenable to numerical solutions. Here we will deal only with one degree of freedom: the roll motion $\Phi(t)$. Then, (20) and (22) simplify to

$$\ddot{\Phi} + b(\Phi,\dot{\Phi}) = e(\Phi,\dot{\Phi},t) \qquad (20a)$$

and

$$\frac{\pi}{2}(S_e p)_{\dot{\Phi}\dot{\Phi}} - \dot{\Phi}p_{\Phi} + (bp)_{\dot{\Phi}} = 0 \qquad (22a)$$

where S_e designates the spectrum of roll exciting moments, again assumed to be independent from frequency ω.

NUMERICAL DETERMINATION OF $p(\Phi,\dot{\Phi})$

We will restrict further upon the case of a ship rolling symmetrically to both sides. In that case, the solution p of (22a) will be the same in all four quadrants $(\pm\Phi,\pm\dot{\Phi})$, and we compute p for $\Phi \geq 0$ and $\dot{\Phi} \geq 0$ only. Due to smoothness conditions of p, we have the boundary conditions

$$p_{\Phi}(\Phi,\dot{\Phi}) = 0 \quad \text{for} \quad \Phi = 0 \qquad (23)$$

and

$$p_{\dot{\Phi}}(\Phi,\dot{\Phi}) = 0 \quad \text{for} \quad \dot{\Phi} = 0 \qquad (24)$$

Because as well the differential equation and the boundary conditions are homogeneous, we need one additional condition which determines the absolute size of the solution. Instead of a condition like

$$\int_{-\infty}^{\infty}\int_{-\infty}^{\infty} p(\Phi,\dot{\Phi}) = 1 \qquad (25)$$

we use the simple condition

$$p(\Phi,\dot{\Phi}) = 1 \qquad (26)$$

If necessary, we could satisfy another inhomogeneous condition later by multiplying the preliminary solution found with (26) by a suitable factor.

(22a) is a parabolic equation, containing second-order derivatives in $\dot{\Phi}$ only. Therefore, the numerical solution in Φ direction is easily found by the 'method of lines': We write

$$p_k(\Phi) = p(\Phi,k\,\Delta\dot{\Phi}) \qquad (27)$$

and correspondingly for S and b. Then, the derivatives in (22a) may be aproximated by finite difference ratios:

$$\frac{\frac{\pi}{2}(S_{k-1}p_{k-1} - 2S_kp_k + S_{k+1}p_{k+1})}{(\Delta\dot{\Phi})^2} - (k\Delta\dot{\Phi}p_{k\Phi})^2 + \frac{(b_{k+1}p_{k+1} - b_{k-1}p_{k-1})}{2\Delta\Phi} = 0 \qquad (28)$$

for $k = 1$ to K. The value p_{K+1} occurring here is set to zero, and the value p_o is approximated as

$$p_o = \frac{4}{3}p_1 - \frac{1}{3}p_2 \qquad (29)$$

which follows from (24) if p is approximated locally by a second-order polynomial in $\dot{\Phi}$.

(28) is a system of first-order ordinary differential equations which - for $k>0$ - is easily solved by means of the Runge-Kutta method. Before starting this procedure, however, we have to determine the initial values $p_k(0)$. That is done by solving the linear system of equations (28) for $\Phi=0$. In this case, due to (23) the term involving $p_{k\Phi}$ is zero, and we have the additional condition $p_o(0)=1$. To satisfy (24), we have also to use (29) and omit simply (28) for

$k = K$.

To derive the capsizing probability P_R from p, we consider the time rate $f(\Phi,\dot\Phi)\Delta\dot\Phi$ with which the ship's state of motion crosses the hatched area in the Φ-$\dot\Phi$-plane of Fig. 7. This rate is related to $p(\Phi,\dot\Phi)$ and to the time

$$\Delta t = \frac{\Delta\Phi}{\dot\Phi} \tag{30}$$

which the motion state needs to cross the hatched area once in the limit $\Delta\Phi\to 0$, $\Delta\dot\Phi\to 0$:

$$p(\Phi,\dot\Phi)\Delta\Phi\Delta\dot\Phi = f(\Phi,\dot\Phi)\Delta\dot\Phi\Delta t \tag{31}$$

Using (30), we obtain

$$\dot\Phi p(\Phi,\dot\Phi) = f(\Phi,\dot\Phi) \tag{32}$$

Integrating f over all positive $\dot\Phi$ values gives the time rate $F(\Phi)$ of upcrossings of Φ:

$$F(\Phi) = \int_0^\infty \dot\Phi\, p(\Phi,\dot\Phi)\, d\dot\Phi \tag{33}$$

For a lightly damped system like a rolling ship, even in white noise excitation there is normally just one roll maximum between two zero-upcrossings. Roll maxima with negative value amount, typically, to not more than 2% of all roll maxima. If we omit these cases, we obtain an approximation for the cumulative probability of the roll angle maxima as

$$P_M(\Phi) = \frac{F(\Phi)}{F(0)} \tag{34}$$

Then the capsizing probability is

$$P_R = P_M(\Phi_c) \tag{35}$$

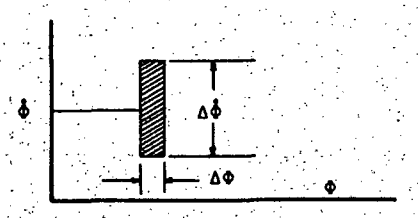

Fig. 7: Motion state plane Φ-$\dot\Phi$

APPLICATION

Applied to the linear motion equation

$$\ddot\Phi + d\dot\Phi + c\Phi = e \tag{36}$$

the integration of the Fokker-Planck equation (Fig. 8) gave accurate coincidence with simulations as well as with the theoretical normal distribution

$$p = \frac{1}{2\pi\overline{\Phi^2}\,\overline{\dot\Phi^2}} \exp\left(-\frac{\Phi^2}{2\overline{\Phi^2}} - \frac{\dot\Phi^2}{2\overline{\dot\Phi^2}}\right) \tag{37}$$

with

$$\overline{\Phi^2} = \frac{S_e\pi}{2d}\ ;\ \overline{\dot\Phi^2} = c\overline{\Phi^2} \tag{38}$$

In case of nonlinear motion equations, we compared results (Fig. 9) with those of simulations and found differences which could not yet be resolved. Fig. 10 compares, e.g., cumulative probability distributions $P_M(\Phi)$ of roll angle maxima found from simulations with those determined from the Fokker-Planck equation together with (34).

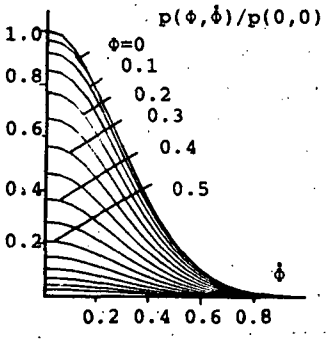

Fig. 8: Joint probability density $p(\Phi,\dot\Phi)$ for the linear motion equation $\ddot\Phi + 0.1\dot\Phi + \Phi = e$ with S_e=0.005

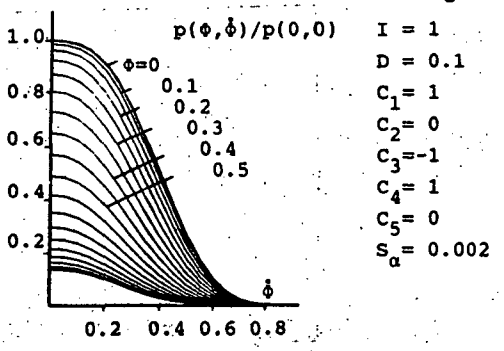

Fig. 9: Joint probability density $p(\Phi,\dot\Phi)$ for the linear motion equation (19)

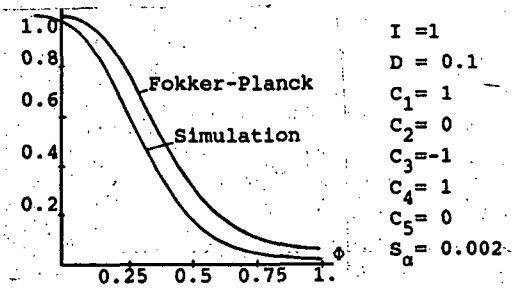

Fig. 10: Cumulative probability distribution of roll angle maxima for the motion equation of Fig. 9

We plan to apply this method for the extrapolation of the results of simulations or, perhaps, also of model experiments in heavy seaways to lower seaways and, correspondingly, quite small capsizing probabilities as follows: The motion history is passed through a low-pass filter to remove high-frequency excitations which have practically no influence on the roll motion. Then for a number of motion state classes $\Phi \pm \Delta\Phi/2$, $\dot{\Phi} \pm \Delta\dot{\Phi}/2$, the mean value and the variance of the filtered roll acceleration are determined from the time history, giving estimations of $b(\Phi,\dot{\Phi})$ and $S_e(\Phi,\dot{\Phi})$. For a seaway with a lower significant height but equal period and angle of encounter, $S_e(\Phi,\dot{\Phi})$ is changed by multiplication with a constant factor. Using these b and S_e functions, $p(\Phi,\dot{\Phi})$ and P_R are determined as described above.

Due to the very stable numerical results of the described integration method of the Fokker-Planck equation and to the extremely small computing effort for 1 degree of freedom systems, it seems possible to extend this method, if worthwhile, by explicitely deeling with more degrees of freedom and/or to excitations with non-constant spectra.

ACKNOWLEDGEMENT

Part of the work was financed by the German Federal Ministry for Research and Technology.

SYMBOLS

A	see Fig. 2
$\underline{b}(\underline{x},\dot{\underline{x}})$	forces and moments upon the ship due to position $\underline{x}$ and motion $\dot{\underline{x}}$
C_1 to C_5	constants in the roll motion equation (19)
D	roll damping constant
$\underline{e}(\underline{x},\dot{\underline{x}},t)$	wave exciting forces and moments upon the ship
f_c	capsizing frequency
f_o	mean zero-upcrossing period of the seaway
$F(\Phi)$	rate of upcrossings of Φ
h	wave height
H	significant wave height of a seaway
H_1	significant height used for simulation
i	designates components of a vector
I	roll moment of inertia
k	index referring to $\dot{\Phi} = k\Delta\dot{\Phi}$
K	number of capsizes simulated
m_o	variance of sea surface height
n	wave component index
N	number of roll periods simulated
p	probability that the ship capsizes after encountering n successive waves exceeding height h
p	probability density of $\Phi,\dot{\Phi}$
P_M	cumulative probability distribution of roll amplitudes
P_R	probability of capsizing during time T_R
P_T	probability of capsizing during time T
S	wave spectrum
S_e	spectrum of roll exciting moment
S_α	spectrum of α
T	time interval
T_c	mean time between successive capsizes
T_R	mean roll period in a seaway
$\underline{x}$	6-component vector of position and orientation of the ship
$\underline{Y}$	transfer function amplitude between seaway and exciting forces and moments
$\underline{\varepsilon}$	phase angle between wave and exciting forces and moments
α	wave slope
$\Delta\dot{\Phi}$	stepsize of $\dot{\Phi}$
Φ	roll angle
$\dot{}$	designates time derivatives
$\underline{\ }$	designates a vector

REFERENCE

/1/Caughey, T. K.
Derivation and application of the Fokker-Planck equation to discrete nonlinear dynamic systems subjected to white random excitation.
Journal of the Acoustical Society of America 35 (1963), No.11, p. 1683.

APPENDIX

We define a motion state vector $\underline{X}(t)$ as a 12-component vector consisting of $\underline{x}$ (1st to 6th component) and $\dot{\underline{x}}$ (7th to 12th component). We further write, similar to /1/, $p_c(\underline{X}|\underline{Z},\Delta t)$ for the conditional probability density that the ship has the motion state $\underline{Z}$ at time $t + \Delta t$ if it had the motion state $\underline{X}$ at time t. We further define for i, j = 1 to 12:

$$A_i(\underline{X})=\lim_{\Delta t\to 0}\frac{1}{\Delta t}\int_{-\infty}^{\infty}\cdots\int_{-\infty}^{\infty}(Z_i-X_i)p_c(\underline{X}|\underline{Z},\Delta t)dZ_1..dZ_{12}$$

and

$$B_{ij}(\underline{X})=\lim_{\Delta t\to 0}\frac{1}{\Delta t}\int_{-\infty}^{\infty}\cdots\int_{-\infty}^{\infty}(Z_i-X_i)(Z_j-X_j)\cdot$$

$$p_c(\underline{X}|\underline{Z},\Delta t)dZ_1..dZ_{12}$$

assuming that these limits exist and that corresponding higher-order quantities involving three or more factors $Z_i - X_i$ are zero. Thus, A_i and B_{ij} are measures of the average change of the state vector with time.

With these definitions, the probability density $p(\underline{X})$ satisfies the stationary Fokker-Planck equation

$$\frac{1}{2}\sum_{i=1}^{12}\sum_{j=1}^{12}(B_{ij}p)_{X_iX_j}-\sum_{i=1}^{12}(A_ip)_{X_i}=0$$

where indices X_i and X_j designate partial derivatives.

To apply this to our problem, we have to determine A_i and B_{ij}, using (20) and (21). For $i = 1,\ldots,6$ we have

$$A_i(\underline{X})=\lim_{\Delta t\to 0}\int_{-\infty}^{\infty}\cdots\int_{-\infty}^{\infty}\frac{x_i(t+\Delta t)-x_i(t)}{\Delta t}\cdot$$

$$p_c(\underline{X}|\underline{Z},\Delta t)dZ_1..dZ_{12}=\dot{x}_i$$

and

$$A_{6+i}(\underline{X})=\lim_{\Delta t\to 0}\int_{-\infty}^{\infty}\cdots\int_{-\infty}^{\infty}\frac{\dot{x}_i(t+\Delta t)-\dot{x}_i(t)}{\Delta t}\cdot$$

$$p_c(\underline{X}|\underline{Z},\Delta t)dZ_1..dZ_{12}=\langle\ddot{x}_i\rangle$$

where $\langle\ \rangle$ designates the mean value over different realizations, i. e. different phase angles ε_n in (21). The mean value will depend on $\underline{x}$ and $\dot{\underline{x}}$ and is, therefore, not a temporal mean.

Inserting into the above equation $\ddot{x}_i$ from (20) leads to

$$A_{6+i}(\underline{X})=\langle e_i(\underline{x},\dot{\underline{x}},t)-b_i(\underline{x},\dot{\underline{x}})\rangle=-b_i(\underline{x},\dot{\underline{x}})$$

Corresondingly, for i, j=1,...,6 we obtain

$$B_{ij}=\lim_{\Delta t\to 0}\Delta t\int_{-\infty}^{\infty}\cdots\int_{-\infty}^{\infty}\frac{x_i(t+\Delta t)-x_i(t)}{\Delta t}\cdot\frac{x_j(t+\Delta t)-x_j(t)}{\Delta t}\cdot$$

$$p_c dZ_1..dZ_{12}=\lim_{\Delta t\to 0}\Delta t\ \dot{x}_i\ \dot{x}_j=0\ ;$$

$$B_{i+6,j}=\lim_{\Delta t\to 0}\Delta t\int_{-\infty}^{\infty}\cdots\int_{-\infty}^{\infty}\ddot{x}_i\ \dot{x}_j\ p_c\ dZ_1..dZ_{12}=$$

$$\lim_{\Delta t\to 0}\Delta t\ \langle e_i-b_i\rangle\dot{x}_j=0$$

because $\langle b_i\rangle=b_i$ is finite and $\langle e_i\rangle=0$. Correspondingly, $B_{i,j+6}=0$.

In the above formulae, writing $\ddot{x}_i$ and e_i is not exact because what is really meant is the temporal mean value of $\ddot{x}_i$ or e_i, respectively, between t and t+Δt for Δt→0. Due to the white-noise assumption, e is an unsteady time function with zero mean and infinite variance. The last fact requires to be more cautios in determining $B_{i+6,j+6}$:

$$B_{i+6,j+6}=\lim_{\Delta t\to 0}\frac{1}{\Delta t}\left\langle\int_t^{t+\Delta t}\ddot{x}_i\,dt\cdot\int_t^{t+\Delta t}\ddot{x}_j\,dt\right\rangle\cdot$$

$$=\lim_{\Delta t\to 0}\frac{1}{\Delta t}\left\langle\int_t^{t+\Delta t}(e_i-b_i)dt\cdot\int_t^{t+\Delta t}(e_j-b_j)dt\right\rangle$$

$$=\lim_{\Delta t\to 0}\frac{1}{\Delta t}\left\langle\int_t^{t+\Delta t}e_i\,dt\cdot\int_t^{t+\Delta t}e_j\,dt\right\rangle$$

With (21) we obtain

$$\int_t^{t+\Delta t}e_i\,dt=\lim_{\substack{\Delta\omega_n\to 0\\ \omega_1\to 0\\ \omega_n\to\infty}}\sum_{n=1}^{N}\sqrt{2S\Delta\omega_n}\ \frac{Y_i}{\omega_n}\cdot$$

$$\left\{\sin\left(\omega_n(t+\Delta t)+\varepsilon_i+\varepsilon_n\right)-\sin\left(\omega_n t+\varepsilon_i+\varepsilon_n\right)\right\}$$

$$=\lim_{\Delta\omega_n\to 0}\sum_{n=1}^{N}\sqrt{2S\Delta\omega_n}\ \frac{Y_i}{\omega_n}\cdot$$

$$2\cos\left(\omega_n(t+\frac{\Delta t}{2})+\varepsilon_i+\varepsilon_n\right)\sin(\omega_n\frac{\Delta t}{2})$$

Inserting this into the expression for $B_{i+6,j+6}$ yields.

$$B_{i+6,j+6}=\lim_{\Delta t\to 0}\lim_{\Delta\omega_n\to 0}\sum_{n=1}^{N}\sum_{m=1}^{N}2S\sqrt{\Delta\omega_n\,\Delta\omega_m}\cdot$$

$$\frac{Y_iY_j}{\omega_n\omega_m}\cdot\frac{4}{\Delta t}\cdot\left\langle\cos\left(\omega_n(t+\frac{\Delta t}{2})+\varepsilon_i+\varepsilon_n\right)\cdot\right.$$

$$\sin(\omega_n\frac{\Delta t}{2})\cos\left(\omega_n(t+\frac{\Delta t}{2})+\varepsilon_j+\varepsilon_m\right)\cdot$$

$$\left.\sin(\omega_m\frac{\Delta t}{2})\right\rangle$$

Terms with $m\neq n$ are zero because ε_n and ε_m are uncorrelated. Further, we have

$$\langle\cos(\varepsilon_n)\sin(\varepsilon_n)\rangle=0$$

and

$$\left\langle\left(\cos(\varepsilon_n)\right)^2\right\rangle=\left\langle\left(\sin(\varepsilon_n)\right)^2\right\rangle=\frac{1}{2}$$

Using these relations after splitting in the above cosine functions the random phase angle from the non-random angles leads to

$$B_{i+6,j+6}=\lim_{\Delta t\to 0}\lim_{\Delta\omega_n\to 0}\sum_{n=1}^{N} 2\,S\,\Delta\omega_n\frac{Y_iY_j}{\omega_n^2}\cdot\frac{4}{\Delta t}\cdot$$

$$\frac{1}{2}\left(1-\cos(\omega_n\Delta t)\right)\cdot<\left\{\cos\left(\omega_n(t+\frac{\Delta t}{2})+\varepsilon_i\right)\cos\varepsilon_n-\sin\left(\omega_n(t+\frac{\Delta t}{2})+\varepsilon_i\right)\sin\varepsilon_n\right\}\cdot\left\{\cos\left(\omega_n(t+\frac{\Delta t}{2})+\varepsilon_j\right)\cos\varepsilon_n-\sin\left(\omega_n(t+\frac{\Delta t}{2})+\varepsilon_j\right)\sin\varepsilon_n\right\}>$$

$$=\lim_{\Delta t\to 0} 2\,S\,\frac{Y_iY_j}{\Delta t}\cos(\varepsilon_i-\varepsilon_j)\cdot\int_0^{\infty}\frac{1-\cos(\omega\Delta t)}{\omega^2}\,d\omega$$

Because the integral is equal to $\frac{\Delta t\cdot\pi}{2}$, we obtain

$$B_{i+6,j+6} = \pi\,S\,Y_i\,Y_j\cos(\varepsilon_i-\varepsilon_j)$$

Inserting A_i and B_{ij} into the Fokker-Planck equation leads immediately to equation (22).

AUTHORS

H. Söding, Institut für Schiffbau der Universität Hamburg, Federal Republic of Germany
E. Tonguc, Institut für Schiffbau der Universität Hamburg, Federal Republic of Germany

Third International Conference on Stability of Ships and Ocean Vehicles, Gdańsk, Sept. 1986

STAB'86

SHIP MOTION CALCULATION IN A SEAWAY BY MEANS OF A COMBINATION OF STRIP THEORY WITH SIMULATION

PETER KRÖGER

1 Abstract

This paper deals with the simulation of the rolling motion of a ship in an irregular seaway. The angles between ship's course and direction of approach of waves are of any size desired. The seaway is approximated by a substitute wave. Surging can be considered.

2 Introduction

Strip theory is known to give relatively reliable results even in heavy seaways for heaving and pitching motions. For other motion components, however, results are hardly acceptable or, notably for rolling motions, unacceptable for practical purposes. On the other hand, strip motion simulations are either unreliable (because couplings or hydrodynamic effects are disregarded) or extremely complicated. Therefore, if we are interested mainly in rolling motions and capsizing, a mixed strategy may be the best choice: The rolling motions, being highly nonlinear, have to be treated by simulation. Fortunately, hydrodynamic effects are less important for rolling motion alone, so that a predominantly hydrostatic calculation method for the righting moments may be used. Coupling with the other motions, however, influences the rolling motion severely by means of inertial terms and of the position of the actual waterline along the ship which has to be used to compute rigthing moments. These other motions are less nonlinear and influenced less severely by hydrodynamic forces; thus they are treated best by the strip method.

3 Method of Simulation

This paper deals with the simulation of the rolling motion of a ship in an irregular, stationary, short crested sea, i.e. solving the time function $\varphi(t)$ starting with an initial state. The problem is solved by means of a method, which has been developed by Söding [1] for the solution of continuous, stochastic processes. This general applicable method is shown in figure 1.

The method combines a given exciting process $z_1(t)$ with responses which are linearly dependent ($z_k(t)$, k = 2....,NZ), and those which are not linearly dependent ($x_l(t)$, l= 1,...,NX and $y_m(t)$, m = 1,...,NY). The definition of the exciting process is given in (1). The equations for the other $z_k(t)$ are given in (2). $\hat{Y}_{k,j}$ are the response amplitude operator which are used during the rolling simulation to determine the coupling between the rolling motion and the other five degrees of freedom.

$$z_1(t) = \sum_{j=1}^{N} Re\left[\hat{z}_j \cdot e^{i\omega_j t}\right] \qquad (1)$$

$$z_k(t) = \sum_{j=1}^{N} Re\left[\hat{Y}_{k,j} \cdot \hat{z}_j \cdot e^{i\omega_j t}\right] \qquad (2)$$

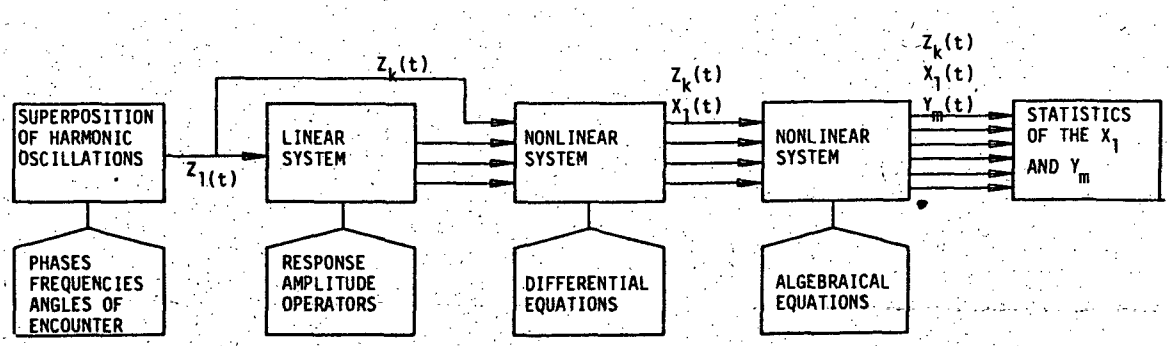

FIGURE 1

The differential equations for the definition of the x (t) are given in (3)

$$\dot{x}_1(t) = f_1(x_1(t), \ldots, x_{NX}(t), z_1(t), \ldots, z_{NS}(t), t) \quad (3)$$

$$\dot{x}_{NX}(t) = f_{NX}(x_1(t), \ldots, x_{NX}(t), z_1(t), \ldots, z_{NS}(t), t) \quad (4)$$

The definition of the $y_m(t)$ is given by the algebraical equation (5).

$$y_m(t) = g_m(x_1(t), \ldots, x_{NX}(t), z_1(t), \ldots, z_{NS}(t), t) \quad (5)$$

The differential equations are numerically solved with a Runge-Kutta-Method of fourth order with constant step size.

The stochastic sea state is approximated by the superposition of regular wave components with random and constant distributed phases, frequencies and angles of encounter.

The linearly dependent processes are:

z_1	wave elevation at the midship section
z_2	heaving motion at the midship section
z_3	heaving acceleration at the midship section
z_4	pitch angle of the ship
z_5	pitch angle acceleration of the ship
z_6	sway acceleration of the ship
z_7	yaw acceleration of the ship
z_8	exciting moment of rolling
z_9	amplitude of the mean lowering of the substitute wave in the region of the ship's length
z_{10}	amplitude of the mean inclination of the water surface (substitute wave)
z_{11}	complex amplitude of the substitute wave with crest or trough at the midship section

z_2 to z_8 are calculated by the strip-method, z_9 to z_{11} are discribed more precise in chapter 4.

4 Seaway and Substitute Wave

The seaway is represented by the superposition of wave components, which are computed from a sea spectrum. The wave components have random phases, directions of run and, in a given range, random circular frequencies.

In the computer program the above described seaway is substituted by a substitute wave. This substitute wave, is first discribed for the case surging is neglected.

The water level, dependent on the length coordinate x and the time t, is given in (6).

$$\zeta(x,t) = \sum_{n=1}^{N} Re\left[\hat{\zeta}_n \cdot e^{i(\omega_{en}t - k_n x \cos\mu_n)}\right] \quad (6)$$

The lever of the righting moments which are used for the simulation are calculated hydrostatically. The righting arms are highly non linearly dependent on the parameters of shape of the underwaterbody. Therefore the resulting righting arm cannot be calculated as a sum of the righting arms of the regular component waves. The actual water contour is approximated by a similar acting, substitute wave, which is regular in x-direction and stochastically oscillating in time. This is given in (7).

$$\zeta_a(x,t) = \sum_{n=1}^{N} Re\left[\left(\hat{a}_n + \hat{b}_n x + \hat{c}_n \cos\left(\frac{2\pi}{\lambda}x\right)\right) \cdot e^{i\omega_{en}t}\right] \quad (7)$$

Each item in (7) approximates a corresponding item in (6). In (7) $\hat{a}_n$ is the amplitude of the mean depth of the trough as a result of the regular wave components in the region of the ship's length; $\hat{b}_n$ is the amplitude of the mean inclination of the water surface and $\hat{c}_n$ is the amplitude of a wave with crest or trough at the midship section. The $\hat{a}_n$, $\hat{b}_n$ and $\hat{c}_n$ are computed by using the method of the least squares of errors:

$$\int_{-\frac{L}{2}}^{+\frac{L}{2}} (\zeta(x,t) - \zeta_a(x,t))^2 \, dx \longrightarrow Min! \quad (8)$$

Using the symmetry $\frac{\hat{a}_n}{\hat{\zeta}_n}$ and $\frac{\hat{c}_n}{\hat{\zeta}_n}$ are real, $\frac{\hat{b}_n}{\hat{\zeta}_n}$ is imaginary. Then (7) can be written as (9).

$$\zeta_a(x,t) = \sum_{n=1}^{N} Re\left[\left(\hat{\zeta}_n\left(a_n + ib_n + c_n \cos\left(\frac{2\pi x}{\lambda}\right)\right)\right) e^{i\omega_{en}t}\right] \quad (9)$$

So a_n, b_n and c_n can be computed as (10), (11) and (12), with the abbreviations $f(w) = \frac{\sin w}{w}$; $s = \frac{\pi L}{2}$ and $r_n = \frac{k_n L}{2}\cos\mu_n$.

$$a_n = \frac{f(r_n)\,[1 + f(2s)] - [f(r_n - s) + f(r_n + s)]\, f(s)}{1 + f(2s) - f(2s)^2} \quad (10)$$

$$c_n = \frac{f(r_n - s) + f(r_n + s) - 2f(r_n)f(s)}{1 + f(2s) - f(2s)^2} \quad (11)$$

$$b_n = \frac{6}{L}\left[\frac{\cos r_n}{r_n} - \frac{\sin r_n}{r_n}\right] \quad (12)$$

If surging is taken into consideration, the amplitudes of the wave components at the midship section are different from the amplitudes which were computed without surging because the ship now is moved forward by the extent ξ.

If surging is considered the complex amplitudes of the waves at the midship section are computed by (13).

$$\tilde{\zeta}_n = \hat{\zeta}_n e^{ik_n \xi \cos\mu_n} \quad (13)$$

Putting (13) into (6) gives (14).

$$\zeta_n(x,t) = \sum_{n=1}^{N} Re\left[\tilde{\zeta}_n e^{ik_n \cos\mu_n \xi} e^{i(\omega_{en}t - k_n \tilde{x}\cos\mu_n)}\right] \quad (14)$$

with (15)

$$\tilde{x} = x + \xi \quad (15)$$

The coefficients a_n, b_n and c_n of the substitute wave change to (16) - (18) if surging is considered.

$$\hat{a}_n = \tilde{x}\hat{i}_n a_n = \hat{x}\hat{i}_n e^{-ik_n \xi \cos \mu_n} a_n \qquad (16)$$

$$\hat{b}_n = \tilde{x}\hat{i}_n b_n = \hat{x}\hat{i}_n e^{-ik_n \xi \cos \mu_n} b_n \qquad (17)$$

$$\hat{c}_n = \tilde{x}\hat{i}_n c_n = \hat{x}\hat{i}_n e^{-ik_n \xi \cos \mu_n} c_n \qquad (18)$$

5 Equations of motions

Rolling is simulated according to the nonlinear equation of motion (19)

$$\theta_x \ddot{\varphi} + d_L \dot{\varphi} + d_Q \dot{\varphi} |\dot{\varphi}| + AR = M + MW \qquad (19)$$

with:

θ_x	moment of inertia about x-axis
d_L	linear damping constant for rolling about x-axis
φ	roll angle about x-axis
d_Q	quadratic damping costant for rolling about x-axis
M	exciting moment about the x-axis induced by waves and sway and yaw motion, computed by a strip method
MW	constant heeling moment
AR	righting moment acc. to (20)

$$AR = (g - \ddot{z})\, m h(\varphi, T, t) + \ddot{\vartheta} \theta_{xz} \sin \varphi \qquad (20)$$

with

g	gravity acceleration
$\ddot{z}$	vertical acceleration of ship at midship section computed by strip method
m	mass of ship
h	righting lever depending on position afloat computed by simulation
$\ddot{\vartheta}$	pitch angle acceleration
θ_{xz}	deviation moment

Linear and quadratic damping constant of rolling are computed following Blume [2].

The actuel draught and trim are determined by (21) and (22).

$$T_e = T + z - a \qquad (21)$$

$$t_e = t + L_{pp}(\vartheta + b) \qquad (22)$$

with

T	mean draught in smooth water
z	actuel heave of ship
t	mean trim in smooth water
ϑ	actuel pitch angle

The righting lever is interpolated quadratically between the levers computed hydrostatically for crest, trough and plane surface:

$$h(T,t,\varphi) = h_P(T,t,\varphi) + \frac{c}{2\zeta_R}(h_C(T,t,\varphi) - h_T(T,t,\varphi)) + \frac{c^2}{2\zeta_R^2}(h_C(T,t,\varphi) - 2h_P(T,t,\varphi) + h_T(T,t,\varphi)) \qquad (23)$$

with

ζ_R	amplitude used for computation levers
h_P	lever in smooth water
h_C	lever in crest wave
h_T	lever in trough of wave

Test computations show a small dependence of the results of the simulation an wave height and length used for hydrostatic lever computation. This is given in table I.

wavelenght	waveheight	φ_{min}	φ_{max}
127.5 m	8.5 m	-23.08	20.93
102.0 m	8.5 m	-22.46	20.70
153.0 m	8.5 m	-23.37	21.00
127.5 m	12.75 m	-24.59	21.58
127.5 m	6.38 m	-22.33	20.71

TABLE I.

This justifies the introduction of the substitute wave.

6 Surging

The equation of equilibrium for a surging ship is (24):

$$R - T_e + \delta R + m^* \ddot{\xi} = 0 \qquad (24)$$

with

R	Resistance of ship
T_e	Thrust without thrust deduction
ΔR	added resistance by waves and ship motion depending on position of ship relative to waves
m	mass of ship including hydrodynamic mass for surging
$\ddot{\xi}$	acceleration of ship in direction of progress
μ	angle between ship's course and direction of approach of waves measured from stern of ship

Constant thrust is assumed. Thus $\ddot{\xi}$ is given by (25):

$$\ddot{\xi} = -\left(\frac{2R(v_0)}{v_0 m^*}\dot{\xi} + \frac{R(v_0}{v_0^2 m^*} + \frac{\delta R}{m^*}\right) \qquad (25)$$

with

$$\Delta R_n = \sum_{n=1}^{NOM} \varrho \left(g - \ddot{z} + x_s \ddot{\vartheta}\right) e^{-k_n \overline{T}} \qquad (26)$$

$$Re\left[\hat{\zeta}_n i k_n \cos\mu_n e^{i\omega_m t} e^{-ik_n \cos\mu_n} \int_{-\frac{L}{2}+\epsilon}^{\frac{L}{2}+\epsilon} A(x) e^{-ik_n x \cos\mu_n} dx\right]$$

7 Results

Computed results for the container vessel E.L.M.A. Tres are given in the figures 2-8. The seaway is represented by the superposition of 25 wave components. The significant period is 12.64 s, the significant wave height is 8.5 m. Figure 2 gives the speed of rolling and the rollangle. Figure 3 gives the change of speed in direction of progress in the seaway and the additional way caused by the surging motion. Figure 4 gives the righting lever and the acceleration in the direction parallel to the deck. Figure 5 gives the amplitude of the mean lowering and the amplitude of the mean inclination of the water surface (substitute wave). Figure 6 gives the actual draught and the amplitude of the substitute wave. Figure 7 gives the actual trim and the wave elevation at the midship section. Figure 8 gives the frequency curve of the roll angle.

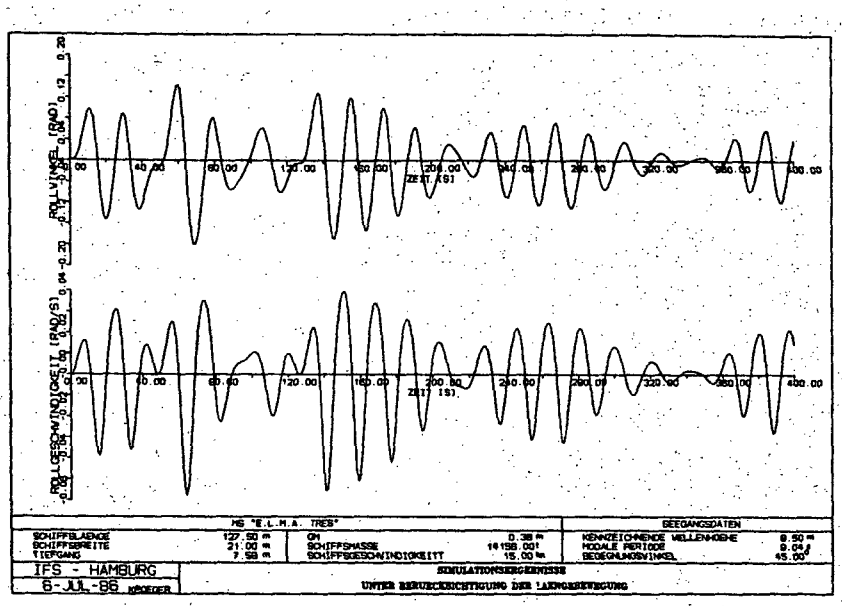

FIGURE 2

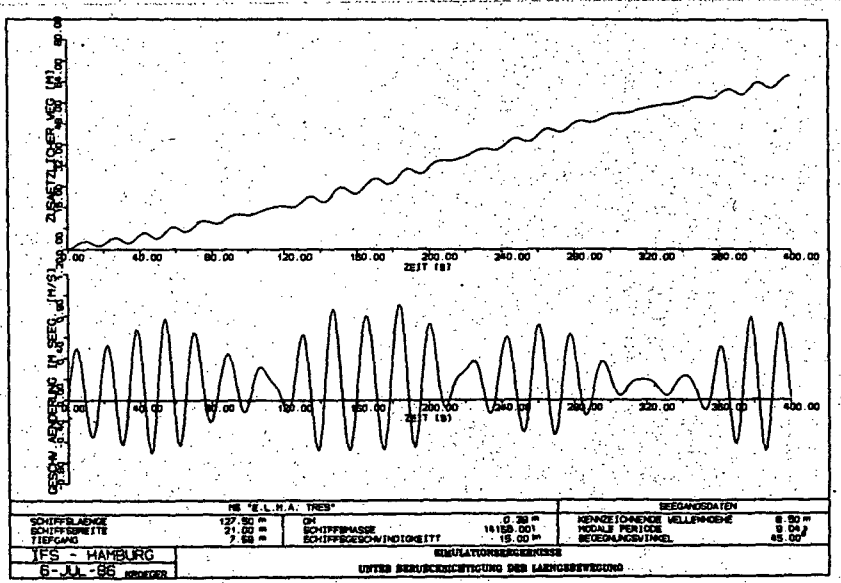

FIGURE 3

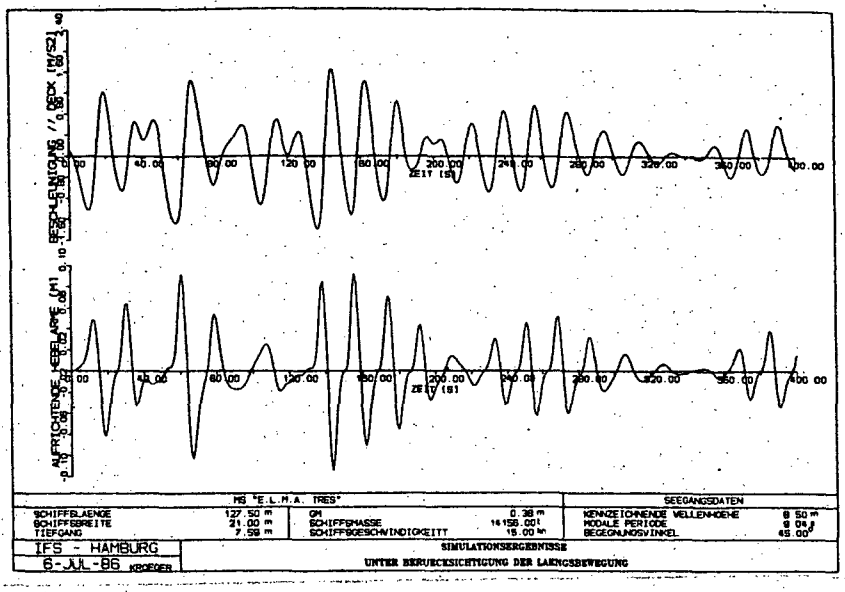

FIGURE 4

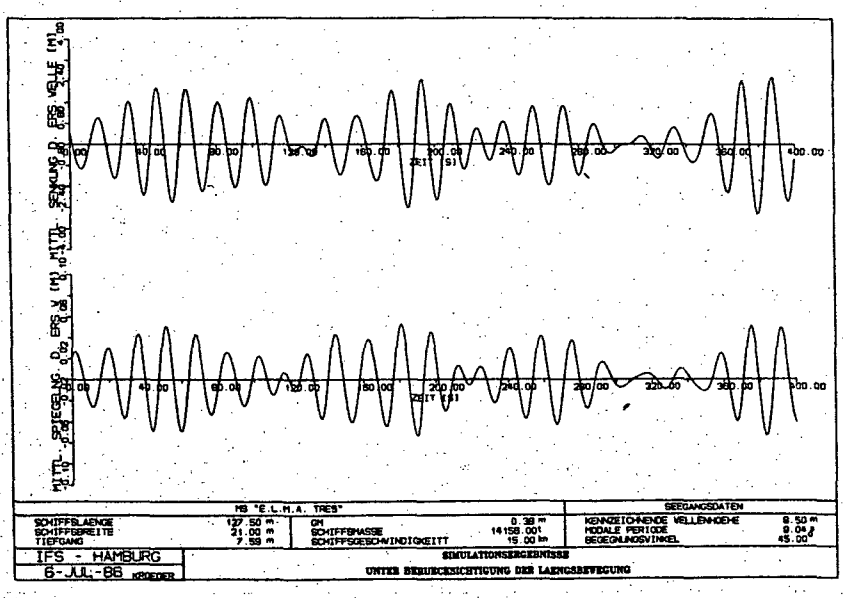

FIGURE 5

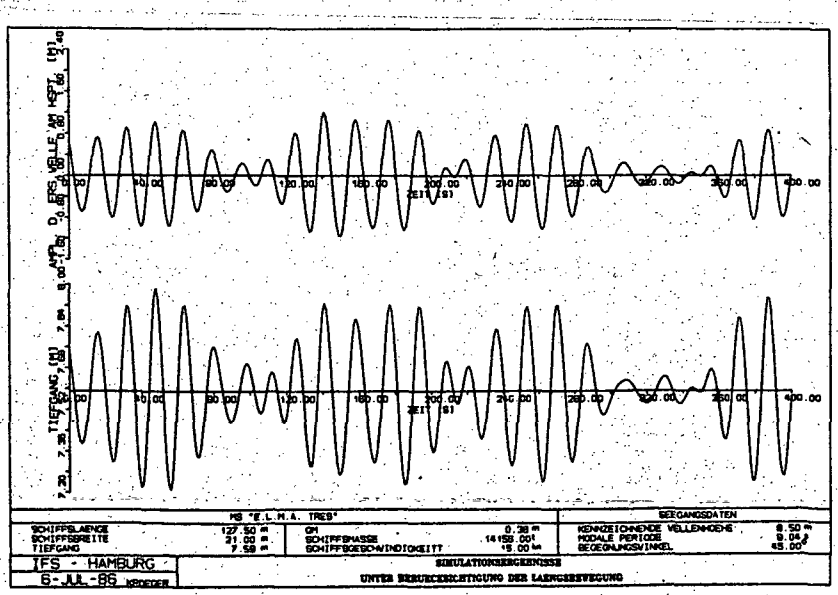

FIGURE 6

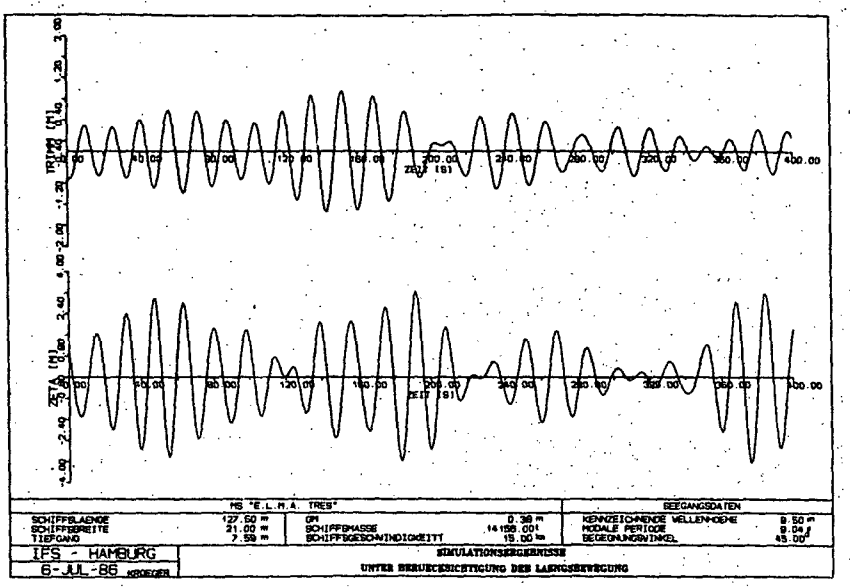

FIGURE 7

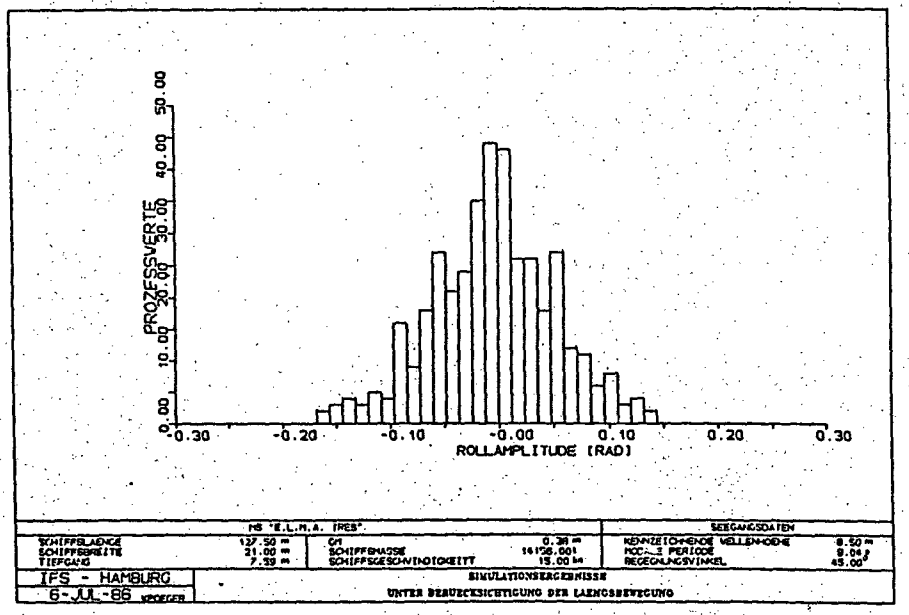

FIGURE 8

Literatur

[1] Söding, H.
Gutachten über Belastungen des Schiffes E.L.M.A. Tres durch Seegang am Vormittag des 26.11.1981
IfS-Schrift Nr.2327, 1982

[2] Blume, P.
Experimentelle Bestimmung von Koeffizienten der wirksamen Rolldämpfung und ihre Anwendung zur Abschätzung extremer Rollwinkel.
Schiffstechnik, 1979, S.3/29

8 Author

Peter Kroeger, Institut fuer Schiffbau der Universitaet Hamburg, Federal Republic of Germany.

Third International Conference on Stability of Ships and Ocean Vehicles, Gdańsk, Sept. 1986

STAB'86

INVESTIGATION OF THE STABILIZING MOMENT GENERATED BY PASSIVE STABILIZING TANKS

V. Rakitin, Tz. Tzvetanov

1. ABSTRACT

The problem of investigating the stabilizing moment generated by passive stabilizing tanks with the aid of model tests is rather interesting from the viewpoint of improving the methods for calculation of stabilized ship's motion and creation of methods for stabilizing tanks design. This, however, requires the conduct of a large-volume cycle of model tests of the ship-tank system.

The paper presents part of the results from model tests carried out on passive stabilizing tanks in conditions of forced roll motion with variable amplitude and frequency. Graphic dependences of the stabilizing moment on parameters varying during the tests, e.g. metacentric height, water level in the tank, etc., are quoted. With the aim of obtaining reliable experimental data on the stabilizing moment and horizontal and vertical forces, a three-components measuring system was specially designed and manufactured; it is designated both for model tests in experimental tank and for carrying out of model investigations on a stand.

2. INTRODUCTION

The model tests of the ship-tank system for investigation of the stabilizing moment built by passive stabilizing tanks is connected with considerable preliminary preparation. This preparation includes design and manufacture of suitable tank and ship models as well as set up of reliable and accurate force-measuring system.

In order to meet the requirements for clear measurements of this moment it is often necessary to built complex multicomponent dynamometers which need sophisticated static and dynamic balancing. It should be noted that considerable attention should be paid also to the internal damping coefficients of the tanks considering the scale effect. The accurate determination or setting of the damping coefficient is separate problem, which has to be solved during the preparation of the tests. Hence the reliability of the experimental results depends considerably on the factors stated above.

The present paper discusses the approach applied at BSHC for conducting model tests with account on all these considerations. The tests were carried out with flume-tanks and free surface tanks. A reliable three-component force-measuring system was designed. The behaviour of ship model equipped with stabilizing tank was investigated in both regular and irregular waves. In addition, forced rolling tests of the system ship-model-stabilizing tank were carried out. On the specially designed single component stand, tests of isolated models of the investigated tanks were carried out as well.

3. TEST PROGRAM

The investigation of the behaviour of the ship model-stabilizing tank system is carried out in the BSHC manoeuvring and seakeeping tank, at two tank states:

- "off" tank state - the tank was dried up and the water in it is replaced by a rigid cargo equivalent to it in weight, which is located so that the mass inertia characteristics of the model-tank system are preserved;
- "on" tank state - the tank is filled with water to the level necessary for the investigations

The following experiments are realized:

- regular wave tests with wave parameters:
  λ = 2.14 - 6.24 m $\alpha_o \approx 5°$
- irregular wave tests at two spectra with the following characteristics in model scale:

τ_{z_1} = 1.5 sec	$h_{1/3}$ = 10.0 sm
τ_{z_2} = 2.0 sec	$h_{1/3}$ = 9.5 sm

- forced rolling tests by gyroscope oscillator-carried out with the aim of comparative analysis; for the purpose harmonic heeling moment is generated in the frequency range of the regular waves;

- stand (roll simulator) tests.

In the course of the investigations the water level in the tanks is varied, as well as the coefficient of their internal damping and the metacentric height. The coefficient of internal damping in the two tanks is varied by means of perforated bulkheads located transverse to the water flow. Regular wave tests, irregular wave tests and forced rolling tests are carried out at zero speed.

During the experiments the following values are registrated:

- roll amplitude;
- stabilizing moment amplitude;
- horizontal force amplitude;
- vertical force amplitude;
- heeling moment amplitude;
- wave parameters in the tank.

The experimental data are recorded and processed by a computer.

4. EXPERIMENTAL SET-UP

The experimental investigation of the roll stabilization is performed in two basic directions:

- investigation of stabilizing tanks effectiveness in conditions close to real ones;
- investigations of tanks' internal hydrodynamic characteristics, which imposes the carrying out of two type of tests;
- tests of ships models equipped with passive stabilizing tanks and
- tests of separate models of stabilizing tanks on a special stand.

The tests of the ship model - stabilizing tank system are carried out in a test tank in regular or irregular waves without speed and under the action of a harmonic heeling moment generated by a forced rolling oscillator at necessity for ship model movement. The following values are measured in the course of the tests:

- roll motion amplitudes of non-stabilized and stabilized ship model;
- harmonic heeling moment amplitude;
- stabilizing moment generated by the passive stabilizing tank;
- horizontal force generated by the fluid moving in the tank;
- vertical force generated by this fluid (only during tests in waves).

The data are recorded on a minicomputer, which is part of the automated system for acquisition and processing of experimental results. A principle scheme of the experimental set up is given in Fig. 1.

The tests of separate models of passive stabilizing tanks are conducted on a special stand creating harmonic oscillating motion round a fixed axis. The following values are measured during the investigations:

- stabilizing moment amplitudes of the tanks;
- horizontal force amplitudes of the liquid motion;
- oscillating motion amplitudes.

The measurements are performed at different coefficients of internal damping in the tanks and at different levels of the liquid in them. The data are recorded on a minicomputer. The principle scheme of the experimental set-up is shown in Fig. 2.

In both test types a three-component force measuring system is used.

The principle scheme of this system is shown in Fig. 3. It is three-component one and allows measurement of the stabilizing moment, horizontal transverse force and vertical force generated by the stabilizing tank at different test conditions (1) .

The whole force measuring system is mounted into the ship model 1, where the tank 2 is located on the platform 3. The force loadings (Y, Z, M) are measured by the transducers 4 and 5. The roller connections 6 and 7 and the shafts 8 and 9 allow, on the one hand, transmitting to the pick-ups of the forces and moment being measured, and, on the other, protection of the pick-ups from parasitic loadings. The unit 10 serves for feeding of the pick-ups and output of the signals from them.

5. TEST RESULTS

As mentioned above, the processing of the data from the tests conducted is done by a computer, using programs based on FFT. For the sake of convenience the results from the processing are systematized in tabular form. Graphic dependences of the values being measured on the varying parameters are developed as well.

In the first stage of the investigations, the experiment preparation, the coefficients of internal damping in the tanks are determined by the method of freely decaying oscillations at different levels of the fluid in them. On this stage the permeability coefficients of the perforated bulkheads used for varying the damping are determined as well.

For the sake of convenience, in the course of the work the period of natural oscillations of the water in the tanks is discussed in the form of a fuction

$$T_z = f(h_s; S_o),$$

and the internal damping coefficient as a function of T_z :

$$M_z = f(T_z).$$

These dependences are presented in Figs. 4 and 5 for a free surface tank.

The second stage of the investigations covers the carrying out of all tests, the experimental data acquisition and initial processing. A typical example of the time histories is shown in Fig. 6. In the course of the experimental results processing, the amplitudes of the values being measured and the phase differences relative to the external disturbing influence are obtained.

During the stand tests the basic harmonics of the moment amplitude M_T' and its phase angle ε', corresponding to the circular frequency ω of the external disturbing influence, are determined. The "frozen" liquid moment M_F, necessary for the pure calculation of the stabilizing moment, is obtained from a "off tank" tests. The corrected value of the summed up moment M_T amplitude and the phase angle ε are determined by the formulae (4):

$$M_T = \sqrt{(M_T' \cos\varepsilon' - M_F)^2 + (M_T' \sin\varepsilon')^2}$$

$$\varepsilon = \operatorname{arc\,tg} \frac{M_T' \cdot \sin\varepsilon'}{M_T' \cdot \cos\varepsilon' - M_F}$$

The characteristic thus obtained are exemplified in Fig. 7 for a flume stabilization tank.

The same theoretical approach is used in the processing of the results from the forced rolling tests and the regular wave tests. For convenience's sake, in this case pure rolling motion round a longitudinal axis, passing through the ship's centre of gravity, is discussed. In first approximation the equation of this motion has the form

$$\ddot{\phi} + 2\nu_\phi \dot{\phi} + n_\phi \phi = m$$

where:

m - disturbing moment.

In the problem being discussed the disturbing moment applied is assumed to be strictly harmonic ; in this way the resultant motion will have the same nature. The moment m of an "on"stabilizing tank will have two components - heeling moment and the moment generated by the shifting of the fluid in the tank. The lather can also be assumed to be harmonic in the frequency range of interest (3) . Taking account of the allowances, the equation of roll motion assumes the form

$$\ddot{\phi} + 2\nu_\phi \dot{\phi} + n_\phi \phi = \alpha_m n_\phi^2 \sin\omega t + m_{ST}$$

where:

$$m_{ST} = \mu_\alpha \nu_s \cdot n_\phi^2 \sin\omega t$$

moment from the shifting of the fluid in the tank.

This dependence for the stabilizing moment is used as a basic one in the drawing up of analytical expressions taking account of the varying parameters' influence, with the aid of the regression analysis. In Fig. 8 are presented part of the initial results illustrating the influence of metacentric height, fluid level in the tank and amplitudes of motion on this dynamic moment. The general form of the approximating expression for the stabilizing moment is the following:

$$M_{ST} = \sum_j C_j (h_s)^{x_{1j}} \cdot (h_o)^{x_{2j}} \cdot (\phi_o)^{x_{3j}} \cdot (\omega)^{x_{4j}}$$

where

C_j - coefficients of transformation,

x_{ij} - calculated power values.

Usually, for convenience's sake it is assumed to present the dynamic moment from the tanks by means of two components $M_{ST} \cdot \cos\varepsilon$ and quadrature component $M_{ST} \cdot \sin\varepsilon$, depending on circular frequency ω. This arbitrary division is done in the course of investigating the effective work of the stabilizing tanks and plotting of the amplitude frequency characteristics of the stabilized ship.

In conclusion, it should be pointed out that the comparative analysis performed between the results from the regular wave tests and the forced rolling tests in still water gives a good coincidence. This allows the assuming the forced rolling tests, as basic in the investigation of the ship model-stabilizing tank system's behaviour.

6. FINAL REMARKS

The model tests carried out with the ship-stabilizing tank system in regular and irregular waves, the forced rolling tests in still water and the stand roll simulation tests with isolated models of the tanks aided the obtaining of a large volume of experimental results. These results afford the possibility to determine the dependences of the stabilizing moment on the parameters varried in the course of the tests. It should be pointed out that the problem formulation and the main conclusions are drawn assuming linearity of the oscillating ship- stabilizing tank system in the frequency range of interest. This allows the discussion of the amplitude-frequency characteristics of the values being investigated as linear transverse functions in the prediction of the tanks' effectiveness and the stabilized ship's behaviour in real sea waves. The data from the irregular wave tests with specified wave spectrum confirmed the correctness of the experimental set-up.

As the end results of the investigation, the creation could be pointed out of an empirical method which may be used at the preliminary stabilization tanks design stage.

7. ACKOWLEDGMENTS

The authors would like to express their appreciation and gratitude to Dr.ing. T.Zdybek from CTO - Gdansk for their valuable directions concerning the roll simulators experiment conduct technique.

8. NOMENCLATURE

h_o - metacentric height,
$h_{1/3}$ - significant wave height,
H - half-height of the tank's active volume,
h_s - level of the fluid in the tank,
M_F - "frozen" liquid moment,
M_{ST} - stabilizing moment,
n_ϕ - natural frequency of roll motion,
P - weight of the fluid in the tanks,
S_o - relative area of the free water surface,
T_z - period of the natural oscillations of the fluid in the tanks,
α_0 - maximal wave slope angle,
Δ - weight displacement,
ϵ - phase angle,
μ_z - dimensionless coefficient of internal damping in the tanks,
μ_α - proportionality coefficient,
s - static characteristic of the tanks,
ω - circular frequency .

9. REFERENCES

1. Rakitin V., Tz. Tzvetanov " Three Components Force-Moment Measuring System for Passive Stabilizing Tank Model Test", the 4th NSESAMT, Brasov , Romania, 1986.

2. Rorke J., "Ship Stabilizers - Fins and Tanks" Brown Brothers and Company Limited, Edinburgh,1969.

3.Vugts J.H., Bosh J.J., "Roll Damping by Free-Surface Tanks", Shipp. World and Shipbuilder, No. 3792, 1966.

4. Zdybek T., "The Use of Bench Test Results for Calculating Roll Response of the Tank Stabilized Ship","International Shipbuilding Progress" , April, 1980.

V.K.Rakitin, Research Scientist
Tz.T.Tzvetanov, Research Scientist
BSHC, 9003 Varna
BULGARIA

FIGURES

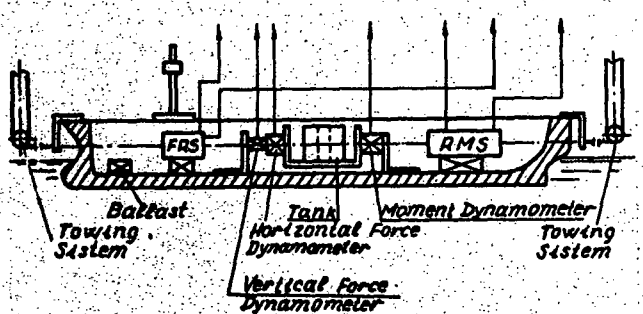

Fig. 1

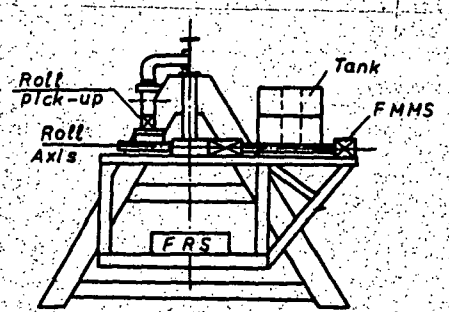

Fig. 2

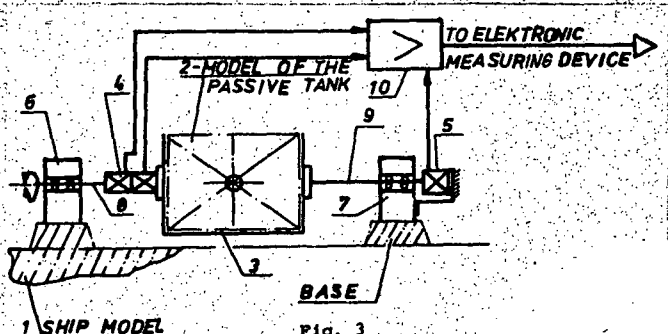

Fig. 3

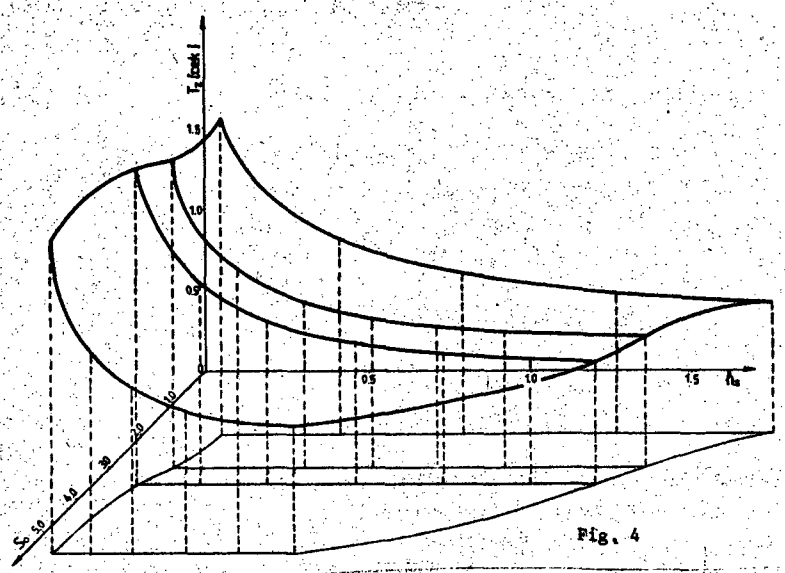

Fig. 4

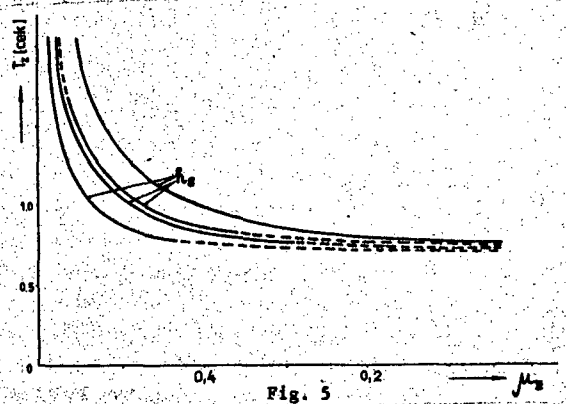

Fig. 5

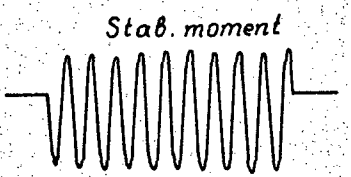

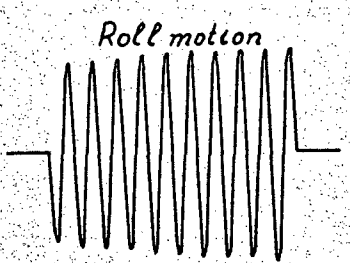

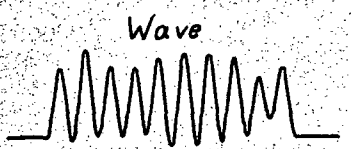

Fig. 6

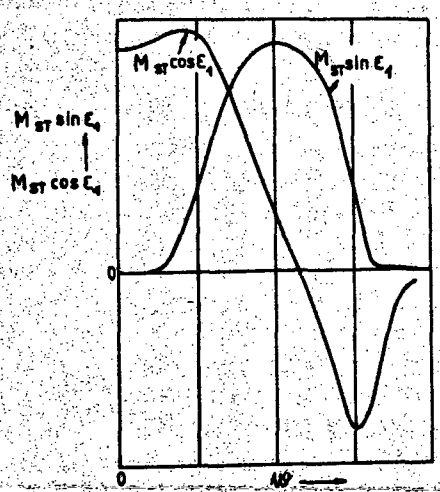

Fig. 7

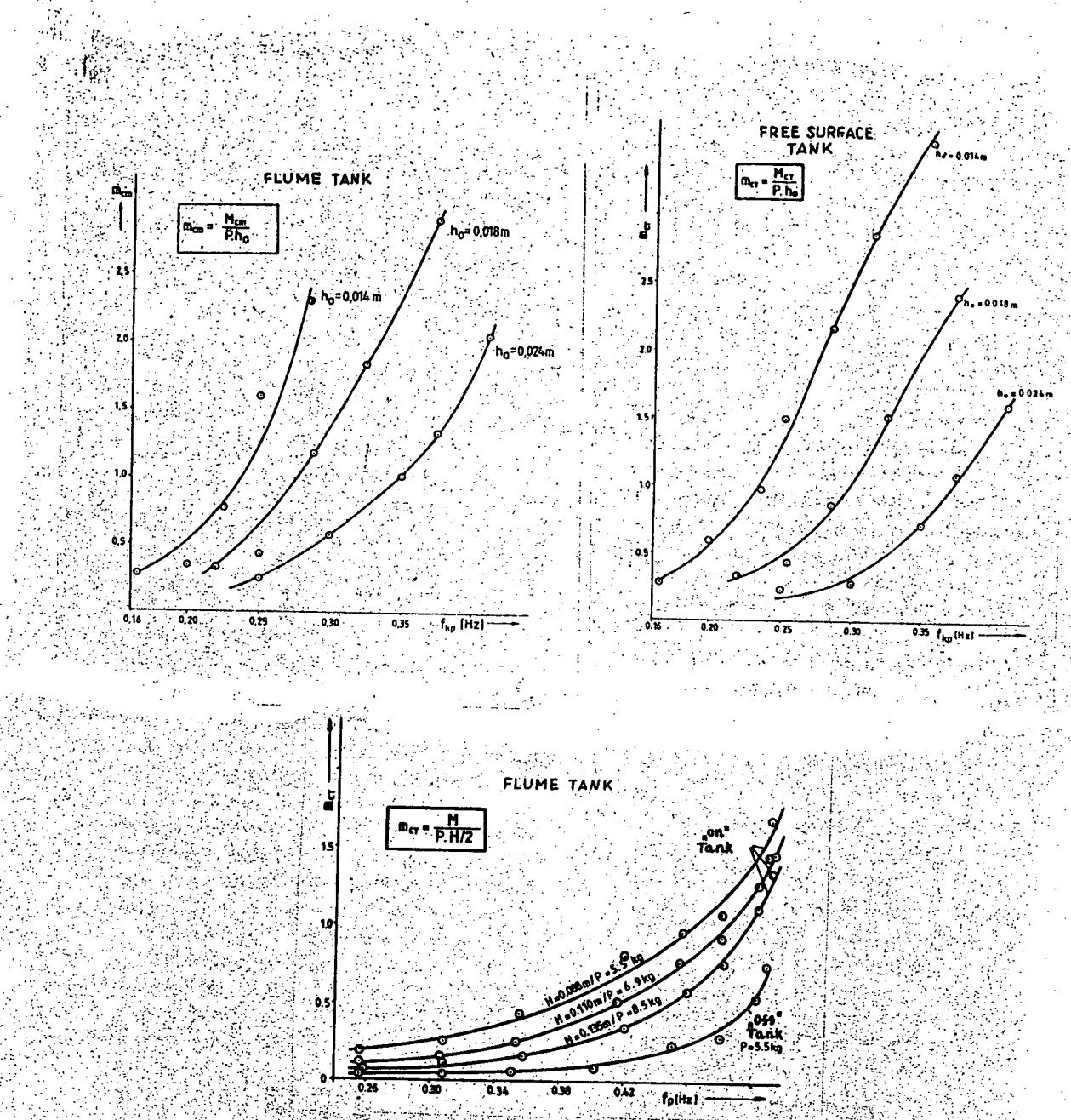
FLUME TANK
$m_{cm} = \frac{M_{cm}}{P.h_0}$
h_0=0,018m
h_0=0,014 m
h_0=0,024m
0.16
0.20
0.25
0.30
0.35
f_{kp} [Hz]
FREE SURFACE TANK
$m_{cT} = \frac{M_{cT}}{P.h_0}$
h_0 = 0.014m
h_0 = 0.018 m
h_0 = 0.024 m
0.16
0.20
0.25
0.30
0.35
f_{kp} [Hz]
FLUME TANK
$m_{cT} = \frac{M}{P.H/2}$
"on" Tank
H=0.088m/P=5.5kg
H=0.110m/P=6.9kg
H=0.135m/P=8.5kg
"off" Tank P=5.5kg
0.26
0.30
0.34
0.38
0.42
f_p[Hz]

Fig. 8

Third International Conference on Stability of Ships and Ocean Vehicles, Gdańsk, Sept. 1986

STAB'86

THE INFLUENCE OF STABILITY CRITERIA ON TLP DESIGN

A.S. Schafernaker, D.P. Peace

1.0 INTRODUCTION

The aim of this paper is to introduce the reader to the stability aspects of the design of a Tension Leg Platform (TLP) and to illustrate the various requirements influencing the geometry and subdivision of the vessel.

The TLP is an established concept for the development of offshore oil reserves since the installation of the first platform of this type in 146 metres of water in the North Sea Hutton Field.

The platform consists of a deck supported on a buoyant hull which is moored to the sea-floor by vertical tethers which are in tension by virtue of excess buoyancy of the hull. The tethers provide a high degree of stiffness in the vertical direction and suppress roll, pitch and heave while allowing the structure to undergo relatively large horizontal excursions.

Subsequent to the installation of the TLP there are a number of temporary phases in which the platform floats freely and the appropriate intact and damaged condition hydrostatic stability criteria have to be fulfilled in these conditions. Likewise, it is necessary to ensure the stability of the platform in the installed condition. In the latter condition the platform stability is governed by the tension in the tethers and the concept of stability changes to one in which the basic requirement is for the installed platform to maintain positive tension in the tethers. Since this concept of stability for the installed condition differs from the usual concepts for freely-floating platforms involving familiar criteria as area ratios, down flooding points and limiting heel angles, it is worthy of some discussion.

The paper begins with a concise introduction to the TLP with emphasis on the influence of the functional requirements on the general arrangement and subdivision of the platform.

Having been familiarised with the TLP, the reader is then introduced to the temporary and installed conditions of the TLP and to the corresponding stability criteria used in the assessment of the design.

Next, after identification of the design criteria, the paper continues with a description of the design methodology for TLPs, which is applied to a parametric study presented in this paper. The objective of this study is to illustrate the effect of the geometrical design parameters on the characteristics of TLP's for different payloads, and to demonstrate the application of design constraints to the selection of a configuration for a particular payload. The North Sea has been assumed as the operating environment for the platforms since this is a hostile environment for which the TLP is particularly well suited. The parametric study includes an investigation into the interaction between the free-floating hydrostatic stability requirements with the stability requirements for the installed condition.

Finally, the paper concludes with a summary of the findings and makes recommendations for the TLP design procedure.

2.0 INTRODUCTION TO THE GENERAL ARRANGEMENT OF THE TLP

2.1 THE DECK

The TLP deck supports the platform payload which normally consists of:-

- production and drilling facilities
- rigid riser system for transmitting fluids between the platform and sea-floor
- support utilities
- accommodation

Deck design is principally dictated by facilities space requirements. Many types of decks have been proposed and these include the Hutton type orthogonal system of plate girders or a modular truss deck construction into which pre-fabricated and equipped modules can be installed. The decks may be constructed with a double bottom but there is no stability requirement which makes this necessary.

2.2 THE HULL

The hull consists of a number of columns which are braced at the bottom by pontoons, and Fig. 1 shows three possible hull configurations adopting four, six and eight-columns respectively.

The primary function of the hull is to support the deck as well as to provide the platform buoyancy and the anchorage for the top of the tethers. Additionally, the hull carries a payload consisting of such items as:-

- heating and ventilation
- ballast
- tether handling equipment
- diesel, fresh water

A discussion on the advantages and disadvantages of different numbers of columns for supporting the deck is outside the scope of this paper, with the exception of one of the aspects of TLP fabrication i.e. mating, which is discussed in this paper.

The fabrication method used for the world's first TLP (CONOCO Hutton) and proposed for most subsequent projects is to build the vessel in two separate parts: a hull, and an integrated deck which may be outfitted to an advanced stage before being joined to the hull.

The two structures are "mated" afloat, with the hull ballasted to a suitably deep draught, when the deck is floated into place on a suitable transportation barge. The two structures are initially joined with temporary restraints until a welded connection is effected at each column top. Once welding is completed and various systems within the two structures are connected and commissioned, the TLP vessel can be towed to site and installed.

Two design constraints on the hull configuration arise from the adoption of the above described "mating" procedure. Firstly, the "mating" operation is only possible in the case of a four or six column hull. Secondly, the columns have to be sufficiently apart to allow a barge of adequate stability to float into place in-between the columns of the hull.

Although the configuration of the hull is predetermined to a degree by the constraints imposed by the deck size and fabrication method, there are additional considerations in the form of hydrodynamic, hydrostatic and structural requirements. The effect of column draught and the distribution of hull displacement, between the columns and pontoons, are amongst the factors influencing hull configuration which are discussed in Section 6.0.

A specific feature of the TLP is that the deck is positioned at a considerable height above the water-line and consequently the vertical centres of gravity of these platforms tend to be very high. The reason for this is the need to minimise the impact of waves on the underside of the deck by providing an adequate air-gap between the deck and still water-surface. The air-gap is usually determined by combining the maximum wave crest elevation above the still surface with the variation in water depth due to tide, and the set-down of the platform.

The set-down of the platform is the increase in column immersion due to the motion of the platform as it moves along an arc described by the motion of the tethers. See Fig. 2.

2.3 TLP MOORING SYSTEM

The mooring system consists of four groups of vertical tethers which are attached at the top to each of the four corner columns and at the bottom, to a foundation template on the sea-floor.

The number of strings in each tether group is dependent on the size of the platform, magnitude of extreme tether loads and installation constraints.

The Hutton TLP uses tethers made up of 9.5m long forged steel elements with an outside diameter of 260mm. These type of elements are suitable for shallow water application but because their weight in water contributes towards the buoyancy requirement of the hull they have been found to be unsuitable for deep water.

Tether weight may be reduced by various methods but the use of buoyant tethers has been found to be most effective.

Typically, neutrally buoyant tethers are thin walled, large diameter elements, having an outside diameter of about 1000mm, and their application significantly reduces hull size.

Tethers may be installed by:

- TLP tow-out with on-board tether storage and installation by free-stabbing of tethers deployed from a mooring compartment within the hull column.
- On-site pre-installation of tethers from suitable vessel followed by connection to TLP.
- Tow-out of tethers themselves to site, uprighting, pre-installation and connection to TLP.

The first mentioned method, was adopted for the Hutton TLP. The second and third methods are only suitable for tethers which are buoyant.

One of the aspects of hull design when adopting the Hutton-type installation is that of storage space for on-board tethers. This may be on the weather deck or within the columns.

For large platforms in shallow waters, requiring short tether elements, storage within the mooring compartment may be considered. The mooring compartment is a watertight compartment in the column located above sea-level and houses dedicated equipment used in free-stabbing and tensioning of the tethers.

In the case of deepwater TLP's, having tethers made up of longer elements to simplify installation and reduce costs, storage may be possible in the central part of each column.

The number of tethers carried on-board is dependant on installation criteria which are based on anticipated environmental conditions in the installation "weather window". A requirement to carry a minimum number of tethers to secure the TLP to its foundation so that it would survive a summer storm, for example, could be the criterion adopted for setting the number of tethers carried. In deciding this, it is necessary to consider, for example, the requirements of tow-out stability of the TLP to the installation site, which may not be met due to the tether weight and its effect on the platform's centre of gravity.

The use of pre-installed tethers which can be anchored to the column base, averts the problems of platform stability caused by on-board tether storage as well as removing the necessity for a mooring compartment. These aspects of hull subdivision are described in the following section.

2.4 HULL SUBDIVISION

This section describes the hull structures of TLP's to show how they are compartmentalised to meet the functional requirements.

As described in the previous section, the tethers may be anchored on the mooring flat within the mooring compartment.

The mooring flat is a horizontal bulkhead within the column on which the tether installation and tensioning equipment is located. An alternative, is to attach the tethers to either internal or external anchorage points located at the column base.

In the case of TLP's with mooring compartments, various options are available for the arrangement of the internal column structure. The subdivision of the columns may be as shown in Fig. 3 - 6.

The annular spaces around the mooring compartments, shown in Fig. 3, are known as the damage control ring (d.c.r.). The purpose of the d.c.r., which itself may be subdivided, is to protect the mooring compartment from flooding as a result of damage at the waterline.

The extent of the damage control ring is determined by applying the rules and recommendations of the regulatory bodies in conjunction with the requirements imposed by the platform's operator.

All figures show a central shaft around which are arranged smaller shafts. These shafts are the column access shaft and tether shrouds respectively.

The access shaft, which is of the order of 5 - 7m diameter, gives access to equipment located at the column bottom and the pontoons.

The tether shrouds, which are about 2m diameter for buoyant tether moorings, are conduits in which the tethers pass through the hull structure to the outside.

The size of the access shaft, tether shrouds, spacing of tether strings and fabrication considerations, obviously imposes a restriction on the minimum diameter of the corner column.

Fig. 3 shows the internal arrangement of the column as in the Hutton TLP in which the structure was subdivided by horizontal watertight bulkheads.

Recent designs adopt vertical subdivision of the columns which facilitates the storage of longer elements. Vertical compartmentation of the columns enables tether lengths of up to 30m to be stored. The number of vertical bulkhead subdivisions is dependent on the diameter of the column, number of tether strings and damage stability considerations. Unlike in the case of the Hutton TLP columns which are ring stiffened, vertical bulkheads serve to support ring stiffeners and the external shell plate which leads to lower column steel weights.

Fig. 5 shows an option in which the double shell which forms the damage control ring is extended to the bottom of the column. Double-skinned columns provide more redundancy in the structure since they provide alternative load paths for column axial loads. In the case of this option, the subdivision within the double skin is designed to satisfy damaged condition stability requirements thereby removing the number of watertight compartments required within the inner shell.

Fig. 6 shows the internal arrangement of a TLP column in which the tethers are anchored at the column base. In this case there is no requirement for a mooring flat and tether shrouds but a damage control ring may still be introduced to obviate the necessity of denser compartment subdivision in the vicinity of the damage zone.

Figs. 7 - 9 show the internal subdivision of column-pontoon nodes.

Fig. 7 shows a node arrangement as in the Hutton TLP in which case the main vertical bulkheads are provided in line with the pontoon sides, dividing the node into inner and outer cores, the inner core containing the access shafts and tethers shrouds and the outer core tanks for ballast adjustments.

The section of a pontoon is shown in Fig. 10 showing the pontoon access tunnel at the centre. The distortion of the pontoon is resisted by web-frames which support longitudinal stiffeners. The pontoon is subdivided by watertight bulkheads as necessary to satisfy damage condition requirements and to provide ballast compartments.

3.0 TEMPORARY FREE-FLOATING STABILITY CONDITIONS

3.1 INTRODUCTION

During the construction and installation of a TLP there are several vessel conditions all of which must be checked for hydrostatic stability and all of which will affect the design and geometry of the vessel.

The several conditions arise because of the usual method of fabrication for TLP's and the change from a free-floating to a tethered structure at installation.

3.2 DECK AND HULL TRANSPORTATION

The requirements for mating are for a sheltered deep water inshore location. Since suitable mating sites do not exist close to many suitable fabrication yards, it may be necessary to plan for an extended open-water tow of the TLP hull and barge/deck before they arrive at the mating site. Since the hull will later be required to meet stability criteria with the deck in place (higher VCG and wind heeling moments), it is easy to understand that the hull alone will not pose any stability problems.

The deck transportation however poses significant problems since the requirements for mating are detrimental to barge stability. Mating requires that the deck is carried as high above the water surface as possible (to reduce the draught requirement of the hull), and on a barge that is as narrow as possible (to allow adequate clearance between the hull columns). Both these factors will reduce the stability of the barge/deck and the latter factor demonstrates how the temporary phases can effect the geometry of the structure. The TLP designer must allow an adequate gap for a suitable barge and arrange the number, diameter and distribution of his columns accordingly.

3.3 HULL/DECK MATING

During mating, (See Fig. 11) ballasting the hull to below its normal operating waterline raises the problem of impact damage prevention. The normal hull subdivision provided to protect the vessel around the operating draught (damage control zone), Fig. 3, does not provide protection at this deep temporary draught and the very large mooring compartment normally protected at the operating draught, becomes vulnerable. The risks involved in operating at this draught are therefore minimised by:

- minimising the duration at which the vessel stays at the mating draught,
- protecting the column shell with elastomeric fenders,
- excluding all vessels, other than the deck barge and attendant tugs, from the area.

As soon as the deck is in place on the hull column tops the hull is deballasted to a weld-out draught within the damage control zone.

3.4 PLATFORM TOW-OUT AND INSTALLATION

After the completion of the various post mating hook-up commissioning activities the hull is towed to the installation site. During its free floating phase the TLP can be considered as a Mobile Offshore Drilling Unit (MODU) for the purposes of stability. The maximum allowable vertical centre of gravity (KG) will determine how much equipment (tethers, risers and drilling equipment for instance) can be carried out on the vessel. This condition will also provide one limitation on the maximum allowable compartment size i.e. a compartment which when damaged allows the same maximum KG as the intact criteria.

One special feature of TLP's must be considered during the vessel tow and installation, that is the presence of tether shrouds passing up through the base of the column the mooring compartments. During vessel tow the tether shrouds must be sealed to prevent the top of the shroud being a down flooding point into the mooring compartment. During installation these seals must be removed thus lowering the potential downflooding point from the column top to the mooring flat and imposing limitations on wind strength during the installation operation.

4.0 TEMPORARY PHASE STABILITY CRITERIA

4.1 INTRODUCTION

The TLP, being a relatively new concept and with only a single vessel in operation, is not yet covered by detailed rules and regulations. Preliminary rules and recommended practices do exist and are actively being developed by the bodies concerned. Details of these documents by Lloyds Register, Det Norske Veritas and the American Petroleum Institute are given in Refs. 1, 2 and 3 respectively.

All three documents agree on the need to examine both the installed and the temporary free-floating phases, and consider that MODU type rules are applicable to the free floating TLP.

4.2 CRITERIA FOR TEMPORARY CONDITIONS

4.2.1 Hull and Vessel

For temporary phases the hull and vessel should be subject to MODU type codes suitably interpreted for the marine operation under consideration. A comparison of the various existing MODU codes can be found in Ref. 4 from which it can be seen that most codes are broadly consistent. The current U.K. Department of Energy are summarised in Table 1. The North West European Conference on harmonisation of rules is consistent with these rules and the DnV and NMD are similar except that they require the loss of the buoyancy in one complete column to be considered.

For the examples given in this paper the U.K. Department of Energy proposed guidlines have been used, with some noted modifications (see Section 6).

All the relevant codes quote two windspeeds for the intact vessel, these being for maximum operating/transit and the survival condition. The question of whether the survival condition is applicable to the vessel tow will depend on the duration of the tow and the route taken. For all such marine operations final agreement must be obtained with Marine Insurance Surveyors covering the operation.

4.2.2 Deck Transportation

For the case of the barge carrying the deck the MODU (surface vessels) rules are generally applicable although some criteria (particularly the range of stability to the second intercept) may need relaxation. Ref. 4 details the criteria used in the case of Conoco Hutton and Table 2 compares these with the U.K. Department of Energy Regulations for surface vessels.

5.0 INSTALLED STABILITY CONDITIONS

5.1 INTRODUCTION

Once the tethers are installed and pretensioned (by deballasting the hull) the stability of the vessel is completely governed by the tethers.

If it is considered that following the loss of tether tension in the installed condition the platform would undergo excessive motions, tether buckling and "snatching" loads in the tethers which could result in failure of the tether system, then there is a basis for the formulation of stability criteria for the installed condition. Such criteria have been formulated and applied in TLP design and their basic premise is that such hazardous situations as tether system failure and its possible consequences be avoided by requiring that the tethers should remain in tension at all times for all combinations of expected loadings.

This section looks at the possible causes of tension loss with varying degrees of severity, considers the consequence of tension loss and reviews the stability criteria recommended by various regulatory bodies for application in the intact and damaged installed conditions.

5.2 THE CAUSES AND CONSEQUENCES OF TENSION LOSS

Loss of tension in a tether or group of tethers can occur as a result of any one of the following causes:-

- error in ballasting, weight or tension control
- gas blow-out in the vicinity of the columns due to riser failure, for example, leading to buoyancy loss
- earthquakes or seaquakes and other extreme environmental conditions
- damage to tethers due to dropped objects
- tether failure due to fatigue
- flooding of hull due to collision or structural failure due to fire, for example.

The tension loss can appear with varying degrees of severity and the following conditions can be envisaged.

- loss of tension in a single tether in a corner
- loss of tension in a tether group in a corner
- loss of tension in all tethers in two corners.

The first condition could arise from failure of the tether, large wave loads or from an incorrect adjustment of the tension required. Since the remaining tethers would take up the load of the "missing" tether, the horizontal restoring stiffness of the platform would be maintained and the proper design of the mooring system would ensure the retention of axial stiffness at an acceptable level. Consequently there would not be any dynamic effects which would significantly affect the structural integrity of the tether system and platform safety.

The second condition would result from tether group failure, large wave loads in quartering seas or from accidental flooding of a compartment. The tether groups in the tensioning corners would, however, maintain tension and stiffness of the platform for all motions.

The loss of tension in all tethers in two corners, which could occur due to large wave loads in head or beam seas or a combination of accidental flooding and oblique seas, represents a potentially hazardous situation since there would be insufficient axial stiffness to suppress the motions of the platform. Consequently the platform would pivot about the cross-load bearing points at the column base of the remaining taut tethers and large bending stresses could develop in the slack tethers. An upward motion of the platform could lead to "snatch" loads in the tethers which could result in tether failure.

The installed stability criteria are formulated to prevent the occurrence of the situations described above. However, since the specification of unnecessarily onerous installed condition criteria would lead to unnecessarily high pretensions and platform weights, it would be expedient to carry out a thorough assessment of the consequences of low tension. Recent studies (Ref. 5) have indicated that momentary tether slackness does not represent failure as has been assumed previously. The authors of Ref. 5 conclude that:

- minimum tension loss, which occurs in the short interval during which a wave trough passes a column, does not lead to excessive tether loads since the tether deflections are limited because the lateral forces are low compared with the tether inertia as well as the drag and added mass of the surrounding water. Moreover, axial compression of the tether can be precluded by designing the bottom tether latch to stroke down when the tension is lost.

- regardless of whether tension is lost in one or two tether groups, the motions are limited and inexcessive.

- brief tether slackening does not lead to significant tension amplification due to "snatching". In the two corner slack condition, "snatch" loads were found to be acceptable even for very large waves.

The above stated conclusions were based on a linear platform motions analysis coupled with a time-domain, non-linear, finite element analysis for the computation of the tether bending stress. The analysis showed that state-of-the-art analysis tools can be used to gain an improved understanding of the behaviour of a TLP under extreme design conditions.

If it were found that the results were generally applicable then pretension could be set on the basis of preventing overstress, thereby considerably relaxing the limitations imposed by the installed condition, minimum tension criteria. The subsequent reduction of platform steel weight costs could prove to be extremely beneficial to the total cost of a TLP floating production system.

5.3 MAINTENANCE OF INSTALLED PLATFORM STABILITY AND THE FORMULATION OF INSTALLED INTACT AND DAMAGED CONDITION CRITERIA

The basic requirement for stability is that the tethers should remain in tension at all times.

Intact Condition

In the intact installed condition, in which neither damage to the hull or tethers or accidental flooding is assumed to have occurred, overstressing or slackening of the tethers can be caused by extreme environmental loads, with or without an imbalance in the weight distribution on the platform.

A weight imbalance for a TLP will not be shown as an angle of heel as in the case of a freely floating unit and for this reason it is important to have on-board monitoring equipment to provide personnel with information, enabling them to maintain the loading and centre of gravity of the platform within certain prescribed limits. The effects of an imbalance due to an accumulated weight error, for example, may be compensated by ballasting.

An order of magnitude for the ballast required may be determined by assuming a maximum error in weight of about 10% of the topside load. Other causes of weight imbalance are hook loads due to cranes operating on the platform and these two may be corrected for by appropriate ballasting. Any causes and sources of imbalance should be carefully considered during the design of the TLP since, as in the case of tether weight in water, the penalty for carrying more ballast than is necessary is a higher platform displacement and weight.

In order to prevent overstressing or slackening of the tethers due to extreme environmental conditions, the tether pretensions are set to sustain effects of extreme wave, wind and tidal conditions. In this respect, it is common to specify design storms in terms of a return period of 100 years.

Earthquake excitation and gas blow-outs resulting in buoyancy loss are other extreme environmental conditions which may have to be considered when checking the tether stress capacity to sustain extreme loads and the pretension capacity to maintain positive tension in the tethers.

Damaged Condition

The damaged condition is herein construed to be one in which either the hull or tether is damaged or an imbalance in weight occurs due to accidental flooding of a compartment.

Flooding causes an imbalance in the platform weight which results in a redistribution in the tether tension which provides a moment to counterbalance that due to the added weight in the flooded compartments. The flooding of a column compartment is more onerous than the flooding of a pontoon since the column floodable spaces tend to be larger in volume and are positioned the furthermost from the heel axis of the platform. The redistribution of tension due to flooding in a column may be estimated as shown in Appendix 1.

Such flooding may be the result of either:

- low energy impact damage
- leakage of ballast due to failure of system mismanagement
- leakage due to structural failure.

In general, only one tank adjacent to the sea or connected to the ballast system may be subjected to flooding. An impact in the region of the waterline, however could cause damage to a bulkhead and consequently flooding of two compartments must be envisaged.

Precautions to limit flooding damage include protection of the vulnerable areas of the hull by a double shell or damage control ring (d.c.r.), as has already been explained in Section 2.0. Furthermore, it is necessary to limit the volumes for potential flooding by subdivision of the hull.

The limitation in the compartment volume may be dependent on free-floating temporary phase stability considerations, which were discussed in the previous sections, or on the requirement to maintain positive tension in the tethers. As shown in Appendix 1, the flooding of a column would result in detensioning of the tethers on that corner and the purpose of the damaged condition criterion in this case, is the prevention of further detensioning to slackness due to the action of the environmental loads.

The compartment damage criteria which are applied by designers, are, generaly, formulated on an intuitive basis and therefore vary amongst designers. The conditions specified in the criteria may be generalised as follows:

The minimum effective tension at the bottom of any tether (or tether group), at the bottom of the tethers in one (or two) of the corners, must be zero or greater when any one (or two) compartment(s) are flooded during a specified storm.

Obviously, the maximum size of a floodable compartment is dependent on how onerous the criterion is. The smaller the allowable compartment sizes, the greater number of bulkheads required and, therefore, the greater the platform weight. This is further discussed in Section 6.0.

Another condition defined as damaged is one in which the mooring system has been damaged.

In the event of a tether failure due to a sudden fracture caused by a crack or by extreme loads, the remaining tethers would increase in tension. For such a condition it is necessary to demonstrate that the remaining tethers would not be overloaded following failure and that the platform would remain safe in the damaged condition with an unsymmetric axial stiffness and reduced tension capacity.

The flooding condition is, however, the one which has the greatest effect on the overall stability of the platform in all the encountered conditions, since the compartment volume sizes based on installed criteria must also satisfy temporary phase requirements. This aspect of the design is given further consideration in Section 6.0.

Flooding of Tethers

In the case of thin walled, large diameter buoyant tethers a further damaged condition needs to be considered, namely that of a flooded tether, which can be onerous in deep water for which long tether elements are used. Limitation of flooding can be effected by internal subdivision of the tether. This topic has not, however, been considered in this paper.

An advantage of buoyant tethers is that condition monitoring of the tether structure is possible by sensing leak before break.

5.4 REVIEW OF RULES AND GUIDELINES OF SOME REGULATORY BODIES ON INSTALLED STABILITY CRITERIA

Because the TLP is a relatively new concept there are no formal design rules, and recommended practices are at various stages of development.

The rules which are documented agree on the need to maintain positive tension in the tethers but differ considerably in detail.

DnV and NPD

The Det Norsk Veritas (DnV) and Norwegian Petroleum Directorate (NPD) rules (Ref. 2 and 6) are similar and are based on load combinations designed to prevent overstressing or slackening of the tethers.

The rules distinguish between various design conditions. The two most relevant to the topic under discussion are referred to as the ultimate limit state (ULS) and the progressive limit state (PLS). Generally, the former ULS condition considers the effect of specified environmental conditions on the intact platform and mooring system whereas the PLS is used to assess conditions which may lead to a progressive failure of the tether system caused by successive overstressing of the tethers due to accidental loads and damage to the TLP.

Combinations of loads and load factors are applied in carrying out the check and these are tabulated in the Refs. 2 and 6. The partial load factors are applied to account fo the uncertainty in the prediction of loads.

The selection of the loads used in the checks is based on annual probabilities of exceedance which are tabulated in the Refs.

The design resistance of the tethers to overstressing or slackening is related to the yield stress of the tether material, and the stress levels for the ULS and PLS checks are given in the Refs.

In the case of the flooded condition the DnV rules specify:

- any one compartment adjacent to the sea is assumed to be flooded regardless of location
- or, the platform is assumed to be damaged at any level between the waterlines shown in Fig. 12, which also shows the extent of damage to be assumed. Damage can only occur to columns which are exposed and on the periphery of the unit, as shown in Fig. 12.

The rules also specify the permeability factors which should be applied and provide guidelines on the overall watertight integrity of the structure.

Lloyds Register of Shipping (LRS)

LRS rules are to be found in Ref. 1. The rules stated that in the intact conditoon the tension is to be positive at all times for the most unfavourable combination of weight, centre of gravity and buoyancy, in the most unfavourable environmental conditions having return periods of not less than 50 years, or 100 years in certain cases. In the damaged condition, the platform must be able to survive flooding of any one underwater watertight compartment and the tension in all tethers must remain positive in the most unfavourable conditions as described above, in environmental conditions which could be expected to occur within a return period of not less than one month.

Within 12 hours following flooding commencement, the loading of the platform has to be adjusted for all tethers to remain in positive tension under the most unfavourable environmental conditions occurring within a return period of not less than one month.

American Petroleum Institute (API)

The API has prepared draft guidelines on the design procedures for a TLP (Ref. 3).

The intact condition should include the full range of possible centre of gravity variations permitted by acceptable operations procedures during extreme tether conditions. In the damaged case, the accidental flooding of any one compartment below the waterline should be considered and the environmental conditions should be assumed to be normal i.e. those expected to be occurring frequently during service life.

6.0 PARAMETRIC STUDY

6.1 INTRODUCTION

The objectives of the study were as follows:

- to explain the methodology for sizing a TLP
- to illustrate the effect of the platform geometry on the design characteristics of TLP's for different payloads
- to demonstrate how design constraints are applied in an optimisation exercise to select geometrical parameters of a platform
- to demonstrate the influence of platform offset restriction, air-gap and water-depth on the compartment sizes and platform characteristics
- to check the free-floating stability of the platforms in order to ascertain whether there are any conflicts between the temporary and installed condition stability requirements.

6.2 SIZING METHODOLOGY

The basis of the sizing methodology is the static equilibrium equation for the TLP which may be written

$$\Delta = Pd + Ds + Hs + Pn + Tw + Pr + Rt$$

where Δ = platform displacement
Pd = deck payload
Ds = deck steelweight
Hs = hull steelweight
Ph = hull payload
Tw = tether weight
Pr = tether pretension
Rt = riser tension

The objective of the design methodology is to determine the displacement, weight and pretension of a platform which will support a specified deck payload, and satisfy the hydrostatic, hydrodynamic and structural design criteria.

During initial sizing, this is normally achieved by sizing algorithms based on a combination of empirically and analytically derived information on platform weights, loads and motion characteristics.

The sizing was carried out by using a program developed in-house at John Brown. Design projects have shown that the predictability of platform weights and pretensions by the algorithms is good and that the trends revealed by the sizing procedure are correct.

A flow diagram of the sizing methodology in the TLP design process is given in Figure 13, which may be described as follows.

The input data is assumed to consist of information on the required deck payload and the environmental characteristics of the operating site such as water depth, wave heights, wind and current velocities.

The geometry of the hull is derived for an assumed displacement.

The deck weight of a deck spanning the columns and carrying the specified deck payload is then estimated from a steel weight algorithm together with the hull steelweight which is dependent on the dimensions of the columns e.g. column length, plate thickness, internal bulkhead area, and pontoons. An estimate of the total platform steelweight is made and the pretension can therefore be calculated from the static equilibrium equation.

The platform centre of gravity and dynamic properties can be estimated on the basis of the calculated weight distribution. The environmental loads acting on the platform are estimated. Wave dynamic tether loads may be estimated by Morison's equation based algorithms. Wind forces are estimated for an assumed wind profile and current loads on the hull and tethers are calculated.

Fig. 2 shows the forces acting on the platform.

In the sizing carried out herein it has been assumed that the environmental forces are considered to be acting uni-directionally and simultaneously in the most onerous combination and the resultant platform excursions and tether loads are estimated by superimposing, where applicable, the effects of the individual load components due to first and second order (drift) wave forces and moments, wind and current force and moments, tide, foundation misplacement etc. The platform is assumed to be positioned so that the load acts in the diagonal i.e. 45 degrees, direction (See Fig. 14) thereby tensioning and detensioning upwave and downwave tethers respectively.

The platform excursions and maximum and minimum tether loads are checked against the design criteria to ascertain whether the offset requirements and installed intact and damaged stability criteria are satisfied.

If any of the requirements are unfulfilled, the design procedures described above is repeated iteratively until the design criteria are met.

6.3 PLATFORM GEOMETRY AND INPUT PARAMETERS

The geometrical input parameters greatly influence the characteristics of the sized configuration and are selected on the basis of an optimisation procedure which involves sizing and computing many configurations.

A description of the geometrical parameters and their influence on TLP design is given below. Fig. 14 shows the overall dimensions of a four column TLP.

Platform draught:

The platform draught has to be deep enough to:

- prevent pontoon emergence in the trough of a design wave
- provide adequate clearance between the pontoon top and barge keel during a mating operation
- maximise the advantage to be gained from depth attenuation of wave force acting on the column and pontoons

Other constraints are:

- hydrostatic stability deteriorates as draught increases
- hydrostatic loading of the column imposes limits on the draught since column shell thickness and therefore column steel weight increases
- graving dock dimensions and maximum tow-out water depth.

Column Spacing

The column spacing has to be sufficiently wide to:

- support the required deck area
- enable a barge to slot in-between the columns for hull-deck mating, if necessary
- fulfill the stability requirements of the platform in the temporary free-floating conditions
- maximise the advantages to be gained from a reduction in dynamic wave induced tether loads due to increase in spacing
- give adequate clearance between risers and the pontoons
- prevent undesirable disturbance of flow beneath the platform, due to hydrodynamic blockage effects.

Other considerations are:

- the width of the graving deck may impose limits on the column spacing
- the advantage of a wide spacing have to be considered in relation to the increase in deck steelweight resulting from an increase in deck span.

Displacement Ratio

This is an important hydrodynamic parameter defined in Fig. 14, which enables the platform tether responses to be detuned from the environmental wave excitation thereby reducing tether loads. A compromise solution usually has to be sought in reconciling hydrodynamic, hydrostatic and structural requirements.

Generally speaking, low displacement ratios are preferable from the point of view of minimising tether loads and tether fatigue as well as improving hydrostatic stability. In certain cases, structural requirements indicate the use of stubbier pontoons, and hence high displacement ratios, to resist stress concentration at the pontoon-column nodes due to wave racking moments.

Pontoon Aspect Ratio

This ratio too has an important effect on platform responses and high and narrow rectangular pontoons are preferable since they reduce wave heave forces. However, squarer pontoons are better at resisting racking and bending moments. Pontoon aspect ratio may also be constrained by fabrication requirements e.g. lining up pontoon sides with column bulkheads.

The pontoon shape is of little importance from the point-of-view of hydrostatic stability since TLP pontoons are usually deep below the surface, even at free-floating draughts.

6.4 PARAMETRIC STUDY INPUT PARAMETERS AND DESIGN CRITERIA

Payload and Riser Tension

The platform data was chosen to represent small, medium and large sized TLP's for carrying deck payloads of 5,000, 15,000 and 25,000 Te respectively.

Table 3 lists the deck and hull payloads and riser tensions assumed in the study.

ENVIRONMENTAL DATA PARAMETERS

The environmental data parameters characterise the extreme environmental conditions at the platform's operating site.

The extreme storm conditions are those which produce the most unfavourable loading conditions of the structure. It is common to specify design storm conditions in terms of a return period which is related to annual probabilities and the 100 year return period storms are usually applied.

The environmental data used in the sizing of the platform is typical for the North Sea environment. The following data was assumed:

Water depth (m)	=	400 m
100 year wave significant wave height (m)	=	16.0 m
100 year wave spectral period (s)	=	15.0 - 18.6s
100 year wind speed (m/s, 1 min. average)	=	49.5 m/s
100 year current speed (m/s)	=	1.4 m/s
Tidal variation from lowest design waterline	=	2.2 m

Geometrical Design Parameters

Table 4 gives a summary of the platform input geometrical design parameters used in this study. Fig. 14 defines the dimensions used and shows the assumed geometry of the TLP.

Other Assumptions

It has been assumed that the platform would use buoyant tethers.

The pontoon aspect ratio has been kept constant throughout the study.

The designs which have been adopted in the sizing study are the N.P.D. installed condition intact and damaged condition criteria referred to in Section 5.4.

The ULS check requires:

$So\ (P+Ws) + S\ (1.3\ E+) \leq Rc/\gamma m$
$So\ (P+Ws) + S\ (1.3L) - S\ (0.7E-) \geq 0$
$So\ (P+Ws) + S\ (L) - S\ (1.3E-) \geq 0$

The PLS check requires:

$So\ (P+Ws) + S\ (E+) \leq Rc$
$So\ (P+Ws) - S\ (L) - S\ (E) \geq 0$

where So = pretension due to permanent loads P and weight of submerged tether Ws.

S (1.3+) = tension due to environmental loads at maximum water level, multiplied by load factor 1.3.

S (L) = reduction of tension due to live loads.

S(E-) = tension due to environmental load at minimum water level.

Rc = yield stress

γm = material factor = 1.15.

6.5 EFFECT OF GEOMETRICAL PARAMETERS ON PLATFORM CHARACTERISTICS

Platform Steelweight displacement and pretension

As seen in Fig. 15 - 17 the minimum of the steelweight, displacement and pretension for a particular payload do not necessarily occur at the same parameter value and are particularly sensitive to column spacing and displacement ratio. The shape of the curves can be explained by considering the effects of changing a parameter on steelweight and pretension requirements. Thus, increasing column gap (or spacing), and hence deck span, increases steelweight but reduces pretension requirements and the displacement is proportional to the difference between the two.

The sensitivity to displacement ratio demonstrates how important this parameter is in detuning the plaform from the wave excitation thereby reducing pretension requirements and, hence, platform size and weight.

Compartment Size

Fig. 18 - 20 shows the hull compartment sizes as a function of the geometrical parameters. (The compartment sizes within the d.c.r. would be half those elsewhere, since a two compartment damage criterion at the waterline would determine d.c.r. compartmentation).

The compartment size is proportional to the reserve of tension in the tether group at the minimum tension condition in the design storm used in setting compartment size. Consequently, the compartment size is proportional to the pretension. Therefore, the minimum compartment size corresponds to the minimum pretensions which do not themselves correspond to minimum steelweight as seen in Fig. 15 - 17.

Fig. 21 - 23 shows the ratio of pretension to displacement as a function of the geometrical parameters for the different payloads. It can be seen that in general, the pretension ratio decreases as payload increases. This indicates that the compartment size of a smaller platform is a larger proportion of the column volume than for a bigger platform designed to carry a greater payload.

Metacentric heights of TLP following tether disconnection

Although there is no requirement to investigate the stability of the TLP following disconnection of all tethers, since such an event is highly improbable, it is nevertheless instructive to investigate the hydrostatic stability in this condition since it is indicative of the temporary phase stability and shows the effect thereon of the geometrical parameters.

The metacentric heights for the free-floating post tether-disconnection state were calculated on the basis of the c.g. and platform weight estimates determined by the sizing algorithm.

Fig. 24 - 26 shows that as may be expected, stability deteriorates as:

- displacement ratio increases
- draught increases
- column spacing decreases.

The figure also shows that the stability of the larger platform is relatively better than that of the smaller platforms, and that in many cases the metacentric heights are negative so that platform would adopt an angle of loll.

These aspects of TLP stability are also discussed in Section 6.8

6.6 SELECTION OF PLATFORM CONFIGURATION

The optimisation procedure involves the selection of the parameters of a configuration which satisfies the design criteria for the lowest cost. The total cost of platform and tether steelweight may be used as a basis of cost comparison and as an indicator of the best solution. Fig. 27 - 29 shows the platform costs as a function of the geometrical parameters.

A configuration for each payload was selected from among the platform geometries derived in the parametric study, on the basis of the following assumptions.

- deck space and hull-deck mating requirements limit the column gaps to minimum value of 40, 50 and 60 metres for the 5,000, 15,000 and 25,000 Tonne payload platform
- draughts are limited to less than 40m.

The particulars of the selected TLP's and their characteristics are given in Table 5. Although the TLP geometries were selected from a limited data base and the column gap constraints were probably too conservative, the configurations given in Table 5 are not untypical of those which could be chosen for platforms of the payloads under consideration.

A number of interesting characteristics may be deduced from the data for these TLP's.

- Larger payload platforms are relatively more stable. This may be explained as follows. Higher payload platform draughts do not increase in proportion to $\Delta 1/3$ (Δ = displacement) and are relatively shallower than the draughts of smaller platforms due to draught limitations imposed by structural and fabricational considerations.

  Consequently, the metacentric radii (BM) of the smaller platforms tend to be relatively smaller than those of larger platforms of a similar displacement ratio. Similarly, a comparison of the platform air-gaps show that the smaller platform air-gaps are also relatively higher. (Platform air-gaps are set by combining maximum wave elevation with the set-down, and wave crest enhancements due to diffraction effects. The latter two components of air-gap are a function of the platform size). Consequently the c.g.'s and wind levers of the smaller platform are relatively higher.

- The metacentric heights of TLP's following tether disconnection tend to be negative.

- Smaller payload platforms need pretensions which are a higher proportion of their displacements. Compartment sizes of smaller platforms are also relatively higher. This is another indicator that the temporary phase stability of smaller TLP's could be expected to be worse than for higher payload platforms.

- The $\frac{\text{steelweight}}{\text{deck payload}}$ and $\frac{\text{displacement}}{\text{payload}}$ ratios of smaller payload platforms are higher indicating that smaller platforms are less efficient payload carriers. It is interesting to note that the smaller platforms have more displacement per tonne of payload but are nevertheless less stable. The reasons for this have already been discussed above.

It is interesting to consider the estimated set-downs of the configured platforms in relation to the damage zone requirements of, say, DnV (See Section 5.4) which require the damage zone to be 8 metres above the maximum waterline and 6 metres below the minimum waterline. The maximum offset estimates indicate that the smaller platforms undergo larger excursions but in all cases the waterlines at the mean offset are well within the damage zones specified by the DnV rules.

6.7 EFFECT OF COMPARTMENT SIZE ON PLATFORM SIZE

Fig. 30 shows the effect of compartment size on platform steelweight and displacement. This was calculated for the 15,000 Tonne payload TLP, details of which are in Section 6.7.

Halving the compartment size for the 15,000 TLP increases steelweight and displacement by about 10 and 20 per cent respectively. Doubling the compartment size, however, decreases the steelweight and displacement by about 5 and 2.5 per cent respectively. The estimated reduction in cost could be of the order of 5%.

Varying the compartment size is approximately equivalent to changing the installed damaged condition criterion, particularly for small changes in compartment size which have little effect on the platform displacement. A lower compartment size would correspond to a more onerous criterion than that applied to sizing the 15,000 Tonne payload TLP compartment, and a higher compartment size would mean a less onerous criterion. It is estimated that the relaxation of the criterion to give a 2,000 Tonne compartment would result in a saving in platform cost of the order of 5%. There is therefore a small if not insignificant gain from reducing compartment sizes.

Increase of the compartment size from 1025 to about 2000 Tonnes corresponds approximately to the relaxation of the damage criterion to one allowing one compartment flooding in a one year summer storm.

Bar charts showing the constitution of the tether loads for the original and relaxed criteria are shown in Fig.31

6.8 INFLUENCE OF OFFSET, AIR-GAP AND WATER DEPTH ON COMPARTMENT SIZE AND PLATFORM CHARACTERISTICS

Platform Offset

If a constraint is imposed on the maximum excursion of a TLP, then the pretension will have to be sufficiently high to provide the necessary horizontal restoring stiffness from the tether system.

An offset limitation of 10% on the 15000 Te payload platform increases compartment size, steelweight and displacement by 218, 1 and 12% respectively. The constraint trebles the allowable compartment size. However even if the compartment size satisfies temporary phase requirements in the unlimited offset case, it may not do so on, for example, on trebling, even though there is an increase in displacement.

Air-Gap

Since the air-gap affects the column length and hence hull steelweight it will influence the compartment size. A reduction in air gap i.e. a relaxation in the air gap setting criteria, reduces platform steelweight, displacement and hence pretension and compartment size. An increase in the air gap has the opposite effect.

Water Depth

An increase in water depth will result in an increase in air-gap and hence steelweight. However, the tether pretension ratio decrease with water depth and the nett result is an insignificant change in the compartment size.

6.9 COMPARISON OF FREE-FLOATING PROPERTIES OF VESSELS IN THE PARAMETRIC STUDY

6.9.1 Introduction

In order to inter-relate the vessel parameters of a TLP it is necessary to assess stability of the free floating vessel. In the course of a detailed design this would be carried out over the full range of draughts and load conditions experienced by the vessel but in this study is limited to the analysis to the case which is typically the most onerous; that of towing the vessel to its installation site. Figure 32 illustrates the range of vessel draughts encountered by a TLP during its 'life cycle'. The TLP hull alone has no stability problem since it has no deck and thus a low wind heel moment and low VCG. During mating and weld-out the vessel will be temporarily moored in sheltered conditions. During installation of the TLP a temporary situation exists for vessels with internal mooring arrangements. The tether shrouds are blanked off at the mooring flat for ice sea tow, but must be opened for installation, introducing a lower hull downflooding point than exists at other times during the vessels operations.

6.9.2 Method of Analysis

In order to accommodate the large number of vessels in the parametric study some simplifying assumptions were made in the modelling of the structures, i.e.:-

- Deck structure assumed to make no contribution to stability;
- Wind heeling moment constant with angle of heel;
- Damaged tank modelled as equivalent cylinder within the damage control zone (that is, modelling a typical damage control ring).
- Tethers were assumed not carried on the vessel during tow-out.

Each vessel was analysed at a tow-out draught equal to the installed draught, with pontoon ballast used to achieve this condition (i.e. effectively replacing tether pre-tension with an equivalent amount of ballast).

The maximum allowable vertical centre of gravity (KG) was calculated against the intact and damaged criteria proposed by the U.K. Department of Energy with the exception that in the damaged condition the limiting angle of heel of 15 degrees after damage was calculated with the effect of wind included (as per NMD/DnV) which the authors consider to be a more realistic criteria. The criteria used to set the maximum permissible KG's are summarised in Table 6. A wind strength for 100 knots was applied to the intact case thus covering the worst condition that could be encountered during the tow-out. The analysis wa carried out using the 'SIKOB-PLP' suite.

6.9.3 Analysis Results

The object of the analysis was to demonstrate that the TLP can be towed to the installation site with the topsides facilities complete and loaded with consumables even under survival conditions and that the maximum tank size allowed in the installed case does not seriously reduce the allowable KG for the free floating structure.

Table 7 gives a summary of the TLP characteristics determined from the sizing methodology. In Table 8 the maximum allowable KG according to each criteria is tabulated for each vessel, together with the actual (calculated) KG.

In the majority of cases the KG is within the limits set by all criteria. Where this is not the case the maximum KG is imposed by one of two criteria, the intact area ratio, or the damaged limiting heel angle, and in most of these instances the difference between actual and allowable is small.

A typical remedy for this situation is demonstrated by looking at vessel 257 again at a higher and deeper draught. The deeper draught, with more ballast and a lower KG brings the vessel within allowable limits.

The results also indicate that when the vessel is constrained by a damage limit the intact limit is very close also, implying that there would be little benefit from reducing the allowable tank size for the free-floating criteria.

Comparison of the free floating stability results with the vessel sizing parameters clearly demonstrates that the narrow (column spacing) vessels (057, 157, 257) are the weakest, with the deep draft vessels (053, 153, 253) also being poor. Conversely the shallow draft and wide vessels (**1 & **6) being particularly strong. It shouold be noted that for a constant displacement and displacement ratio, column diameter is proportional to the inverse square root of draught, which compounds the problems of the deep draught vessels.

Low displacement ratios, leading to large column diameters give good stability (**4) and the converse is equally true (**5). However, the smaller displacement ratios particularly for the smaller payload vessels may have inadequate pontoon volume for the required ballast leading to ballasting in the columns and an increased KG.

Finally, a definite size effect can be deduced. The smaller platforms having, relatively larger airgaps have relatively larger wind moments and thus are penalised by low wind heel area ratios.

7.0 INTERACTION OF TEMPORARY AND INSTALLED CONDITIONS

In the previous sections it has been demonstrated that there are a number of conflicting stability constraints which will influence the TLP designer. He must consider the temporary phases prior to installation as well as the installed criteria, though the extent to which each of the temporary constraints will be allowed to effect the design will depend on the nature of the marine operations and the associated risks involved, and the likely environmental conditions.

A floating mating operation will impose a definite column gap limitation, since barge stability will in general (given the draught restrictions of load-out etc.) be a function of beam squared. However, in the case of some small platforms with minimal topsides equipment, such as well-head platforms, it may be preferable to build the vessel in one piece.

The foregoing free-floating analysis has assumed the worst probable sea-tow conditions (100 knot winds) but in certain circumstances, such as a short tow to a deepwater site relatively close to shelter, the tow might be performed over one or more short predictable weather windows, thus allowing a reduction of the environmental criteria and making the free floating stability parameters less important.

Ideally the structure would be built with a shallow draft, large column span with a low displacement ratio to achieve the best free floating stability. This would immediately conflict with the overall aims of the project. The shallow draft would reduce pontoon immersion and increase wave loads and tether tensions. The large column span would increase steelweights and costs, and the low displacement ratio would reduce pontoon section moduli and platform rigidity.

Therefore in a TLP project it is important to balance and resolve these conflicting interests at an early stage of the design.

8.0 CONCLUSIONS AND RECOMMENDATIONS

- TLP free-floating temporary phases must be considered in addition to the installed phase.
- Typical MODU codes are applicable to the TLP in its free-floating condition.
- The stability criteria applied to the temporary phases will depend on the type of marine operations involved and relaxation of the codes normally applied to free-floating units may be possible.
- Installed stability of TLPs is governed by tension in the tethers and the stability criteria are usually based on the assumption that the tethers should not slacken at any time.
- In the installed damaged condition, the criteria require that tethers should not slacken on flooding of a hull compartment in a specified design storm.
- Installed stability criteria are at various stages of development and differ considerably in detail.
- Relaxation of the "no-slackening" criteria may be possible without impairing the safety of the platform.
- TLP's design to carry low payloads tend to have poorer free-floating stability characteristics than higher payload carrying platforms.
- The metacentric heights of TLPs in the free-floating condition after the unlikely event of all tether disconnection, are generally negative.
- Compartment sizes based on installed damaged condition criteria are proportional to the pretension in the tethers, and
- smaller platforms require a higher pretension as a proportion of their displacement, consequently
- the floodable compartment sizes of smaller platforms tend to be a higher proportion of the column volume than those of larger platforms.

- Relaxation of the installed damaged criteria increases allowable compartment sizes and reduces platform costs.

- Compartment sizes based on the installed damaged condition criteria generally satisfy temporary phase stability criteria for the range of North Sea TLP's considered. This indicates that

- for such platforms, compartment sizes should be based on the installed condition.

- The design constraints which the temporary and installed phase requirements impose, are frequently in conflict and must be resolved at an early stage.

It is recommended that in the TLP design:

- State-of-art technique are applied to check whether tether slackening is allowable since a relaxation of the installed condition criteria could have a significant impact on TLP size and cost.

- Stability criteria in the temporary and installed phases should be based on a probabilistic analysis of the joint occurrences of events which would lead to situations in which the safety of the platform would be impaired. This too could lead to relaxation of design criteria and, hence, TLP size and costs.

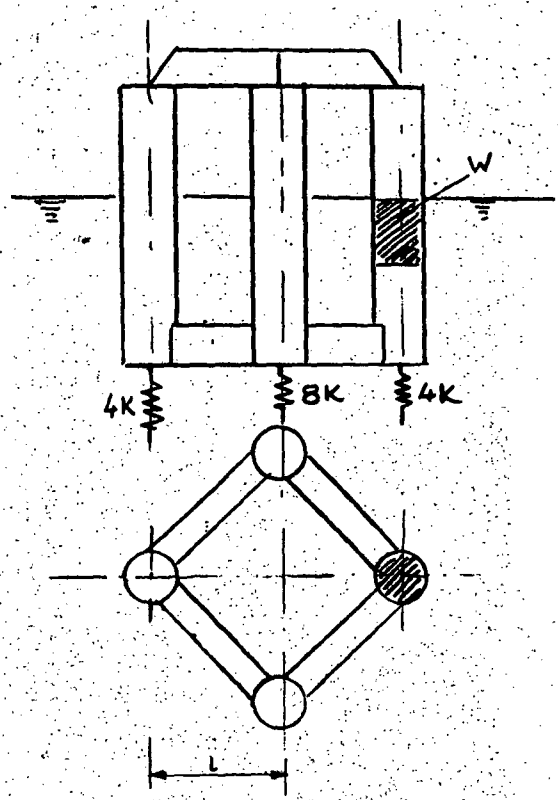

Ref 1 "Preliminary Guidance Rules for Tension Leg Installation" 1983, Lloyds Register of Shipping.

Ref 2 "Recommended Practice: Tension Leg Platform Design" RP 0202 1986, Det Norske Veritas.

Ref 3 "Recommended Practice for Planning, Designing and Constructing Tension Leg Platforms" (RP 2T) 1986, American Petroleum Institute.

Ref 4 "The Hutton TLP Deck/Hull Mating Operation", N. Ellis, J. Chivvis, D. Tutures, A. Lydon, OTC 4911 1985.

Ref 5 "Analysis of Brief Tension Loss in TLP Tethers", J.N. Brekke and T.N. Gardner, OMAE, 1986.

Ref 6 "Regulations for Load Carrying Structures", NPD 1984.

APPENDIX 1

If it is assumed that:

- waterplane stiffness is negligible
- platform flexibility is negligible
- stiffness of foundation, cross-load bearing is small compared with tether axial stiffness
- each tether group is represented by e.g. 4 tethers per corner, each having a stiffness K
- the effect of the distances between tethers in one corner is negligible.

then the following method may be applied to estimate the redistribution of tension due to water of weight W flooding a corner column compartment.

If the vertical displacements are z1, z2 and z

For vertical equilibrium

$$4Kz1 + 8Kz2 + 4Kz3 = W$$

For moment equilibrium

$$8K.lz3 + 8Kaz2 = 2l.W$$

Since

$$z1 - z2 = z2 - z3$$

and since the incremental tension due to a displacement z is given by $\Delta T = K2$

$$\Delta T1 = 1/4\ W$$

$$\Delta T2 = 1/4\ W$$

$$\Delta T3 = 3/4\ W$$

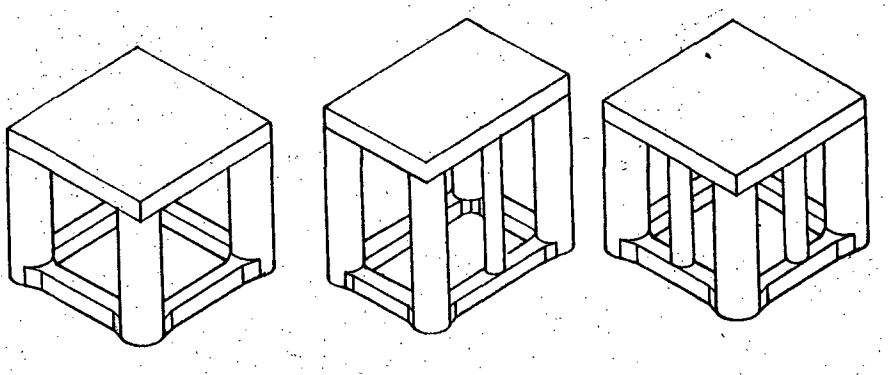

DIFFERENT TENSION LEG PLATFORM CONFIGURATIONS
(4,6 and 8 column hulls)

FIGURE 1

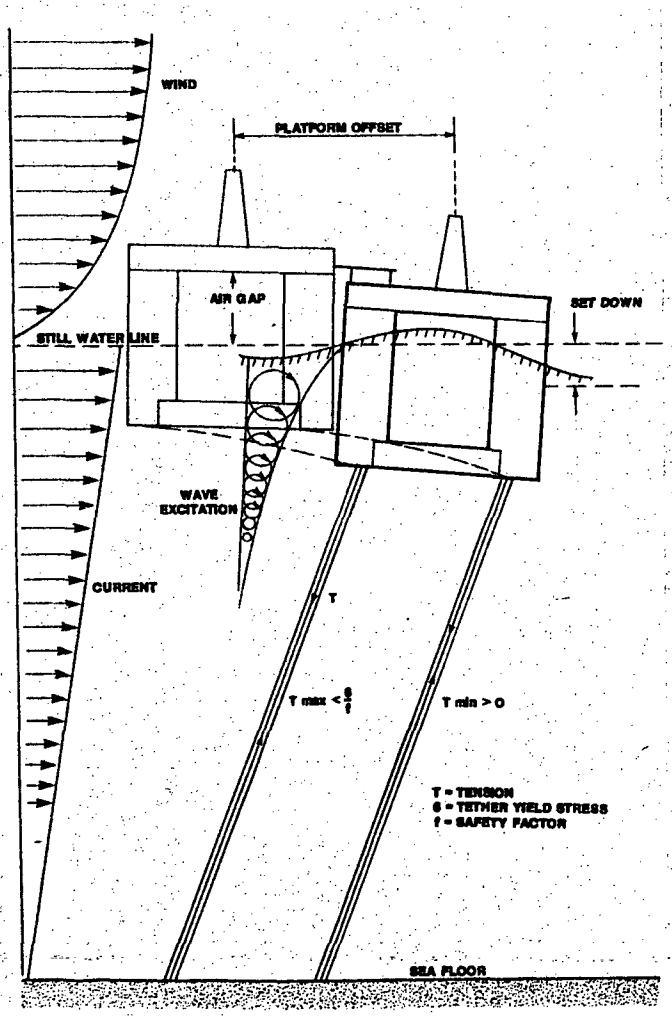

FIGURE 2

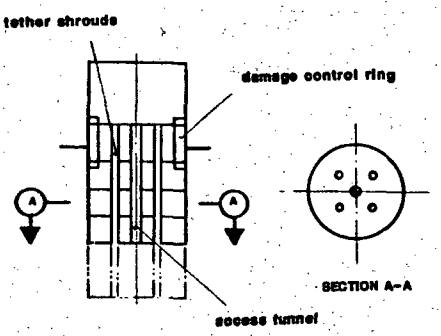

FIGURE 3

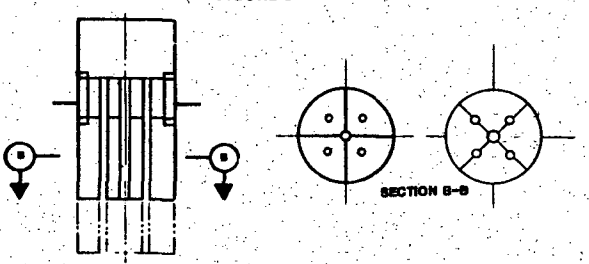

FIGURE 4 COLUMNS

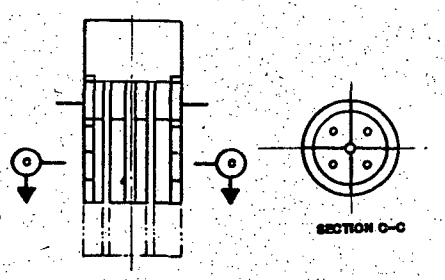

FIGURE 5

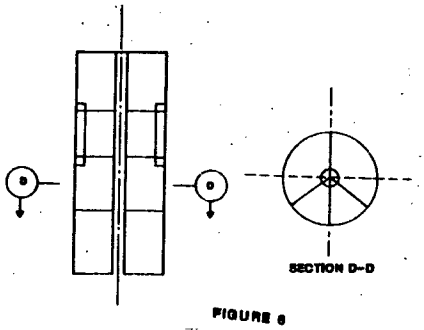

FIGURE 6

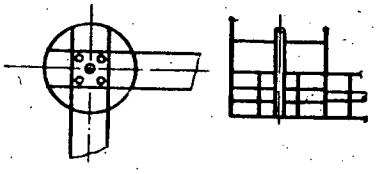

FIGURE 7

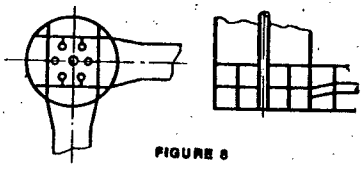

FIGURE 8

NODES

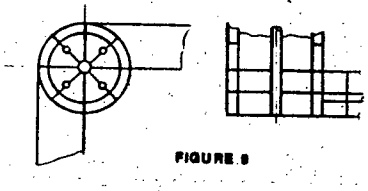

FIGURE 9

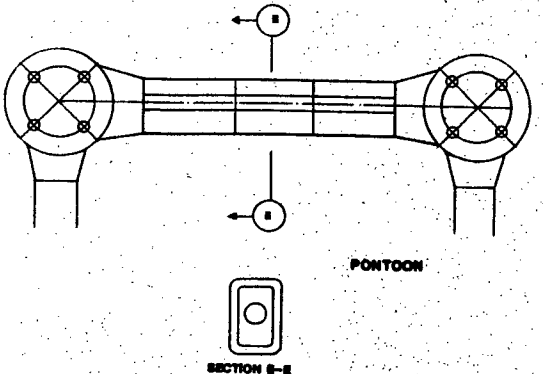

PONTOON

FIGURE 10

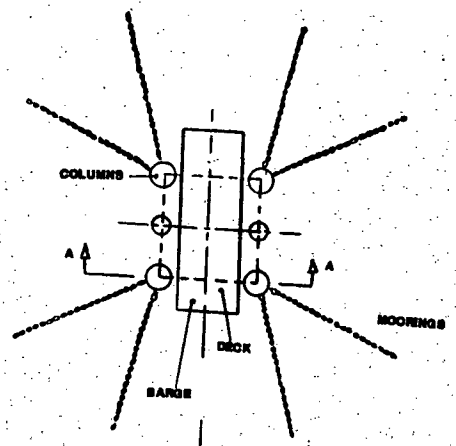

DECK SUPPORT STRUCTURE

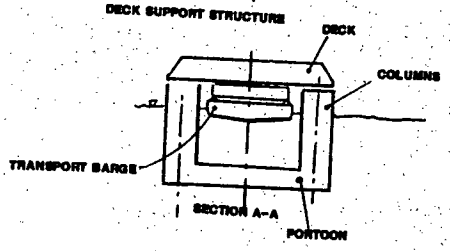

SCHEMATIC OF TLP MATING OPERATION

FIGURE 11

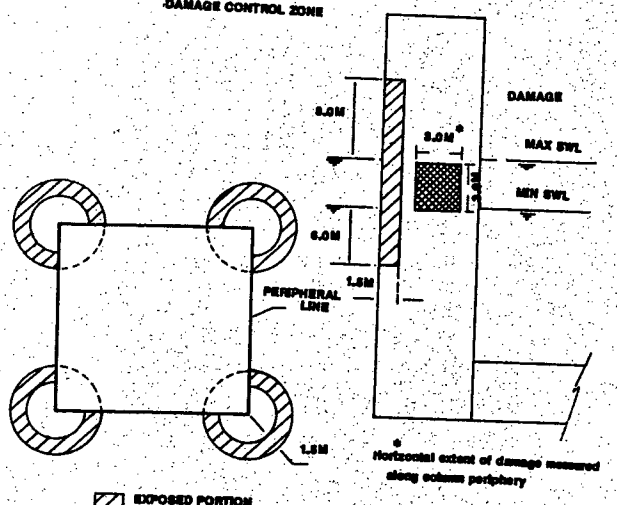

FIGURE 12

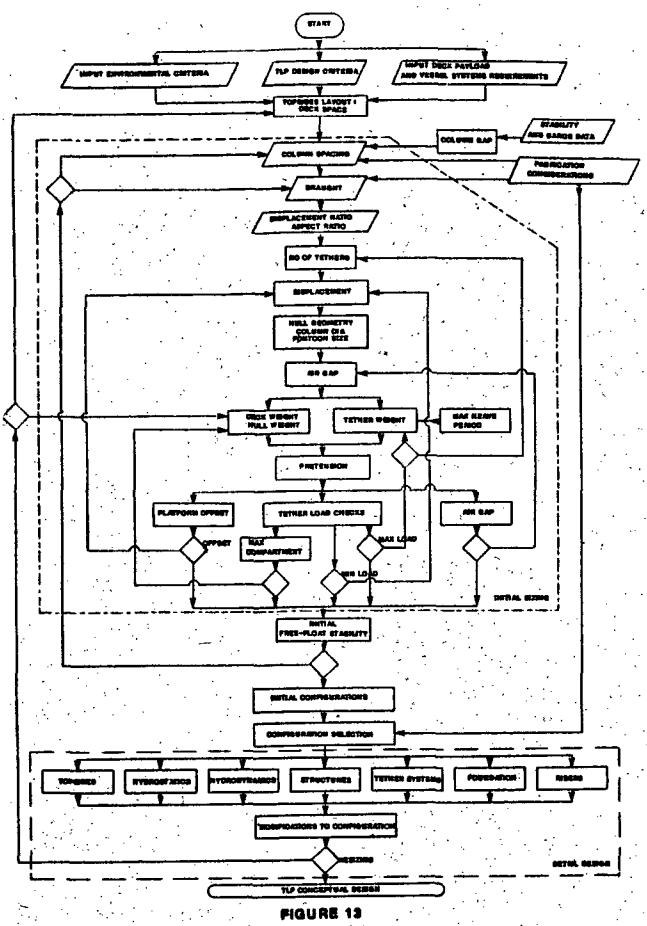

FIGURE 13

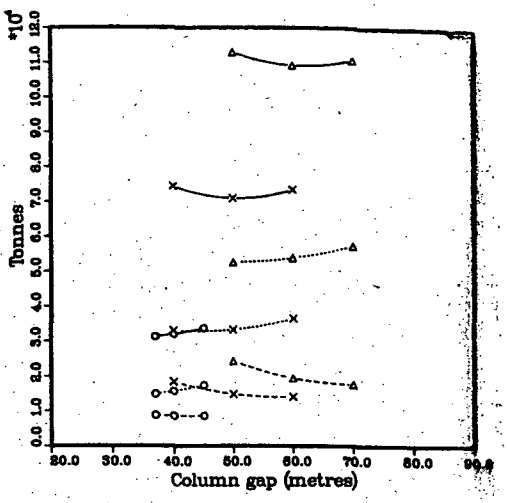

LEGEND

- o steelweight 5000
- × steelweight 15000
- △ steelweight 25000
- o pretension 5000
- × pretension 15000
- △ pretension 25000
- o displacement 5000
- × displacement 15000
- △ displacement 25000

FIGURE 15

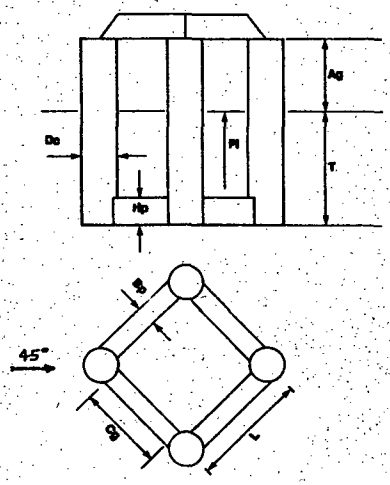

PLATFORM GEOMETRY DEFINITIONS

Ag=AIR GAP
T=COLUMN DRAUGHT
Pl=DRAUGHT TO TOP OF PONTOONS
L=COLUMN CENTRE-CENTRE SPACING
Cg=COLUMN GAP
Dc=CORNER COLUMN DIAMETER
Hp=PONTOON HEIGHT
Bp=PONTOON BREADTH
DISPLACEMENT RATIO=PONTOON VOLUME/TOTAL DISPLACEMENT
PONTOON ASPECT RATIO=Hp/Bp

FIGURE 14

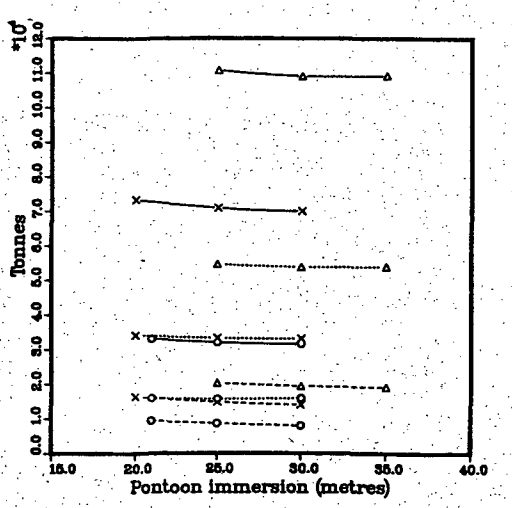

LEGEND

- o steelweight 5000
- × steelweight 15000
- △ steelweight 25000
- o pretension 5000
- × pretension 15000
- △ pretension 25000
- o displacement 5000
- × displacement 15000
- △ displacement 25000

FIGURE 16

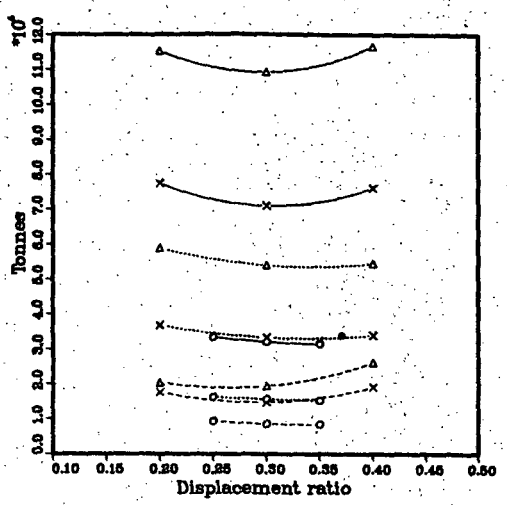

LEGEND

- steelweight 5000
- steelweight 15000
- steelweight 25000
- pretension 5000
- pretension 15000
- pretension 25000
- displacement 5000
- displacement 15000
- displacement 25000

FIGURE 17

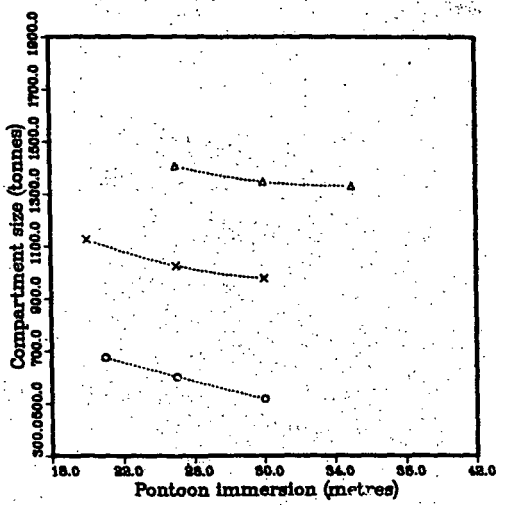

LEGEND

- payload 5000
- payload 15000
- payload 25000

FIGURE 19

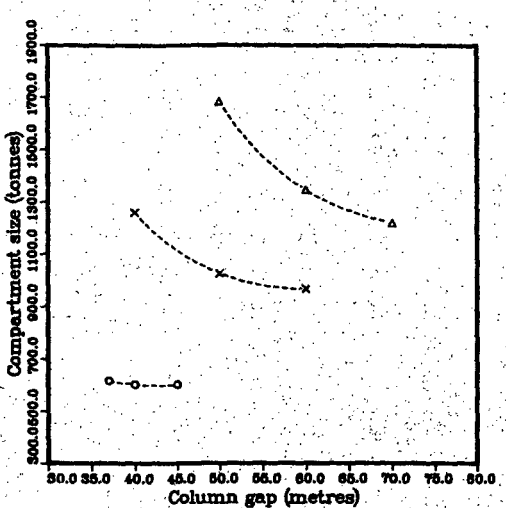

LEGEND

- payload 5000
- payload 15000
- payload 25000

FIGURE 18

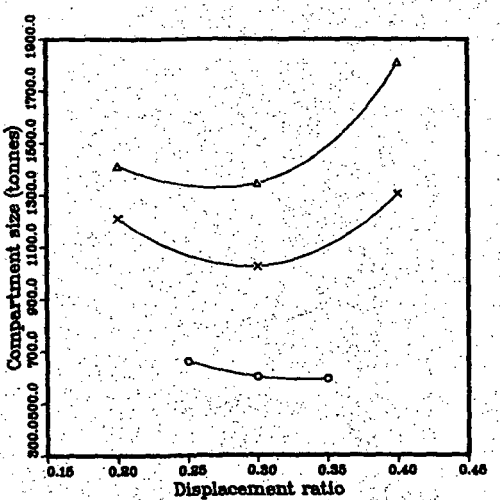

LEGEND

- payload 5000
- payload 15000
- payload 25000

FIGURE 20

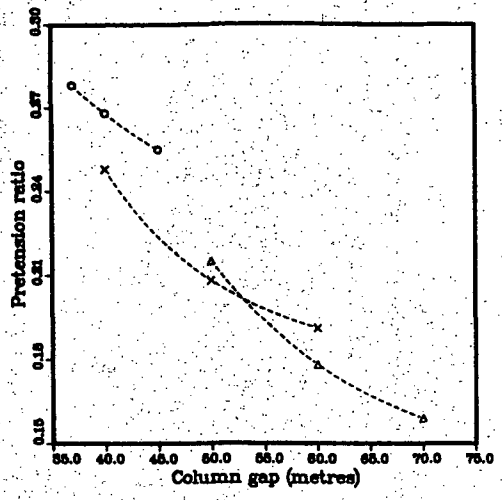

LEGEND
- payload 5000
- payload 15000
- payload 25000

FIGURE 21

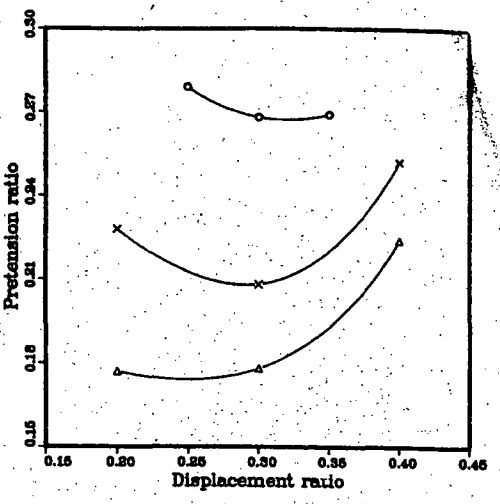

LEGEND
- payload 5000
- payload 15000
- payload 25000

FIGURE 23

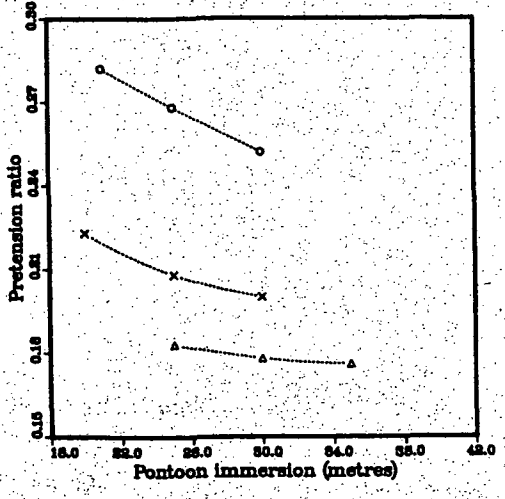

LEGEND
- payload 5000
- payload 15000
- payload 25000

FIGURE 22

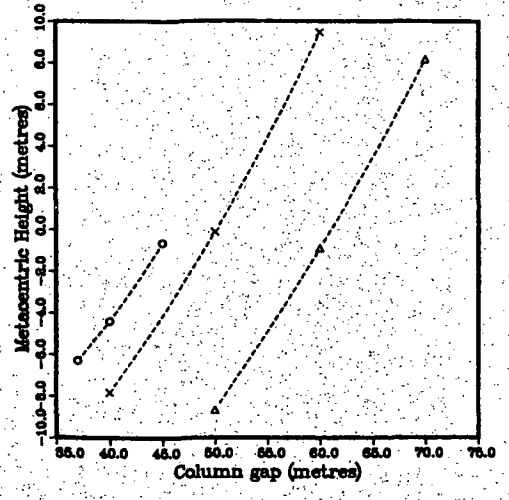

LEGEND
- payload 5000
- payload 15000
- payload 25000

FIGURE 24

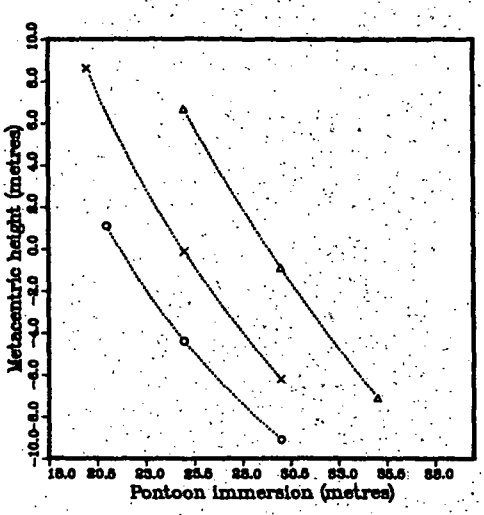

LEGEND
- payload 5000
- payload 15000
- payload 25000

FIGURE 26

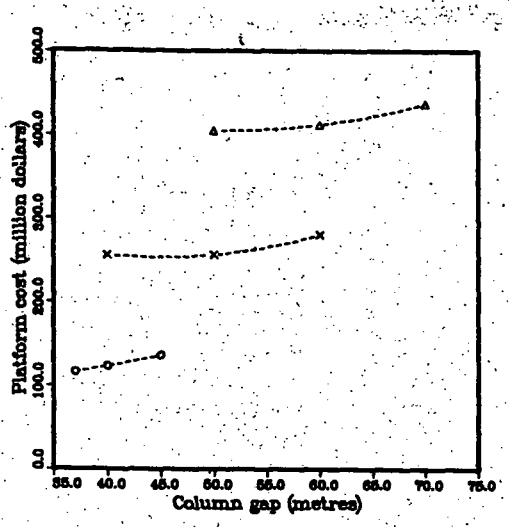

LEGEND
- payload 5000
- payload 15000
- payload 25000

FIGURE 27

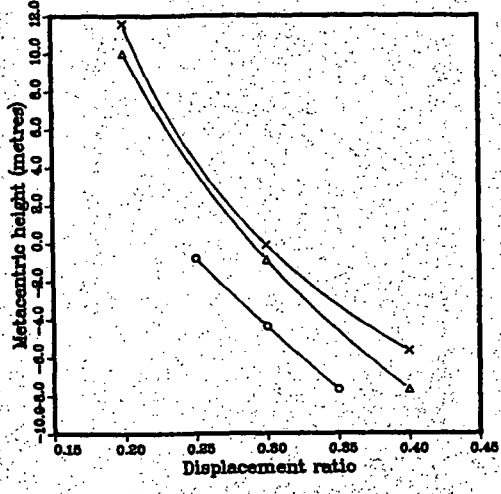

LEGEND
- payload 5000
- payload 15000
- payload 25000

FIGURE 28

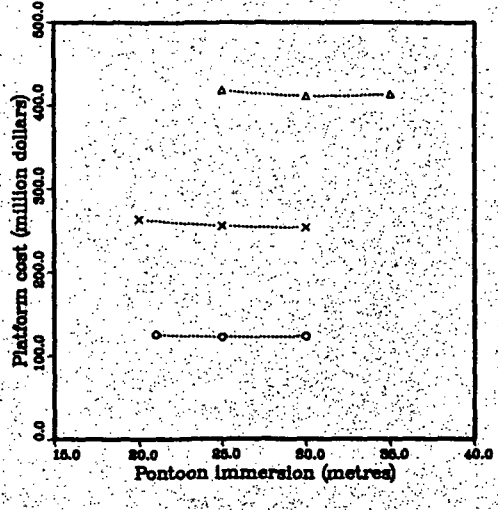

LEGEND
- payload 5000
- payload 15000
- payload 25000

FIGURE 29

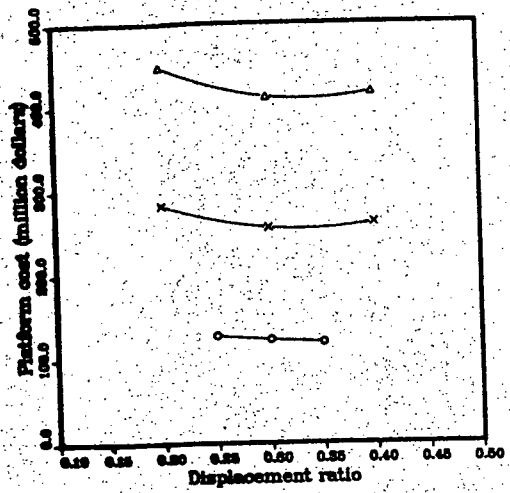

LEGEND

- payload 6000
- payload 15000
- payload 25000

FIGURE 29

BAR CHARTS SHOWING COMPOSITION OF TETHER LOADS IN THE MINIMUM TENSION "SLACKENING" TETHER CONDITION

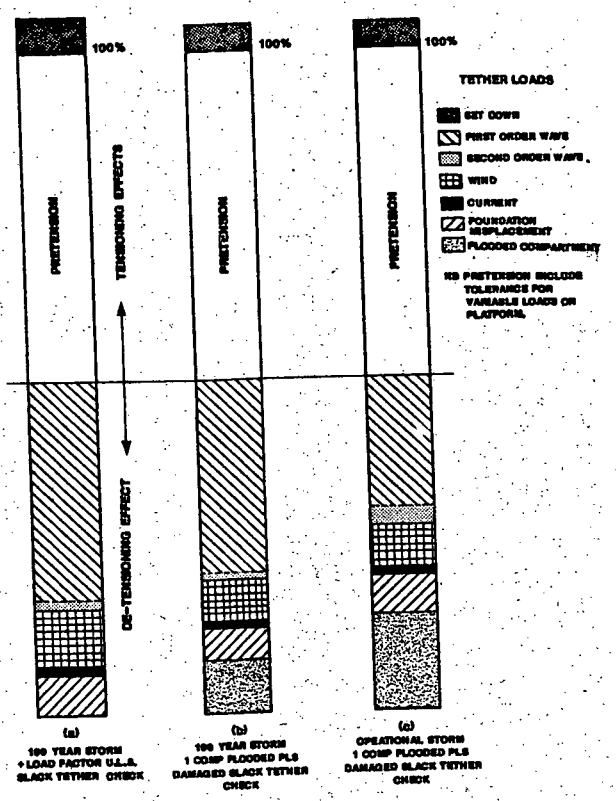

(Length of a shaded "load segment" gives load as a percentage of tether pretension)

FIGURE 31

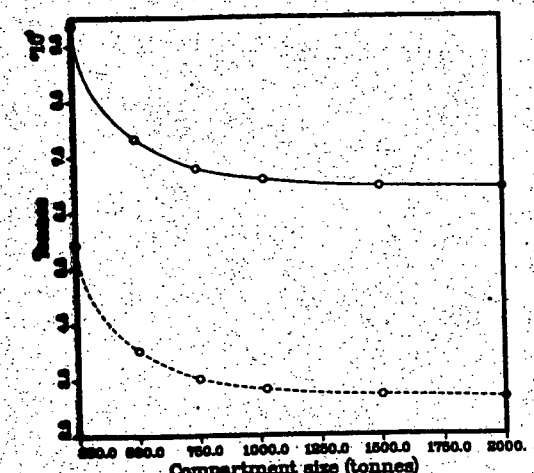

LEGEND

- steelweight
- displacement

FIGURE 30

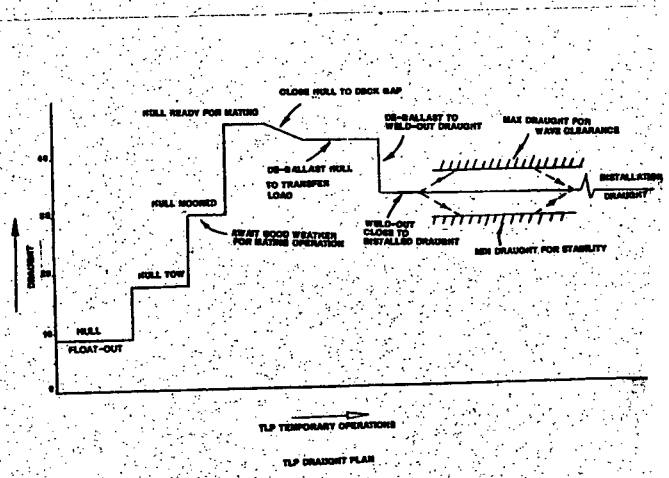

FIGURE 32

WIND SPEEDS

INTACT SURVIVAL	100 knots
INTACT OPERATING	70 knots
DAMAGED	50 knots

METACENTRIC HEIGHTS

OPERATING/SURVIVAL	>1.0 metre
TEMPORARY CONDITION	>0.3 metre

INTACT CRITERIA

AREA RATIO (SEE NOTE 1)	>1.3
STATIC HEEL DUE TO WIND	<15 DEGREES

DAMAGE ASSUMPTIONS

ANY ONE COMPARTMENT
OR
ANY COMPARTMENTS WITHIN
SPECIFIED DAMAGE ZONE

DAMAGE ZONE

VERTICAL EXTENT	+5 METRES)
	-3 METRES) FROM D.W.L
DEPTH OF PENETRATION	1.5 METRES
DAMAGE PATCH	3 X 3 METRES

DAMAGE CRITERIA

AREA RATIO (SEE NOTE 1)	>1.0
STATIC HEEL DUE TO DAMAGE*	<15 degrees
NO PROGRESSIVE DOWNFLOODING	

NOTE 1:

Area ratio is ratio of areas under wind heel and righting moment curve from point of zero heel moment to second intercept or downflooding point.

NOTE 2:

* Department of Energy do not require damaged heel with wind, but this has been applied in this analysis.

COLUMN STABILISED MOBILE OFFSHORE UNITS
CURRENT U.K DEPARTMENT OF ENERGY GUIDELINES

TABLE 1

CRITERIA	U.K DEPARTMENT OF ENERGY	HUTTON BARGE TOW
WIND SPEED (INTACT)	70/100* knots	71 knots
AREA RATIO	1.4	1.4
GM	0.3 metres	POSITIVE
STATIC HEEL ANGLE	<15 degrees	-
WIND SPEED (DAMAGED)	50 knots	50 knots
DAMAGED ASSUMPTIONS	TWO TANKS IN DAMAGE ZONE ONE TANK ELSEWHERE	ONE TANK
DAMAGED AREA RATIO	1.0	1.4
STATIC HEEL WITH DAMAGE	<15 degrees	-
DOWNFLOODING	NO PROGRESSIVE FLOODING	NO PROGRESSIVE FLOODING

* SURVIVAL CONDITION ONLY

BARGE STABILITY
COMPARISON OF PROPOSED U.K DEPARTMENT OF ENERGY AND HUTTON CRITERIA

TABLE 2

Payload (tonnes)	Hull Payload (tonnes)	Riser Tension (tonnes)
5,000	1,333	700
15,000	4,500	2,100
25,000	5,500	3,500

TABLE 3

Payload (tonnes)	Pontoon Immersion (metres)	Displacement Ratio	Column Gap (metres)
5,000	21	0.3	40
	25	0.3	40
	30	0.3	40
	25	0.25	40
	25	0.35	40
	25	0.3	45
	25	0.3	37
15,000	20	0.3	50
	25	0.3	50
	30	0.3	50
	25	0.2	50
	25	0.4	50
	25	0.3	60
	25	0.3	40
25,000	25	0.3	60
	30	0.3	60
	35	0.3	60
	30	0.2	60
	30	0.4	60
	30	0.3	70
	30	0.3	50

TABLE 4

DECK PAYLOAD (tonnes)	DRAUGHT (metres)	PONTOON IMMERSION (metres)	COLUMN GAP (metres)	DISPLACEMENT RATIO	AIR-GAP (metres)	COLUMN DIA (metres)	STEELWEIGHT (tonnes)	PRETENSION (tonnes)	DISPLACEMENT (tonnes)	COMPARTMENT SIZE (tonnes)	DISCONNECT GM (metres)	PLATFORM OFFSET (% water depth)	SET-DOWN	COMP SIZE DISPLACEMENT (metres)	PRETENSION DISPLACEMENT x 100	STEELWEIGHT PAYLOAD
5000	34.6	25	40	0.35	23.9	13.6	15311	8462	31459	593	-7.7	13.9	4.1	1.88	0.27	3.06
15000	36.9	25	50	0.3	26.5	20.4	33248	14809	70880	1025	-.13	12.7	3.5	1.45	0.21	2.22
25000	38.5	25	60	0.3	29.5	25.0	54645	20306	110742	1407	6.67	12.9	3.7	1.27	0.18	2.18

TABLE 5

INTACT STABILITY CRITERIA

1. Area ratio righting-moment curve/windheeling-moment curve to second intercept or downflooding, greater or equal than 1.30.
2. GZ positive from upright to second interception.
3. Heeling due to wind less or equal 15.00 deg.
4. Second interception between righting-moment curve and wind heeling-moment curve bigger or equal 30 deg.
5. GM bigger or equal 0.3m, for temporary conditions.
7. GM bigger or equal 1.0m, for stationery conditions.

DAMAGED STABILITY CRITERIA

1. Area ratio righting-moment curve/windheeling-moment curve to second interception or downflooding, greater or equal than 1.
3. Heeling due to wind less or equal 15.00 deg.
6. All progressive flooding and downflooding points above surface after flooding and with wind imposed.

MAXIMUM PERMISSIBLE RS'S FOR PARAMETRIC STUDY VESSELS

TABLE 6

PAYLOAD (Te)	No.	INSTAL DRAFT (m)	PONT DIM (m)	DISP RATIO	COL SPACING	COL GAP (m)	AIR GAP (m)	COL DIA (m)	PONT HT (m)	PONT WIDTH (m)	INST'D VCB (m)	PLATFORM MASS (Te)	WIND FORCE (kn)	C.OF ACTION (m)	INST'D DISP (Te)
5000	051	30.1	21	0.3	55.5	40	24.6	15.8	9.1	6.7	+1.8	22690	4424	32.0	33122
	052	33.9	25	0.3	54.3	40	24.3	14.3	8.9	6.6	- .32	22420	4214	32.0	32006
	053	30.9	30	0.3	53.3	40	24.1	13.3	8.9	6.6	-3.25	22660	4036	32.1	31818
	054	33.3	25	0.25	55.3	40	24.5	15.3	8.3	6.2	+0.42	23020	4304	32.0	33360
	055	34.6	25	0.35	53.6	40	23.9	13.6	9.6	7.1	-1.26	22010	4061	31.9	31459
	056	33.6	25	0.3	59.8	45	24.9	14.8	8.6	6.4	+0.88	24100	4708	32.8	33700
	057	34.2	25	0.3	51.1	37	24.0	14.1	9.2	6.8	-1.0	21530	3938	31.6	31198
15000	151	32.1	20	0.3	72.3	40	27.7	22.3	12.1	8.9	6.55	54240	6830	34.4	73397
	152	36.9	25	0.3	70.4	50	26.5	20.4	11.9	8.8	4.1	53330	6328	33.7	70880
	253	41.8	30	0.3	69.1	50	25.7	19.1	11.8	8.7	1.51	53270	5977	33.2	70062
	154	35.1	25	0.2	73.4	50	28.4	23.4	10.1	7.5	5.56	56910	7129	34.8	77355
	155	39.2	25	0.4	69.0	50	24.5	19.0	14.2	10.5	.63	54060	5848	32.4	75997
	156	36.0	25	0.3	81.0	60	27.7	21.0	11.0	8.2	5.46	56560	7556	35.5	73369
	157	38.6	25	0.3	60.5	40	25.9	20.5	13.6	10.1	2.15	53210	6734	35.4	74421
25000	251	38.5	25	0.3	85.0	60	29.5	25.0	13.5	10.0	8.0	85940	8666	36.6	110742
	252	43.4	30	0.3	83.4	60	28.1	23.4	13.4	10.0	5.41	85220	8119	35.7	109106
	253	40.5	35	0.3	82.1	60	27.1	22.1	13.5	10.0	2.68	85520	7722	35.0	109180
	254	41.3	30	0.2	86.3	60	30.8	26.3	11.3	8.4	7.6	90190	9157	37.5	115149
	255	46.1	30	0.4	81.7	60	25.7	21.7	16.1	11.9	1.53	85890	7504	34.0	116625
	256	42.5	30	0.3	93.8	70	29.3	23.8	12.5	9.3	6.65	88580	9504	37.6	110669
	257	45.0	30	0.3	73.4	50	27.5	23.4	15.1	11.1	3.65	84110	8977	38.1	112890

VESSEL GEOMETRIES FROM PARAMETRIC STUDY

TABLE 7

VESSEL NO.	CRITERIA 1	2	3	4	6	7	3d	3d	5d	CALCULATED RS
51	27.54	30.24	28.02	-	29.94	29.24	30.42	27.23	30.84	23.29
52	25.62	28.72	26.29	-	28.42	27.72	28.57	25.85	29.02	24.86
53	24.80	27.90	25.32	-	27.60	26.90	27.89	25.33	28.30	26.81
54	28.30	31.12	28.82	-	30.82	30.12	31.24	28.15	31.66	24.55
55	23.68	26.65	24.21	-	26.25	25.65	26.43	23.78	26.87	24.77
56	28.71	32.09	29.57	33.16	31.79	31.09	31.99	29.18	32.48	25.88
57	24.31	26.96	24.62	-	26.66	25.96	27.05	24.11	27.41	24.34
157	40.35	42.35	41.25	44.19	42.05	41.35	42.08	39.96	43.24	30.14
152	36.49	38.69	37.40	39.47	38.39	37.69	38.07	36.65	39.15	32.32
153	34.48	36.88	35.46	37.42	36.58	35.88	36.72	34.56	37.03	34.35
154	44.80	46.65	45.58	48.66	46.35	45.65	47.34	44.23	47.75	31.25
155	30.92	33.16	31.86	33.10	32.86	32.16	32.15	30.27	32.46	30.39
156	43.75	46.73	45.33	46.18	46.43	45.73	46.78	44.45	47.21	33.22
157	30.34	32.61	30.97	-	32.31	31.61	32.45	29.99	32.80	31.07
251	47.19	49.24	48.43	49.35	48.94	48.24	49.47	47.11	49.83	37.60
252	43.59	45.90	44.95	45.22	45.60	44.90	45.62	43.78	45.98	39.59
253	41.23	43.73	42.68	42.87	43.43	42.73	43.07	41.52	43.42	41.55
254	52.63	54.58	53.79	55.38	54.28	53.28	55.40	52.62	55.73	39.53
255	36.72	39.09	38.16	37.47	38.79	38.09	37.57	36.15	37.83	37.20
256	50.75	53.76	52.73	51.20	53.46	52.76	53.47	51.78	53.89	40.59
257	38.93	39.47	38.04	40.08	39.17	38.47	39.03	38.05	39.38	38.17 (DRAUGHT = 45m)
258	37.72	39.21	-	-	38.91	38.21	37.86	-	40.17	40.75 (DRAUGHT = 40m)
259	38.79	40.04	38.72	37.99	39.75	39.04	38.65	37.69	38.98	35.98 (DRAUGHT = 50m)

TABLE 8

Third International Conference on Stability of Ships and Ocean Vehicles, Gdańsk, Sept. 1986

STAB'86

AN EXPERIMENTAL TECHNIQUE FOR INVESTIGATION INTO PHYSICS OF SHIP CAPSIZING

S. Grochowalski, I. Rask
P. Söderberg

ABSTRACT

The Institute for Marine Dynamics of the National Research Council of Canada have started a long term research program aimed at formulating a set of appropriate stability criteria. The project is concentrated on smaller fishing vessels.

SSPA Maritime Consulting AB was contracted to carry out a comprehensive test program with both free-running and captive tests to determine the response as well as the forces acting on a 20 m stern trawler in large breaking waves.

This paper describes the test technique used for free-running tests, completely captive tests and captive tests with freedom to heave and pitch. It also gives some examples of the results of the test analysis.

1. INTRODUCTION

The lack of stability criteria which would be applicable to small fishing vessels and frequent capsize disasters occurring in this class of vessels, have prompted the Ship Safety Branch of the Canadian Coast Guard to request the Institute for Marine Dynamics of the National Research Council of Canada to formulate and undertake a corresponding long term research program.

The study commenced about two years ago and is aimed at formulating a set of appropriate stability criteria founded on a rational basis. Therefore, attention is focused on developing a theoretical model of ship capsizing since there is still no such model capable of adequately representing the general case of ship capsizing in extreme wave conditions.

Although a considerable amount of research is being carried out in this field, the efforts are usually concentrated either on studies of some selected simplified cases such as roll resonance, Mathieu instability, beam breaking waves and broaching in following seas or on some improvements of traditional approaches as e.g. "sufficient" stability curves, energy balance, etc. While it is difficult to generalize the results of studies of particular situations, the rationality of improvements of traditional methods can be questioned.

After some studies, and a review of results of various model tests, the instance of a ship moving in quartering breaking waves has been selected as the subject of NRC's research. It has been concluded that this is the most dangerous and also the most general case, in which all particular dangerous situations, usually investigated separately, may be focused in one event. The resonance or sub-harmonic roll, reduction or loss of stability on a wave crest, large amplitude motions with strong coupling between roll-sway-yaw-heave, etc, could be observed. Capsizing in quartering waves may also occur as a totally transient event due to some factors normally not considered in equations of rolling, i.e. broaching and centrifugal moments, impact of breaking waves, immersion of deck edge and bulwark with simultaneous large lateral motion which causes additional strong coupling effects, etc.

In studies of such complicated dynamic phenomenon, it is essential to evaluate the contribution of different dynamic factors, to find a correlation between them and to select the most decisive ones from the capsizing point of view. Obviously, it cannot

yet be done by theoretical considerations alone. Appropriately designed, precisely instrumented and scrupulously carried out model experiments can help not only to analyze and better understand the physics of ship capsizing, but also to evaluate the quantitative influence of particular elements.

These were the reasons that a special experimental program was designed. The objective was not to examine systematically the stability quality of a certain vessel or class of vessels in various environmental conditions, but to investigate the physics of capsize phenomenon in general and most critical situations. The results should help to define a mathematical model suitable for the prediction of capsizing in extreme quartering seas and to validate or calibrate the numerical simulating programs.

2. PHILOSOPHY OF THE EXPERIMENTS

The dynamic identification of a ship from the capsizing point of view could be completed if two components of the phenomenon are fully identified:

- composition of acting forces and moments generated by waves;
- characteristics of a corresponding response of a ship.

However, the problem lies in the fact that it is impossible to measure the exciting hydrodynamic forces and the model response at once. Therefore, the usual practice in experimental investigations of ship capsizing is measuring the behaviour of a free model in various wave configurations. These types of tests may be very useful for stability estimation of a particular ship in specified environmental conditions but they do not give any information about either exciting forces or the relationship force-response during complicated motion and capsizing. Obviously, the identification methods based on linear theory and used in seakeeping are not applicable to this case.

A special composition of experiments was designed to solve this complex problem. The principles of the idea could be summarized as follows:

(A) the dynamics of large amplitude motions and capsizing in specified waves, loading and propulsion-steering conditions will be simulated by use of the free-running model technique;

(B) the hydrodynamic forces, generated on the ship by the same specified waves, and at the same conditions as for a free-running model, can be measured on a model restrained at a specified 'frozen' position, moving with the same forward speed. These have been named 'captive model tests'.

Measurements on a fully restrained model (fully captive model tests) are the most convenient for a validation of theoretically developed computer programs, while it is more valuable for investigations into capsizing mechanism to measure the forces in the captive modes on the model, which is free to heave and pitch (partly captive model tests).

(C) In order to reproduce the real capsizing mechanism the free-running and the captive model tests must be correlated so that for every instantaneous position of the model in respect to the wave profile in the free-running situation, the appropriate 'frozen' situation in the captive tests can be found and the composition of the hydrodynamic forces can be interpolated. That can be achieved if in both cases the wave profiles and forward speeds are the same and the range of headings and heel angles in the captive tests cover the range of changes of those parameters in free-running tests.

Proposed procedure requests test facilities with a special capacity. A high quality wavemaking system producing extremely steep repeatable waves, precision instrumentation and, first of all, a wide wave basin spanned by a carriage which would be able to move the fastened model with a desired path -- are the basic necessary features.

Such exacting conditions can be provided at the SSPA Maritime Dynamics Laboratory in Göteborg, Sweden. SSPA has designed and set up appropriate measuring systems which make the proposed experiments possible. The main characteristics of the facilities and the developed experimental technique as well as the description of the carried out experiments are presented below.

3. TEST FACILITIES

The SSPA seakeeping basin which measures 39 x 88 m has wavemakers of flap-type along one short and one long side for generating sinusoidal or breaking regular or irregular long-crested waves of any kind. Along the opposite sides there are wave absorbers. The water depth can be varied between 0 and 3 m.

A computer-controlled multi-motion carriage system spanning the basin can be used for towing or tracking a model moving in an arbitrary way.

The onboard standard data acquisition system can provide recording of 38 measurement signals at a sampling frequency of 25 Hz.

4. FREE-RUNNING TESTS

At the free-running tests the model is self-propelled and autopiloted.

The multi-motion carriage is used to accelerate the model prior to each test and to catch it after test completion.

After release from the carriage the model is controlled by the autopilot, of a proportional regulator-type.

In order to keep the model within the working range of the electro-optical system used for measuring yaw the carriage can be controlled with a joy-stick.

Power supply and data logging system as well as two video cameras, one behind and one beside the model, a high-speed movie camera and necessary lighting were located on the carriage. The test arrangement is shown in Fig 1.

At the tests the waves were measured with one wave probe in a fixed position in the basin and another located on the carriage to measure the waves close to the model.

Roll and pitch were measured with a gyro horizon and yaw with an electro-optical system (Selspot).

The model speed is measured with a Pitot tube located amidships under the keel.

Longitudinal, transverse and vertical accelerations were measured with accelerometers located in the center of the model at CWL.

The rudder angle is measured with a potentiometer on the rudder shaft.

Vertical motions of the water surface relative to the ship side were measured amidships on both the starboard and port sides. As a complement to the relative motion measurement the model had a system of marks on the sides. The wave profile at the sides could therefore be determined from the video recordings which were synchronized with the data logging system.

5. CAPTIVE MODEL TESTS

5.1 Fully Captive Tests

The fully captive test arrangement is shown in Fig 2.

The model is connected to the carriage by a six-component balance and has no freedom to move relatively to the carriage. The model follows the carriage motion and is thus forced to move in the horizontal plane with controlled forward speed, drift speed and required heading angles in relation to the wave direction.

The model can be fixed in different heeling angles up to 45 deg. The heave position is adjusted for different heels to get the same displacement for the ship as in upright position in calm water.

The model is equipped with self propulsion arrangements. The propeller revolutions are adjusted to a constant value corresponding to the model self propulsion point in calm water.

During the tests the forces and moments in six modes are registered, i.e. heave, surge, sway, roll, pitch and yaw. Furthermore, the relative motion of the waves is measured on both sides of the model. Propeller revolution and rudder force can also be measured. The model speed and heading are given from the carriage position.

5.2 Partly Captive Tests

The partly captive test arrangement is shown in Fig 3. It is composed of a statically balanced frame including a four-component balance for measuring forces in the ship surge and sway and moments in yaw and roll. Further a light-weight measuring arm capable of registering motions in all six degrees of freedom is used. Thus a control of the free motions of the ship as well as of the flexibility of the captive frame is made.

The model is free to heave and pitch,

but fixed to the carriage in all other directions. Similarly to the fully captive tests the model is forced to move in the horizontal plane by the carriage motions. The model speed and course are also calculated from the carriage position.

Some problems occur when arranging a partly captive test set-up. As some motions will be restrained there will be forces on the model in the connection point. If these forces should not influence the free motions the connection point has to be in the center of buoyancy. This point is, however, not fixed in the hull but dependent on the position in the wave. To minimize the influence on the free motions the model is attached to the balance in a point close to the center of gravity.

In these tests, demanding a watertight model, it was not possible to arrange the connection under deck. The model was instead connected to the test arrangement in a point on the deck immediately above the center of gravity.

Similarly to the fully captive tests the model can be adjusted to different heel angles up to 45 deg.

As for the fully captive tests the model was equipped with self propulsion arrangements. During the tests the propeller revolutions are adjusted to a constant value corresponding to the self propulsion point in calm water. When the model is restrained in surge motion, connected in a point not equal to the center of flotation, a pitch moment will be introduced on the model. However, this effect can be minimized by the model being self-propelled.

In this test set-up the model displacement, longitudinal center of gravity and radius of gyration for pitch have to be correctly scaled.

5.3 Static Influence of Frame on Partly Captive Tests

So as to give no static influence on the model in the vertical direction in calm water the test frame has a counter balance.

When the heave position of the model is changed from calm water level, a vertical force will be transferred to the model from the frame. With a maximum heave amplitude of 0.14 m the force will be about 8 N.

This vertical load on the model is small compared to the model displacement. It will, however, result in a small increase of heave motion.

5.4 Dynamic Influence of Frame on Partly Captive Tests

The mass inertia of the test fram will give some dynamic influence on the model when the ship is moving in waves.

The angular motion of the test frame will result in a vertical force acting on the ship model. The force will vary harmonically with the ship heave motion and will reach its maximum value in the extreme heave positions. The magnitude of this force is dependent on the heave frequency.

The mass inertia of the frame is approximately 10 kg m^2. With a maximum wave frequency of encounter in these tests of 5.7 rad/sec this results in a maximum heave force acting on the model of about 32 N.

From previous investigations with another model it is known that the static and dynamic influences on the measurements give a small increase of the heave motion of the ship but the influence on the measured forces and moments in surge, sway, yaw and roll direction is not significant.

5.5 Wave Measurements

Wave measurements were made in two different points simultaneously with one fixed wave probe at a position 10 m perpendicular to the long side from the basin center and the other positioned close to the model, being fixed to the carriage and following the model, measuring the encountering waves.

Registrations of the relative wave motions were carried out amidships on both the starboard and port sides.

Using the registrations from the wave probe following the model at a known distance it is possible to calculate the phase lag between forces and encountering waves.

5.6 Data Processing

The directly registered forces and moments refer to a fixed point in the balance. These values are then recalculated to the model center of gravity by means of a coordinate transformation. As the position of the model in relation to the carriage is measured simultaneously with the forces it

is possible to carry out this recalculation for each sample.

6. PERFORMED EXPERIMENTS

A model of a typical Canadian stern trawler of 19.75 m length was used in the experiments. The main particulars of the model are the following:

L_{OA} = 1.413 m Displacement:
L_{WL} = 1.328 m Δ_1 = 53.1 kg (port departure)
B = 0.435 m Δ_2 = 65.7 kg (fully loaded)
d = 0.190 m Scale 1:14
D = 0.263 m

The shape of the body is shown in Fig 4.

The model was built with the decks, forecastle, deckhouse and bulwark. The draft marks on every station were painted to enable the estimating of a wave profile at the model side.

According to the developed conceptual frame the experiments were split into three different categories: free, fully captive, and partly captive model tests.

The tests with the free-running model were carried out in regular and irregular waves for two displacements and two metacentric heights for each one. The model was tested at three forward speeds, mostly in quartering waves at the heading angle ~30° but the behaviour in beam waves was investigated as well. The notion 'regular wave' refers here to waves with the constant period and constant wave height but with the wave profile not sinusoidal.

The regular waves were generated with 1/7 height to length ratio to achieve the maximum steepness and the breaking effect. Seven wave lengths were selected so that the most important range of frequency was covered, including the roll resonance. The range of corresponding wave height was [0.18 m - 0.65 m] which corresponds to [0.68 - 2.47] of the model moulded depth.

The irregular waves were generated according to JONSWAP spectrum for two different combinations of significant wave height and modal period so that the pattern of big breaking and plunging waves could be formed frequently. The significant wave heights for the spectra were 0.30 m and 0.36 m.

The performed program which consisted of 117 runs covered a wide range of possible dangerous situations, and many capsize events have been recorded.

While the experiments with the free-running model were concentrated on the investigations in quartering extreme waves with different frequencies, the captive tests were performed in regular waves with one nominal wave period T = 1.1 sec and one corresponding height of 0.27 m, and in irregular waves of one JONSWAP spectrum (γ = 3.3, $H^{1/3}$ = 0.30 m, T = 1.5 sec). These waves were selected from the program for free model tests. One loading condition was tested.

The program contained combinations of three forward speeds (the same as for free-running tests), three forced drift speeds, five heading angles (30°, 40°, 50°, 60°, 90°) and five angles of heel (0°, 10°, 20°, 35°, 45°).

The combinations of these parameters were formed in such a way that the interpolation of the results for other combinations within the frame of this pattern can be made.

The investigation of the influence of the heading angle, the heel position and the possible lateral motion on the value of generated hydrodynamic forces was focused in the captive tests.

The fully captive and partly captive model tests were carried out according to the same program. The number of runs amounted to 320.

7. EXAMPLES OF THE RESULTS

As many as 437 tests were carried out all together. The analysis of the records has not yet been completed and therefore final results and conclusions cannot be given at present.

The form in which the physical values were recorded is illustrated by reproduced fragments of the time histories, which also indicate the kind of immediately accessible information.

An example of a time record from the free model experiments is shown in Figs 5-6. That run was performed in the same regular waves as all the captive tests were carried out. The final part of the record showing the process of capsizing is presented.

All the components of the motion and their interrelation can be analyzed. As the measured data are recorded in digital form

it is easy to reproduce any specific part of the plots in desired form and scale for a detailed analysis or to use the values directly for any computations, transformation, etc.

The positions of the wave crest in respect to the model length are shown at the bottom of the figures and the corresponding time points are marked on the time histories. This is possible by the fact that the time which is monitored on the video records, is synchronized with the time base of the digital recording. As can be seen from the graphs, the confrontation of the motion components with the wave crest passing along the model creates a new excellent tool for studies of ship capsizing.

The additional interesting information can be gained through analysis of the water relative motions at the model sides and the bulwark position in respect to the water surface. In Fig 5 the time, when the bulwark is under water, has been indicated. From the records of yawing and the instantaneous forward speed it is possible to evaluate the centrifugal moments due to yawing and broaching.

Since for any point in time the wave profile at the model side and the instantaneous position of the model in space can be determined, the test records provide valuable data for the validation of numerical time domain simulations of ship motions in extreme wave conditions.

Examples of time records from the captive model tests are shown in Figs 7-9.

The selected fully captive model test was carried out in regular waves at heading angle of 30^{o} with the model fastened in the upright position, without forward speed and without drift. All the six components of the total hydrodynamic force, their orientation in space and the water relative motions at the midship, are presented. The time points corresponding to the position of the wave crest at the stern, quarter of the model length, midship, etc, are marked on the graphs.

The wave profile at the model side can be found from the video records which are synchronized with the time base of the digital records as it is done for free model tests. Thus, the dependence of the generated forces on the position of the passing wave crest can be analyzed. Furthermore, the measured values can be directly compared with theoretical calculations performed for the same 'frozen' wave-model configurations, which is essential for validation of computer programs calculating the hydrodynamic forces at such extreme conditions.

A record of a partly captive model experiment which was carried out at the same conditions as the fully captive one, is presented in the same pictures. The same wave profiles and the position of the wave crest in respect to the model, were the synchronizing factors making the comparison of both cases possible.

For an illustration of the dependence of the hydrodynamic forces and moments on the angle of heel, the appropriate fragments of the time histories from the fully captive tests have been drawn on Fig 10 and for the partly captive tests on Fig 12. The graphs were synchronized in respect to the wave profile and the position of the wave crest at the model side.

The same approach was applied in preparation of a comparison of the forces and moments at different heading angles. The time plots for some of the tested heading angles are presented for the fully and partly captive model on Figs 11 and 13 respectively.

It can be seen from the presented examples that the following information can be obtained immediately from the captive tests:

- maximum values of the moments and forces for a particular hull shape in waves for which the theoretical calculations still fail;
- phase lags between the components of the total hydrodynamic force;
- phase lags between the forces and the wave crest position at the model;
- position of a wave crest at which the heeling moment reaches the maximum, changes its sign, etc;
- what difference in the roll moment distribution is caused by free heave and pitch;
- dependence of the particular forces and moments on heading angle, heel angle, forward speed, drift, etc.

This information improves our understanding of the dynamics of large amplitude motions and is essential in formulating an adequate theoretical model of ship capsizing in quartering breaking waves.

8. CONCLUSIONS

The preliminary analysis of the test results confirms that the developed experimental system affords possibilities for detailed studies of:

1. hydrodynamic forces and moments generated on the body by a passing arbitrary wave, in particular the composition of the forces and moments, their interrelation and dependence on the instantaneous position of the ship in respect to the wave profile;
2. motions of a ship in extremely steep or breaking waves, in particular,
   - the interrelation of the components of the motion and their dependence on the instantaneous ship position in the wave;
   - analysis of factors which affect the ship dynamics in waves and selection of the most decisive ones;
   - selection of the most dangerous situation from the capsizing point of view.

The incorporation of the video recording technique with the synchronized time base into the measuring system, makes it possible to combine the free and captive model tests by using an appropriately composed program of the experiments. In this way, the components of the chain: wave profile - position of a ship; generated hydrodynamic forces - ship motion, can be fully identified.

This creates the capability to:

- analyze the stability safety of a particular ship in severe seas, select the most dangerous situations, and find the limiting conditions;
- validate deterministic models of ship dynamics in extreme and breaking waves and calibrate appropriate computer programs for calculations of the hydrodynamic forces and motion simulations in time domain;
- investigate fully the mechanism of ship capsizing in the most general case.

It is hoped that the designed experimental approach and the developed sophisticated measuring technique will provide a useful tool for studies of ship capsizing phenomena for which the theoretical models still fail.

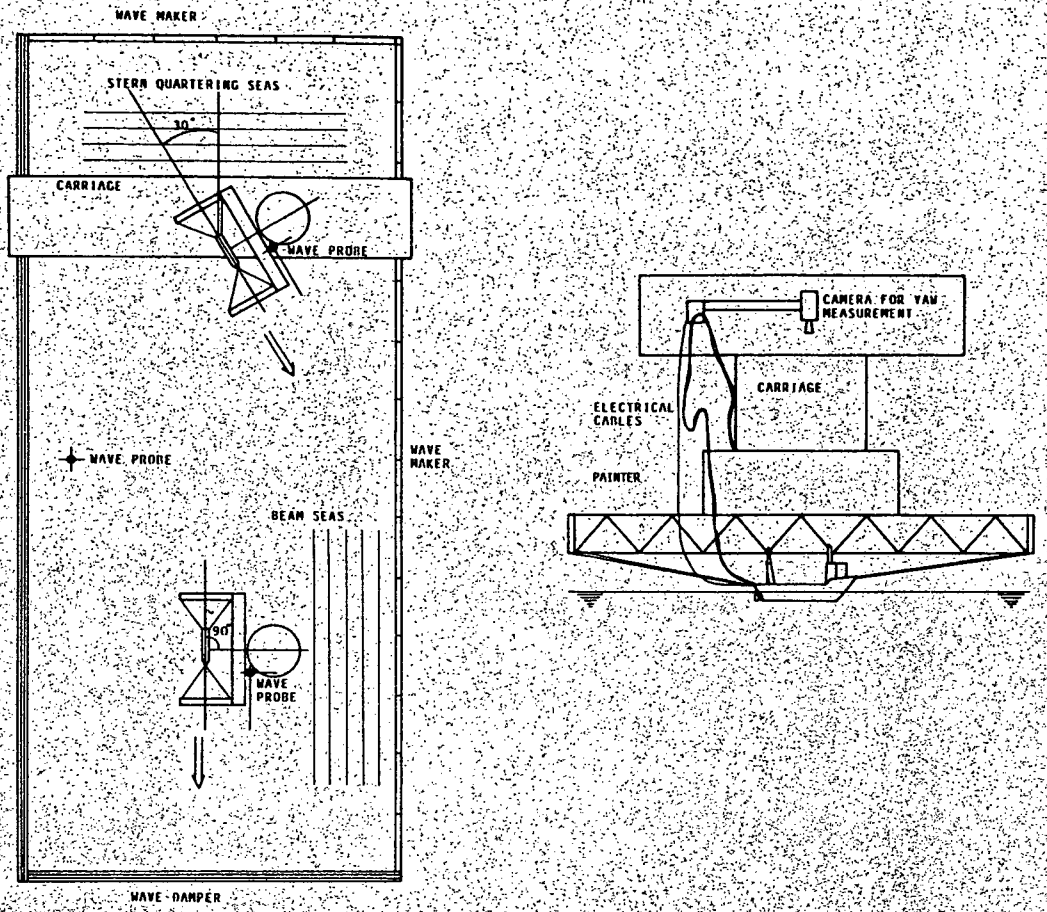

Fig 1. Free run test.

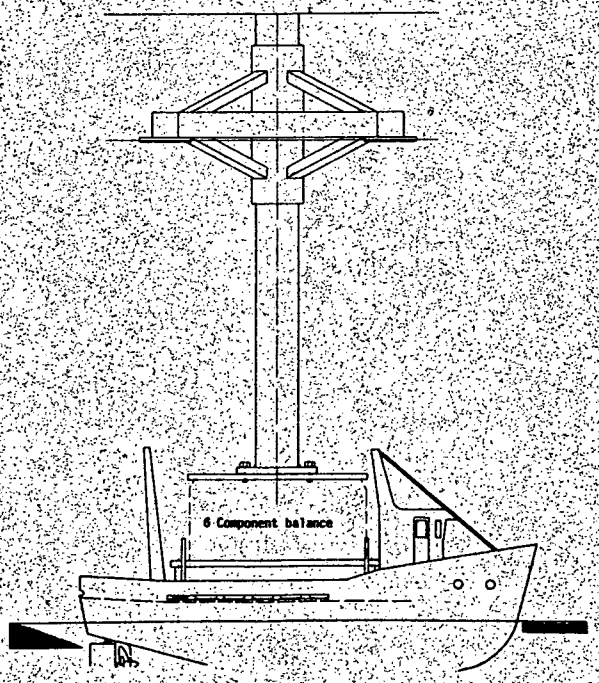

Fig. 2 Fully captive test

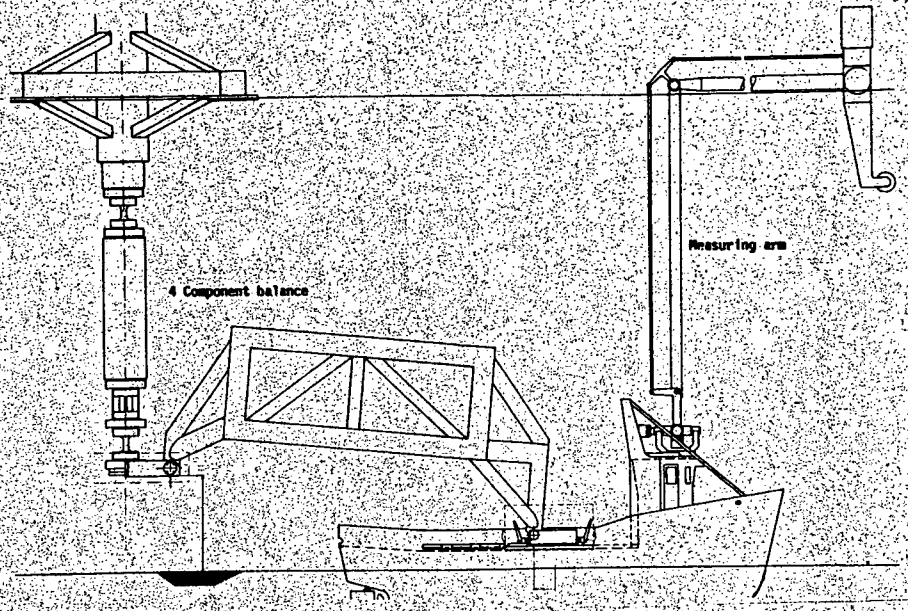

Fig. 3 Partly captive test

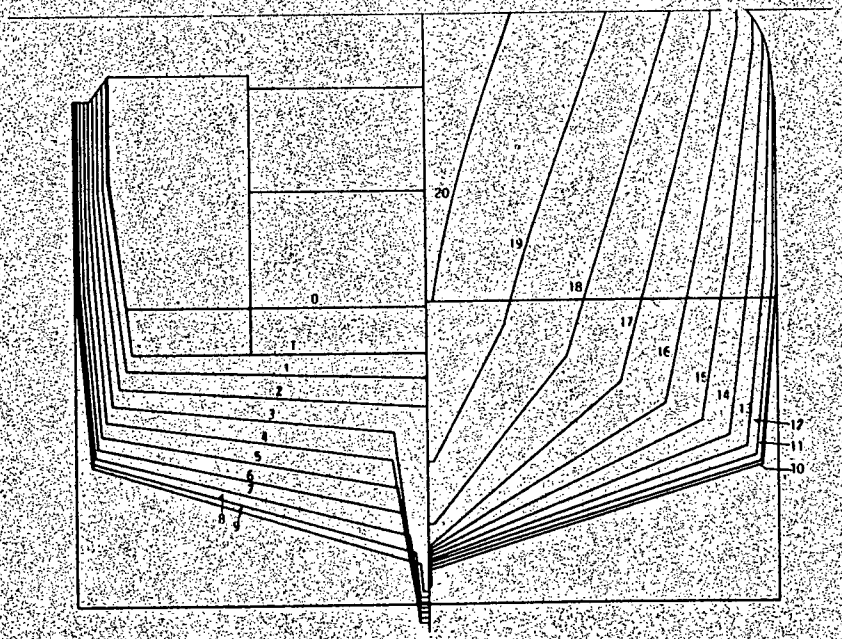

Fig. 4 Body plan

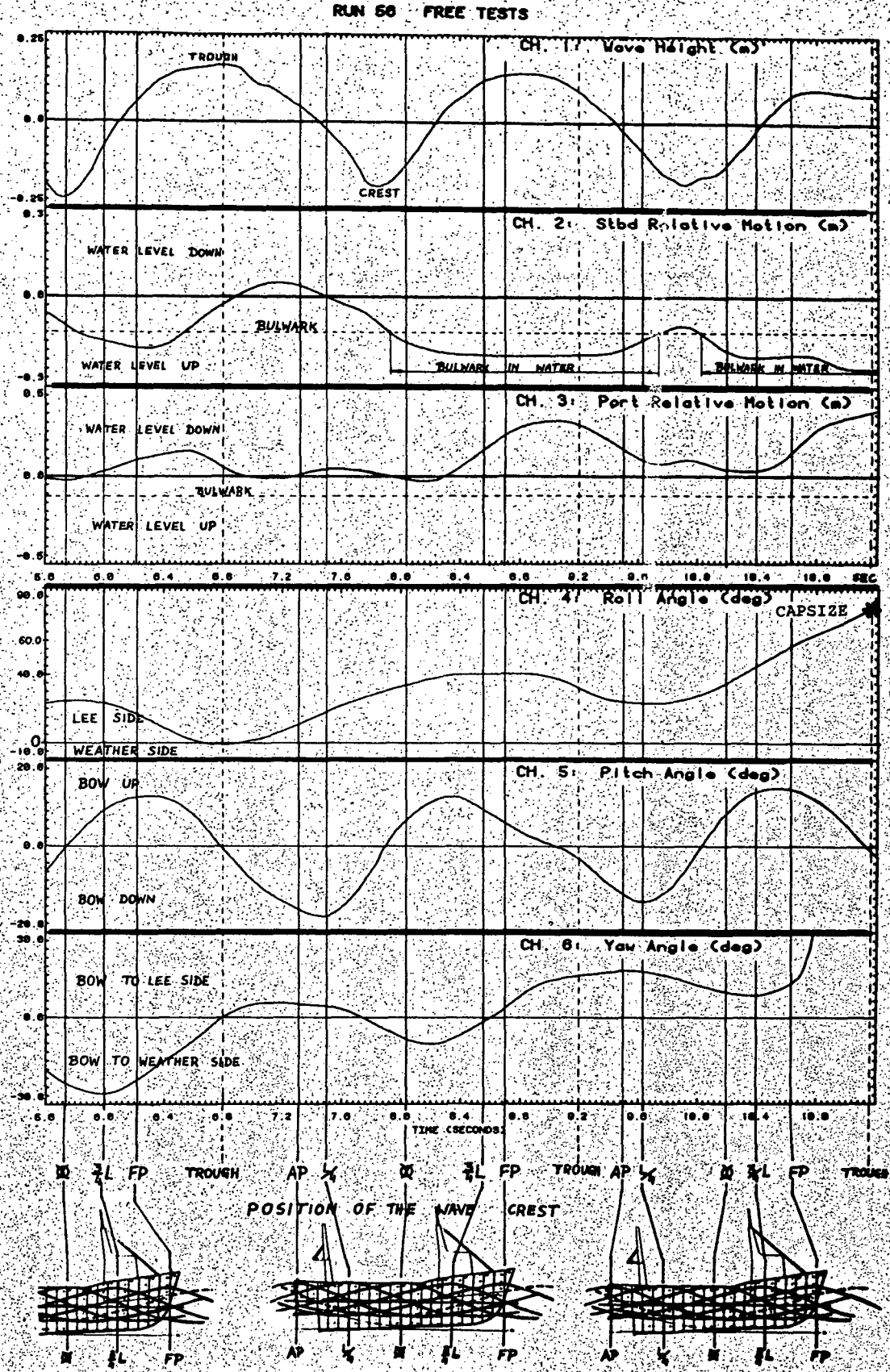

FIG.5 FREE RUNNING MODEL.
A FRAGMENT OF TIME HISTORY OF MOTIONS INCLUDING CAPSIZING.

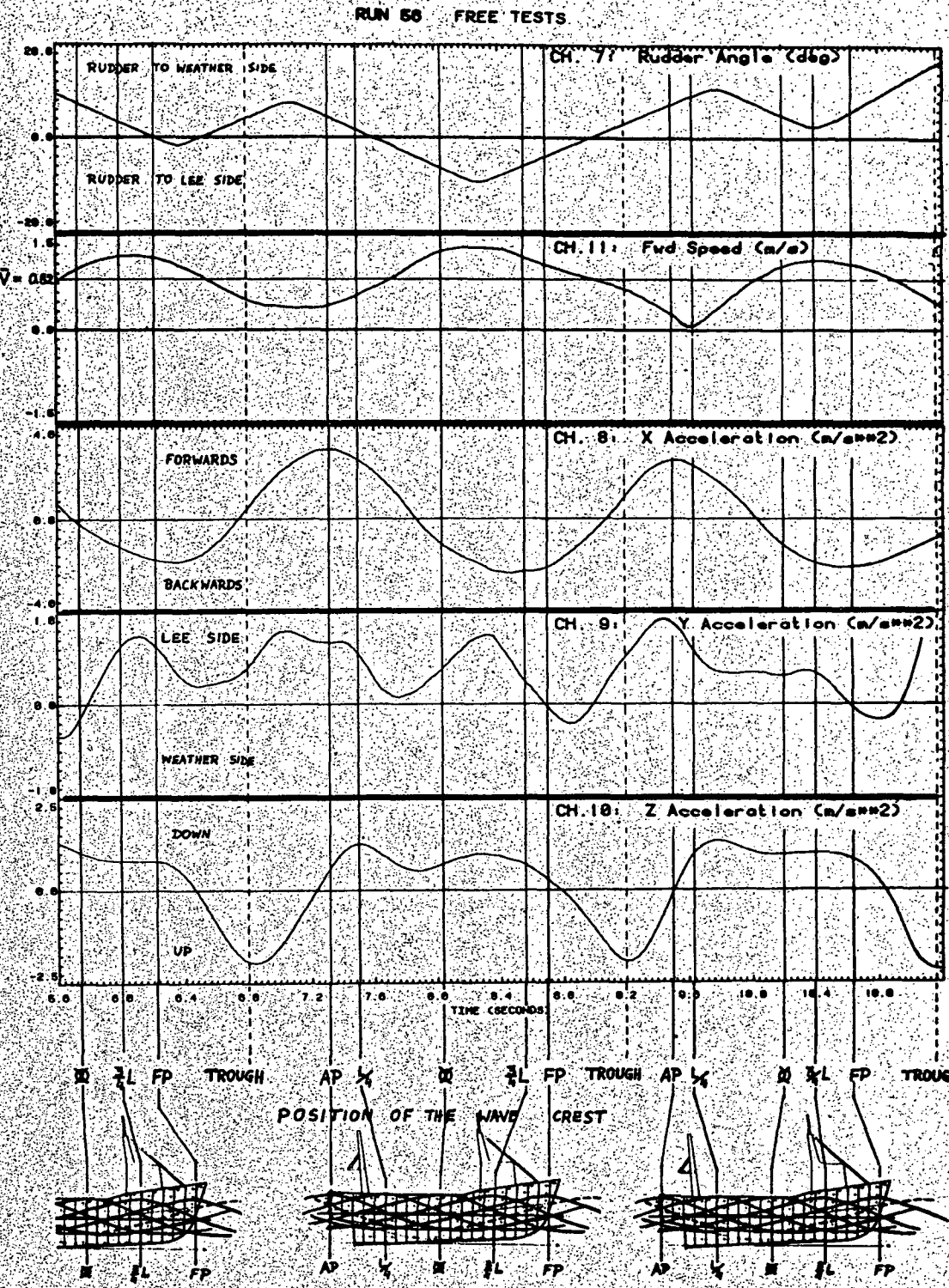

FIG.6 FREE RUNNING MODEL.
A FRAGMENT OF TIME HISTORY OF MOTIONS INCLUDING CAPSIZING (Cont.).

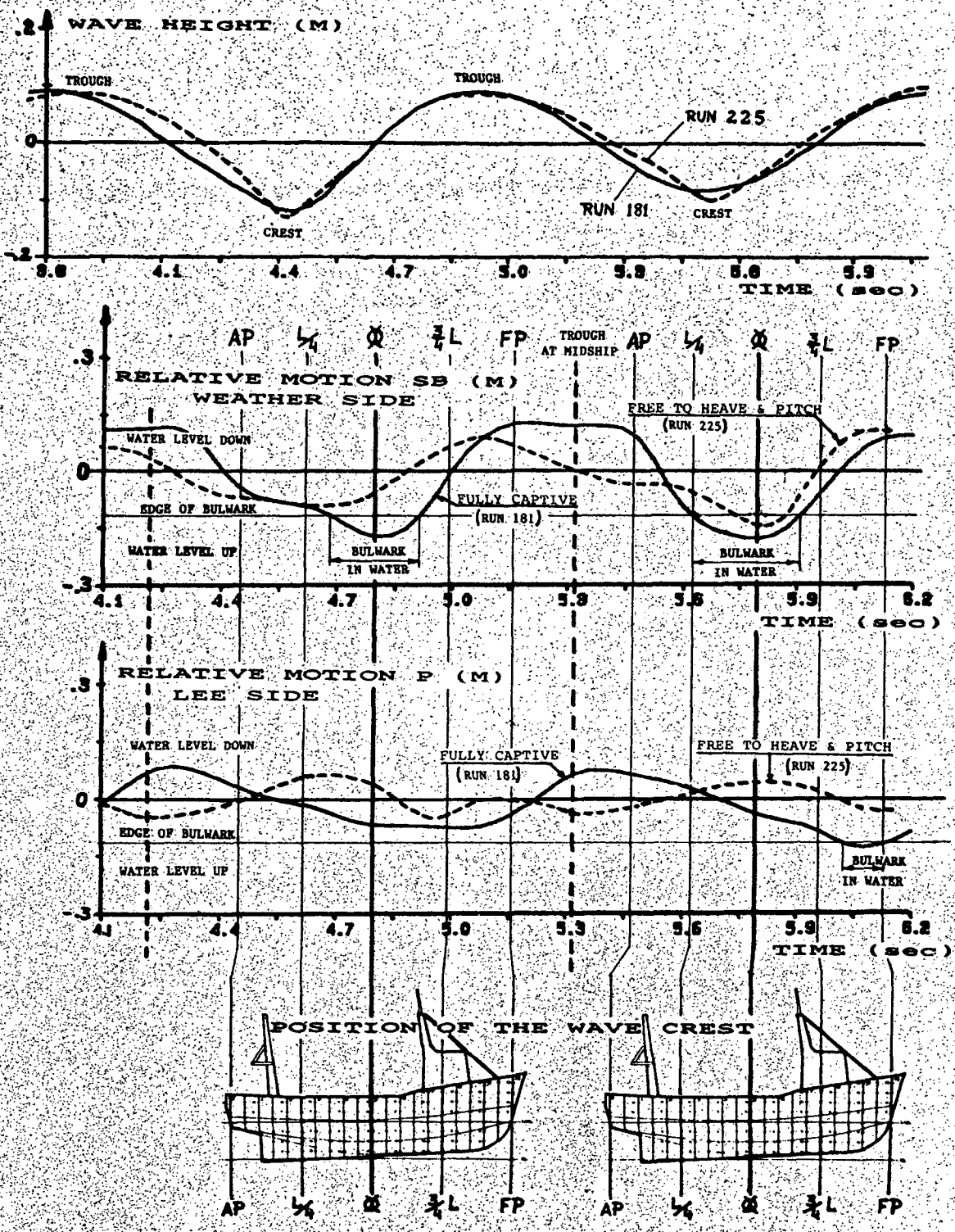

FIG.7 COMPARISON BETWEEN FULLY AND PARTLY CAPTIVE MODEL TESTS

WAVE PROFILE AND WATER RELATIVE MOTION DURING 2 WAVE CYCLES

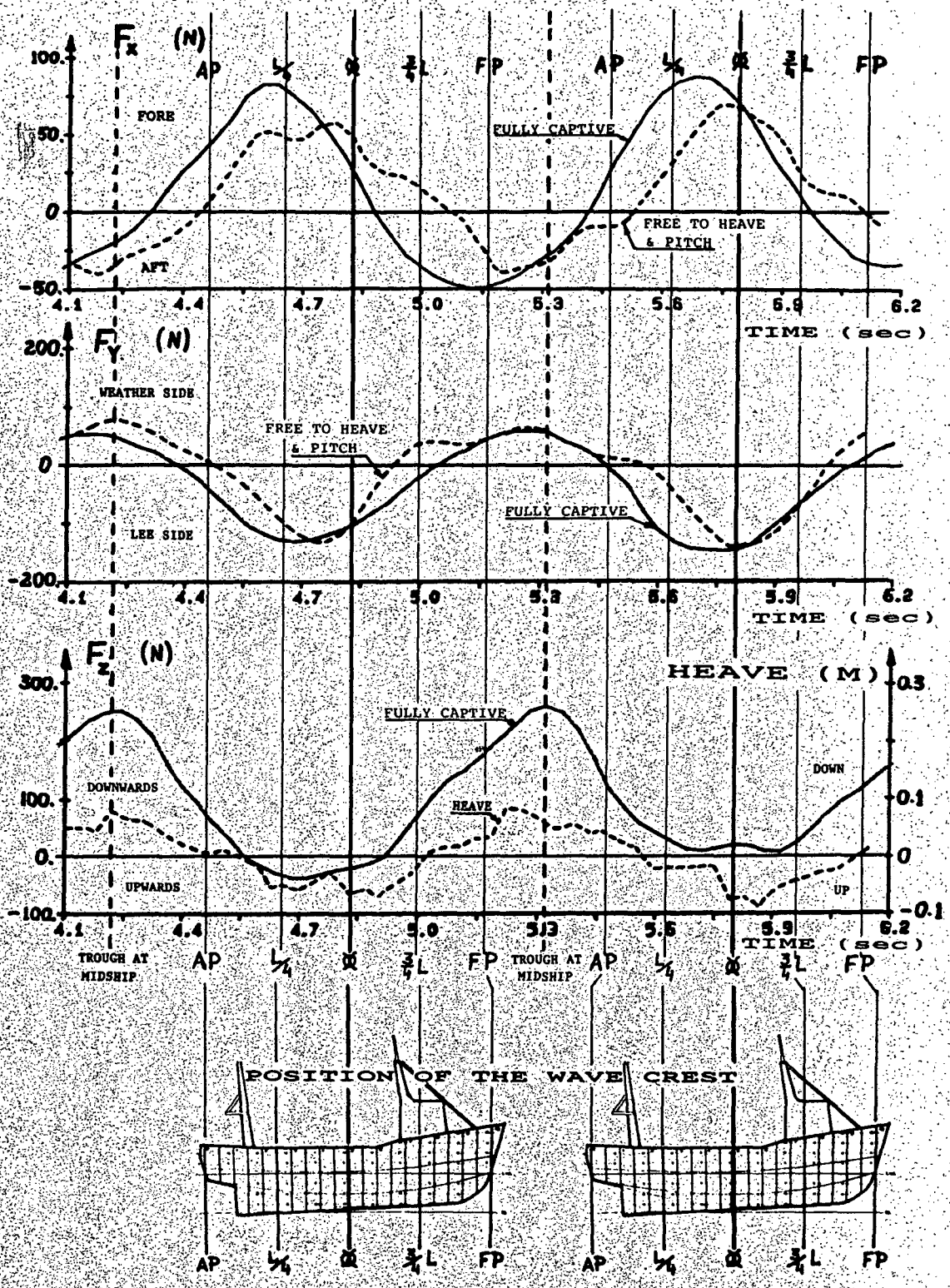

FIG.8 COMPARISON BETWEEN FULLY AND PARTLY CAPTIVE MODEL TESTS

HYDRODYNAMIC FORCES DURING 2 WAVE CYCLES

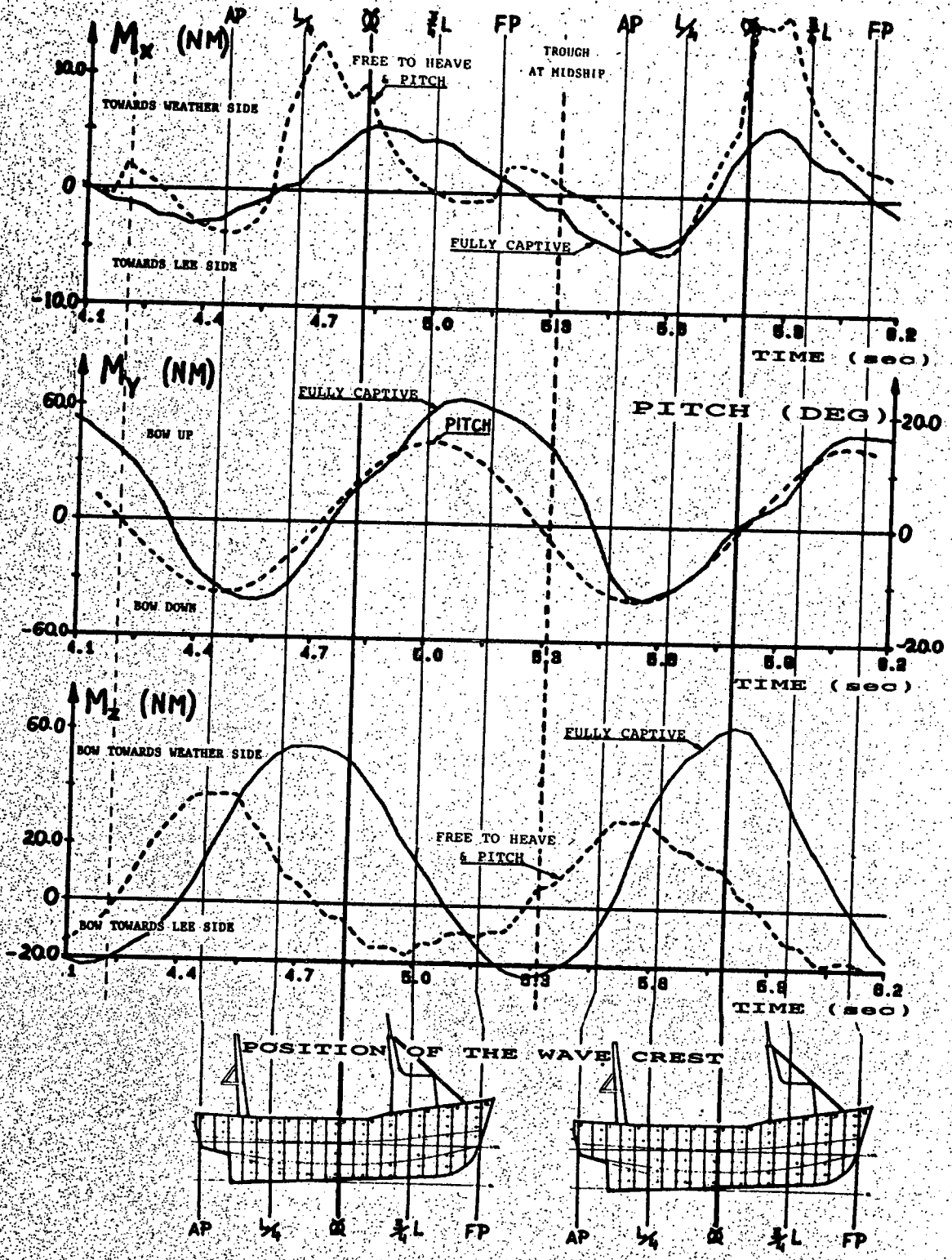

FIG.9 COMPARISON BETWEEN FULLY AND PARTLY CAPTIVE MODEL TESTS

HYDRODYNAMIC MOMENTS DURING 2 WAVE CYCLES

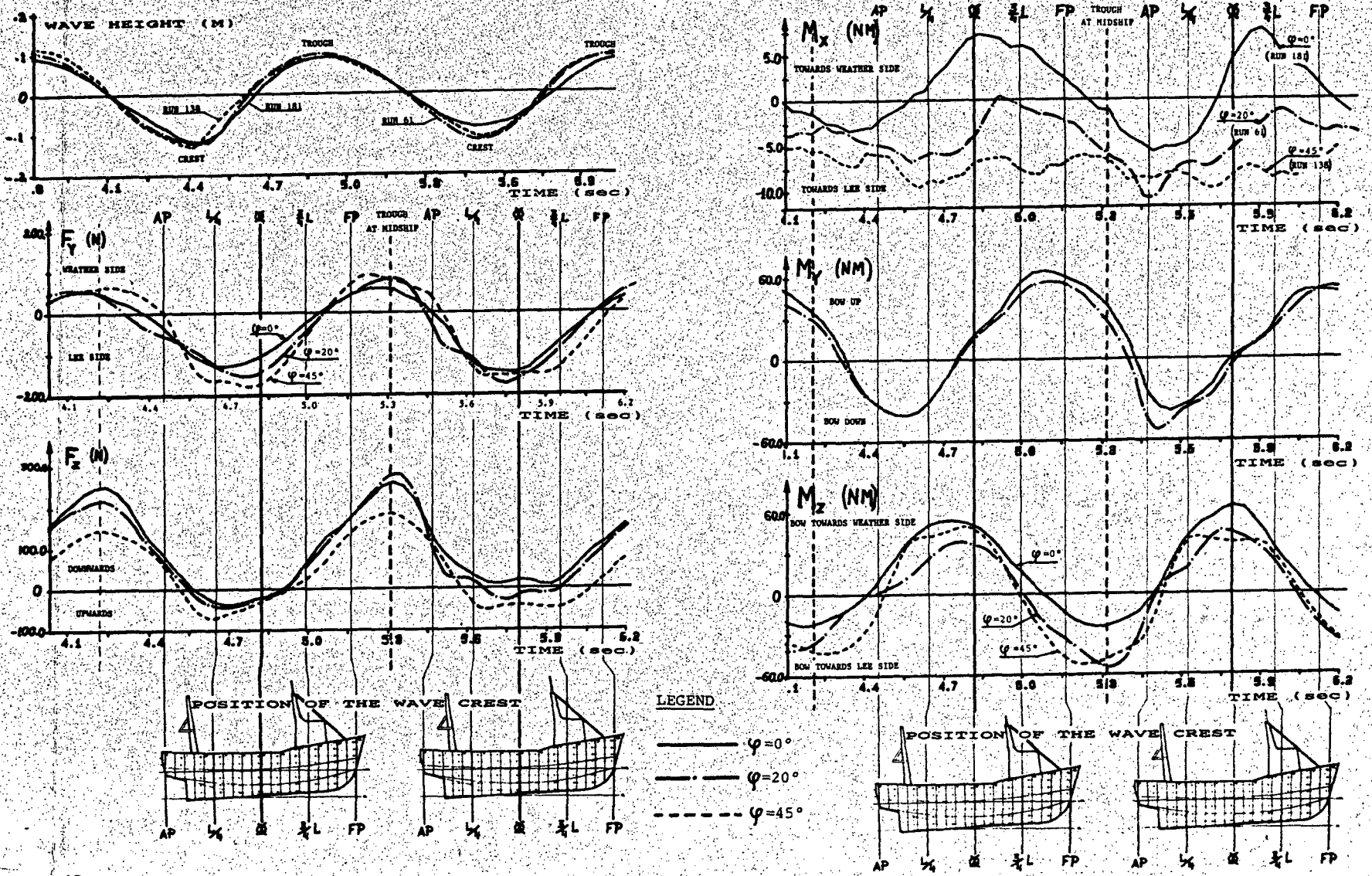

FIG.10 FULLY CAPTIVE MODEL TESTS
HYDRODYNAMIC FORCES & MOMENTS AT VARIOUS ANGLES OF HEEL

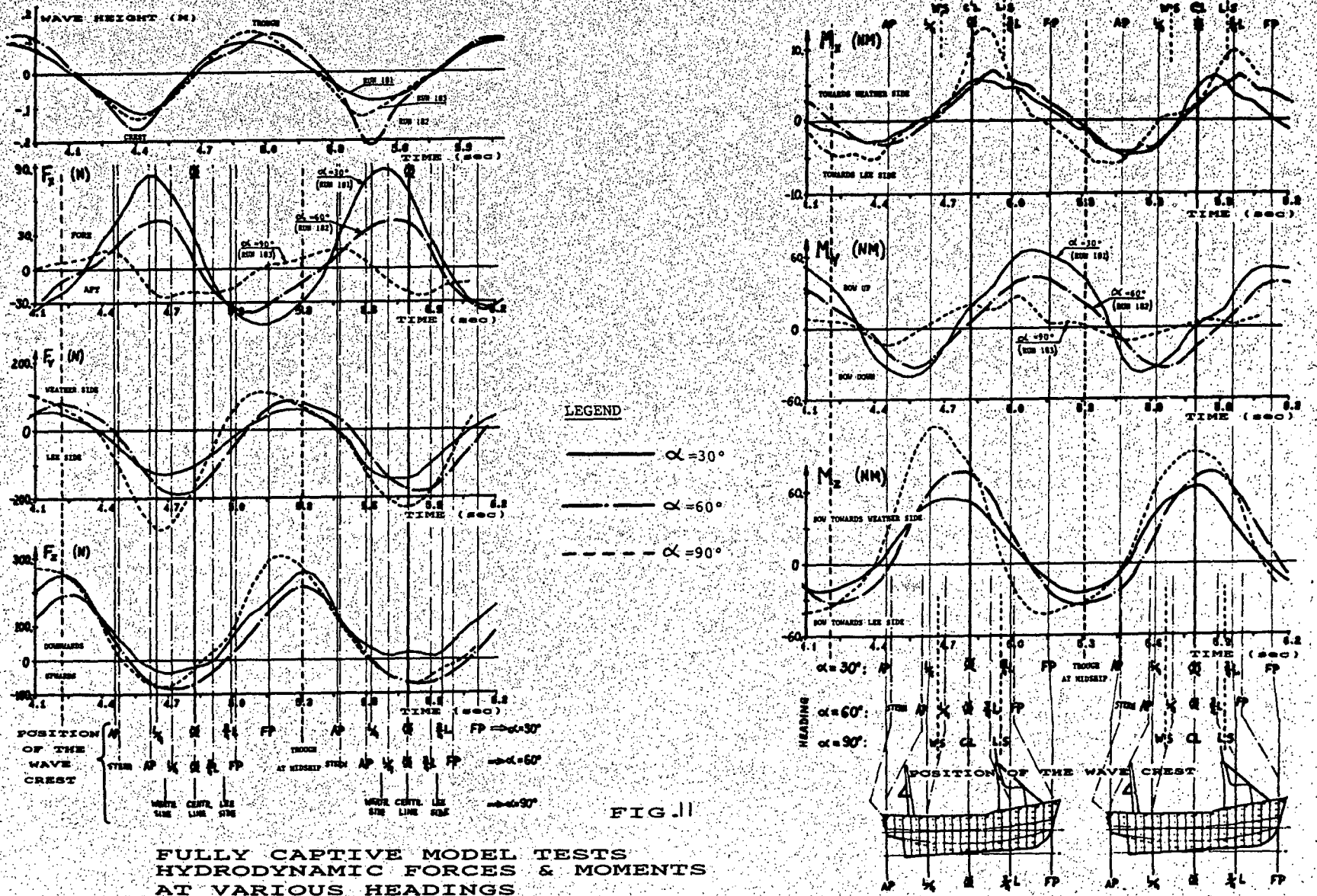

FIG.11

FULLY CAPTIVE MODEL TESTS
HYDRODYNAMIC FORCES & MOMENTS
AT VARIOUS HEADINGS

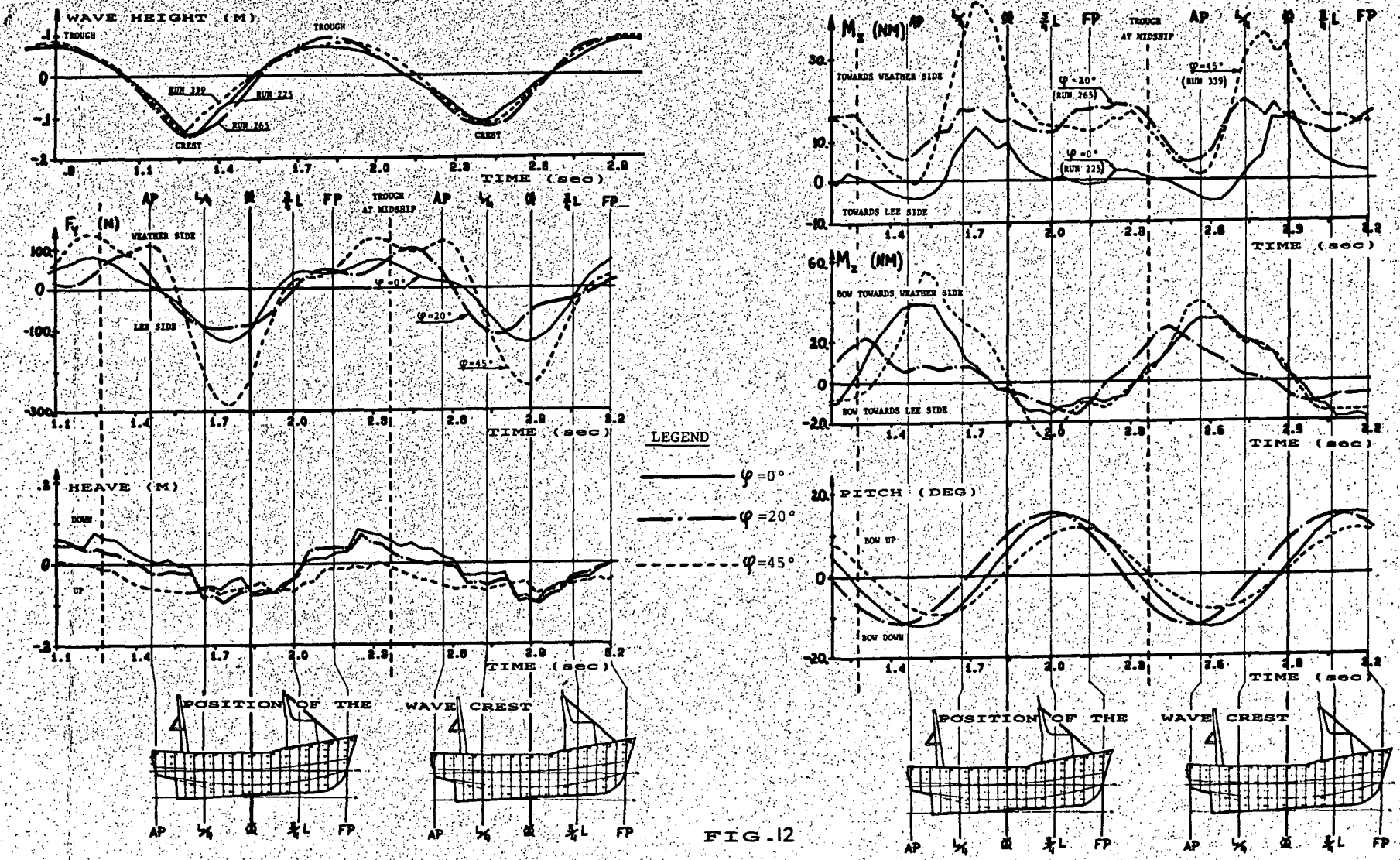

FIG.12

PARTLY CAPTIVE MODEL TESTS
HYDRODYNAMIC FORCES & MOMENTS AT VARIOUS ANGLES OF HEEL

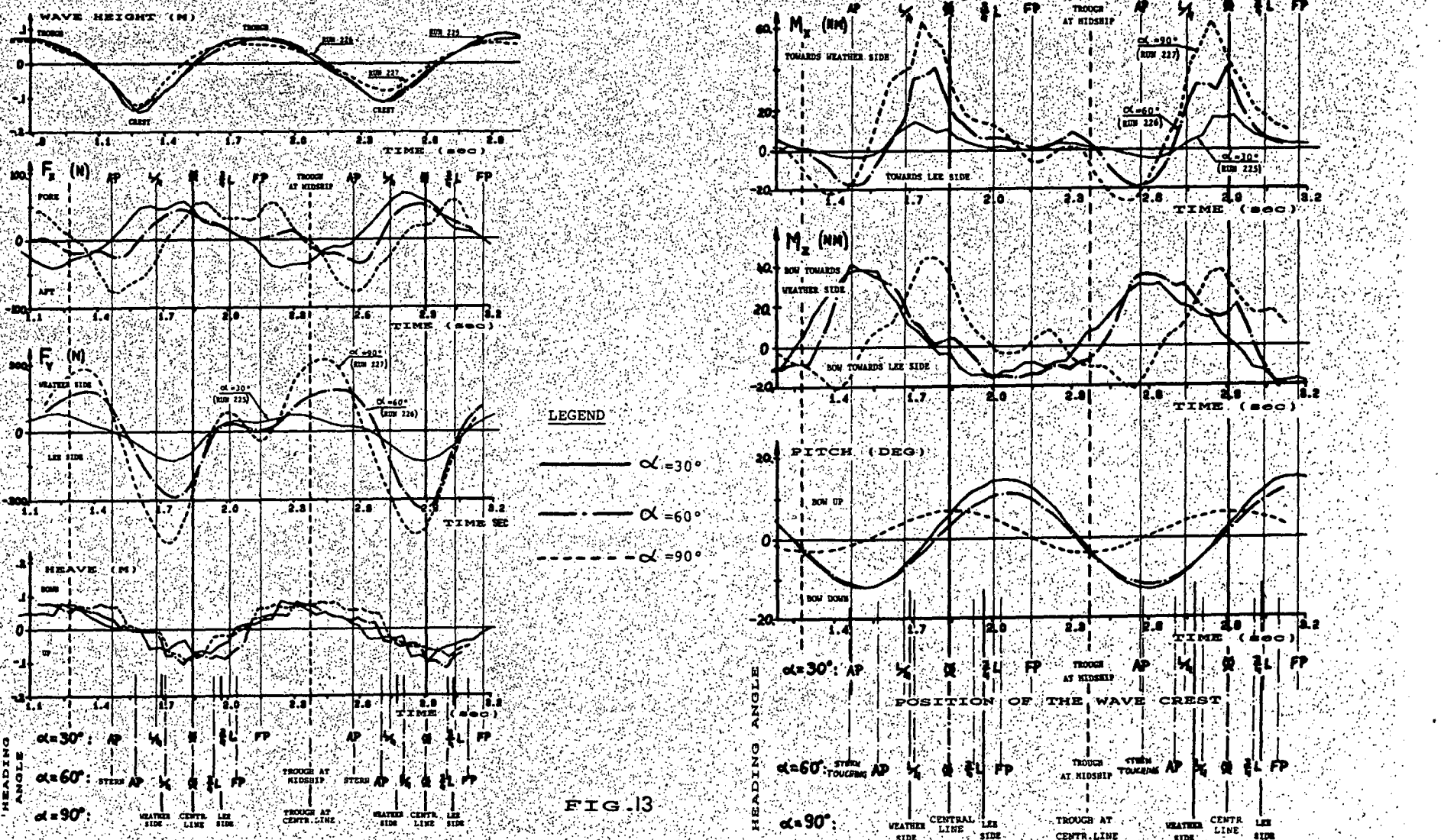

LEGEND

——— α =30°

—·—·— α =60°

- - - - - - α =90°

FIG.13

PARTLY CAPTIVE MODEL TESTS
HYDRODYNAMIC FORCES & MOMENTS AT VARIOUS HEADINGS

SUBDIVISION STANDARD AND DAMAGE STABILITY FOR DRY CARGO SHIPS BASED ON THE PROBABILISTIC CONCEPT OF SURVIVAL

Magne Sigurdsen and Sigmund Rusaas

Det norske Veritas

Norway

ABSTRACT

The question of subdivision standard for dry cargo vessels has gained considerable international interest during the past few years, espesially in connection with the probabilistic concept of survival. This paper describes a subdivision standard for dry cargo vessels, developed by Det norske Veritas. The standard is offered as an Optional Class Notation: The SC-Class.

The subdivision standard is based on the probabilistic concept found in IMCO resolution A.265 (VIII), but modified for dry cargo vessels. The theoretical background with the basis in resolution A.265 is discussed, together with the modifications necessary to adopt the method to dry cargo vessels.

1. INTRODUCTION

The safety of ships has always been a topic of great concern for ship designers, shipbuilders, shipowners, national authorities and classification societies. Important instruments to achieve an acceptable level of safety are the rules and regulations given by national authorities and classification societies. The objectives of these rules are twofold:

a) Minimize the risk for accidents

and

b) Reduce the consequences if an accident should happen.

Examples of rules and regulations aimed at reducing the consequences of an accident are the damage stability requirements found in several international codes and conventions, like SOLAS, MARPOL, The Gas Code, The Chemical Code etc. Provided these standards are followed, the ship is assumed to have a certain level of survival capability in case of damage.

However, the damage stability requirements do not cover all types of ships. There has been a tendency to emphasize on the consequences and the effect on the environment. Ships carrying dangerous cargo are therefore well covered, whereas ordinary dry cargo vessels have been neglected.

The development of new types of ships, like for instance Roll on/Roll off vessels has brought forward the issue of damage stability for dry cargo ships. The Roll on/Roll off concept invites to "open" ship solutions, which makes these vessels vulnerable from a damage stability point of view. It is therefore an increasing international opinion that also dry cargo ships should have a minimum subdivision standard.

2. THE PROBABILISTIC CONCEPT

The ship which can not sink is not yet built. Therefore, one always have to face the question: How safe is the ship in case of damage? A ship designed to sustain any one- compartment damage, is just as safe as the probability of not damaging one of the transverse bulkheads. It is obvious that the probability of such damage increases with number of bulkheads. The one-compartment damage standard may therefore offer a rather arbitrary level of safety, e.g. dependent on number of bulkheads. It is also very common to assume a limited damage penetration, one fifth of the breadth is a very often used figure, and damages exceeding this limit is not investigated.

Instead of using traditionally 'deterministic' methods such as the one-compartment standard, an attempt to calculate the probability of surviving a hyphothetical damage can been made. Such a method was first described by Wendel /10/, and implemented in IMCO Res. A.265 (VIII). Ref /1/ and /2/. If such a probability can be found, it is quite obvious that it gives a far more objective measure of the ship's survival capability in case of damage than any other damage stability standards.

The probability of a ship's survival includes the following probabilities:

- the probability of flooding each single compartment and each possible group of two or more adjacent compartments.

- the probability that the residual buoyancy and stability after damage will be sufficient to provide for survival.

It may be demonstrated by means of the probability theory that the probability of survival should be calculated as a sum of the product of these two probabilities, taking the summation over each single compartment and each group of two or more adjacent compartments.

This probability is called the "Attained Subdivision Index", and is expressed as follows:

$A = \sum a \cdot p \cdot s$ (See fig. 1)

where

$a \cdot p$ is the probability that only the compartment or group of compartments are flooded.

s is the probability of surviving the damage.

The implementation made in IMCO Res A.265 is based on statistics from 296 cases of rammed ships, using the following statistical material:

- Damage position along the ship.
- Damage length density function
- Damage penetration density function

Consult fig. 2. For a more thorough description of the method, it is referred to Wendel /10/ and A.265 (/1/ and /2/).

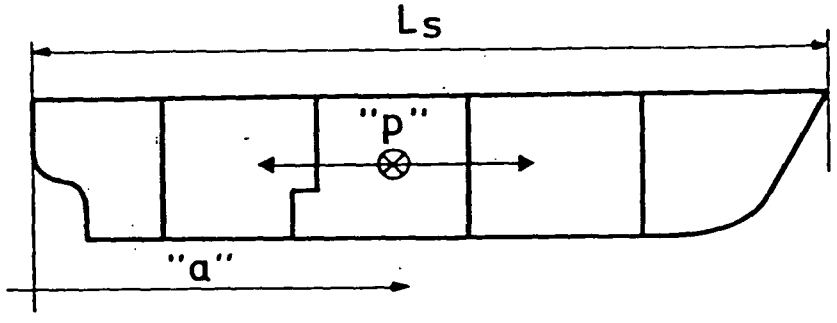

$$A = \sum a \cdot p \cdot s$$

'a' accounts for probability as related to position of compartment

'p' accounts for probability that only the compartment or group of compartments may be flooded

's' account for the probability of survival after damage

Fig 1: Calculation of attained index

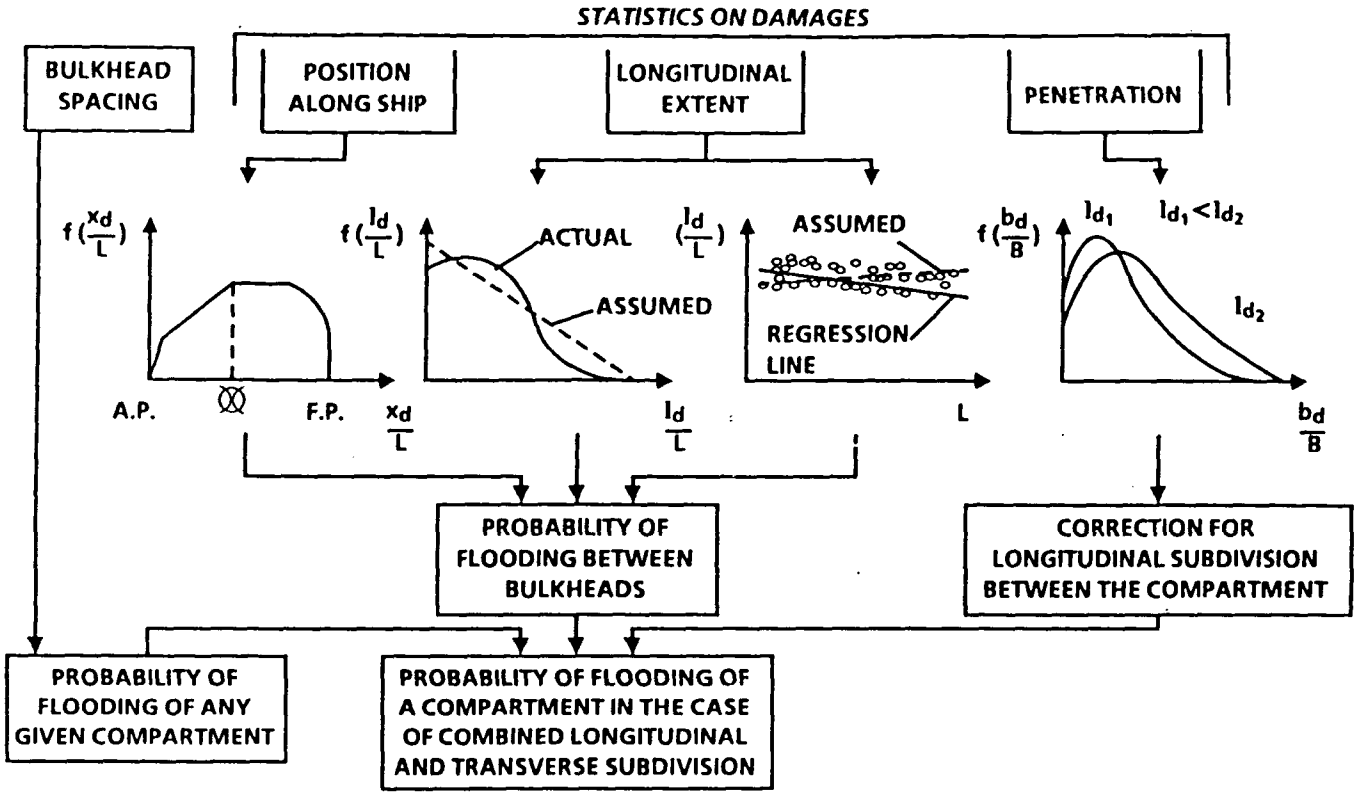

Fig. 2: Statistical distributions used in calculation of subdivision index

3. ADOPTION OF THE METHOD TO DRY CARGO VESSELS

A primary goal when adopting the method to dry cargo vessels was not to make the rules too sophisticated, but still take account of all relevant effects in a reasonable way. Since dry cargo ships are a very in-homogenous group of ships, this cannot be achieved without making some simplifications. Also, since the method in A.265 were developed for passenger ships, some of the assumptions and criteria in A.265 may not be relevant for dry cargo ships.

The simplifications to be made of course imply that the subdivision index does not represent the exact probability of survival, but it is a useful comparative measure of survival capability in case of damage, and it gives a good indication of the safety level.

The damage statistics forming the basis for calculation of the attained subdivision index, were kept unchanged from A.265. It was found nesessary, however, to re-evaluate some of the assumptions and criteria inherent in the method, like:

- Loading conditions
- Permeabilities
- Vertical extent of damage
- Survival criteria
- Required index
- Effect of longitudinal subdivision

Each of these topics are discussed in the following.

Loading_Conditions

In A.265 it is used three different draughts within the draught range, and each draught is given a "weight" corresponding to the probability distribution on draughts. This distribution, however, is believed to have sufficient relevance for passenger ships only, and that similar distribution to be used for dry cargo ships would have been different for each ship type.

Available information on such draught distribution for dry cargo ships is very limited, and another approach were therefore chosen, based on two extreme loading conditions only:

a) Ballast arrival

b) Full load with minimum metacentric height, or if a higher metacentric height is to be specified in the instructions to the master, then that value may be used.

By putting equal weight on each draught, this method is believed to take account of both the light and deeper draughts in a reasonable way. The attained index is then calculated as follows:

$$A = 0.5 \ A_L + 0.5 \ A_B$$

where

A_L = Attained index in loaded condition

A_B = Attained index in ballast condition

Permeabilities_in_loaded_Compartments

Very limited data on permeabilities for dry cargo ships were available, but from ref /5/ and /6/ it was found that reasonable permeabilities were:

0.70 in fully loaded condition.
0.95 in ballast.

Due to the limited information available it was not felt reasonable to distinguish between ship types, although there are reason to believe that e.g. Ro/Ro ships have somewhat higher figures.

Vertical_extent_of_damage

In A.265 the damage is assumed to extend to a so-called "relevant bulkhead deck". This deck is in principle freely chosen, as long as it is a watertight deck. The probability of survival, however, is among other things a function of the freeboard measured from the relevant freeboard deck.

Since the probability of survival in the SC-Class (see Survival Criteria below) is formulated in another way, the concept of a freely chosen "relevant bulkhead deck" cannot be used. An unlimited vertical extent of damage would have been too extensive for ships with large freeboard, e.g. car carriers. Therefore, a limitation of the vertical extent of damage was assumed. Statis-

tics on vertical extent of damage were not readily available, so one had to make a reasonable assumption. Based on the minimum bow-height required in the load line convention a vertical extent above the waterline of 0.03 times the length of the ship, but not more than 5 metres were chosen.

Survival Criteria

The ship's probability to survive after damage is dependent on the residual buoyancy and stability after damage and the environmental conditions (wind, waves) at the time of damage. The residual buoyancy and stability is found by damage stability calculations, and the probability distribution of e.g. wave heights may be found from meteorological statistics. The difficulty with regard to the practical application is, however, to obtain the correct relationship between the residual buoyancy/stability and the meterological statistics.

In A.265 this is solved by making model tests in waves to arrive at a relationship between residual stability and critical wave height, i.e. the wave height necessary to capsize the model. Having established this relationship, the probability that the ship will not capsize is equal the probability that the critical wave height is not exceeded.

From the model tests, it was found that there was a reasonable relationship between the critical wave height and the freeboard and metacentric height after damage. Using this relationship together with the wave height distribution an approximate formula for the probability of not capsizing were derived.

This formula, which is very simple and easy to use, was appraised for use within the SC-Class, but was rejected for the following reasons:

- The model tests were carried out with two different models only. Their relevance for today's dry cargo fleet is therefore questionable.

- The formula gives only the probability of not capsizing. The probability of not sinking was taken into account by setting the probability to zero if any part of the undamaged deck was submerged. This may be a relevant assumption for vessels with high freeboard, e.g. passenger ships, but it cannot be taken as a general approach for dry cargo ships.

Instead, the following general accepted survival criteria from existing rules and regulations were chosen:

- The final waterline, and any waterline during the period of flooding, is to be below the lower edge of any opening through which progressive flooding may take place.

- The angle of heel in final stage of flooding and during the period of flooding is not to exceed 25 degrees.

- In final stage of flooding, the righting lever curve should have a range of at least 20 degrees beyond the angle of equilibrium in association with a maximum righting lever of at least 0.1 metres within the same range.

If all these criteria are fulfilled, then the probability of survival is set to 1.0, else the probability is set to zero.

Required subdivision Index R

In order to find a reasonable level of the subdivision index, a systematic calculation of a sample of the dry cargo fleet were carried out. The result from this study is summarized in the tables 1 and 2 below:

Table 1: Subdivision Index by Distribution on Ship Type

Ship Type	No of ships (T)	No of ships (R)	Average index Full load	Average index Ballast	Average index Mean
Bulk Carrier	3	3	0.54	0.94	0.74
General Dry Cargo	6	1	0.12	0.45	0.28
Ro/Ro	3	0	0.08	0.62	0.35
Container	3	3	0.28	0.86	0.57
Vehicle Carrier	3	0	0.03	0.13	0.08
Total	18	7	0.19	0.57	0.38

No of ships (T) = Total no of ships
(R) = No of ships fulfilling required index

Table 2: Subdivision Index by Distribution on Ship Length

Ship Length	No of ships (T)	No of ships (R)	Average index Full load	Average index Ballast	Average index Mean
Less than 50	1	0	0.07	0.07	0.07
50-99	4	0	0.07	0.36	0.21
100-149	6	3	0.19	0.70	0.45
150-199	4	2	0.20	0.59	0.39
Above 200	3	2	0.40	0.92	0.66
Total	18	7	0.19	0.57	0.38

No of ships (T) = Total no of ships
(R) = No of ships fulfilling required index

Even if one should not draw too firm conclusions from such a limited sample, it can be seen that there is a pronounced tendency of higher index for larger ships, wheras the smaller ones all have very low index. With regards to ship types, it can be seen that the bulk- carriers all have high index compared to the other types.

Ideally, the subdivision index should be independent of ship size, but for practical reasons this is not possible. An approach with increasing index with ship size was therefore chosen. The subdivision index should, however, be independent of ship type.

The formula in A.265, but with number of passengers set to zero was then chosen:

$$R = 1 - \frac{1000}{1500 + 4\,Ls}$$

On fig. 3 this formula is drawn as a function of ship length. The results from the systematic calculation is also indicated on the same figure. The actual probability of survival derived from casualty statistics (see Risk Evaluation following) is also plotted on the same diagram. Even if the subdivision index does not pretend being the exact probability of survival, the statistics should give an indication of the level of subdivision index on today's fleet of dry cargo ships.

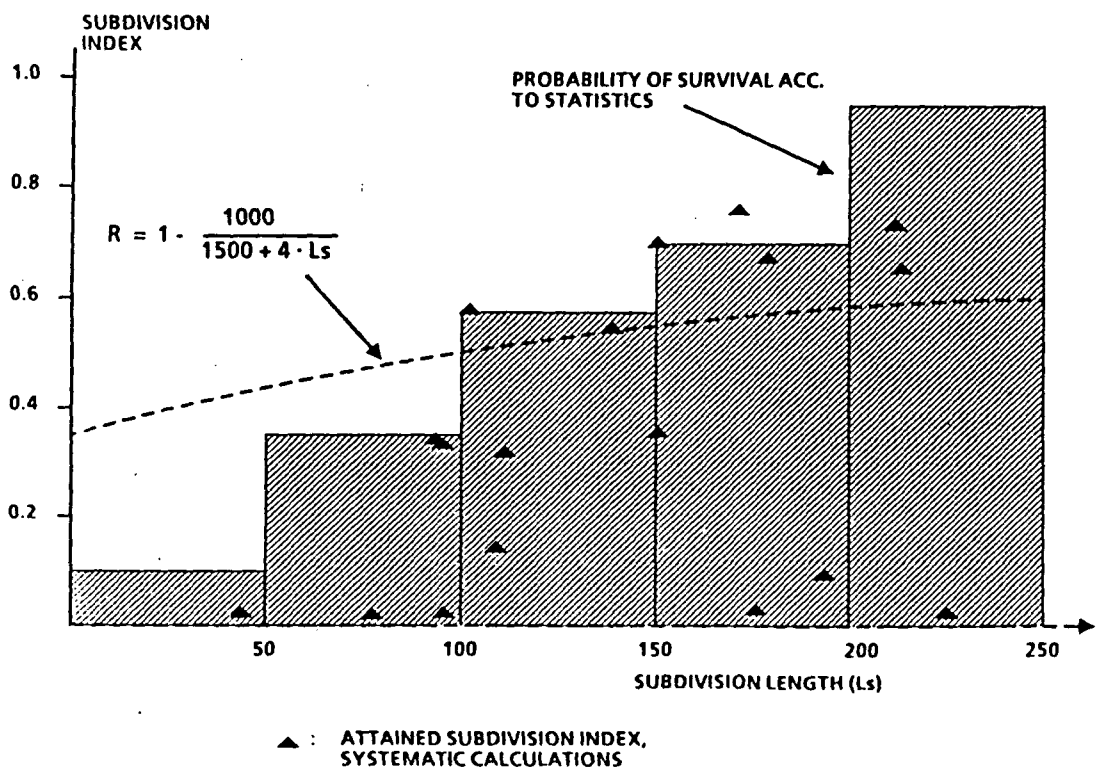

Fig. 3: Subdivision index as function of ship length

Longitudinal subdivision

The effect of longitudinal subdivision is taken into account by a socalled "reduction factor" (r), which accounts for the probability that the damage penetration will not reach the longitudinal bulkhead. As can be seen from the formula in A.265 it approximates the probability function by a straight line from (b/B=0,r=0) to b/B=0.2, causing underestimation of r for small values of b/B. It was found that a better approximation of the probability function was a straight line from (b/B=0,r=0.1) to b/B=0.2. (See fig. 4)

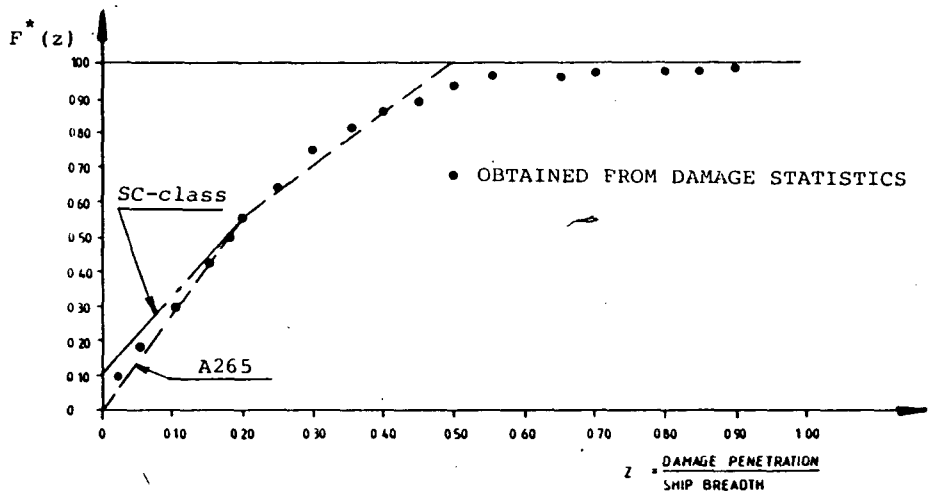

Fig. 4: Probability function of damage penetration

As can also be seen from the original formula for r, it only gives negligible contribution for double skin. Such a contribution is highly recommended, because of the obvious increased safety against e.g. leakages. The enhanced r-factor in the SC-Class always gives a double skin arrangement a factor of at least r=0.1, which is considered to be a reasonable figure, and at the same time gives a better approximation for narrow wing tanks.

4. DESIGN PRINCIPLES

In addition to complying with the "Required Subdivision Index", the ship also have to comply with certain design principles. First, the collision bulkhead should be such positioned that the ship will sustain a simultaneous damage to all compartments forward of that bulkhead.

Secondly, to have some safety in case of grounding (the probabilistic concept only address collision damages) there is a re-

quirement to double bottom underneath all cargo holds, with a height of at least 1/15 of the breadth of the ship.

The SC-Class also includes requirements to watertight integrity, closing appliances and position of openings. Alarm systems are required when access openings in the shell are in use, giving alarm when the distance between the lower edge of the opening and the waterline is below a certain value.

Certain documentation requirements are also set forth, of special importance is a "Damage Control Plan", showing the boundaries of the watertight compartments, the relevant openings with means of closure and arrangement for correction of list due to flooding.

5. CONSEQUENCE STUDY

As can be seen from the tables 1 and 2, 11 out of 18 existing vessels did not meet the requirement to subdivision index. For 9 of these ships, a consequence analysis were carried out to see which changes were necessary to meet the criteria.

There are obviously 3 ways of improving the subdivision index of a ship:

a) increasing number of bulkheads

b) increasing the freeboard

c) increasing the metacentric height

First, additional bulkheads were assumed in reasonable positions within the cargo hold area. Then, the freeboard and metacentric height were increased until the required index were obtained. For the vehicle carriers, however, the study was made assuming one of the decks closed watertight.

The results of the study is summarized in table 3. As can be seen from the results, the required index in most cases can be obtained by adding one or two bulkheads and increasing the freeboard and/or metacentric height.

A general observation is that the vessel's freeboard has a significant influence on the attained index. This is of course not surprising because the vessel's reserve buoyancy is a direct function of the freeboard. One may therefore conclude that paying sufficient attention to these circumstances, it should be quite feasible to design any type of dry cargo vessel meeting the required subdivision index. It is not likely, however, that any ship can reach an acceptable level of survival capability without bulkheads in the cargo area, but it is interesting to see that both RO/RO-ships included in the consequence study gave sufficient index with one extra bulkhead only.

Table 3: Consequense study - results

Ship type	Length (Ls)	No of cargo holds	Subdiv.index 'A'	'R'	No of add. bhds.	To reach required index (with additional bhds) Increase freeboard	or Increase GM
Gen. dry carg	120.50	2	0.163	0.495	2	0.54	1.56
Gen. dry carg	92.50	2	0.340	0.465	2	0.00	0.00
Gen. dry carg	42.45	1	0.068	0.401	3	0.21	0.35
Gen. dry carg	149.16	3	0.349	0.515	2	0.20	0.73
Gen. dry carg	71.30	1	0.089	0.440	3	0.19	0.24
RO/RO	113.45	1	0.310	0.488	1	0.05	0.33
RO/RO	92.50	1	0.365	0.465	1	0.06	0.36
Vehicle carr.	193.00	2	0.115	0.550	*)		
Vehicle carr.	94.30	1	0.051	0.462	*)		

*) The Vehicle Carriers both obtained the necessary index by closing one of the decks watertight.

6. RISK EVALUATION

To evaluate collision data for Dry Cargo Ships and to assess the probability of survival, collisions occured between 1978 through 1983 have been analyzed. The analysis includes ships above 100 grt and less than 15 years of age.

Totally 616 collisions have been studied. Of these, 149 led to ingress of water, and 81 of these did not survive the damage. This gives a survival capability of 45.6 %. General Cargo ships which are by far the biggest group, show a survival capability of 39 %.

The results are summarized in tables 4 through 6.

n = Number of collisions with water ingress.
x = Number of non survivals after collisions with water ingress.

Table 4: Distribution on Ship Type

Ship Type	n	x	Survival %
Bulk Carrier	20	6	70.0
General Dry Cargo	110	67	39.1
Ro/Ro	9	6	33.3
Pass./Cargo/Ferry	2	2	0.0
Container	5	0	100.0
Other	3	0	100.0
Total	149	81	45.6

Table 5: Distribution on Ship Length

Ship Length	n	x	Survival %
Less than 50	17	15	11.8
50-99	68	43	36.8
100-149	39	18	53.8
150-199	18	5	72.2
Above 200	7	0	100.0
Total	149	81	45.6

Table 6: Distribution on Damage Location

Damage Location	Number of Collisions	Percent of all
Bow/forepeak	178	53.6
Forepeak + hold/tank fwd	15	4.5
Hold/tank fwd	24	7.2
Midship	40	12.0
Hold/tank aft	18	5.4
Hold/tank aft + Eng. room	3	0.9
Engine room/superstructure	35	10.5
Aft	19	5.7
Total	332	99.8

As shown, the tendency is the same as found in the calculations: The safety increases with ship length. As regards ship types, it appears that Bulk Carriers have better safety record than other ship types.

From the distribution on Damage Location it appears, as expected, that a majority of the collisions take place in the bow/forepeak area. This is not reflected properly in the method, and is the background for a special requirement to damage stability to this part of the ship.

7. CONCLUSION

Even if the probabilistic concept have been known for some years, and the resolution A.265 has been available as an alternative to the damage stability in SOLAS, it has not been very much used. The reason is believed that the method described in A.265 appears to be more complicated than the deterministic method in SOLAS. A.265 in itself also includes a deterministic part, (minimum one- compartment damage), and as such does not appear as a completely probabilistic concept.

The philosophy behind the probabilistic concept is that two ships with the same index are of equal safety, and there should not be any need for special treatment of certain parts of the ship. The only part of the ship which may be given special attention, is the forward part, e.g. forward of the collision bulkhead. The reason should be quite obvious: In all collisions, damage to the forward part must be expected, and this is not properly reflected in the method, which mainly consentrates on the rammed ship, and not the ramming one.

The SC-Class uses the main ideas behind the probabilistic concept as it is described in A.265, but as can be seen from this paper, some simplifications and adjustments had to be made to adapt the method to dry cargo ships. Recognizing that this is a first step in the direction of subdivision standard for Dry Cargo ships, Det norske Veritas has issued the standard as "Tentative Rules". This means that it is expected that adjustments have to be made, not least on the background of the ongoing international activity in this area.

It is believed that the method presented herein will prove to increase the level of safety for dry cargo ships. Even if the method itself does not pretend to calculate the exact probability of survival, it gives a good indication of the level of safety in case of damage, and is a useful comparative measure between different arrangement alternatives.

7. REFERENCES

/1/ IMCO Resolution A.265 (VIII)
"Regulations on Subdivision and Stability of Passenger Ships as an Equivalent to Part B of Chapter II of the International Convention for the Safety of Life at Sea, 1960".

/2/ IMCO MSC/Circular 153
"Regulations on Subdivision and Stability of Passenger Ships as an Equivalent to Part B of Chapter II of the International Convention for the Safety of Life at Sea, 1960, Explanatory notes to the Regulations".

/3/ Det norske Veritas Technical Report 82-1139:
"Roll on/Roll off Vessel's Casualty Statistics in the Period 1965-1982".

/4/ Det norske Veritas Technical Report 82-1140:
"Survival Capability of Roll on/Roll off Vessels".

/5/ George G. Sharp Inc, New York:
"Study of the Permeability of Cargo Ships. Volume I".
Prepared for U.S. Coast Guard, Washington, D.C., Nov, 1976

/6/ U.S. Maritime Administration:
"An Investigation into the Permeability of Container and Ro/Ro Vessels".
Prepared for U.S. Coast Guard, Washington, D.C., Nov, 1975.

/7/ Tagg, Robert D:
"Damage Survivability of Cargo Ships".
SNAME Trans., Vol 90, 1982.

/8/ Cleary, William A. Jr:
"Subdivision, Stability, Liability".
Marine Technology, Vol 19, No.3, July 1982.

/9/ Grochowalski, S. and Pawlowski, M:
"The Safety of Ro/Ro vessels in the light of the probabilistic concept for standardizing unsinkability".
International Shipbuilding Progress, Vol. 28, 1981.

/10/ Wendel, Kurt:
"Subdivision of Ships".
SNAME Paper No 12, Diamond Jubilee International Meeting, New York, 1968.

/11/ Det norske Veritas:
"Subdivision Index and Survival Probability of Dry Cargo Vessels. Tentative Rules".
Rules for Steel Ships, Pt.5, Ch.2, Sec.8

LIST OF PARTICIPANTS

A U S T R A L I A

· RENILSON Martin

Australian Maritime College
PO BOX 986,
7250 Launceston,
tlx: 58827

B U L G A R I A

· KISHEV Roumen

BSHC
9003 Varna
tlx: 77497 BSHC BG

: TOMCZEV Dimitr

Ship Research Institute
Varna

D E N M A R K

· NIELSEN John Koch

Danish Maritime Institute
Hjortekaersvej 99
2800 Lyngby
tlx: 37223 SHILAB DK

· GULDHAMMER Hans Erik

Department of Ocean Engineering, D.T.H.
Bld.101E, DK 2800 Lyngby
tlx: 37529 DTHDIA DK

FEDERAL REPUBLIC OF GERMANY

· HORMANN Hartmut

Germanischer Lloyd
PO Box 111606
D-2000 Hamburg 11
tlx: 212828 glhh d

· WAGNER, Diether

Germanischer Lloyd
PO Box 111606
D-2000 Hamburg 11
tlx: 212828 glhh d

· KRAPPINGER Odo

Hamburgische Schiffbau-
Versuchsanstalt GmbH
Postfach 600929,
D-2000 Hamburg 60,
tlx: 2 174 236 hsva d

. KASTNER Sigismund

Langemarckstrasse 116
2800 Bremen 1,
HOCHSCHULE BREMEN
tlx: 244804 SENAT D

· FEEDER F.L.

HOCHSCHULE BREMEN
Langemarckstrasse 116
2800 Bremen 1,
tlx: 244804 SENAT D

. BÖTTCHER Harald

Institut für Schiffbau der
Universität Hamburg
Lämmersieth 90
D-2000 Hamburg 60,

. PETEY, Fernando

Institut für Schiffbau der
Universität Hamburg
Lämmersieth 90
D-2000 Hamburg 60,

· SÖDING, Heinrich

Institut für Schiffbau der
Universität Hamburg
Lämmersieth 90
D-2000 Hamburg 60,

· ABICHT, Walter

Institut für Schiffbau der
Universität Hamburg
Lämmersieth 90
D-2000 Hamburg 60,

· BLUME, Peter

Hamburg Ship Model Basin
Bramfelder Strasse 164
D-2000 Hamburg 60,

G R E A T B R I T A I N

· VASSALOS Dracos
University of Strathclyde,
Dept. of Ship and Marine
Technology,
100 Montrose str.,
Glasgow, U.K.

· BROOK Keith A.
British Maritime Technology LTD.,
Wallsend,Tyne and Wear NE286UY

· CHEESLEY N.R.
Plymouth Polytechnic
Department of Marine Technology
Drake Circus, PLYMOUTH
Devon, PL48AA
tlx: 45423 PPLRC G.

· DEAKINS E.
Plymouth Polytechnic
Department of Marine Technology
Drake Circus, PLYMOUTH
Devon, PL48AA
tlx: 45423 PPLRC G.

· PETROV A.
International Maritime Organization
I.M.O
4 Albert Embankment,
London SE1 7SR

KUO Chengi
University of Strathclyde
Department of Ship and Marine
Technology
100 Montrose Street, Glasgow G40LZ,
Scotland
tlx: 77472

· MORRALL A.
British Maritime Technology LTD.,
Feltham,
Middlesex TW140LQ
tlx: 263118

· SCHAFERNAKER ANDRZEJ
John Brown Offshore LTD.,
LONDON

· WINKLE I.E.
Dept. of Naval Architecture and
Ocean Engineering
University of Glasgow,
G12 8QQ
tlx: 777070 unigla g

GERMAN DEMOCRATIC REPUBLIC

· LAU, Kurt
Schiffbau-Versuchsanstalt Potsdam
VEB Kombinat Schiffbau
Marquardter chaussee 100,
1503 Potsdam
tlx: SVA Pdm 15403

I T A L Y

· CAMPANILE Antonio

Department of Naval Engineering
v.Claudio, 21-80125 Napoli

· CARDO Antonio

Institute of Naval Architecture
Via A.Valerio 10
134127 Trieste

· CASSELLA Pasquale

Department of Naval Engineering
Via Claudio, 21
80125 Napoli

· FRANCESCUTTO Alberto

Department of Physics
University of Trieste,
Via A. Valerio 2,
134127 Trieste

J A P A N

· HIRAYAMA,Tsugukiyo

Yokohama National University
Tokiwadai-156, Hodogaya-ku,
Yokohama 240
tlx: 3822614 YNUENG J

· IKEGAMI,Kunihiro

Ship Hydrodynamics Research Laboratory
Nagasaki Technical Institute,
Mitsubishi Heavy Industries, Ltd.
5-717-1, Fukahori-machi,
Nagasaki 851-03
tlx: 752451 MHINGA J

· NAKAJIMA, Toshio

Sumitomo Heavy Industries, Ltd.,
63-30,Yuhigaoka, Hiratsuka-shi,
Kanagawa-ken 254,
tlx: 3882423 SSM J

TAKARADA, Nakajima

Sumitomo Heavy Industries, Ltd.,
63-30,Yuhigaoka, Hiratsuka-shi,
Kanagawa-ken 254,
tlx: 3882423 SSM J

· MASUYAMA, Yutaka

Kanazawa Institute of Technology
Dept. of Mechanical Engineering
7-1 Ohgigaoka, Nonoichi,
Ishikawa 921,
tlx: 5122456KIT LC J

HAMAMOTO, Masami

Osaka University, SOYA 2-28-16
Hirakata, OSAKA

OHKUSU, Makoto

Kyushu University
Kasuga-koen 6, Kasuga, Fukuoka

· KAN,Makoto

Ship Research Institute
6-38-1, Shinkawa, Mitaka,
Tokyo 181,

· TAKEZAWA Seiji

Yokohama National University
Tokiwadai, Hodogaya-ku,
Yokohama 240,
tlx: 3822-614 YNUENG J

· UMEDA, Naoya

National Research Institute of
Fisheries Engineering
5-5-1, Kachidoki,Chuo-ku,
Tokyo 104,

MOTORA, Seizo

Foundation for Shipbuilding Advancement
Senpaku Shinko Bldg. 15-16 Toranomon
10-CHO-ME, Minatoku, Tokyo 105
tlx: 2222652 ISIF J

N E T H E R L A N D S

· VERMEER, H.

Directorate General of Shipping and
Maritime Affairs
Post Box 5817,
2280 HV RYSWYK

N O R W A Y

· DAHL Sverre J.

Norwegian Maritime Directorate
PO BOX 8123-DEP, N-0032 Oslo 1
tlx:76997 SDIR N

· DAHLE Emil Aall

Det Norske Veritas,
P.O. Box 300, N-1322 Høvik

· JULLUMSTROE, Egil

MARINTEK A/S
Haakon Haakonsonsgt. 34
PO Box 4125 Valentinlyst N-7001 Trondheim

· MYRHAUG Dag

UNIT/NTH, Marin Hydrodynamikk
N-7034 Trondheim - NTH
tlx:55146 NSFIT N

· NEDRELID Terje

MARINTEK A/S
Haakon Haakonsonsgt. 34
PO Box 4125 Valentinlyst N-7001 Trondheim

· RUSAAS, Sigmund

Det Norske Veritas,
PO Box 300, N-1322 Høvik

P O L A N D

· KOBYLIŃSKI, Lech	Ship Research Institute Technical University of Gdańsk ul. Majakowskiego 11/12 80-952 Gdańsk tlx: 512967 IOPG PL
· KRĘŻELEWSKI, Mieczysław	Same as above.
· GERIGK , Mirosław	Same as above.
· BŁOCKI, Witold	Same as above.
· JAGIEŁKA, Mikołaj	Same as above.
· STASIAK, Janusz	Same as above.
· FRĄCKOWIAK, Miłosz	Same as above.
· WEŁNICKI, Wiesław	Same as above.
· PAWŁOWSKI, Maciej	Same as above.
· JAROSZ, Andrzej	Same as above.
· FRĄCKOWIAK, Ryszard	Same as above.
· TRAN HUNG NAM	Same as above.
· DURU, Stephen	Same as above
· WIŚNIEWSKI, Jerzy	Same as above.
· SZELANGIEWICZ, Tadeusz	Technical University of Szczecin Shipbuilding Institut Al.Piastów 42 71-065 Szczecin tlx: 0422141 ps
GNIEWSZEW, Jerzy	WSM Gdynia
DUDZIAK, Jan	CTO-OHO Gdańsk-Oliwa ul. Szczecińska
ZDYBEK, Tadeusz	Same as above.
ŻOCHOWSKI, Cezary	WSM Gdynia
BANACKI, Marian	CTO-OHO Gdańsk-Oliwa ul. Szczecińska

POLAND

· MIEDZIŃSKI, Franciszek	Polish Steamship Company Szczecin, ul.Małopolska 44 tlx: 0422136
· MICHALEC, Zygmunt	Maritime Board at Gdynia ul.Chrzanowskiego 10 81-338 Gdynia tlx: 054285
· PISKORZ-NAŁĘCKI, Jerzy, Wojciech	Marine Consultants ul. Lyskowskiego 16 70-966 Szczecin tlx: 0425105 ctw pl
· JANKOWSKI, Jan	Polish Register of Shipping ul.Wały Piastowskie 24, 80-855 Gdańsk 1 tlx: 0512373
· DOBROMIRSKI, Walerian	Technical University of Wrocław ul. Wybrzeże Wyspiańskiego 27, 50-370 Wrocław
· MOREK, Bronisław	Polish Register of Shipping ul. Wały Piastowskie 24 80-855 Gdańsk tlx: 0512373
· SAMOŁYK, Józef, A.,	Technical University of Wrocław ul.Łukasiewicza 7/9 50-371 Wrocław tlx: 0712254 pwr pl
· MICHALIK, Leszek	Polish Ocean Lines ul. 10 Lutego 24 81-364 Gdynia tlx: 054396
· TURECKI, Władysław	The Gdańsk Shipyard ul. Doki 1 80-958 Gdańsk tlx: 0512273 pl
· JAKLEWICZ, Przemysław	Same as above.
· ŻYCHSKI, Wojciech	The Gdynia Shipyard Design Office ul. Czechosłowacka 3 81-963 Gdynia tlx: 054571 bpk
· NIEBIESZCZAŃSKI, Janusz	Same as above.
· ORZECH, Kazimierz	Same as above.
· OTREMBA, Ernest	Technical University of Szczecin Shipbuilding Institute Al.Piastów 42 71-065 Szczecin tlx: 0422141 ps

S W E D E N

· KARLSSON Roger	Dep. of Marine Hydrodynamics Chalmers University of Technology 41296 Göteborg tlx: 2369 CHALBIB S
· REGNSTRÖM Björn	Dep. of Marine Hydrodynamics Chalmers University of Technology 41296 Göteborg tlx: 2369 CHALBIB S
· SÖDERBERG Peter	SSPA Maritime Consulting AB PO Box 24001 S-400 22 Göteborg tlx: 20863 SSPAGBG S
SANDELL, Anders	SEASAFE AB Ingenjörscentrum S-19178, Sollentuna

T U R K E Y

· ÖZALP Teoman	Technical Adviser Gepa Group of Companies Miraley Sefik Bay Sok. Antalya Palas 5110 Taksim, Istanbul

U S A

· Chen Hsao H.	American Bureau of Shipping 45 Eisenhower Drive Paramus, New Jersey 07652,
· Nehrling Bruce C.	United States Naval Academy Annapolis, Maryland 21402
· Cleary, William A.,Jr.	U.S. Coast Guard 2100 Second Street-Washington D.C.20593
· Pantazopoulos Michael S.	University of Washington Meb, FU-10, Seattle, WA, 98105
· Adee, Bruce H.	University of Washington FU-10, Seattle, WA 98177 tlx: 470096 uw ui
· Palzarano, Jeffrey M.	University of Michigan Ann Arbor, MI 48109 tlx: 4320815 um ui
. Bhattacharyya Rameswar	Naval Systems Engineering Department U.S. Naval Academy Annapolis, Maryland 21402
. St.Denis, Manley	Home address: 6750 Hawaii Kai Dr.No.1301,Honolulu Hawaii, 96825
MAZUREK, Joseph	WEBB Inst. of Naval Architecture New York

U S S R

. BORODAY I.K.

Krylov Shipbuilding Research Institute
Leningrad 196158

· RAKHMANIN N.N.

Krylov Shipbuilding Research Institute
Leningrad 196158

. KHOLODILIN A.N.

Leningrad Shipbuilding Institute
Leningrad 190008

ERRATUM

"Towards Rational Stability Criteria for Semisubmersibles - A Pilot Study" H.H. Chen, Y.S. Shin, J.L. Wilson, Page 5, Fig. 11.

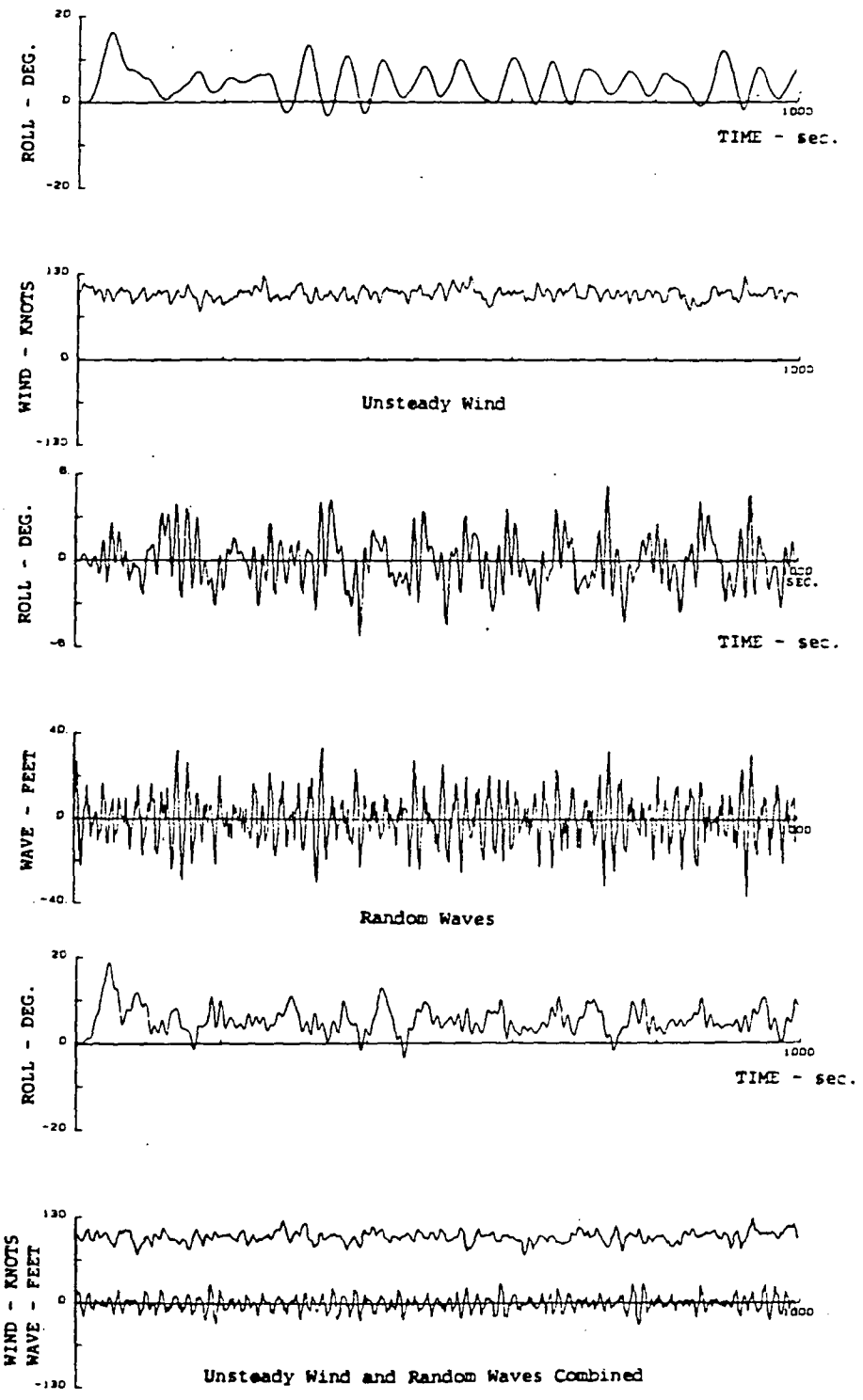

Fig. 11 Time Histories of Roll Motion for the 8-Column Unit subjected to Three Different Environmental Conditions